

GROUTING FOR PILE FOUNDATION IMPROVEMENT

Almer E.C. van der Stoel

Grouting for Pile Foundation Improvement

Proefschrift

ter verkrijging van de graad van doctor
aan de Technische Universiteit Delft,
op gezag van de Rector Magnificus prof.ir. K.F. Wakker
voorzitter van het College voor Promoties,
in het openbaar te verdedigen

op dinsdag 11 september 2001 om 11.30 uur

door

Almer Engelbert Carl VAN DER STOEL

Civiel Ingenieur
geboren te Amsterdam

Dit proefschrift is goedgekeurd door de promotoren:

Prof. ir. A.F. van Tol

Prof. ir. J. van Stigt

Toegevoegd promotor:

ir. L.G.W. Verhoef

Samenstelling promotiecommissie:

Rector Magnificus,	voorzitter
Prof. ir. A.F. van Tol,	Technische Universiteit Delft, promotor
Prof. ir. J. van Stigt,	Technische Universiteit Delft, promotor
ir. L.G.W. Verhoef,	Technische Universiteit Delft, toegevoegd promotor
Prof. ir. E. Horvat,	Technische Universiteit Delft
Prof. ir. J. Maertens,	Katholieke Universiteit Leuven
Prof. dr. R.J. Mair,	University of Cambridge
Prof. ir. C. van Weeren,	Technische Universiteit Delft

Published and distributed by: DUP Science

DUP Science is an imprint of

Delft University Press

P.O. Box 98

2600 MG Delft

The Netherlands

Telephone: +31 15 27 85 678

Telefax: +31 15 27 85 706

E-mail: DUP@Library.TUdelft.NL

ISBN 90-407-2223-4

Keywords: grouting / pile foundation improvement / geophysical verification methods

Copyright © 2001 by A.E.C. van der Stoel

All rights reserved. No part of the material protected by this copyright notice may be reproduced or utilised in any form or by any means, electronic or mechanical, including photocopying, recording or any information storage and retrieval system, without permission from the publisher: Delft University Press.

Printed in the Netherlands



Dit proefschrift is opgedragen aan mijn ouders,
Edward en Viviënne van der Stoel,
van wie ik heel erg veel hou.

ACKNOWLEDGEMENTS

This research project was carried out at Delft University of Technology, more specifically at the Geotechnical Laboratory of the Faculty of Civil Engineering and at the Renovation and Maintenance Techniques Section of the Faculty of Architecture. Partial financial support of Ingenieursbureau Amsterdam and Noord/Zuidlijn Consultants is gratefully acknowledged.

First, I would like to express my appreciation to my supervisors, Frits van Tol, Joop van Stigt and Leo Verhoef for their support and guidance during this study. I would also like to express my gratitude to my Noord/Zuidlijn colleagues, in particular to Jacco Haasnoot, Harro van Ree, Marc Everaars and Luuk Achterbosch, who assisted me during the analysis of the test results, while Frank Kaalberg's support in creating optimal working conditions was greatly valued. My appreciation also extends to my friends Paul Rebel, Erwin Bijlhouwer and Martin de Kant and my colleagues at Ingenieursbureau Amsterdam for their encouragement and interest during the study. The efforts of Lorraine van Dam and Susan Gourvenec in reading the thesis and making very useful suggestions for improving the quality of the English language are also gratefully acknowledged.

My special gratitude goes out to Holger Netzel, who has been my roommate and friend throughout the research period. Without his companionship and the discussions, reflections and many laughs we shared, this study would have been twice as hard to complete.

Finally, I would like to thank my parents, Hilda, my family and my friends. Without their constant love, support and, above all, patience it would not have been possible for me to complete this thesis.

Almer van der Stoel

*Twee regels voor succes:
1) vertel nooit alles wat je weet
(Roger J. Lincoln)*

ABSTRACT

The aim of this research was to examine the use of grouting methods for *pile foundation improvement*, a generic term that is used here to define both foundation renovation (increasing the bearing capacity of a pile foundation that has insufficient bearing capacity) and foundation protection (safeguarding the piles of the foundation against possible damage resulting from underground construction activities in the vicinity). First some definitions and standards relating to pile foundations are outlined after which a short account of pile foundation history is given. Subsequently the causes and detection of foundation damage and possible methods for foundation renovation are explained. One of these methods, foundation improvement by means of grouting techniques, can usually be executed from outside the structure and therefore the need to shore up the structure is avoided. However this application did raise questions regarding the response of the foundation piles to the installation process and to the grouting process, thus it was considered necessary to conduct further research. A full-scale test, of which the general set-up and consistency check are outlined in the thesis, was conducted in Amsterdam. By using the pile displacements, soil stresses, pore pressures and pile bearing capacity measured in this test it was possible to examine the influence of grouting methods on pile foundations.

The main part of the thesis focuses on permeation grouting, jet grouting and compaction grouting. For each method, first some more general aspects like history, grouting equipment, grouting parameters and fields of application are outlined. Subsequently existing theories used in modelling the grouting process are examined and compared. It could be generally concluded that all the techniques, and especially jet grouting, are so complex that modelling serves only to increase understanding of the process. The existing models are not designed for use in engineering practice.

There are many similarities between the processes of installing the permeation grouting TAMs or compaction grouting tubes and of drilling the jet grouting monitor to depth. From the tests it was concluded that in most cases significant pile displacements caused by installation effects occur only when the minimum distance between the TAM/tube/monitor and a wooden pile is less than 0.5 m.

Permeation groutability tests were conducted. These showed that the known applicability limits for permeation grouting using a silica gel, are fairly correct for the Amsterdam situation. The influence of grouting on pile displacements, total stresses and pore water pressures during the actual grouting process is insignificant, which confirms the non-disturbing character of the grouting process when properly conducted. The bearing capacity and stiffness of the piles can be considerably increased by the use of this method.

When jet grouting for foundation protection, the pile settlement during the jetting stage remained limited to 2 mm for each column, regardless of the distance between the pile and the jet grouted column and the diameter of the column. Neither the bearing capacity nor the stiffness of the wooden piles was negatively influenced. When jet grouting for foundation renovation, the pile displacements increased exponentially, especially when grouting just below pile toe level. After grouting the extended concrete piles showed almost exclusively elastic deformations and showed no sign of reaching their ultimate bearing capacity. From the samples obtained from the jet grouting columns, it was deduced that although satisfactory

ABSTRACT

strength and stiffness parameters had been achieved, the variation coefficients of the grout parameters were high. Some empirical relations have been derived from the test results.

During the test, compaction grouting subsequently caused the soil and piles to heave (caused by the large volumes of grout that are injected) and to settle (as a result of consolidation). Generally the measurement points closest to the injection point showed the largest displacement and excess pore pressures. When the excess pore pressures had dissipated the settling of the piles ceased. The bearing capacity could be considerably increased, which agreed with the calculations of the compaction ratio.

The use of and suitability of geophysical verification methods for grouting, which were necessary to determine the shape and position of grouted elements, were also considered. On the whole, the results of electrical resistance measurement seem to be in accordance with the actual geometry of the grouted elements. The use of Bore Hole Radar measurements in permeation grouting applications is not considered feasible. Verification by using BHR measurements in jet grouting columns showed that they usually underestimate the actual column diameter.

To determine how grouting methods can best be applied for foundation renovation purposes, the cost of grouting methods and the hindrance that they cause have been compared with those of conventional foundation renovation methods. The construction cost of grouting can be up to about 50% lower than that of conventional methods of underpinning a structure. Taking cost, hindrance and the test results into consideration, it can be concluded that permeation grouting and compaction grouting are economic and effective alternatives to conventional underpinning methods for renovating pile foundations. The methods may also be used for pile foundation protection. Jet grouting is only suitable for use in the renovation of end bearing piles when the structure is strong and stiff enough to redistribute the loads from the grouted pile. Jet grouting is very suitable for use in protecting pile foundations because it can be applied in any type of soil.

The future perspective regarding jet grouting is that until a database containing the relation between the input and output parameters is available, trial columns should be constructed before the actual project is started. Because of the wide scatter that is generally found when analysing strength and stiffness parameters, adequate risk assessments should be made or material factors of 2 to 3 should be used. In addition, because of the risk of blowouts, the significance of careful monitoring of the jet grouting process is emphasised. To counteract this risk, the spoil return flow and the pressure at the monitor should be constantly monitored.

The most important recommendations on compaction grouting are that the volume of the grouted element should be carefully controlled and that it is necessary to ensure that the installation procedure is accurate.

TABLE OF CONTENTS

ACKNOWLEDGEMENTS..... VII

ABSTRACT..... VIII

TABLE OF CONTENTS XI

CHAPTER 1 INTRODUCTION 1

1.1 Scope.....1
 1.2 Aim of the Research2
 1.3 Short Outline of the Thesis.....2

CHAPTER 2 CAUSES, DETECTION & RENOVATION OF PILE FOUNDATION DAMAGE..... 3

2.1 Introduction3
 2.1.1 Scope3
 2.1.2 Resume of Amsterdam Pile Foundation History.....3
 2.1.3 Dutch Pile Foundations5
 2.2 Pile Foundation Design5
 2.2.1 Definitions5
 2.2.2 Pile Bearing Capacity Calculations6
 2.3 Causes of Pile Foundation Damage.....7
 2.3.1 Introduction7
 2.3.2 Scope of the Research.....8
 2.3.3 Inadequate Design or Poor Workmanship during Construction8
 2.3.4 External Causes9
 2.3.5 Concluding Remarks11
 2.4 Detection of Foundation Damage11
 2.4.1 Introduction11
 2.4.2 Damage Detection Methods.....11
 2.4.3 Concluding Remarks12
 2.5 Foundation Improvement13
 2.6 Conventional Underpinning13
 2.6.1 Introduction13
 2.6.2 Pile Types15
 2.6.3 Examples of Foundation Renovation.....15
 2.7 Grouting Techniques16
 2.7.1 Introduction16
 2.7.2 Grouting Techniques17
 2.7.3 Examples of Foundation Renovation.....18
 2.7.4 Examples of Foundation Protection.....19
 2.8 Concluding Remarks19

CHAPTER 3 TEST SET-UP & CONSISTENCY CHECK.....21

3.1 Introduction21

3.2 Aim of the Test22

3.3 Stages of the Test22

3.4 Associated Full Scale Tests23

3.5 Soil and Groundwater Characteristics24

3.6 Pile Foundation and Construction25

3.7 Monitoring Equipment28

3.8 Data Acquisition and Processing29

3.9 Consistency Check of the Monitoring Data30

 3.9.1 General30

 3.9.2 Explanation of the Graphs30

 3.9.3 Consistency of Pile Displacement Measurements31

 3.9.4 Consistency of SMS en Piezometer Measurements32

 3.9.5 Influence of Pile Load Fluctuation32

 3.9.6 Irregularities33

 3.9.7 TAM Installation34

3.10 Reference Load Tests on Piles35

 3.10.1 Introduction35

 3.10.2 Determination of the Theoretical Bearing Capacity of Piles35

 3.10.3 Determining the Ultimate Bearing Capacity by Pile Load Tests35

 3.10.4 Observed Differences in Ultimate Bearing Capacity of the Wooden Piles36

3.11 Conclusions and Recommendations38

CHAPTER 4 PERMEATION GROUTING39

4.1 Introduction39

4.2 Permeation Grouting Technique39

 4.2.1 History39

 4.2.2 Grouting Equipment40

 4.2.3 Grout Types41

 4.2.4 Field of Application: Groutability44

 4.2.5 Grouting Pressure47

 4.2.6 Grouting Pattern47

4.3 Modelling Permeation Grouting47

 4.3.1 General47

 4.3.2 Empirical Modelling48

 4.3.3 Analytical Modelling48

 4.3.4 Model Applied to the Amsterdam Situation50

 4.3.5 Conclusions50

4.4 Literature References on Grout Strength52

4.5 Amsterdam Groutability Tests53

 4.5.1 General53

 4.5.2 Injection Pressure and Flow54

 4.5.3 Strength of the Samples55

 4.5.4 Geophysical Verification of the Dimensions of the Grouted Elements56

 4.5.5 Conclusions57

4.6 Detailed Set-up of Stage 3a57

 4.6.1 General57

 4.6.2 Piles and Monitoring Equipment59

 4.6.3 TAMs and Grout Elements59

TABLE OF CONTENTS

4.7	Results of TAM Installation Test	61
4.7.1	General	61
4.7.2	Pile Displacement	61
4.7.3	Correlation of Pile Displacement - Minimum Distance between TAM & Pile.....	63
4.7.4	Pore Water Pressures & Effective Stress	64
4.8	Results of Permeation Grouting Test	65
4.8.1	Pile Displacement	65
4.8.2	Pore Water Pressure & Effective Stress	65
4.8.3	Bearing Capacity	66
4.9	Conclusions and Recommendations	67

CHAPTER 5 JET GROUTING..... **69**

5.1	Introduction	69
5.2	Jet Grouting Process	70
5.2.1	History	70
5.2.2	Definitions, Process and Equipment	70
5.2.3	Jet Grouting Elements	74
5.2.4	Jet Grouting Structures	74
5.2.5	Field of Application	75
5.2.6	Grout Strength	75
5.2.7	Jet Grouting Parameters	76
5.2.8	Horizontal Position of the Jet Grouted Column	77
5.3	Assessing the Influence of Jet Grouting on Pile Foundations	78
5.3.1	Introduction	78
5.3.2	Assessing the Jet Grouting Process	78
5.3.3	Modelling Jet Grouting	79
5.3.4	Conclusions	82
5.4	Details of Jet Grouting Test Set-up	82
5.4.1	General	82
5.4.2	Piles	85
5.4.3	Jet Grouted Columns	85
5.4.4	Monitoring Equipment	86
5.5	Jet Grouting Process Parameters	87
5.6	Grout Quality	87
5.6.1	General	87
5.6.2	Unconfined Compressive Strength	89
5.6.3	Tensile Strength	92
5.6.4	Young's Modulus	92
5.6.5	Shear Strength	94
5.6.6	Relations between Grout and Spoil Parameters	96
5.6.7	Conclusions	97
5.7	Jet Grouting for Foundation Protection	98
5.7.1	Pile Displacement	98
5.7.2	Pore Water Pressure	100
5.7.3	Total Stress and Effective Stress	103
5.7.4	Soil Movement	104
5.7.5	Bearing Capacity	106
5.7.6	Conclusions on Jet Grouting for Foundation Protection	107
5.8	Results of Jet Grouting for Foundation Renovation	107
5.8.1	Pile Displacement	107
5.8.2	Total Stress, Pore Water Pressure and Effective Stress	111
5.8.3	Soil Movement	113

TABLE OF CONTENTS

5.8.4	Bearing Capacity	113
5.8.5	Conclusions on Jet Grouting for Foundation Renovation.....	115
5.9	Correlation Pile Displacement - Distance.....	116
5.10	Influence of Jet Grouting on CPT.....	117
5.11	Diameter Determination by Excavation.....	118
5.12	Conclusions on Jet Grouting for Pile Foundation Improvement	120
5.13	Recommendations and Future Perspectives	122

CHAPTER 6 COMPACTION GROUTING.....123

6.1	Introduction.....	123
6.2	Compaction Grouting Technique	123
6.2.1	History.....	123
6.2.2	Compaction Grout	124
6.2.3	Grouting Equipment	125
6.2.4	Grouting Pressure and Pumping Rate.....	125
6.3	Field of Application	126
6.4	Modelling Compaction Grouting	128
6.4.1	Compaction Grouting Models	128
6.4.2	Modelling Compaction Grouting in Amsterdam	130
6.5	Detailed Test Set-up	135
6.5.1	General	135
6.5.2	Piles and Monitoring Equipment.....	135
6.5.3	Grout Composition	137
6.5.4	Compaction Grouting Wooden Piles in the 1 st Sand Layer	137
6.5.5	Grouting the Elements.....	137
6.6	Results of Tube Installation.....	140
6.7	Results of Compaction Grouting.....	141
6.7.1	Introduction	141
6.7.2	Pile Displacement.....	141
6.7.3	Surface Displacements.....	144
6.7.4	Pore Water Pressure & Total Stress.....	146
6.7.5	CPTs.....	149
6.7.6	Bearing Capacity	150
6.8	Conclusions	151
6.9	Recommendations and Future Perspective.....	152

CHAPTER 7 GROUTING VERIFICATION METHODS.....153

7.1	Introduction.....	153
7.2	Determining the Position of a Grouted Element.....	153
7.3	Determining the Geometry of a Grouted Element	154
7.4	Results of the Full Scale Injection Test.....	155
7.4.1	General	155
7.4.2	Stage 1: Determining Suitable Geophysical Detection Methods	155
7.4.3	Stage 2: Measuring the Geometry of Permeation Grouting Bodies	156
7.4.4	Stage 3: Measuring the Geometry of Jet Grouted Columns.....	157
7.5	Conclusions	162
7.6	Future Perspective.....	162

CHAPTER 8	SUITABILITY OF GROUTING FOR FOUNDATION IMPROVEMENT.....	163
8.1	Introduction.....	163
8.2	Considerations Regarding the Influence of the Test Set-Up.....	163
8.3	Using Permeation Grouting for Foundation Improvement.....	164
8.4	Using Jet Grouting for Foundation Improvement.....	166
8.5	Using Compaction Grouting for Foundation Improvement.....	167
8.6	Economic Feasibility of Grouting for Foundation Improvement.....	168
8.7	Conclusions.....	169
CHAPTER 9	CONCLUSIONS & FUTURE PERSPECTIVE.....	171
9.1	General.....	171
9.2	Conclusions.....	171
9.3	Future Perspective.....	173
LITERATURE REFERENCES	175
APPENDICES	181
DUTCH ABSTRACT / SAMENVATTING	213
CURRICULUM VITAE	217

APPENDICES

APPENDIX I GROUTING VOCABULARY.....	183
APPENDIX II CHARACTERISTIC SOIL PARAMETERS.....	186
APPENDIX III INSTALLATION TIMES PERMEATION GROUTING.....	186
APPENDIX IV CHRONOLOGICAL SEQUENCE OF THE BALLAST FRAME CONSTRUCTION.....	187
APPENDIX V DATE OF JET GROUTING ACTIVITIES.....	188
APPENDIX VI MONITORING EQUIPMENT.....	189
APPENDIX VII RESULTS OF LOAD TESTS 1 AND 2.....	192
APPENDIX VIII PILE LOAD TESTS BEFORE AND AFTER PERMEATION GROUTING.....	194
APPENDIX IX PILE LOAD TESTS BEFORE AND AFTER JET GROUTING.....	199
APPENDIX X PILE LOAD TESTS BEFORE AND AFTER COMPACTION GROUTING.....	203
APPENDIX XI DISTANCES BETWEEN PILES AND TAMS.....	205
APPENDIX XII SCATTER PLOTS MINIMAL DISTANCE TAM/PILE VERSUS PILE DISPLACEMENT.....	206
APPENDIX XIII LIST OF FIGURES AND TABLES.....	207

Chapter 1 INTRODUCTION

1.1 Scope

All buildings, from individual houses to major civil engineering structures, are constructed on foundations. To properly transfer the loads from the structure to the soil the foundations must be strong, rigid and stable. This means that the foundations must ensure that unacceptable deformation, that might possibly even lead to the collapse of the structure, does not occur.

Until the mid 20th century, architects, engineers and contractors tended to pay insufficient attention to or have inadequate knowledge about proper dimensioning of the foundations of structures. Regretfully, this has frequently resulted in inadequate foundations, some of which were intended to support buildings of major historic significance. In Figure 1.1 three typical examples of late 19th century Amsterdam buildings that have had, or still have, foundation problems are shown. From left to right these are Amsterdam Central Station (built from 1882 to 1889), the Beurs van Berlage (Berlage Exchange; built from 1898 to 1903) and the Amsterdam Royal Concert Hall (built from 1883-1886). Figure 1.2 shows an example of the facades of Amsterdam canal-side houses on the Herengracht, some of which have undergone foundation renovation.



Figure 1.1 Amsterdam Central Station, Beurs van Berlage and Amsterdam Royal Concert Hall (l→r)

During the last 50 years, people have become increasingly aware of the importance of making comprehensive and meticulous designs for foundations. This growing awareness was accompanied by recognition of the necessity to repair, renovate or replace existing foundations that do not meet the current criteria relating to strength, stiffness and stability. The result has been the development of a variety of methods for foundation renovation. This thesis focuses on one of the relatively newest methods: pile foundation renovation using grouting. In the next section the aim of the research will be defined, while the subsequent section gives a brief outline of the thesis.



Figure 1.2 Amsterdam Mansions (Herengracht 174-150; Philips, 1769)

1.2 Aim of the Research

There are a great variety of foundation problems that may lead to deterioration of foundations and the subsequent need for foundation restoration. The specific foundation problems to which this research applies are described below.

Historically, a variety of causes have led to too small bearing capacities in pile foundations. In many cases, this reduction has led to an ongoing, even settlement process, which has not usually caused any problems. In some cases however, the differential settlement are such that measures have to be taken to combat their effects. Moreover, in the event of later underground construction in the vicinity, the bearing capacity of the pile foundations of nearby structures can be negatively influenced, which calls for similar measures. The measures that have to be taken generally involve restoring the bearing capacity of the foundation. Up till now this has usually been done by the placement of additional foundation piles. Because this conventional foundation renovation method has to be executed from inside the structure, it may cause significant hindrance and economic damage. Moreover, the cost of these techniques is so considerable that it is desirable to develop alternative methods that cause less hindrance and are more cost effective.

The aim of this research is to examine the use of grouting methods for pile foundation improvement, a generic term that is used here to define both the renovation and protection of pile foundations. These relatively new foundation renovation methods have the major advantage that they can generally be applied from outside the structure, and will therefore cause significantly less hindrance and economic damage. The next section outlines how the above subjects have been considered in this thesis.

1.3 Short Outline of the Thesis

In Chapter 2, first some definitions and standards relating to pile foundations are outlined. A short outline of the history of pile foundation is also given. Subsequently the causes and detection of foundation damage and possible methods for foundation renovation are explained. The chapter concludes with an outline of how permeation grouting, jet grouting and compaction grouting could be effective foundation renovation methods.

Chapter 3 deals with the general set-up and an assessment of the consistency of the results of a full-scale test that was conducted in Amsterdam to examine the influence of grouting methods on pile foundations.

In Chapters 4, 5 and 6, respectively, permeation grouting, jet grouting and compaction grouting are considered. For each method first some more general aspects like history, grouting equipment, grouting parameters, field of application and modelling are outlined. Subsequently these chapters focus on the full-scale test, by describing a detailed test set-up and focusing on the test results. At the end of each chapter guidelines are given for the application of grouting close to pile foundations.

The use of and suitability of geophysical verification methods for grouting, which is necessary to determine the shape and position of grouted elements, is explained in Chapter 7.

In Chapter 8 the results of the previous chapters are examined to determine how grouting methods can best be applied for foundation renovation purposes. Moreover, in this chapter both the cost of grouting methods and the hindrance that they cause will be compared with those of conventional foundation renovation methods.

Finally, Chapter 9 summarises the main conclusions that have been drawn from this study. In this chapter the most important recommendations for the application of grouting methods for foundation improvement are also given.

Chapter 2 CAUSES, DETECTION & RENOVATION OF PILE FOUNDATION DAMAGE

2.1 Introduction

2.1.1 Scope

Pile foundation improvement is a generic term that is used here to define both the renovation and protection of pile foundations. Before the subject of grouting for pile foundation improvement can be thoroughly examined, it is necessary to increase the understanding of pile foundations. Therefore, to start with, in the first section of this chapter an outline is given of pile foundation history. Consequently, in the next section pile foundation definitions and design, with an emphasis on Dutch pile foundations, are outlined. Section 2.3 deals with the causes of foundation damage and more specifically for which type of foundation damage grouting for pile foundation improvement will be examined. Damage detection, which facilitates the determination of whether or not the cause of the damage falls within the scope of this research project, is outlined in Section 2.4.

After explaining the concept of foundation improvement in 2.5, Section 2.6 focuses on structural improvement of the foundation. The improvement of the impermeability of the foundation to humidity and groundwater is beyond the scope of this study. In conclusion, in Section 2.7 the possibilities of using grouting techniques for foundation improvement are outlined.

2.1.2 Resume of Amsterdam Pile Foundation History

Most of the developments described in this sub-section are specific to the Amsterdam situation and are merely illustrative of Dutch Pile foundation History. The developments in other major cities in the western part of the Netherlands (for instance in Rotterdam, Haarlem and The Hague) show similar developments.

One of the earliest uses of wooden piles *in Dutch* ground is found beneath a late Roman bridge over the River Maas at Cuick (Verhoef, 1999). From dendrological investigations it appears that this bridge was built in the period of 330-350 AD. The rectangular oak piles were fitted with wrought iron points to facilitate the piling work. A framework of wooden beams was laid on the piles, on top of which the masonry was laid.

The first houses built in Amsterdam, in the *12th century*, were very light constructions of timber without foundations*. Because of the soft peat layers found in Amsterdam, the houses there suffered from damage due to settlement.

In the *13th century*, castles and churches were increasingly built of bricks, which made it necessary to provide support for bigger loads. Under the wall of the construction a trench was dug, and this was filled on either side by alder faggots†. Between the faggots small wooden piles were driven (by hand) on which another series of faggots was put. On top of this construction, were placed oak slabs on which the bricks were then laid. From that moment on, a problem was caused by the decay of wooden foundation elements in the humid soil.

In *1503* a law was introduced forbidding building foundations on public streets without permission of the Building Inspection (to keep the fronts of the buildings in a straight line). In *1528* a law requiring permission from the local authorities for all building activities replaced this law. In this period developments started which led to the use of the type of foundation that can be considered the mother of the current "typical" Dutch pile foundation. The piles used in this period were shaft-bearing piles about 5 to 7 meters long. The mostly pine piles were driven between oak beams, which were placed on either

* The folk stories claiming some buildings were built on animal skin has not proven to be correct (Van Tol, 1982)

† *In Dutch: takkenbos*

sides of a trench, after which other oak beams were laid across at regular spaces: the so called “cross beam” pile foundation (Figure 2.1).



Figure 2.1 Early Cross Beam Pile Foundation (Bureau Monumentenzorg Amsterdam)

In the 17th century the “cross beam” pile foundation was still used, with the difference that the piles were now driven until reaching the sand layer. This was called driving “on stop” or in Dutch “op stuit”. This pile driving required a gigantic effort of up to 40 men lifting the heavy ram that was used to drive the piles. To keep the piles in a vertical position, a special frame, as shown in Figure 2.2, was used. Because of the effort required to move the frame, this was often done inadequately which led to some piles being driven out of true.

In 1638 it was ordained that all foundation wood should be at least half a foot below the groundwater table reduced problems caused by decay of the foundation wood. To get an impression of the way houses were built in the 17th century, in Figure 2.3 a schematic representation is given of building a typical Amsterdam house in a street bordering the canal.



Figure 2.2 Pile Driving in the 17th Century



Figure 2.3 Building a Typical Amsterdam Canal-Side House

In the 19th century, some specific problems arose with very special buildings. At Amsterdam Central Station, built in 1886, the absence of the bearing sand layer due to erosion by of the river IJ caused many problems. The same problem arose at the Berlage Exchange (see Figure 1.1).

In the 20th century there was a big development in pile driving equipment, for example the use of diesel hammers, making it possible to drive piles deeper and build bigger and higher structures. Since the nineteen-fifties, concrete piles driven to the 2nd sand layer at about 20 meters deep have almost exclusively been used. Recently, some major high-rise structures have been constructed using pile foundations extending to the 3rd sand layer, at a depth of 60 meters.

2.1.3 Dutch Pile Foundations

In the Netherlands two different types of wooden pile foundations are used. The principle difference between the two types, the *Amsterdam* and the *Rotterdam* pile foundation, is found in the number of pile rows. The Amsterdam pile foundation consists of piles driven in pairs on top of which a crossbeam is placed. The foundation plates are laid on the crossbeam. The Rotterdam pile consists of one row of driven piles and no crossbeam is used (see Figure 2.4).

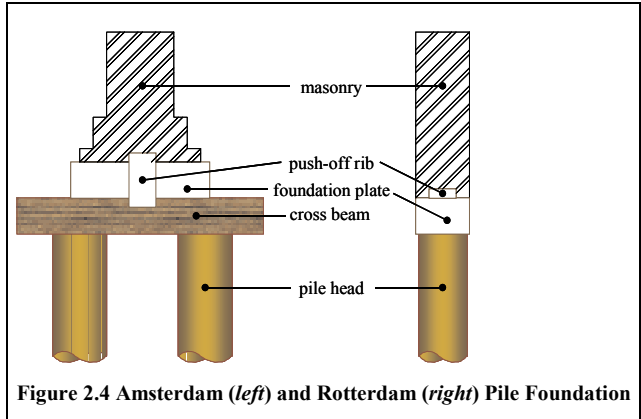


Figure 2.4 Amsterdam (left) and Rotterdam (right) Pile Foundation

2.2 Pile Foundation Design

2.2.1 Definitions

The focus in this sub-section is on wooden pile foundations, because the problem of an insignificant bearing capacity is found relatively often in this foundation type. Because this thesis deals with improving the bearing capacity of pile foundations, it is important to specifically understand which foundations elements are considered to be pile foundations. Here the definition of a pile foundation as described by Dutch Standard *NEN6743* (Geotechnics, Calculation method for bearing capacity of pile foundations, Compression Piles) is used. This standard states that a *pile* is a foundation element the length of which is at least 5 times the smallest cross section of its foot. The *pile foot* is described as the geometrical form of the broadened lower part of the pile, the *pile toe* as the lowest full cross section of the pile foot and the *pile shaft* as the outline of the pile between the pile foot and the pile head. The installation method of a pile greatly affects its bearing capacity. Three installation methods are distinguished:

1. Driving the pile using a drop hammer (dynamic).
2. Pushing (and screwing) the pile using dead weight (static).
3. In-situ pile construction.

The majority of Dutch pile foundations are of the driven type. Static installation is mainly used for foundation renovation purposes and working in restricted height. In-situ piles are more commonly used for large civil engineering structures.

When the pile settles relatively more than the soil surrounding it, it will experience *positive skin friction*. When some or all of the soil along the shaft of the pile moves downward relative to the pile, it will drag the pile down. This phenomenon of shaft resistance acting downward on the pile is called *negative skin friction*. There are two classic situations in which this phenomenon can occur (Lambe & Whitman, 1979). The first and most common situation is that in which the pile is driven through the profile consisting of fill, soft soil and firm soil. The fill causes the soft soil to compress and thus the fill and most of the soft soil move downward and drag on the pile. The second situation can arise when fill is placed around a pile already driven through the soft soil in the firm soil. To fully develop the negative skin friction only 20 to 30 mm downward displacement of the soil surrounding pile shaft is necessary. Therefore it is essential to include negative skin friction as part of the design load of the piles (Van Weele, 1964).

If a pile derives most of its support from adhesion or friction along its shaft, it is called a *friction pile*. A pile that derives most of its support from its toe is called a *point- or end-bearing pile*. The deep

foundation layer in which the pile toes are driven and that is carrying most of the pile load is called the *bearing stratum*. The maximum bearing capacity of a pile is defined as the sum of the point resistance and the shaft resistance: $F_{max} = F_{point} + F_{positive\ skin\ friction} - F_{negative\ skin\ friction}$ (see Figure 2.5). The reversal point between positive skin friction and negative skin friction lies at a settlement rate of approximately 3 mm/year. If the settlement rate of the pile is 0 mm/year, the reversal point lies in the top of the bearing stratum. More information on pile bearing capacity calculations is given in the next sub-section.

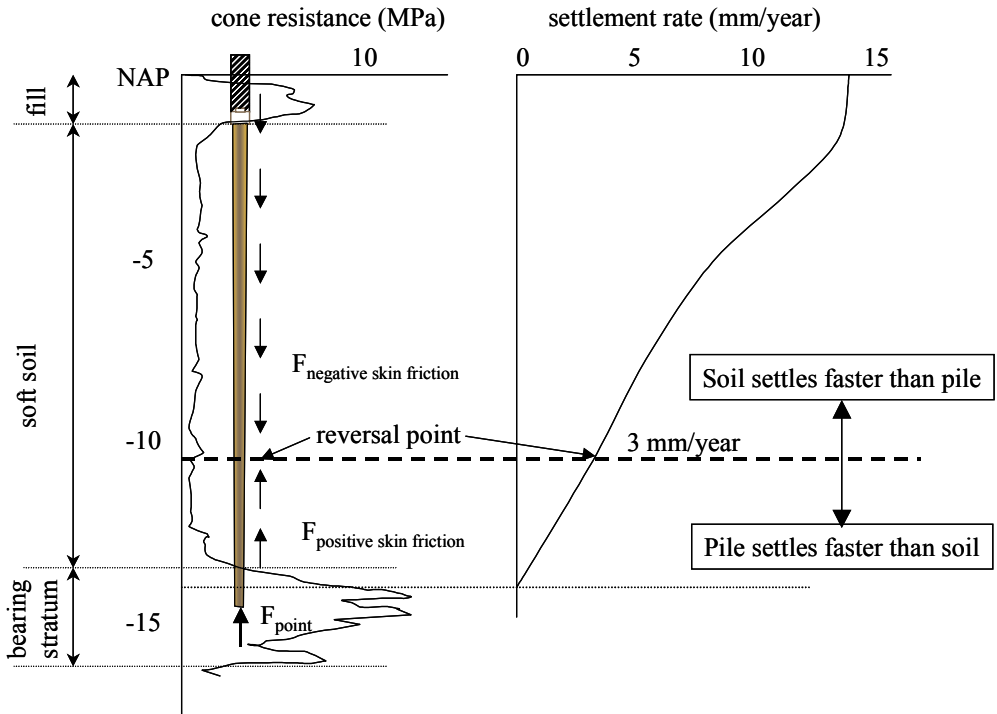


Figure 2.5 Point Resistance, Positive Skin Friction and Negative Skin Friction Graphically Explained (after Van Tol, 1996)

2.2.2 Pile Bearing Capacity Calculations

In the Netherlands there is a clear distinction between pile foundations that were designed and built up to 1940 and pile foundations that were designed and built afterwards.

Before 1940 test piles were used to dimension the pile foundation only for larger public buildings. For private building projects sometimes exploratory drilling was used to determine the soil profile, but usually pile lengths similar to those previously employed for adjacent structures were used. Up till 1945 almost exclusively wooden piles were used.

After 1945 many new types of pile were introduced, of which the driven prefabricated concrete pile is by far the most important. These displacement piles, like driven wooden piles, increase the density and the horizontal effective stresses, which significantly contribute to both friction and end-bearing capacity. Other concrete piles were created in situ using soil removing techniques (like bored cast-in-place piles and bored/continuous flight auger piles). To a certain extent these pile types reduce the effective soil stresses. This should be accounted for in the design.

Another important development was the introduction of the Dutch Cone Penetration Test (CPT), which was first only used to determine the position of the bearing stratum, but was later used as a “test pile”. This was a very economical method to investigate the soil and help calculate the pile bearing capacity.

Negative skin friction was not accounted for until 1950. From then on, it was integrated in the design, but its influence was still often underestimated. It was not until 1965 that in situ measurements of negative skin friction (Horvat, 1978; Van Weele, 1989) and practical tests to determine the effects of negative skin friction were conducted. This led to fundamental understanding of this phenomenon and made it possible to predict the negative skin friction more accurately. In 1975 the results of research on design rules for negative skin friction were published (SBR-47, 1975). Underestimating the effects of negative skin friction, however, remained a problem until the 1980s*.

Until the 1970's the Municipal Building and Housing Inspection Departments all had their own rules for the determination of the bearing capacity of a pile foundation. In the 1980's the Koppejan method for the determination of the bearing capacity of driven piles became commonly accepted and the CPT was normalized (1982). The developments for driven piles were finalized on October 1st 1992, when the standard for building-constructions: Loadings & Deformations[†] (NEN 6702) was introduced. An integral part of these regulations was formed by Dutch standard *NEN6743*. In this standard a method to calculate the bearing capacity of foundation piles, also known as the *4D-8D* or *Koppejan* method, is described. This method is based on using the results of the *Dutch Cone Penetration Test* and several empirically determined factors to calculate the pile toe and shaft resistance. When making an assessment of the quality of existing foundation piles, it should be noted that the safety factors required in these standards are too strict for existing foundations. The application of these standards would therefore result in the large-scale demolition of existing structures (Van Tol, 1982).

Other internationally used methods to calculate the bearing capacity of foundation piles are (Van Tol, 1994):

- the *analytical approach*, based on effective stresses, soil friction and pile area, which is used in many Anglo-Saxon countries;
- *load tests*, used in Germany and some other countries, which are costly and may give conflicting interpretation;
- an approach based on *dictated pile toe or shaft resistance*, which is based on local experience, of a conservative nature and therefore reliable;
- *SPT & Pressiometer method*, which is difficult to use to predict the bearing capacity of pile foundations because the relation between soil stiffness and strength is not unambiguous.

Van Tol (1994) concludes that in general foreign design methods are qualitatively less reliable than the Dutch method, which should be compensated by using larger safety factors to obtain an equally reliable pile foundation. This results in economically less sound pile foundations. Inadequate foundation design is one of the main causes of pile foundation damage, which will be dealt with in the next section.

2.3 Causes of Pile Foundation Damage

2.3.1 Introduction

Damage inflicted on structures due to pile foundation problems may be attributed to several causes. The damage often occurs when the structure is subjected to differential displacements. Too often, much effort is put into restoring the damage caused by these differential displacements, without first thoroughly investigating the problems that caused the damage, although understanding the causes of pile foundation damage certainly helps to solve the problem.

To facilitate investigation of pile foundation damage, an effort has been made by Van der Stoel (2001b) to combine different sources, link them and give a complete overview of causes of pile foundation damage. The results of these investigations can be used to determine the cause(s) of pile foundation damage and as an aid to the prevention of pile foundation damage when designing new projects. Here a short resume is given and the results are used to indicate the scope of the research and for which type of foundation damage foundation improvement by grouting will be examined

* Van Tol (1994) gives an example where, in the late 1980s, 7 different foundation consultants were asked to calculate the negative skin friction; the results considerably differed (variation coefficient of 0.18)

[†] in Dutch: Technische Grondslagen voor Bouwconstructies: belastingen en vervormingen (TGB 1990)

2.3.2 Scope of the Research

A pile foundation is considered to malfunction when it has reached either its Ultimate Limit State (ULS) or Serviceability Limit State (SLS). Usually, the SLS is the criterion considered normative for malfunctioning. A distinction can be made between failure of a pile foundation resulting from three primary processes (see overview in Figure 2.6):

1. inadequate/exceeded pile bearing capacity;
2. settlement of the bearing stratum or layers underneath this;
3. degradation of pile foundation material.

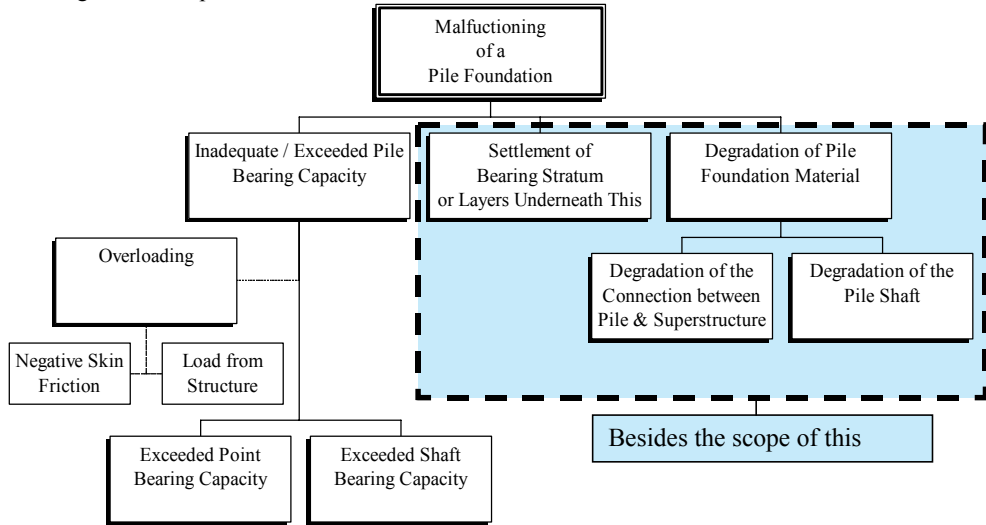


Figure 2.6 Mechanical Processes of Pile Foundation Degradation

The degradation of pile foundation materials can be caused decay of wooden piles as a result of lowering the groundwater table (by artificial water abstractions for drinking water/a porous sewer or by natural water abstraction by big trees or similar vegetation with deep roots). Other causes of degradation are decay of wooden piles below the groundwater table by caused fungi or bacteria and the corrosion of steel piles. This type of damage lies besides the scope of this thesis.

Settlement of the bearing stratum or the layers underneath a pile foundation may be caused by for instance mining activities, biological decay of organic material in the soil, shrinking by drying of clayey soils, creep or consolidation. This type of damage is also beyond the scope of this thesis.

This study is limited to finding foundation improvement solutions for piles with an inadequate or exceeded pile bearing capacity. A distinction is made between causes relating to an inadequate design and/or poor workmanship during construction of the pile foundation and external causes. In the next two subsections these topics will be briefly outlined.

2.3.3 Inadequate Design or Poor Workmanship during Construction

In this sub-section the most important causes related to inadequate design or poor workmanship during construction are summarized.

The most significant historical pile foundation design problems that occurred in the Netherlands, concern not accounting for negative skin friction. As was already outlined in Section 2.2.2, these problems ceased to occur in the 1970's. Another important issue that has caused many problems concerns the omission of the determination of appropriate and reliable geotechnical parameters. Until the 1940's, overestimation of the bearing capacity of the soil was a problem. Even till now, problems

may occur because local discontinuities or non-homogeneity of the soil are not discovered. Some less familiar causes related to inadequate design are:

- inaccurate distribution of the loads over the pile foundation elements or inaccurate positioning of the pile foundation elements under the structure (which has the same consequences); for instance, wooden piles may break at some depth owing to excessive loads (Hoekstra, 1974);
- not taking into account the movements induced or prevented by adjacent structures.

Typical examples of poor workmanship concern the use of piles with an unsuitable diameter, piles made of inadequate material or piles that are damaged during transportation or during installation:

- different material properties of adjoining piles will lead to varying stiffness of the piles, which may result in differential settlement;
- when the diameter of cast-in-place piles deviates from the prescribed diameter due to bulging at the bottom, or constrictions in the top of the pile, the bearing capacity of the foundation will differ; Van Weele & Lencioni (1999) reported extensively on the consequences concerning the pile shaft resistance;
- concrete piles may break owing to pile driving operations;
- use of an inaccurately positioned or wrong elongation piece on a wooden pile;
- missing piles or piles that are too short (before the 20th century).

2.3.4 External Causes

Due to a wide variety of construction activities, which are gathered here under the generic term external causes, changes in soil stresses and soil displacement may occur. These changes may affect the bearing capacity of pile foundations and lead to pile displacements. The most important examples of foundation damage related to external causes are summarized here.

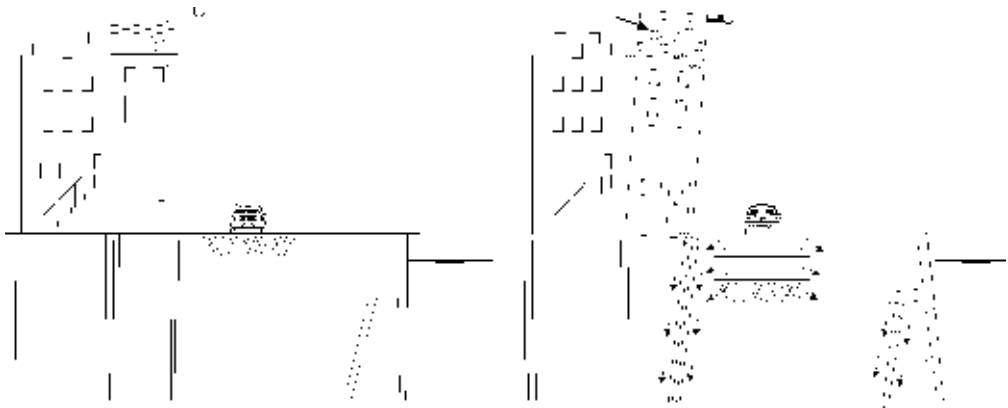


Figure 2.7 Schematic Representation of the Effect of an Embankment

Embankments

A good example of damage caused by embankments is found in city centres, where the roads are located next to the foundation piles (see Figure 2.7). When the road has been elevated many times since the pile foundation was built, this generates additional negative friction on the piles. Because the piles under the front (facade) of the building near the road consequently suffer from higher negative skin friction, these piles settle more than the piles in the back.

Excavations

Excavations that temporarily or permanently remove support from the soil can cause both horizontal and vertical displacements and, in an extreme situation, even instability. Examples are building pits and shafts. In particular deep excavations, like building pits for metro stations, can result in large horizontal movements of the soil adjoining the D-Walls and consequently of the piles in adjoining foundation layers. Boscardin and Cording (1989) reported extensively on building response to excavation-induced settlement. Clough and O'Rourke (1990) report specifically on construction induced movements of in-situ walls. Van Tol (1996) gives an overview for excavations for specific Dutch conditions. A special category of excavations is formed by creating foundation elements like flight auger piles and D-walls. For extensive tests on excavating D-Wall panels located next to pile foundations a reference to De Wit et al (1999) is made.

Tunnelling

A special type of foundation damage due to excavations is caused by tunnelling using a Tunnel Boring Machine (TBM shown in Figure 2.8), the New Austrian Tunnelling Method (NATM) or Micro

Tunnelling. TBM tunnelling (large diameters) and micro tunnelling can cause heave or settlement. When these techniques are used to create tunnels or other structures under existing structures, and the process is not properly monitored and performed, damage may occur. Peck (1969) has been breaking new ground on deep excavations and tunnelling in soft ground, and Sagaseta (1987) has given a fundamental analysis of undrained soil deformation due to ground loss. New and O'Reilly (1991) and Mair, Taylor & Burland (1996) reported on predicting the magnitude and effects of tunnelling-induced ground movement. Mair et al (1993) specifically reported on subsurface settlement profiles above tunnels in clay. For an extensive review of soft ground tunnelling and buried structures a reference to Fujita (1994) is made. Netzel & Kaalberg (1999, 2000) and Standing (1999) report on numerical damage risk assessment and the use of GIS applications for settlement risk management for tunnelling projects.

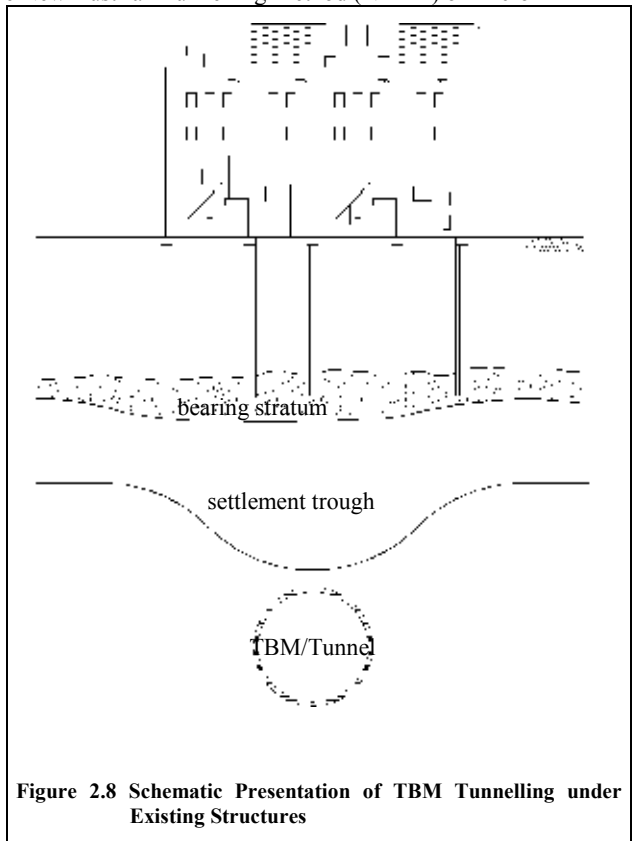


Figure 2.8 Schematic Presentation of TBM Tunnelling under Existing Structures

Other Causes

Other external causes of foundation damage, which are not extensively dealt with here, are:

- settlements due to densification caused by traffic vibrations (Engel, 1975) or earthquakes;
- water abstractions (which may cause both decay of foundation wood or additional negative skin friction);
- structures that are subjected to high temperature changes, which may cause unacceptable differential displacements between the superstructure and the foundation;

- changes in the structure like the construction of additional floors, attics, subsidiary buildings (annexes) or function changes, which may all cause an extra load on the existing pile foundation.

2.3.5 Concluding Remarks

Since there are many possible reasons for the degradation of a pile foundation, it can be very difficult to determine which of these is the principal one. The goal should therefore be to carefully examine all possibilities and then find the sources of the most serious damage. To save valuable restoration resources, it is important to determine as early as possible whether the cause of the damage lies with exceeding pile bearing capacity, with the pile foundation material degradation or with settlement of the bearing stratum or layers underneath, or possibly a combination of these.

2.4 Detection of Foundation Damage

2.4.1 Introduction

Before it is possible to decide if a foundation needs to be renovated, the cause and severity of the foundation damage must be detected. Detection of foundation damage is the most valuable technical tool in the process of determining whether or not to renovate a foundation. To facilitate the set-up of a program for the detection of pile foundation damage, an overview of detection methods has been given by Van der Stoel (2001b). In this section a summary is given. The reason for including this section is that it is necessary to detect the cause of the damage in order to assess whether strengthening by grouting is an option when an improperly functioning foundation has to be renovated .

2.4.2 Damage Detection Methods

Damage to foundations may be detected by using several methods in succession, these being:

1. general visual inspection of the superstructure;
2. desk studies;
3. accurate inspection.

The applicability of each method is largely dependent on the stage that has been reached by the detection process.

A **general visual inspection of the superstructure** is a quick, cheap and non-destructive method of examining the condition of a structure. It will not provide detailed information on the type of foundation and usually only provides limited information about the condition of the foundation.

A **desk study** is a non-destructive method of examining the condition of the foundation. Depending on the effort that has to be made in gaining information, it is fairly quick and reasonably inexpensive. It generally gives detailed information on the type of foundation and usually only limited direct information about its condition.

An **accurate inspection** of both the outside and inside of the structure and, if possible, the foundation elements, may reveal the true extent of the foundation problems. An accurate inspection can be performed by using:

- inspection of the façade (see Figure 2.9) using a *crack guide*; movement of the structure on both sides of the crack and the distortion pattern that historically occurred can give valuable information concerning the location of the malfunctioning foundation; Van Stigt et al. (1995) give a very practical crack guide, as also do Ter Linde (1990/1997) and Hunt et al. (1991); this method is fast and inexpensive;
- *Settlement measurements*, which can be performed over a period of time (not commonly available because measurements usually only start when the problem has already been detected) or by recording differential settlement at a specific moment (by levelling a window head, a layered joint or floors and walls); this method is usually very time consuming and moderately expensive but gives detailed information on the settlement behaviour of the foundation;
- creating an *inspection pit*, which can be used to determine if the pile itself is settling or if the superstructure is settling relative to the pile; the excavation is commonly combined with cutting

samples to gain additional information about the nature and condition of the foundation material and gives quick and moderately expensive results (Netzel & Kaalberg, 2001).

There are various approaches to determining the condition of the foundation. In publications by Van Tol & De Jong (1999), Van Stigt (1995), Hunt et al (1991), Van Tol (1982) and Burland et al (1977, 1996) several examples of these approaches are given. Here two principally different approaches are distinguished. One approach is to roughly calculate the load on the piles, determine the soil profile and dig an inspection pit. After this a pile load test is carried out on one or more piles. The results are interpreted by using a risk assessment resulting in the determination of a true safety factor for the foundation piles. With this method practical information is interpreted on a theoretical basis for a single point of the foundation. The other approach is based on assessing whether the structure has been able to withstand the differential displacements of the foundation, and this method is therefore purely practical. This implies that the strength and stiffness of the structure also play an important role in determining the state of the foundation. Often a combination of both approaches is used.

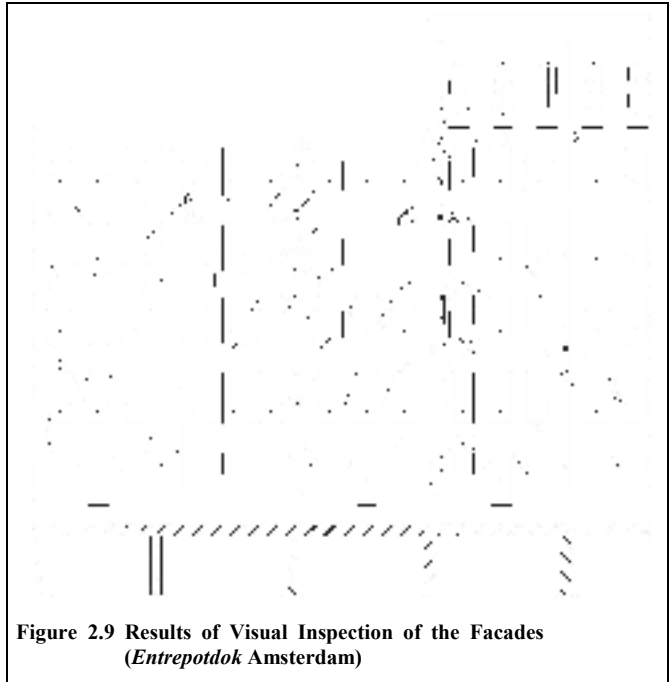


Figure 2.9 Results of Visual Inspection of the Facades (Entrepotdok Amsterdam)

2.4.3 Concluding Remarks

Often there is only limited time and funding available to conduct an investigation program. Therefore it is recommended that the program should be phased and that decision moments be built into it. In this way certain aspects can be advanced, postponed or omitted. Van der Stoel (2001b) has presented a flow chart that can be used in the process of determining whether renovation is needed and which detection methods should be used.

At the end of a complete investigation program, an inventory should be available, at least in broad outlines, including the foundation type, the causes of the damage, the condition of the foundation (damage type), the impact on the superstructure, the damage development in time and the influences on the surroundings. In addition to the very important expert opinion on the results of the foundation damage detection, a quantitative appreciation of the problem should be added to the investigation report. This should indicate the degree of foundation deterioration (x %), the remaining lifetime (y years) of the structure, a cost estimate of foundation restoration and a time schedule.

After determining the causes of foundation damage by using the appropriate damage detection methods, the next logical step is to determine how foundation improvement can be accomplished.

2.5 Foundation Improvement

Foundation improvement is a generic term that is used here to define both the renovation and protection of foundations. In the specific case of foundation renovation, this implies increasing the bearing capacity of a pile foundation that has insufficient bearing capacity. In the case of foundation protection, the focus is on safeguarding the piles of the foundation against possible damage resulting from underground construction activities in the vicinity.

One way of improving the properties of the foundation is by adjustment of the load applied on the foundation. This can be achieved by either reducing the weight of the structure or by reducing the negative skin friction on the piles. The first solution concerns making structural alterations, like demolishing annexes. The second solution relates to reducing the weight of the soil by using lightweight materials, which both directly and indirectly reduce negative pile skin friction. The biggest advantage of this method is that it is about 50% cheaper than the conventional underpinning methods (Oversteegen, 1999). On the other hand the settlement process is only retarded, not stopped and only a limited number of structures can be dealt with at the same time (because of the instability during excavation). This method is not further examined in this thesis.

Another approach to foundation improvement is to strengthen the foundation. Strengthening (of load bearing structures*) is defined here as the process of adding new, permanent support to the foundation of a structure without the need to remove or demolish this structure. Yet another approach to strengthening the foundation involves improving the strength and stiffness properties of the load-bearing stratum, for example by using soil improvement methods like permeation grouting, jet grouting and compaction grouting. The point of departure for foundation strengthening is that the structure remains intact during the renovation process.

The wide range of foundation renewal, upgrading and repair techniques, which here fall under the generic term *conventional underpinning*[†], are dealt with in Section 2.6. Although there is extensive experience in the use of conventional underpinning methods, relatively little use has been made of grouting for foundation strengthening. However this method is considered to have high potential. In Section 2.7 a general outline of grouting techniques and their applications for foundation improvement are given.

2.6 Conventional Underpinning

2.6.1 Introduction

After determining the causes of foundation damage by using the appropriate damage detection methods, the next logical step is to determine how foundation renovation can be accomplished. In this section, a summary of the most important results of investigations on conventional underpinning carried out by Van der Stoel (2001b), are given. These investigations outline the different types of strengthening methods, their fields of application and their advantages and disadvantages.

The principle of conventional underpinning is to transfer the structural load to an underlying bearing stratum where sufficient bearing capacity is available. This system is used for both pile foundations and for shallow foundations that are transformed into pile foundations or 'piled rafts'. A distinction is made between the piles and the load transfer system. The piles are usually made of steel, concrete or grout. The load transfer system consists of concrete or steel beams or steel stools combined with jacks. In the next sub-sections the pile types are summarized and some typical examples of underpinning are given.

* By structures not only buildings, but also bridges, tunnels, roads, factories, ship locks, etc. are mend.

† Underpinning can be achieved by soil improvement and by other more conventional methods.

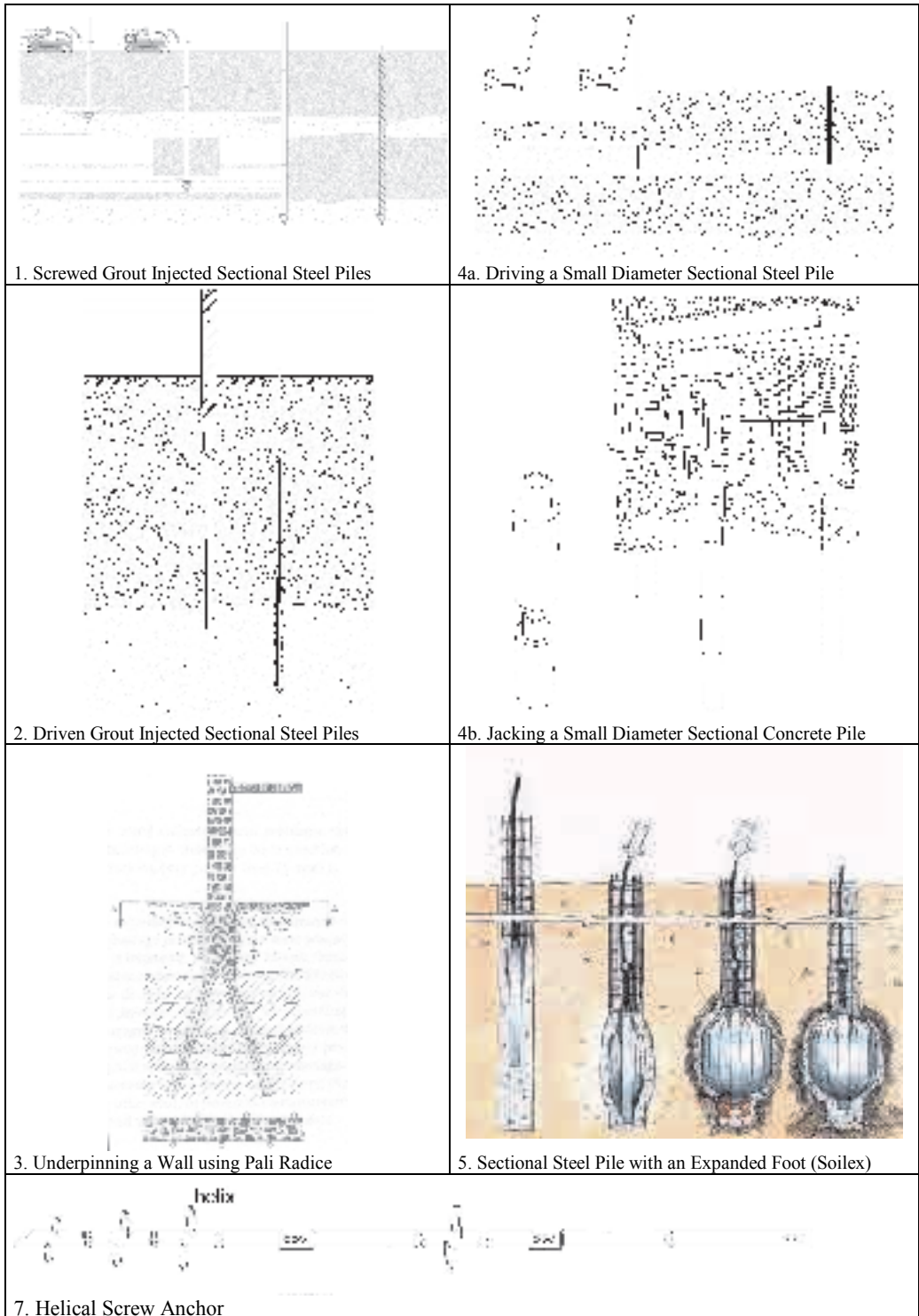


Figure 2.10 Examples of Pile Types

2.6.2 Pile Types

When making an inventory of the pile types available for foundation renovation, the large number of pile types is striking, but closer examination reveals that there are a few basic categories that differ only slightly. These differences usually concern contractors patents (and the efforts of other contractors trying to improve or imitate these patents). A distinction is made between the types of piles mentioned below.

1. Screwed Grout Injected Sectional Steel Piles.
2. Driven Grout Injected Sectional Steel Piles.
3. Micropiles and Root Piles or Pali Radice.
4. Small Diameter Sectional a)Steel, b)Concrete or c)High-Strength Concrete Piles.
5. Sectional Steel Piles with an Expanded Foot.
6. Steel Piles with a Jet Grouted Base.
7. Helical Screw Anchor Piles.

All pile systems are unstressed after installation. Multiple techniques, which are not outlined here, are available for partial stressing of the piles.

2.6.3 Examples of Foundation Renovation

The characteristic buildings of the *Begijnhof* are located in the city centre of Amsterdam. Because of the poor condition of their foundations and the historic relevance of the buildings, new foundations had to be made without damaging the fragile buildings. In Figure 2.11 illustrations of the renovation of the foundations are given. Figure 2.11a shows the initial situation. Piles have been created by using small diameter sectional concrete piles, *after* which the floor at ground level was demolished. The soil was removed and replaced by clean sand and openings (bonding pockets) were made in the load bearing walls (Figure 2.11b). A foil and hard bricks were placed in the openings, after which the alternating openings were created and covered with foil. A PVC foil and 50mm isolation material was placed on the sand and concrete was then poured onto it (Figure 2.11c). The openings provide a connection between the new floor and the load bearing walls.

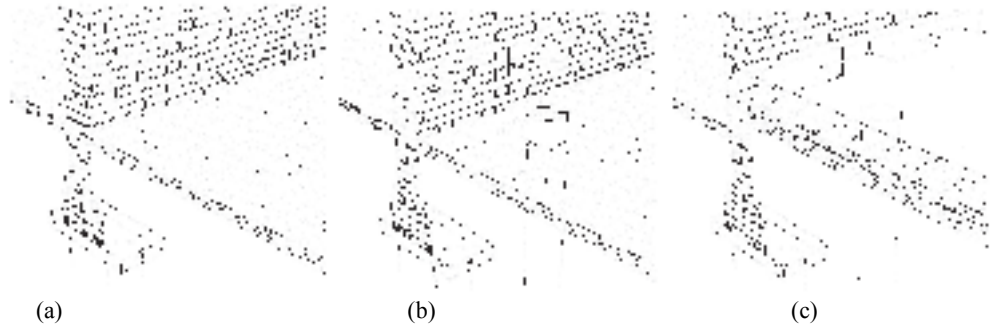


Figure 2.11 Example Begijnhof Amsterdam

The warehouses of the *Entrepotdok* (see Figure 2.9 on page 12) in the city centre of Amsterdam are characterized by having different foundations (depending on the stock that was kept in the warehouse). The main reason for the settlement problems that had occurred were:

- the number of floors differed per building but the foundations did not, so differential settlement between adjacent buildings occurred;
- the facades were in a poor condition, also due to the differential settlement (broken cross beams and piles that were positioned next to the walls instead of under the walls);
- at some locations the weight of two buildings was put on one foundation.

The differential settlement also led to moisture problems which not only affected the quality of the foundations, but also the historic value of the buildings. Therefore foundation renovation was initiated.



Figure 2.12 Example Entrepotdok Amsterdam; Stages

In Figure 2.12 and Figure 2.13 illustrations of the foundation renovations are given. These differ from the Begijnhof in that here first the ground level floor was demolished *after* which the piles were installed (again using small diameter sectional concrete piles). Another difference is that the piles were constructed to create additional bearing capacity instead of creating an entirely new foundation. Figure 2.12a shows openings that were made in the load bearing walls and formwork that was placed to create the connections. Concrete was poured into the formwork, thus creating stiff elements (Figure 2.12b). After that 0.35 m of foam concrete was put onto the sand to reduce the negative skin friction on the piles. Finally concrete was poured onto it and through the openings (Figure 2.12c). The continuous concrete floor also acted as a moisture barrier. Because the warehouses were treated alternately (Figure 2.13) a “Table Construction” was created. Therefore the concrete floor at the piled sections is approximately twice as thick as the concrete floor at non-piled sections.

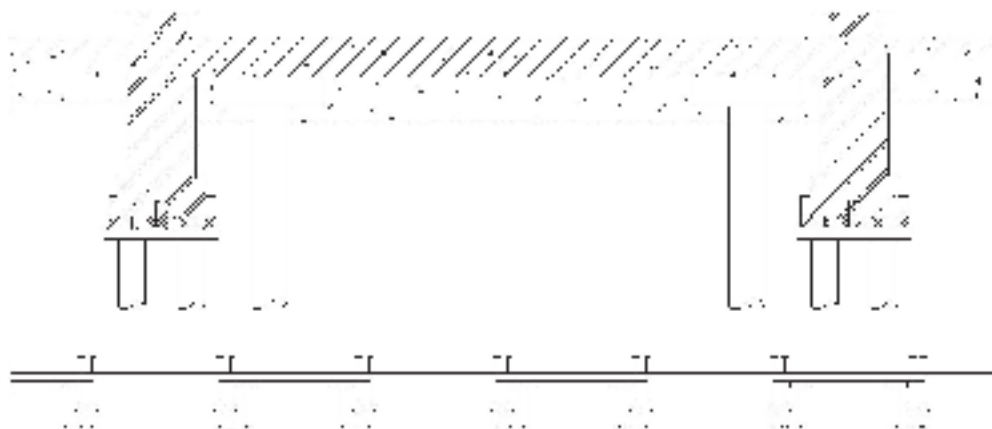


Figure 2.13 Example Entrepotdok Amsterdam; Cross Section of Tables

2.7 Grouting Techniques

2.7.1 Introduction

Compared to conventional underpinning techniques foundation renovation by using grouting techniques is rarely used. Foundation protection, for instance against TBM tunnelling, is much more frequently used. The three techniques that are mentioned in this section, are extensively dealt with in Chapter 3 (Permeation Grouting), Chapter 4 (Jet Grouting) and Chapter 5 (Compaction Grouting). Their suitability for foundation improvement is discussed in Chapter 8. In the next sub-sections some short definitions and examples are given and the basic characteristics/differences are explained.

2.7.2 Grouting Techniques

The most common way of using grouting is to apply permeation grouting to increase the strength and stiffness of the soil. When carried out properly, this technique leaves the soil relatively undisturbed, because only the voids are filled. An alternative that is frequently used for shallow foundations (but only seldom with pile foundations) is an eroding technique called jet grouting, which creates new piles (or extends existing piles). Another option is compaction grouting, which increases the effective soil stresses by compacting the soil near the piles.

A complete list of all terms referring to grouting is incorporated in APPENDIX I. The most important definitions that are given in prEN12715 and prEN12716, are incorporated here.

Permeation grouting (Figure 2.14a) is based on the replacement of pore water (or gas) of a porous medium (soil) with a grout at injection pressures low enough to prevent displacement.

Jet grouting (Figure 2.14b) is a process that consists of the disaggregation of the soil and its mixing with (and partial replacement by) a cementing agent. The disaggregation is achieved by a high-energy jet of a fluid, which can be the cementing agent itself.

Fracturing (Figure 2.14c) is a displacement grouting technique which aims at forcing a mortar of low internal friction into the soil, thus fracturing and displacing it.

Compaction grouting (Figure 2.14d) is a displacement grouting technique, which aims at forcing a mortar of high internal friction into the soil without fracturing it.

Compensation grouting is a generic term employed for controlled displacement grouting and it is intended to counteract ground settlement or effective stress relaxation induced by excavation works. This term refers to a number of grouting techniques like compaction grouting, displacement grouting and fracturing.

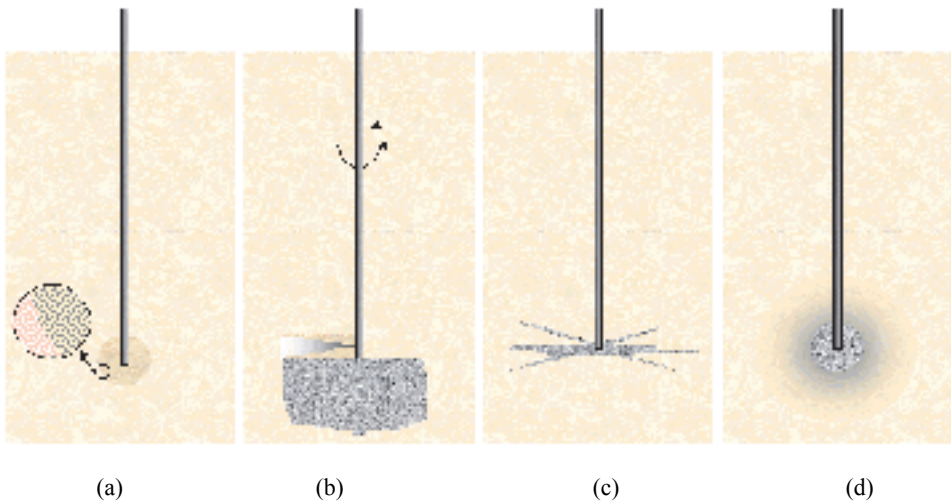


Figure 2.14 (a) Permeation Grouting (b) Jet Grouting (c) Fracturing (d) Compaction Grouting

2.7.3 Examples of Foundation Renovation

To create grouted piles for the purpose of foundation renovation, both permeation grouting and as jet grouting may be used. To extend a pile foundation, existing piles are elongated by adding grouted piles, to reach a deeper and firmer bearing stratum. An example is shown in Figure 2.15.

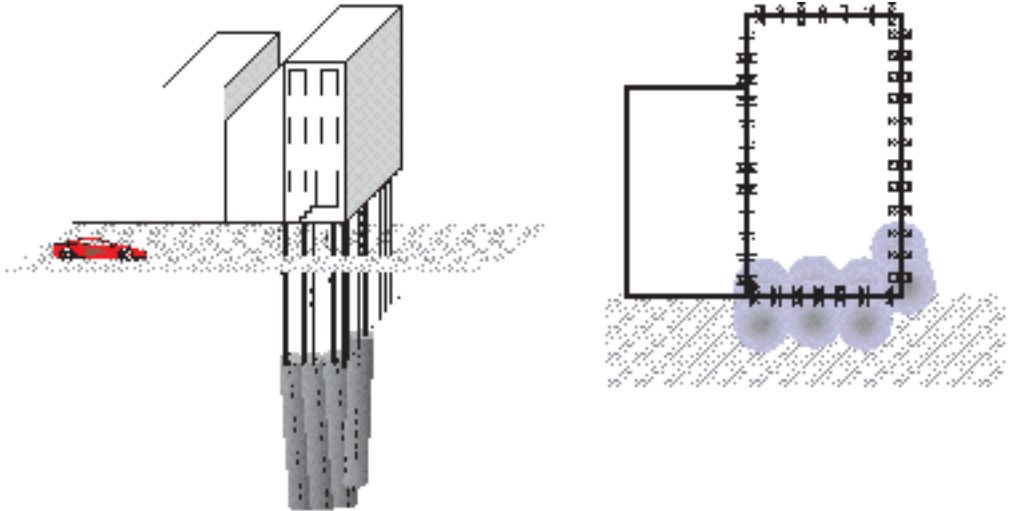


Figure 2.15 Example of Jet Grouted Piles to Extend a Pile Foundation

Another possible application is to increase the bearing capacity of the soil by permeation grouting or compaction grouting near the pile toes. An example of the latter for a typical Amsterdam building is shown in Figure 2.16.

When using compaction grouting, the aim is to increase the horizontal effective stresses in the soil, by injecting a relatively stiff grout into the bearing stratum, next to the pile toes. The soil is thus compacted, the effective soil stresses are increased and consequently the bearing capacity of the wooden piles is increased.

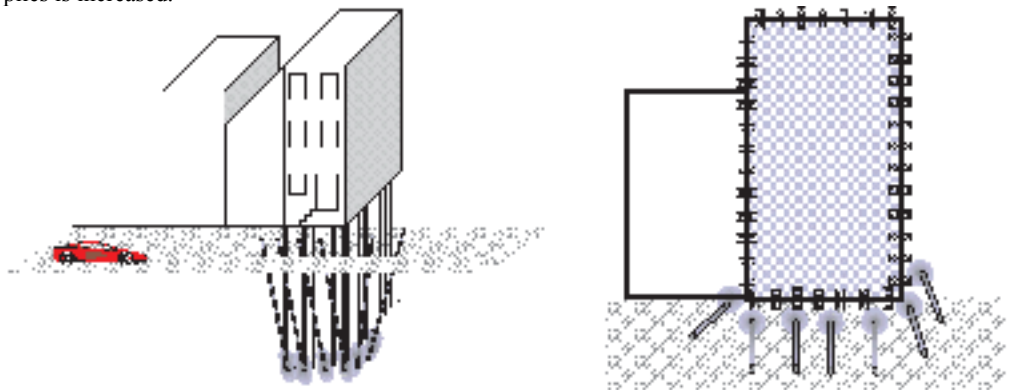


Figure 2.16 Example of Compaction Grouting near a Pile Foundation

2.7.4 Examples of Foundation Protection

An example of foundation protection is shown in Figure 2.17. A permeation grouted or jet grouted structure is created in soft soil before the TBM arrives. When the TBM bores through the grouted structure, the settlement can be significantly reduced owing to the increased stiffness of the soil. Van der Stoel (1997b) has made Finite Element Method calculations using PLAXIS showing this reduction. The extent of the settlement reduction is dependent on the homogeneity, strength and stiffness of the grouted structure and therefore on the grouting process used.

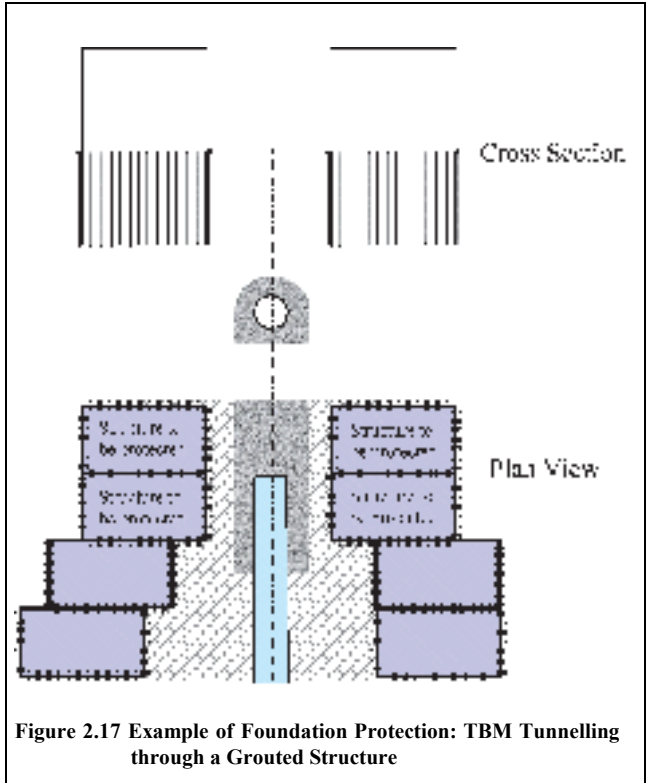


Figure 2.17 Example of Foundation Protection: TBM Tunnelling through a Grouted Structure

2.8 Concluding Remarks

The goal of the foundation investigation program should be to carefully examine all possibilities and then find the sources of the most serious damage. After determining the causes of foundation damage by using the appropriate damage detection methods, the next logical step is to determine how foundation improvement can be accomplished.

Throughout the world a wide range of foundation renewal, upgrading and repair techniques, known as conventional underpinning, is frequently used to strengthen existing foundations. These techniques are very reliable, but often cause considerable disturbance because they require evacuation or partial evacuation, or temporary or permanent closure of the structure. The costs of conventional underpinning are considerable, making it appealing to search for alternatives.

Because foundation improvement by means of grouting techniques can generally be executed from outside the structure, this technique makes evacuation superfluous. It also avoids the need to shore up the structure. The application of grouting techniques for foundation renovation purposes does raise questions regarding the response of the foundation piles to the installation and grouting process. Because practical experience of using grouting techniques for pile foundation improvement is limited, a test in which the pile displacements, soil stresses and pore pressures could be observed and the pile bearing capacity could be studied was conducted. The set-up of this Full Scale Injection Test is outlined in the next chapter. The subsequent chapters consider permeation grouting, jet grouting and compaction grouting in more detail. In Chapter 8 the applicability of using grouting techniques for foundation improvement is explained.

Chapter 3 TEST SET-UP & CONSISTENCY CHECK

3.1 Introduction

The Full-Scale Injection Test (FSIT)* was a full-scale field test carried out to investigate the effect of grouting on Amsterdam deposits, and particularly to investigate the effects on piled foundations.

The test was initiated to answer specific questions concerning the settlement mitigating measures for the Noord/Zuidlijn† project and some more general questions regarding grouting. Delft University of Technology also had an interest in alternative foundation-strengthening methods, and grouting was considered to be a promising option. The test was set up because there is very limited experience of using injection techniques in the vicinity of pile foundations and non-homogeneous, soft, stratified soil (as present in Amsterdam) had previously been injected only to a limited extent. The test location was specifically selected because of the general similarity of the soil conditions to those of the western parts of the Netherlands and more particularly to those along the Noord/Zuidlijn route.



Figure 3.1 Map of Amsterdam Showing the Test Location

For the Noord/Zuidlijn the shield tunnelling method will be used for the construction of two $\text{Ø}6.5$ m metro tunnels. In Amsterdam most of the structures (buildings, bridges, tunnels, and sewers) are founded on piles. Using a Tunnel Boring Machine (TBM) near these structures may induce displacements, including pile displacements or a reduction of pile bearing capacity. These effects are undesirable and must be minimised by taking mitigating measures. These mitigating measures comprise either of the creation of massive grouted elements through which the TBM can be driven or compensating the settlement by compensation grouting. The use of the massive grouted elements is based on the supposition that grouting techniques will improve the soil quality, i.e. the strength and stiffness parameters of the soil improve. By compensation grouting the settlement that may be caused by the TBM are partly prevented and partly compensated.

* in Dutch termed: Praktijk Injectie Proef (PIP)

† a new metro line connecting the northern suburbs, the city-centre and the southern part of Amsterdam.

Grouting techniques can also be used to improve the bearing capacity of existing foundations that are not affected by external factors like a TBM. Opportunities to do this have already been explained in Chapter 2.

Because of Dutch national interest, the Full-Scale Injection Test involved the collaboration of:

- Noord/Zuidlijn Metro/Municipality of Amsterdam;
- Delft University of Technology;
- Centre for Underground Construction Studies (COB*).

The test comprised three stages. Stages 1 and 2, which mainly deal with an investigation into the accuracy of geophysical detection methods for and with (permeation) groutability, are dealt with in Chapter 4 and Chapter 7 respectively. Stage 3 involved three different grouting methods, these being permeation grouting, jet grouting and compensation grouting. In this chapter the test set-up of Stage 3 will be explained. Expert information specific to the grouting methods will be dealt with in Chapter 4, Chapter 5 and Chapter 6 respectively.

3.2 Aim of the Test

The Full-Scale Injection Test was initiated to provide improved understanding and experience of:

- the use of geophysical methods to measure the dimensions of a grouted body;
- the groutability of some specific Dutch soil types;
- mastering and controlling the operational aspects of grouting (pressure, flow-rate, etc.);
- optimisation of the feasibility and practicability of grouting in densely populated urban areas;
- the effect on the surroundings and on the load-settlement behaviour of the piles that results from the placing of injection rods or ‘tubes à manchette’ (TAMs);
- the effect of creating the grouted body on the surrounding area and more specifically on:
 - the bearing capacity of the piles;
 - the load-settlement behaviour of the piles;
 - soil deformations;
 - the changes in piezometric level and soil stresses (at pile toe level).

The reasons for choosing a full-scale test rather than a scaled laboratory test are twofold. Firstly, the behaviour of end-bearing pile foundations is very complex and therefore too complicated to model in a laboratory. Secondly grouting, especially permeation grouting, is extremely difficult to study on a smaller scale, because of the large influence the size of the soil and grout particles has on the results. While full-scale testing also has some disadvantages as compared to laboratory testing, mainly the reduced control over test conditions, the advantages of the full scale test were considered decisive.

3.3 Stages of the Test

To achieve the goals outlined in section 3.2, the Full-Scale Injection Test was split into three stages:

- Stage 1: comparison of different geophysical surveying methods;
- Stage 2: determining the groutability of Amsterdam soil by means of permeation grouting;
- Stage 3: grouting near instrumented pile foundations by using different injection methods, including:
 - permeation grouting (Stage 3A);
 - jet grouting (Stage 3B);
 - compensation grouting (compaction grouting and fracturing; Stage 3C).

Stage 1 was undertaken, because in order to determine the influence of grouting on existing pile foundations, the diameter of the grouted elements has to be determined to an acceptable degree of accuracy. As current practice for verifying the dimensions of grouted bodies at depth is difficult and

* The *Centrum Ondergronds Bouwen* (COB) is a co-operation of Dutch contractors, engineering consultants, specialist institutions and others involved in underground construction.

therefore costly, in this stage different geophysical surveying methods were examined. The results of this stage are integrated in Chapter 7.

Stage 2 was intended to determine the ‘groutability’ of some specific Amsterdam soil layers when using permeation grouting. There were some doubts regarding this injectability because working according to the known criteria did not ensure there would be a good result. The results are integrated in Chapter 4.

Stage 3 involved the three different injection methods: permeation grouting, jet grouting and compensation grouting. In the design of the Noord/Zuidlijn the two latter methods are used as either an alternative or as a back-up measure when permeation grouting is not possible or not considered desirable. The main focus of Stage 3 was to determine the influence of grouting on pile foundations.

Stage 1 was completed in February 1998, Stage 2 was completed in February 1999 and Stage 3 was completed in December 1999.

3.4 Associated Full Scale Tests

For the Noord/Zuidlijn multiple underground construction techniques will be used. Some of these techniques, such as tunnel boring and deep diaphragm walls, will be carried out in the vicinity of the delicate and historically significant structures in the centre of Amsterdam. This has led to the development of a series of tests to investigate the impact of these construction techniques. Two of these tests, the Test Pile Project and the Diaphragm Wall Test, were carried out before the Full-Scale Injection Test and their results have been integrated in the Full-Scale Injection Test.

The main objective of the *Test Pile Project*^{*} was to observe the deformation of pile foundations and the stress and strain behaviour of soil as a tunnel boring machine passes underneath. In the trajectory of the Second Heineoord tunnel, the first bored tunnel in the Netherlands, a special test site was created with ground conditions similar to those of the Amsterdam situation. The test site consisted of a large series of piles driven at varying distances from the tunnel axis, as well as various instrumentation to monitor stress and strain behaviour of the soil, during and after the TBM passage. For more information see Teunissen & Hutteman (1998) and Kaalberg et al (1999).

The main objective of the *D-Wall Test*[†] was to observe the stress and strain behaviour of the soil and the pile foundations during the installation process of a deep diaphragm wall. The test was carried out at the construction site of a high rise building in Amsterdam. Differently shaped wall panels were monitored during their installation and during the subsequent consolidation period. For more information see De Wit, De Kant & Roelands (1999) and De Wit, De Kant & Lengkeek (2000).

During the Test Pile Project and the Diaphragm Wall Test the stress and strain behaviour of the soil and the pile deformations were thoroughly monitored. Lessons learned from these tests included the following: the need for automatic displacement data acquisition, the poor reliability of the absolute readings of Stress Monitoring Stations (SMS) placed in a borehole and the relatively limited influence on the pile bearing capacity.

^{*} in Dutch: *Proef Palen Project*

[†] in Dutch: *Diepwandproef*

3.5 Soil and Groundwater Characteristics

The test location had to be compatible with the general soil conditions of the western part of the Netherlands and more specifically the Amsterdam Noord/Zuidlijn route. The site chosen was located in the northern part of Amsterdam near the Sixhaven. At this location matching soil conditions were combined with sufficient space for the execution of the works and storage of materials.

Figure 3.2 shows the result of a characteristic CPT, Figure 3.3 shows the grain size distribution of the sand layers and intermediate layer and Table 3.1 gives a summary of the different soil layers. The Dutch reference level for height measurements is *NAP**. A detailed description of the soil conditions, including a parameter set, is given in APPENDIX II.

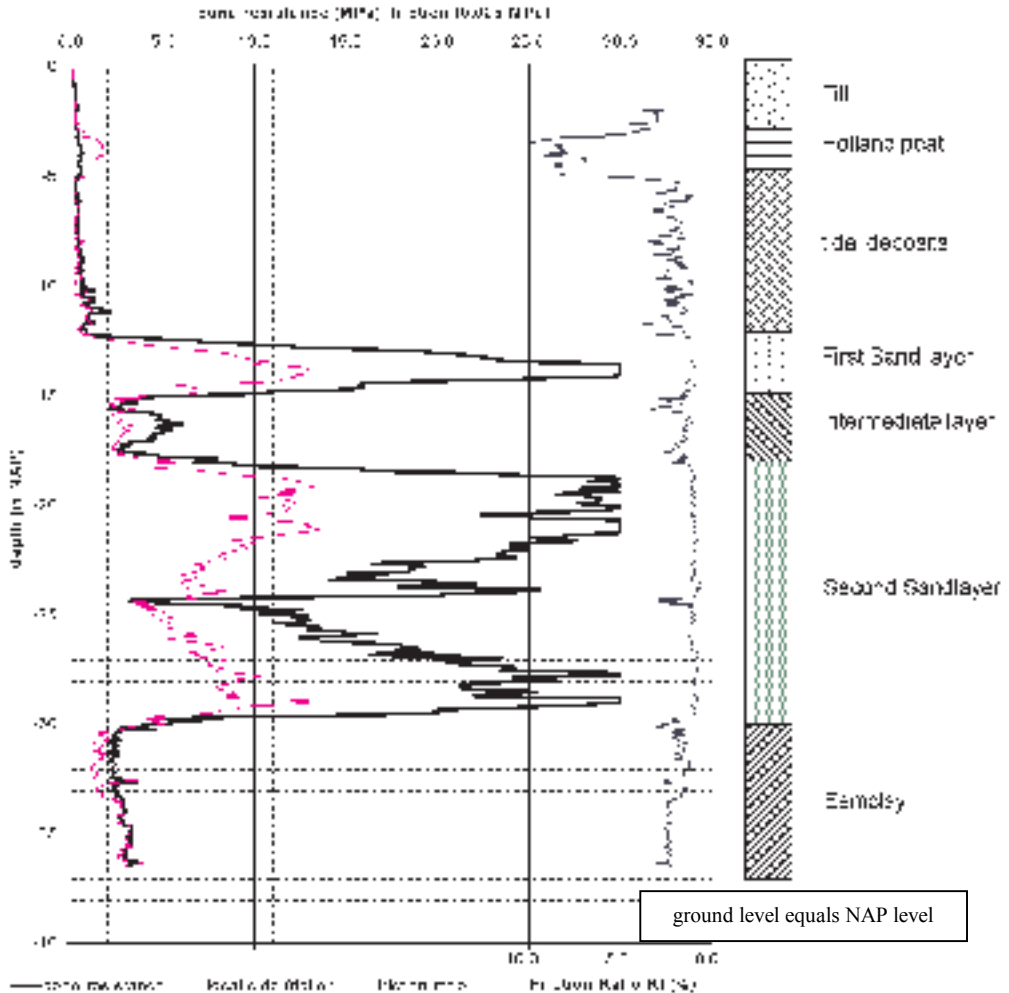


Figure 3.2 Typical CPT at Test Site

* in Dutch: Nieuw Amsterdams Peil

Table 3.1 Soil Characteristics at the Full-Scale Injection Test Site

Layer No.	Layer Name	Composition	Bottom (m; NAP)
0	Greenfield		+0.5
	Made ground	Made ground and rubble	-0.5
1	Peat	Clayey peat	-5.5
2	Upper clay layer	Clay with a low sand content	-8.0
3	Lower clay layer	Silty clay	-12.5
4	1st sand layer	Dense sand	-15.0
5	Intermediate layer (Alleröd)	Silty sand with clay lenses	-18.0
6	Upper 2nd sand layer	Very dense sand	-21.0
7	Lower 2nd sand layer	Dense sand	-30.0
8	Eemclay layer	Stiff to very stiff clay	-45.0

The groundwater levels and the piezometric heads of the 1st and 2nd sand layers were measured. The groundwater level was identified at NAP -0.8 m and the piezometric head of the sand layers at NAP -1.4m ± 0.10 m. Some minor differences between this profile and the characteristic Amsterdam soil profile are apparent, in particular the varying thickness of the peat layer and the position of the bottom of the 2nd sand layer which may vary by 3-4 meters in other parts of the city centre.

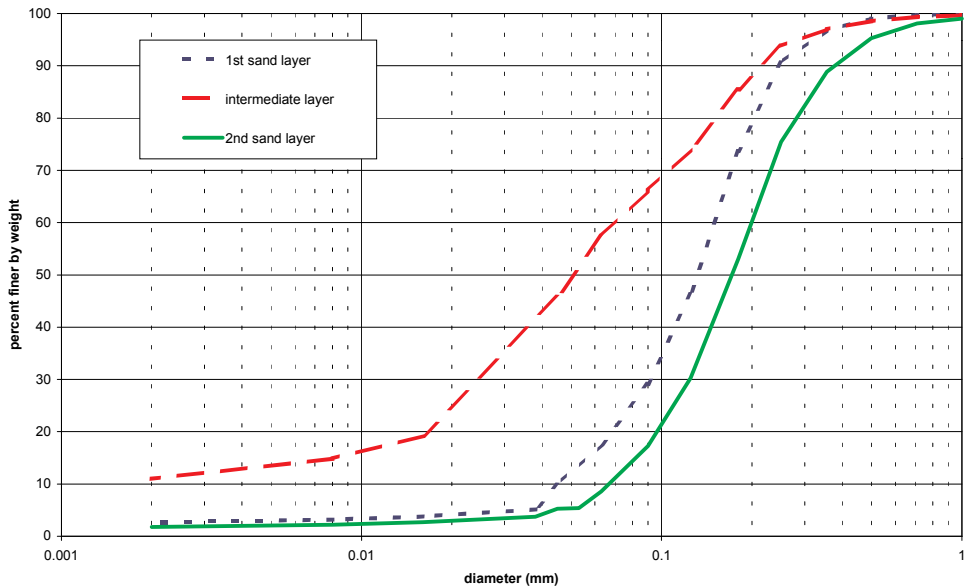


Figure 3.3 Grain Size Distribution of the Sand Layers and Intermediate Layer

3.6 Pile Foundation and Construction

During stage 3 of the test a series of 18 wooden and 3 concrete piles were loaded with a constant working load by using jacks. The loads on and movement of the piles and the water-pressures and stresses in the soil during grouting were measured. For the loading 8750 kN of dead weight was used. Table 3.2 summarises the characteristics of the wooden and concrete foundation piles. These piles are considered to be characteristic for the Amsterdam situation. A total of 18 wooden piles and 3 concrete piles were driven into the soil, these being:

- 9 wooden piles used for Stage 3A and later on for 3C;
- 3 wooden piles and 3 concrete piles used exclusively for Stage 3B;
- 6 wooden piles used exclusively for Stage 3C.

TEST SET-UP & CONSISTENCY CHECK

The possibility to be able to determine the ultimate bearing capacity of the concrete piles was conditional for the design of the frame and the total weight of the ballast. Figure 3.4 shows a photograph of the test site with the ballast frame loaded.

Table 3.2 Pile Characteristics (average values).

Feature	Wooden pile	Concrete pile
<i>Number of piles</i>	18	3
Diameter pile head (mm)	Ø 230	350
Diameter pile toe (mm)	Ø 130	350
Pile toe level (m NAP)	NAP -13.5	NAP -20.0
Length (m)	15	22
Material	<i>Picea Abies</i> (Pine Wood)	Concrete B35
Pile toe resistance (%)	75-85	65-70
Pile shaft resistance (%)	15-25	30-35
Calculated working load* (WL)	135 kN	1000 kN
Ultimate bearing capacity (UBC)	265 kN	3410 kN

* The calculated working load corresponds with the characteristic load of a Amsterdam pile foundation.



Figure 3.4 Photograph of the Test Site

Figure 3.5 and Figure 3.6 show the step by step assembly-up of the construction, a typical cross-section and plan views respectively. In APPENDIX IV photos illustrate chronological sequence of the construction.

Once driven, the piles were loaded by hydraulic jacks, thus providing the ability to adjust the load on each individual pile independently. Various steel profiles were used to distribute the load from Stelcon (concrete) plates and 'big bags' filled with sand that were placed on top of the construction to serve as ballast. Throughout the entire testing program the working load (WL) that was applied on the piles, was adjusted by using the jacks. All piles were loaded simultaneously. In total $18 * 135 \text{ kN} + 3 * 1000 \text{ kN} = 5430 \text{ kN}$ (see Table 3.2) of the 8750 kN of ballast was used to load the piles during this stage, such that the remaining $8750 - 5430 = 3320 \text{ kN}$ was distributed via the Stelcon plates to the surface.

TEST SET-UP & CONSISTENCY CHECK



Figure 3.5 (a) piles

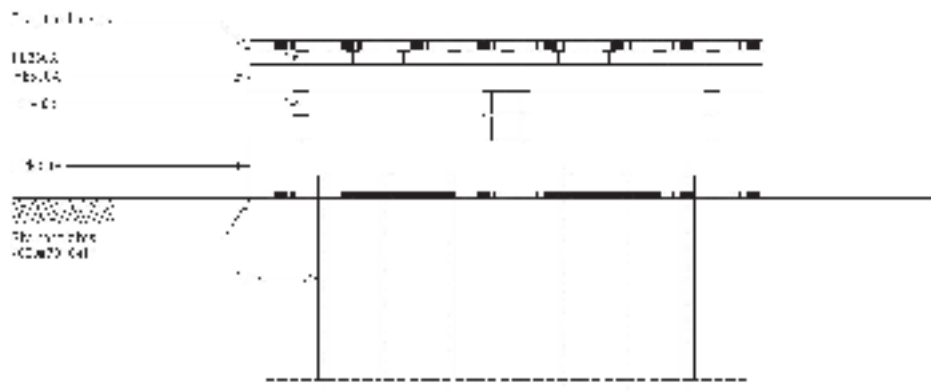


Figure 3.5 (b) steel framework and dragline plates

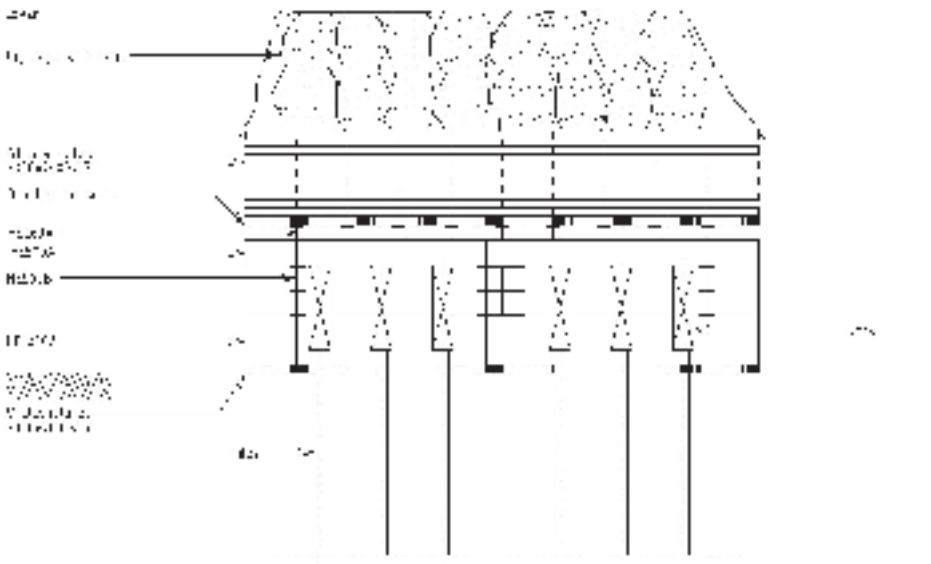


Figure 3.5 (c) stelcon plates and 'big bags' filled with sand for ballast

Figure 3.5 Typical Cross Section of the Ballast Frame Construction

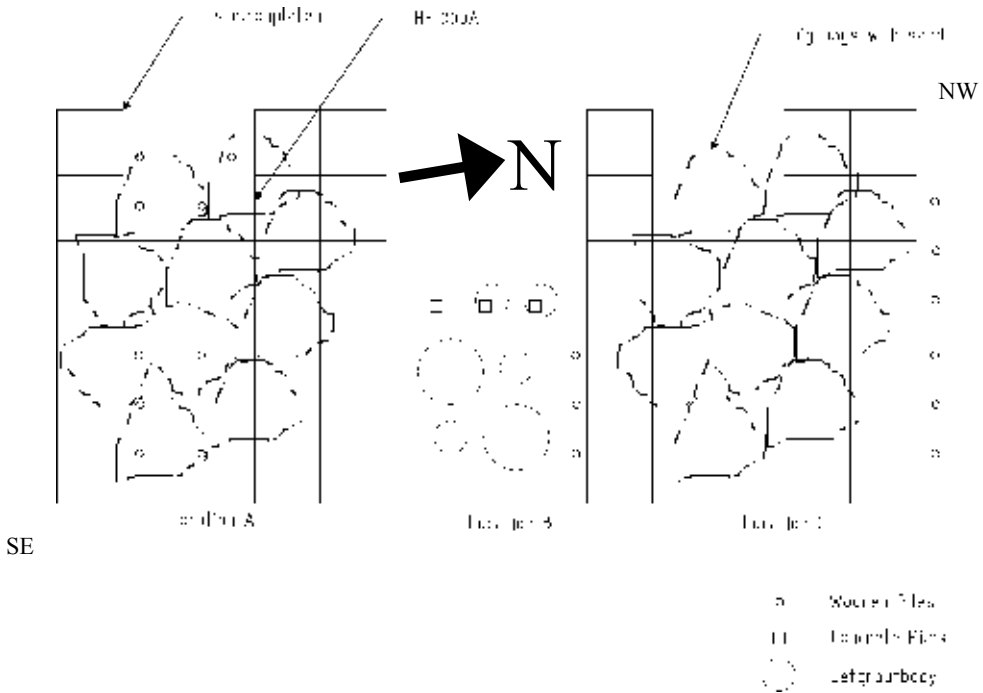


Figure 3.6 Schematic Plan View of the Ballast Frame Construction

Because throughout the tests the jacks maintained the working load on all the piles, the redistribution of loads was kept to a minimum. Pile displacement as a function of time was therefore obtained at constant load, thus being entirely dependent upon the injection process.

Figure 3.7 shows an example of a loaded wooden pile. Figure 3.14 (p.35) shows an example of a concrete pile loaded during ultimate bearing capacity testing.

3.7 Monitoring Equipment

The monitoring equipment that was used for the test consists of various types of instruments. A series of measurements were taken during testing, including soil deformations (in three directions), pile deformations (mainly in the vertical plane, although some lateral measurement were taken), pore water pressures (p), soil pressures (σ) and loads on the piles (F). The following equipment was used:

- VW Piezometers installed in the soil;
- Extensometers installed in the soil;
- Inclinerometers;
- Jointmeters;
- Load-cells;

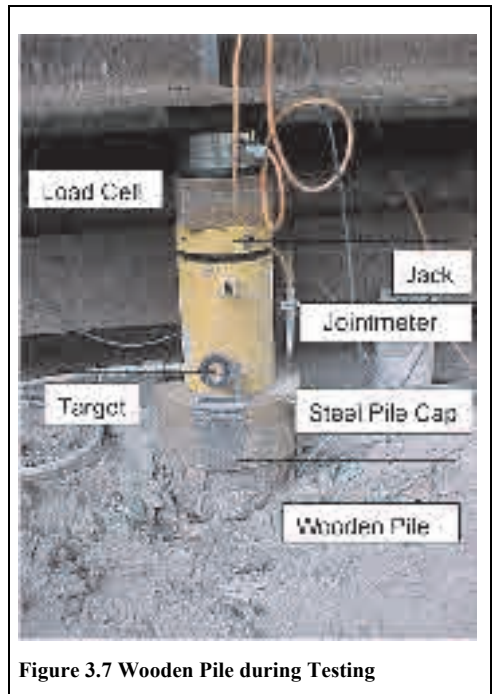


Figure 3.7 Wooden Pile during Testing

TEST SET-UP & CONSISTENCY CHECK

- Total Station (an automatic theodolite; x,y position and vertical levelling) combined with targets (prismatic measurement points);
- Beacons (surface levelling points for measuring vertical movement);
- Stress Monitoring Stations (SMS) and Piezometers installed in the pile-toes.

Due to the large quantity of data to be collected from the test, strict regulations regarding obtaining and processing of the data were specified. Some important aspects were:

- regular synchronisation of all the monitoring equipment;
- predefined format of the data (including the time, temperature and reference location registration; units; accuracy);
- processing and presentation (digitally at the site, including graphs).
- To enable cross-referencing between all available data, output was collected digitally every 2 minutes*. The registration and/or measurement intervals could only be extended, during the consolidation periods after each grouting stage

A description of the monitoring equipment is included in APPENDIX VI. In the next section the details of the method of data acquisition and processing are dealt with.

3.8 Data Acquisition and Processing

In Figure 3.8 a pictorial presentation of the measurement system is presented and Figure 3.9 gives a schematic overview of the data acquisition system.

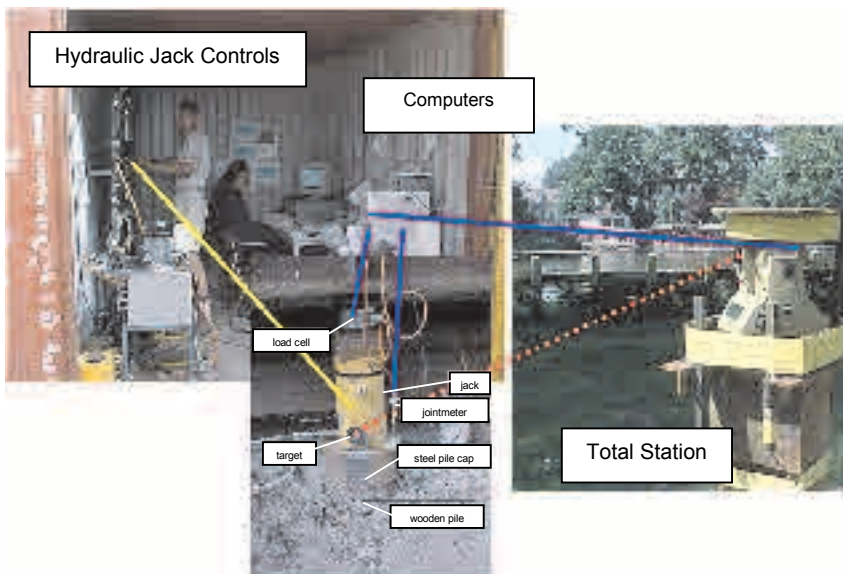


Figure 3.8 Relation Between Different Monitoring Equipment

To permit the correlation of data from the monitoring equipment, a special data acquisition method had to be used. The most important feature of this method was the ability to determine the relation between the absolute measurements of the total station and the relative measurements of the jointmeters. By making corrections via reference points the total station can accurately measure the x,y,z-position of a target. However, the maximum frequency of 5-6 measurement registrations per hour that can be achieved by the total station, is low. The jointmeter can measure at a higher frequency, but the measurements are relative to either a special measurement frame (see Figure 6.15 on page 136) or the

* i.e. the registration interval was 2 minutes even if the measurement interval was much longer

ballast frame. Both such frames are themselves sensitive to surface movements. By making the best possible use of both methods to monitor displacements, a cross-reference check could be made. When the targets on the frames appeared to be stable, the jointmeter measurements could be used without corrections. When the total station targets on the frames moved, the jointmeter measurements were corrected using the absolute total station readings.

The load on the piles was monitored by using load cells on the pile head (Figure 3.7 and Figure 3.14) and using a manometer at the jacking pump unit.

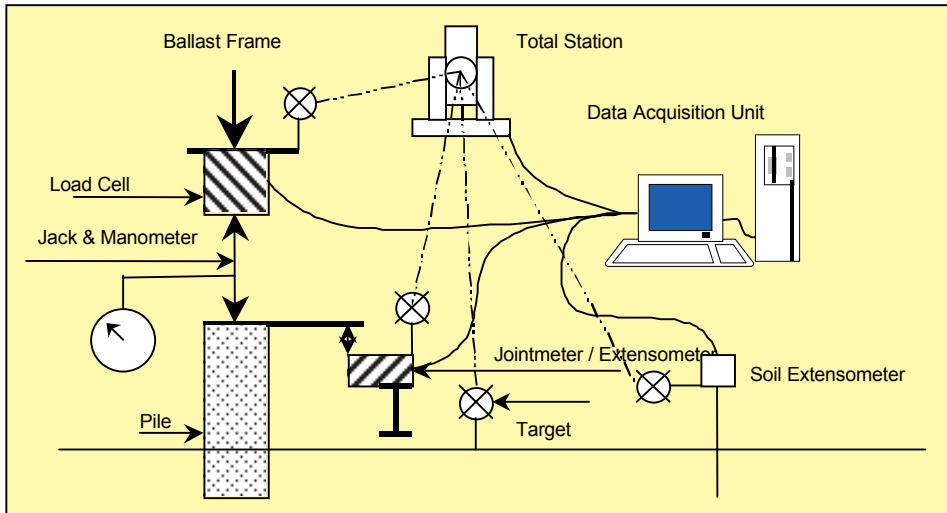


Figure 3.9 Data Acquisition System (Fundamentum, 2000)

3.9 Consistency Check of the Monitoring Data

3.9.1 General

Before analysing the influence of the different grouting methods, a consistency check of the data acquired by the monitoring system had to be performed. Because during the test the conditions constantly change, the data acquired by the monitoring equipment can consequently be influenced by these changes. This section includes general remarks concerning the consistency of the data and more specific information concerning the individual grouting methods. A number of graphs are used to illustrate specific problems. A broader range of graphs and a detailed analysis of these graphs can be found in Van der Stoel (2001). This thesis focuses more on the correlation between the grouting process parameters and the pile and soil displacement, stresses and bearing capacity.

3.9.2 Explanation of the Graphs

In the next chapters the displacement, pile load data, soil stresses and pore water pressures for the different grouting methods are plotted against time. This clearly shows the different trends in pile reaction during installation of the grouted element (see for an example Figure 3.13).

The graphs are generally set up in such a way that:

- time is displayed on the horizontal axis;
- on the horizontal axis, using two identical symbols and an interconnecting line, the grouting activities trajectory is indicated;
- either pile loads (kN) or stresses (kPa) are shown on the right vertical axis;
- the vertical (pile)displacement (mm) is indicated on the left vertical axis.

3.9.3 Consistency of Pile Displacement Measurements

The pile head displacement was monitored using both target readings as well as jointmeters. The monitoring data obtained from these instruments was evaluated by carrying out corrections using statistical parameters:

- for the target readings, because of their irregular character, subtracting the average of the last five readings from the average of the first five; the difference is regarded as the displacement of the pile due to grouting activities;
- for the jointmeter readings, correction by using the target readings of the (ballast)frame; by doing this, some noise is introduced in the data, which is nevertheless small enough not to disrupt the analysis; the last jointmeter reading (immediately after grouting) is then subtracted from the first (start grouting).

Whether pile displacements between start reading and end reading had exceeded the maximum average value or were lower than the minimum average value was always verified. If the verification indicated that this had happened, this was accounted for in the analysis.

When comparing the corrected jointmeter readings with the corrected target readings it could be concluded that they are generally (90%) of the same magnitude. When no discrepancies between the jointmeter and the target readings, the jointmeters are used in the analysis, because they are more continuous and have a higher accuracy. To illustrate this principle of analysis an example is given here. In Figure 3.10 four targets on the reference beam and a reference target are shown. Throughout September 6th the reference beam, used to monitor the pile displacement of the permeation grouting piles, shows a total upward movement of 2 to 3 mm. The uplift is most probably induced by movement of the grouting rig next to the reference beam (to which the jointmeters are attached), causing some lateral squeezing of the peat layer on top of which the beam is positioned. In the next two days a clear consolidation effect can be noticed after the rig has moved away. The jointmeter readings were therefore corrected using interpolated results of reference beam target measurements.

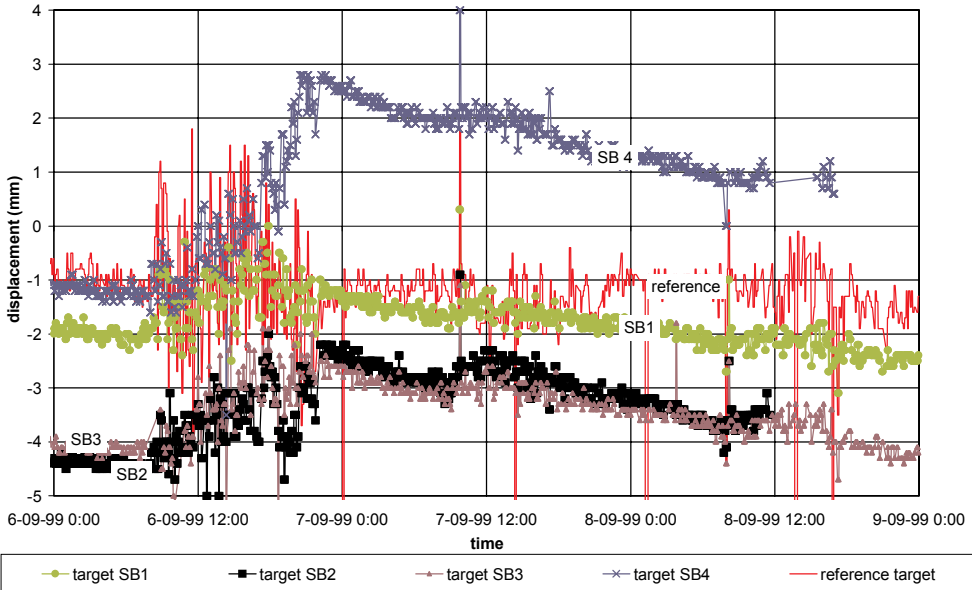


Figure 3.10 Target Readings of the Reference Beam

In conclusion it can be noted that it was extremely useful to use both the jointmeter and the (automatic theodolite) target measurements. Because of the many building activities that took place on the test site, machines often blocked the sight line of the theodolite for a significant time span. There were quite a

number of difficulties when correcting the jointmeter readings for ballast frame or reference frame displacement, because of the sometimes irregular automatic theodolite readings. More automatic theodolites measurements would have been useful. However, because automatic theodolites are very costly (and the test budget was tight) only one theodolite could be used.

3.9.4 Consistency of SMS en Piezometer Measurements

Regarding the total soil stress measurements using the SMS, it could be concluded that the absolute value of these readings was too low. The value should have been at least equal to the pore water pressure. Therefore the reading can best be considered as a relative reading instead of an absolute reading. This phenomenon has previously been encountered (see Bruzzi et al.(1993) and Section 3.4). The piezometers functioned well during the test. Both the absolute pore water pressures and the pressure changes due to grouting activity could be satisfactorily monitored.

Problems with SMS and Piezometers in Wooden Piles

A design that was successfully used in the Test Pile Project, but which did not perform quite as well in the Full-Scale Injection Test, involved the use of the SMS in the wooden pile. In the Test Pile Project piezometers and pressure cells were attached to the wooden pile and performed without any problems. A similar design for the pressure cells was used in the injection test. Unfortunately only two of the eleven ground-pressure cells operated at all. The piezometers did not perform any better in this respect: three of the eleven worked. There were two possible reasons for the non-functioning or malfunctioning of the SMS in the wooden piles:

- the use of a pile hammer that was too powerful ;
- the fixed integration (using a resin) of the measurement cable in the wooden piles; during driving the piles bent somewhat, which could result in tension forces in these cables.

The wooden piles were pulled out of the ground for inspection after the test had finished. Some of the piles were broken (probably because of the pulling force). On the piles that were retrieved in one piece, no visual evidence of the existence of tension forces in the SMS cable was found, but it has to be considered that a very small fracture in the cable is enough to wreck it. The SMS and piezometers in the concrete piles all functioned properly.

3.9.5 Influence of Pile Load Fluctuation

The load cells that were used to measure the load on the pile head proved to be sensitive to temperature fluctuations. As an example, Figure 3.11 shows the fluctuations in pile load during permeation grouting. It can be observed that as the temperature gradually increases during the day, so does the load on the pile. Since this has no correlation with the grouting, the load cell measurements were corrected for temperature changes.

Although during grouting the pile load is supposed to remain constant, it was observed that the load sometimes fluctuated as a result of pile displacement or redistribution of loads from the ballast frame (i.e. a pile settlement causes a decrease in measured pile load). Because this fluctuation might have influenced the pile settlement, in the analysis it was indicated when the standard deviation of the pile load exceeded 2.5% and also when it exceeded 5% of the average of the data during a certain time span. When it was found that this had occurred, the values were qualitatively compared with the pile settlement. The conclusion was that generally the pile load fluctuations had a negligible influence on the pile settlement during the test activities.

TEST SET-UP & CONSISTENCY CHECK

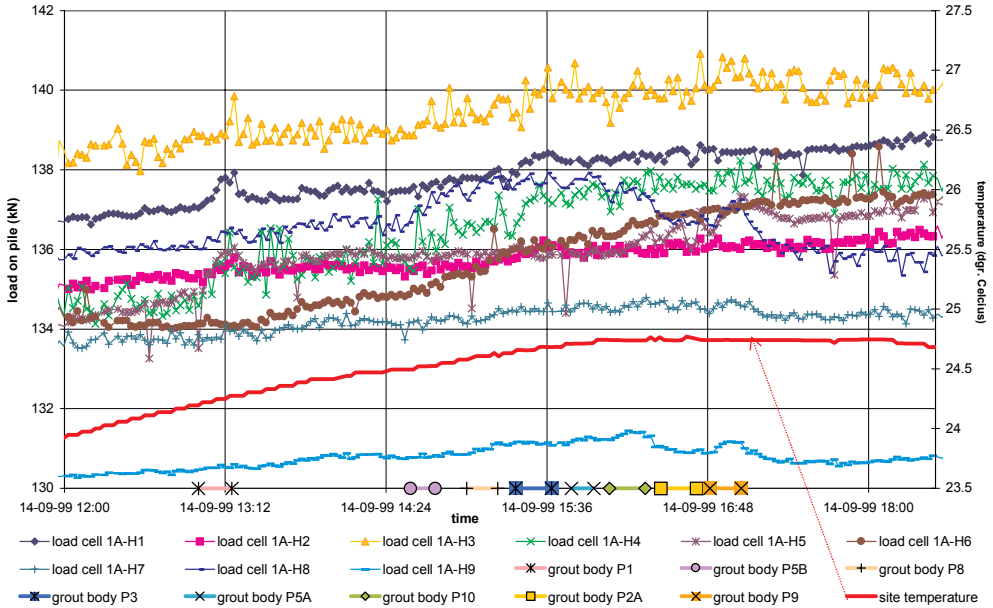


Figure 3.11 Load Cell Readings During Permeation Grouting

3.9.6 Irregularities

During the grouting and monitoring process sometimes irregularities, like grout blow outs, (temporarily) defective measurement equipment and cables getting stuck, occurred. The danger of irregularities is that they are not noticed during the monitoring process and therefore may be mistakenly related to the grouting process when analysing the data. Information in the project log combined with thorough analysis of the data can avoid neglecting irregularities.

An example that occurred several times during the test is given in Figure 3.12. When the total station tries to measure Target 1 that is temporarily blocked (for instance by the jet grouting rig), it can occur that it measures Target 2 that is close in sight.

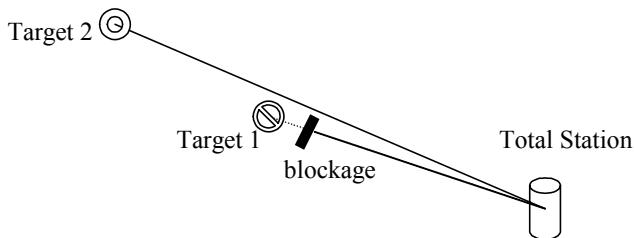


Figure 3.12 Example of Total Station Irregularity

An example that concerns the jet grouting is shown in Figure 3.13 (see Chapter 5 for more information). During the jetting of column C large fluctuations occurred. From the project log it has become clear that during the last part of jetting column C (shallow grouting) a blow out occurred that dislocated many of the targets and jointmeters. Based on this information it could be concluded that the readings obtained after 19:45 on August 11, 1999 are unreliable.

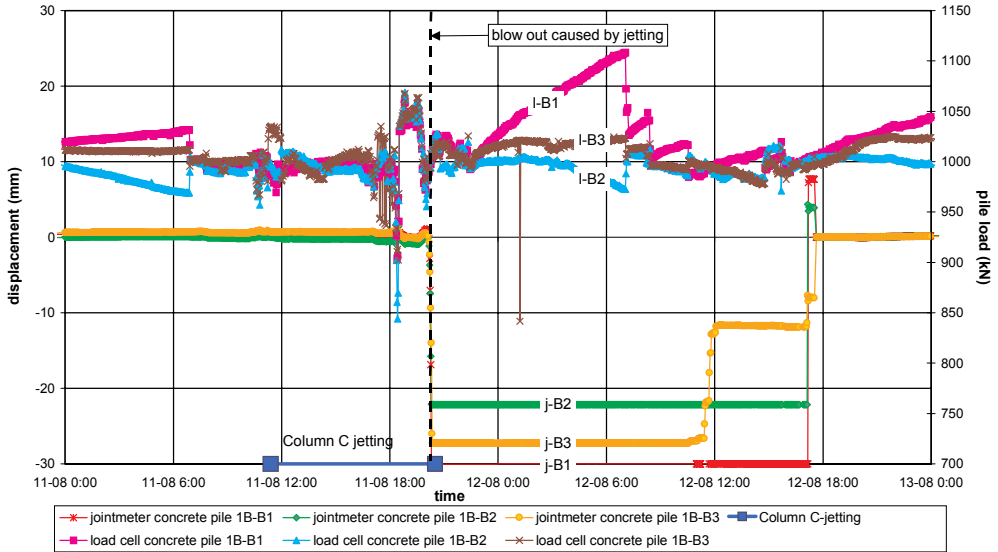


Figure 3.13 Displacement of Concrete Piles during Jet Grouting Installation (Column C)

3.9.7 TAM Installation

The installation time of the tubes-à-manchette (TAMs) and the grout bodies used for the permeation grouting and compensation grouting stages is especially important in the analysis of the monitoring data when the installation of different TAMs took place close after another. For that reason the reported installation time (Fundamentum, 2000) was checked and adjusted using the piezometers readings. In APPENDIX III, A. Table 2 an overview is given of the installation times as reported by Fundamentum and of the installation times after examination of the piezometer data. In the table it can be seen that in most cases the installation time is somewhat shifted or extended compared to the reported values, to extent the time frame of data analysis. From the monitoring data, time frames in which it is certain that installation activities took place were selected. The selected data was then used for quantification or statistical analyses.

Because there was some doubt about the installation accuracy of the TAMs, after installation the exact positions of all the TAMs were measured. Regrettably, the results of these measurements turned out to be unreliable. Van der Stoel (2001) concluded after analysis of the results, that the measurements had not been reliable, because an erroneous orientation for the inclinometers was used. Therefore in the analyses the designed TAM locations are used.

3.10 Reference Load Tests on Piles

3.10.1 Introduction

Pile load tests were carried out to permit the determination of the difference between ultimate bearing capacity of the pile and load-settlement behaviour both before and after grouting. Because all three stages of the test deal with load tests, the testing protocol is explained in this section as well as the load tests that were conducted *before* grouting. The results of the load tests *after* grouting, i.e. the influence of the three different grouting methods on the bearing capacity of the piles will be dealt with in Chapter 4, Chapter 5 and Chapter 6.

3.10.2 Determination of the Theoretical Bearing Capacity of Piles

The theoretical bearing capacity of the wooden and the concrete piles used in the test was determined by using NEN 6743. The method uses the results of five cone penetration tests (CPT), carried out prior to pile installation (see also Figure 3.2). These CPTs showed similar results. For calculation of the ultimate bearing capacity the shaft friction for all layers is included. The results are shown in Table 3.3.

Table 3.3 Theoretical Bearing Capacity of the Piles

Piles	Ultimate Pile bearing capacity (kN)			Working Load (kN)
	Pile toe	Pile shaft	Total	Total
Wood	200	65	265	135
Concrete	1835	1575	3410	1000

During this test, because of practical reasons only individually loaded piles were used. Although in Amsterdam only double piles connected by a cross beam were used (see Section 2.1.3), research conducted by Hoekstra (1974) showed that there is no significant difference when test loading double piles simultaneously or individually.

3.10.3 Determining the Ultimate Bearing Capacity by Pile Load Tests

In situ pile load tests were carried out to determine the influence of the installation of grouting equipment and the actual grouting process on the ultimate bearing capacity of the piles. Because of the large loads necessary to determine the ultimate bearing capacity of the concrete piles, each pile was loaded individually, using four jacks simultaneously (Figure 3.14). The wooden piles were loaded three at a time, using one jack for each pile, and taking into consideration the need to keep sufficient distance between the piles being tested. Because of problems associated with load redistribution during ultimate bearing capacity testing, the remaining piles were **not** loaded.

It was decided that for most of the piles, three pile load tests would be necessary to enable the determination of this influence. For some of the piles at location B (Figure 3.6) an extra test, which will be dealt with in Chapter 6, was carried out.

Pile Load Test 1 was carried out **before grouting** to determine the ultimate bearing capacity of the pile.

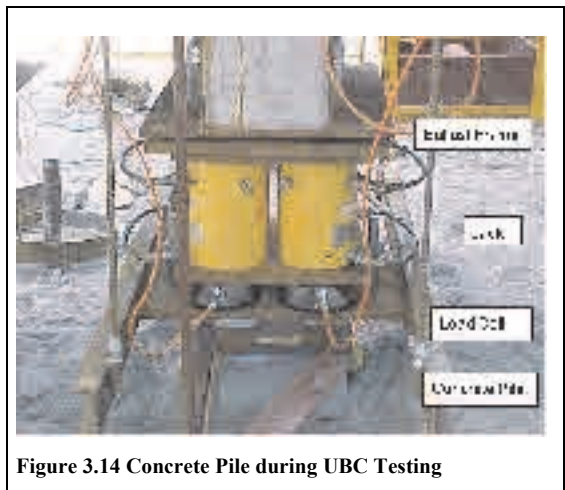


Figure 3.14 Concrete Pile during UBC Testing

Pile Load Test 2, also carried out **before grouting**, had a dual goal. This enabled either verification of the ultimate bearing capacity reached in Test 1 or adjustment of the load steps if Test 1 had revealed that the ultimate bearing capacity did not comply with the theoretical value.

Pile Load Test 3 was carried out **after grouting** to bring the pile to failure, using the same load steps as were used in Test 2. The results of this test are presented in Chapter 4, Chapter 5 and Chapter 6.

The ultimate bearing capacity of the pile was considered to be the load on the pile when the pile toe displacement was 10% of the pile toe diameter (i.e. $\delta_{10\%}=35\text{mm}$ for the concrete piles, $\delta_{10\%}=12\text{mm}$ for the wooden piles; NEN 6743). It should be noted that the difference between pile toe and pile head displacement is only marginal.

In Table 3.4 the pre-defined load steps are given for Pile Load Test 1. For Pile Load Tests 2 and 3 the load steps are presented as a percentage of the ultimate load reached in Test 1 (F_{max}). The load on the pile has been maintained for a minimum of 25 minutes and a maximum of 1.5 hours. For intermediate load steps the load has to be reduced to zero during a minimum of 5 minutes.

Table 3.4 Load Steps Pile Load Tests 1, 2 and 3

Load Step #	Wooden piles		Concrete piles	
	Test 1 <i>kN</i>	Test 2,3 <i>% of F_{max}</i>	Test 1 <i>kN</i>	Test 2,3 <i>% of F_{max}</i>
1	100 / 120 / 150	-	-	-
2	175	65%	700	65%
3	215	80%	1300	75%
4	225	85%	1900	80%
5	240	90%	2500	85%
6	250	95%	3100	90%
7→	If $\delta > 12 \text{ mm}$ $\Delta = 10 \text{ kN}$, else $\Delta = 20 \text{ kN}$	$\Delta = 5\%$	if $\delta > 25 \text{ mm}$ $\Delta = 200 \text{ kN}$, else $\Delta = 400 \text{ kN}$	$\Delta = 5\%$

δ = pile settlement Δ = load increase

A summary of the results of tests 1 and 2 is presented in Table 3.5; the complete results are presented in APPENDIX VII. A surprising result is that the measured ultimate bearing capacity of the wooden piles at location A ($F_{1,average} = 268 \text{ kN}$) is about 50% higher than the ultimate bearing capacity of the wooden piles at location B ($F_{1,average} = 190 \text{ kN}$) and C ($F_{1,average} = 177 \text{ kN}$). The measured bearing capacity of the wooden piles at location A, however, matches the values predicted using the NEN 6743 method most closely. The difference between the 1st and the 2nd load tests is generally small. In 3.10.4 the possible causes of the difference in the ultimate bearing capacity of the wooden piles are discussed.

For the concrete piles also there is little difference between the 1st and the 2nd load tests. Piles 1B-B1 and 1B-B3 could not be loaded up to their ultimate bearing capacity ($\delta_{10\%} = 35 \text{ mm}$). This was because owing to safety regulations (stability of the ballast frame) the maximum load was restricted to 4300 kN. The measured values of the ultimate bearing capacity of the concrete piles are much higher than the predicted values. No explanation has been found for this result.

3.10.4 Observed Differences in Ultimate Bearing Capacity of the Wooden Piles

The most obvious reason for the differing results for the wooden piles at location B and C compared to location would be different CPT values at these locations. However, because sufficient CPTs were carried out at the pile locations, it could be concluded that no significant differences between CPT values occurs. It also seems unlikely that damage was inflicted upon the piles during driving, because the difference between the results at location A and locations B and C is consistent.

The reason that remains, is that during the extensive settlement at location C north of the frame (Table 3.6) and the settlement at the centre, the negative shaft friction on the piles in these locations increased. Subsequently, because of the large settlement compared to the limited displacements during the load tests, the positive shaft friction in the soft soil layers could not be mobilised. This more-or-less corresponds with the fact that the average ultimate bearing capacity of the wooden piles at location C

TEST SET-UP & CONSISTENCY CHECK

(177 kN) approximates the predicted pile toe resistance (199 kN; Table 3.3). The alternative and favoured explanation is therefore that ground settlement near location C reduced the shaft capacity of the piles.

Table 3.5 Bearing Capacity Tests 1 and 2 of the Wooden and Concrete Piles

	Pile code	Displacement	Pile Load Test 1	Pile Load Test 2	Δ Load
		S_l (mm)	F_1 (kN)	F_2 (kN)	$(F_2-F_1)/F_1$ (%)
Location A	1A-H1	12	300	330	10
	1A-H2	12	240	250	4.2
	1A-H3	12	320	310	-3.1
	1A-H4	12	250	310	24
	1A-H5	12	290	250	-14
	1A-H6	12	240	240	0.0
	1A-H7	12	310	310	0.0
	1A-H8	12	270	270	0.0
	1A-H9	12	190	200	5.3
	Average	12	268	274	2.9
Location B	1B-H1	12	200	200	0.0
	1B-H2	12	180	190	5.6
	1B-H3	12	190	160	-5.3
	Average	12	190	183	0.1
	1B-B1	27	4300	4300	0.0
	1B-B2	35	4100	3900	-4.9
	1B-B3	30	4300	4150	-3.5
	Average	31	4233	4117	-2.8
Location C	1C-H1	12	190	190	0.0
	1C-H2	12	180	180	0.0
	1C-H3	12	170	170	0.0
	1C-H4	12	180	180	0.0
	1C-H5	12	170	160	-5.9
	1C-H6	12	170	170	0.0
	Average	12	177	175	-1.0

Since not all the dead weight of the ballast frame was used to load the piles during the load tests and grouting stage, some of the load was transferred to the soil under and near the frame. While the underlying Holocene deposits (peat and clay layers) were known to be sensitive to changes in stress, some consolidation effects were expected. The first two weeks, during which primary consolidation took place, had a significant and surprisingly irregular effect on the position of the frame (Table 3.6). Because of the rather uniform soil conditions at the site and the relatively uniform load distribution of the frame, it was not expected that the settlement would show such an irregular pattern. The possible explanation for the irregularity of ground movements is a variation in the compressibility of the peat

TEST SET-UP & CONSISTENCY CHECK

layers on the north side and on the south side of the frame. No extensive soil investigation was conducted on the Holocene layers and this remains an assumption.

Table 3.6 Vertical Displacement of the Four Corners of the Ballast Frame (mm)

Date	NW Corner	NE Corner	SW Corner	SE Corner
08-07-1999	0	0	0	0
12-07-1999	-26	+16	-5	0
14-07-1999	-35	-20	-6	+2
19-07-1999	-65	-36	-13	+3
20-07-1999	-68	-37	-14	+2
21-07-1999	-70	-40	-15	-1

3.11 Conclusions and Recommendations

Regarding the test set-up and the consistency of the monitoring data the following conclusions and can be drawn and recommendations can be made.

- Installation of the SMS and piezometers in the wooden piles was unsuccessful. This was probably related to effects pile driving had on the cabling. It is recommended that for future applications the cables should be placed in a shaft containing a more-or-less flexible material, thus creating a less rigid connection than that used in this test. The use of SMS and piezometers in the concrete piles was however a success.
- The effective stress measurements using the SMS gave absolute value readings that were too low. Total stress changes however could be monitored.
- The piezometers functioned well during the test. Both the absolute pore water pressures and the pressure changes due to grouting activity could be satisfactorily monitored. Since this is a relatively cheap monitoring tool, its use is recommended.
- The load cells that were used to measure the load on the pile head proved to be sensitive to temperature fluctuations. Load fluctuations had a negligible influence on the pile settlement during the test activities.
- The jointmeter readings and the target readings are of the same magnitude ninety percent of the time. However it was extremely useful and therefore recommended for similar tests to use both the jointmeter and the (automatic theodolite) target measurements.
- There were quite a number of difficulties correcting the jointmeter readings for ballast frame displacement. More automatic theodolite measurements would have been useful.
- The performance of two load tests before grouting proved to be valuable. By this means it was observed that the ultimate bearing capacity of some of the wooden piles had been diminished, probably due to unexpected large ground settlement around the ballast frame, and thus the load steps could be adjusted.
- The test results complied with the NEN 6743 method for calculating the ultimate bearing capacity of most of the wooden piles. With regard to the concrete piles, the calculated NEN 6743 method values significantly differed (underestimation of their capacity) from the test results.

Chapter 4 PERMEATION GROUTING

4.1 Introduction

During the permeation grouting process, the pores in the soil are filled with an injection fluid or *grout*. Permeation grouting induces changes in the soil properties, making it stiffer and stronger without, when properly executed, disturbing the structure of the soil. Because little is known of the effect permeation grouting has on pile foundations, a test was conducted. The general set up of this Full-Scale Injection Test was explained in Chapter 3. This chapter deals with permeation grouting: Stage 2 and Stage 3A of the test. To facilitate understanding of this chapter a list of grouting vocabulary is enclosed in APPENDIX I.

Permeation grouting is the oldest of the grouting techniques dealt with in this thesis. To start with, the history, main characteristics and fields of application of the permeation grouting system are outlined. Subsequently some models that describe the relation between permeation grouting parameters and soil parameters are discussed. To examine the groutability of the Amsterdam soil*, different types of grout were injected and the results were monitored, leading to the determination of an optimum grout for the Amsterdam soil. To investigate the effects on the foundations and the soil near pile foundations, the differential displacements of the soil and piles, the bearing capacity of the piles, the soil stresses and the pore water pressures had to be considered. The main part of this chapter discusses the effects of permeation grouting on pile foundations.

4.2 Permeation Grouting Technique

4.2.1 History

The first known application of “Permeation” Grouting dates from 200 years ago. The French Engineer Charles Berigny in 1802 used a suspension of water and puzzuolana cement to fill up the cavities in the foundation of a sluice in Dieppe, that had been damaged by settlement. In this way alluvial deposits were simultaneously sealed and stabilised. He named this treatment ‘procédé d’injection’. After that, in the 19th century, injection was mainly used in mining applications (Glossop, 1960). The first application of Portland Cement Injection dates from 1839, when Collin used injection to fill fissures in the masonry of the Grosbois Dam in France (Nonveiller, 1989). From 1900 onwards grouting equipment was constantly improved. The introduction of hydraulically driven, high pressure pumps and manometers led to increasing control over pumping pressures and grout flow.

The first known application of permeation grouting using a sodium silicate (gel) dates from 1886 (Jeriorsky patent). In 1909 Lemaire en Dumont patented a single-shot system based on a dilute silicate and acid solution, which however, gave too many practical problems to be applied (Karol, 1983). The Dutchman Joosten solved the practical problems in 1925 by developing an ingenious method for the treatment of sands, in which small volumes of concentrated sodium silicate were injected in stages through a perforated pipe as the pipe was driven to required depth (Littlejohn, 1985). During withdrawal of the pipe a strong calcium chloride solution was injected transforming the soil into “impermeable” sandstone. This system was extensively used when constructing the Berlin underground in 1930.

The next milestone in grouting history was the invention of the tube-à-manchette (TAM) by Ischy in 1933. His invention permitted grouts of different properties to be injected in any order and at any interval of time from the same borehole. Shortly after that, Mayer (1934) developed a one-shot silicate,

* the term Amsterdam soil is used here to indicate the typical soil profile that is found in the centre of Amsterdam

in which gelling was controlled, thus counteracting the disadvantages of the laborious *two-shot* Joosten procedure.

From the 20th century onwards, engineers also started to approach grouting in a more scientific manner. In 1902 a congress on grouting was held during which engineers discussed the effect the number of injection points and the grouting pressure have on the results. The first large-scale permeation grouting stabilisation using cement was applied during the construction of the Hoover Dam from 1932 to 1936. This project made a large contribution to knowledge on grouting.

During the 1939-45 war the development of practical grouting applications was largely halted. However from then on there was a dramatic increase in the development of all sorts of new chemical formulations (mostly resins). Most important was the patent of Mello, Hauser en Lambe in 1953, concerning the acrylate of polyvalent metal (AM-9). This soft gel grout had a viscosity only slightly higher than that of water and thus could also be used in silty soils and it possessed excellent gel time control. In about 1980, this system was replaced by less toxic grouts like AC-400. The disadvantage of these resins is that they are very expensive compared to cement and silica gels. Therefore they are usually only used for the renovation of masonry. Soletanche in 1957 developed a hard silicate gel, using an organic ester, producing strengths of 2-3 MPa in sands.

From the 1980s, the widespread use of permeation grouting for stabilisation purposes was largely discontinued in favour of other techniques, mainly because of problems arising from public opinion about the pumping of chemicals into the ground (because of environmental concerns). This contributed to the development of jet grouting and also to the use of fine cements (micro-cements) for permeation grouting. Important research concerning micro-cement properties has been performed by De Paoli (1992b).

Nowadays both silicate gels and as micro-cements are used on a large scale to stabilise soil and create grouted soil layers with low permeability.

4.2.2 Grouting Equipment

Permeation grouting equipment usually comprises:

- the drilling rig;
- the injection unit (mixing and grouting plant);
- double packers and tubes-à-manchette.

The injection unit consists of storage facilities for grout and other materials, a mixing plant and several high-pressure grout pumps. Usually four or six pumps, the controls and the monitoring equipment are placed in a container (Figure 4.1).

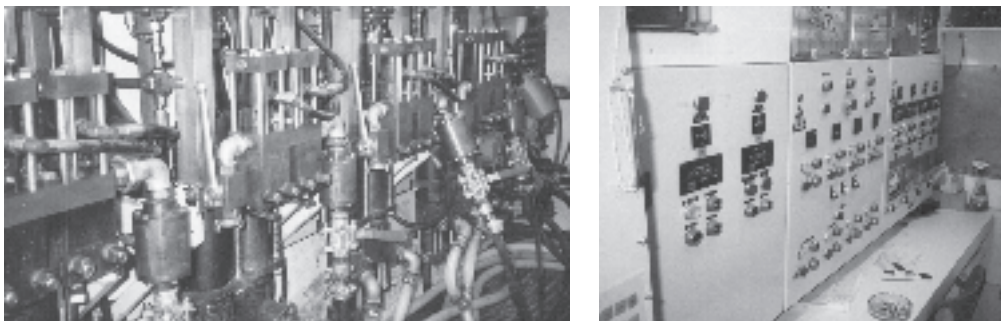


Figure 4.1 Injection Unit: Pumps (left) and Controls & Registration Equipment (right)

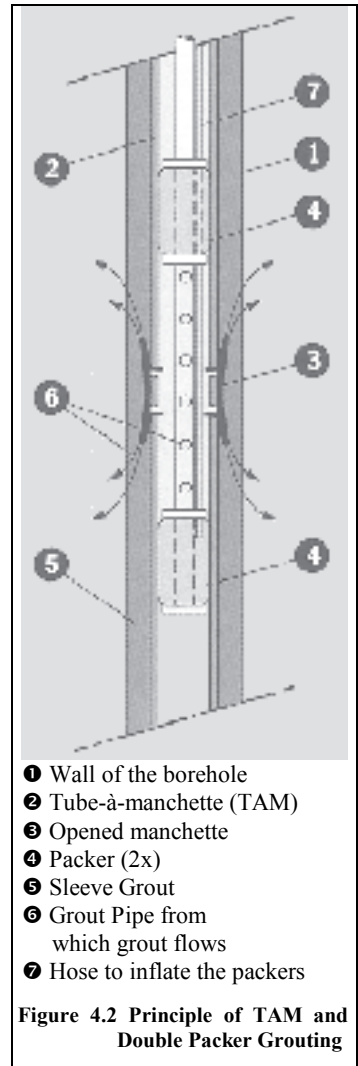
Nowadays usually tubes-à-manchette (TAMs) are used for injecting the grout. This so called *TAM grouting* or *sleeve-grouting* method involves the following operations (Figure 4.2):

- drilling a circa 100 mm diameter hole in the soil and bottom-up filling of the hole with a cement-bentonite *sleeve grout*;
- placing the tube-à-manchette; the TAM is a PVC pipe (usually with a diameter of 50 mm) perforated with rings of small holes at specified (usually 330 or 500 mm) intervals. In most cases, each ring of perforations is enclosed by a short rubber sleeve fitting tightly around the pipe so as to act as a one-way valve;
- leaving the sleeve grout time to gain sufficient strength (circa 1 MPa);
- using a double packer (Figure 4.3) to grout each sleeve individually; the double packer is a device consisting of a pair of inflatable rubber seals with a grouting pipe in-between; the packers are fixed just above and below a manchette and inflated, after which grout is injected under pressure; the grout opens the rubber sleeve and cracks the sleeve grout; when the injection is stopped the rubber sleeve closes again, thus preventing the injected grout from flowing back into the TAM;
- rinsing the TAM with water so it can be re-entered to perform injection of another sleeve at a different location or re-injection of the same sleeve.

In specific poor soil conditions and when drilling horizontally or inclined, the drilling of the hole can be performed by using a casing. The TAM is then placed in the casing and the sleeve is filled with bentonite-cement, after which the casing is withdrawn.



Figure 4.3 Double Packer



4.2.3 Grout Types

Introduction

There are many detailed publications about the different types of grouts and their properties. Here only the basic types of grouts will be characterised; for more information reference should be made to Littlejohn (1985), Nonveiller (1989), Van der Stoel (1997) and Kutzner (1996). Primarily, a distinction can be made between grouts used to stabilise soil and grouts used to reduce soil permeability. As far as gels are concerned, the first category is usually indicated as hard gels, the latter as soft gels. For improvement of the foundation bearing capacity only the stabilising grouts are of interest.

Depending on the intended function of the grout, the *ideal* grout should live up to the following criteria:

- be non toxic/non aggressive/non explosive, not harmful to personnel and material
- give a stable reaction/react stable and not cause any environmental pollution when hardened;
- be soluble in water (so the grout can be mixed with water on site and transport costs can be reduced);
- keep well for an unlimited time independent of storage conditions;
- have chemical reactions that are independent on soil conditions;
- have low viscosity (equal to water) before hardening;
- have a controllable gel time
- be easy to mix;
- have no degeneration with time;
- have good strength and stiffness properties.

Obviously no grout that meets all these qualifications has yet been developed (and probably never will be). However, developments will continue, or as Littlejohn (1985) once postulated: “*However, there is still no relaxation in the quest by Scottish civil engineers for a single fluid grout with the viscosity of water and strength of concrete, where water is the most expensive constituent*”.

To be able to understand the different behaviour of the various grout types, it is necessary to focus somewhat more fundamentally on the composition and rheological properties of the grout.

Grout Composition

A *solution* is defined as a liquid formed by completely dissolving a chemical in water to give a uniform fluid without solid particles. Solutions are Newtonian liquids without rigidity and harden in a predetermined period of time, called the ‘setting time’. They can be either true or colloidal solutions. In the case of colloidal solutions, large molecules are contained in the liquid.

A *suspension* is a mixture of liquid and solid materials. It behaves as a Bingham fluid during flow, possessing both viscosity and cohesion (yield strength). Particulate suspensions contain particles larger than clay size, while colloidal suspensions contain particles of clay size. Unstable suspensions will separate into their components, after which their behaviour will become unpredictable.

The *viscosity* is defined as the internal fluid resistance of a substance that makes it resist a tendency to flow. A distinction is made between kinematic viscosity, ν , and dynamic viscosity, η , for which: $\nu = \eta/\rho$, where ρ = density. *Newton fluids* are purely viscous fluids, which means they have a shear rate (τ) based on a constant viscosity: $\tau = \eta \cdot \dot{\gamma}$, where

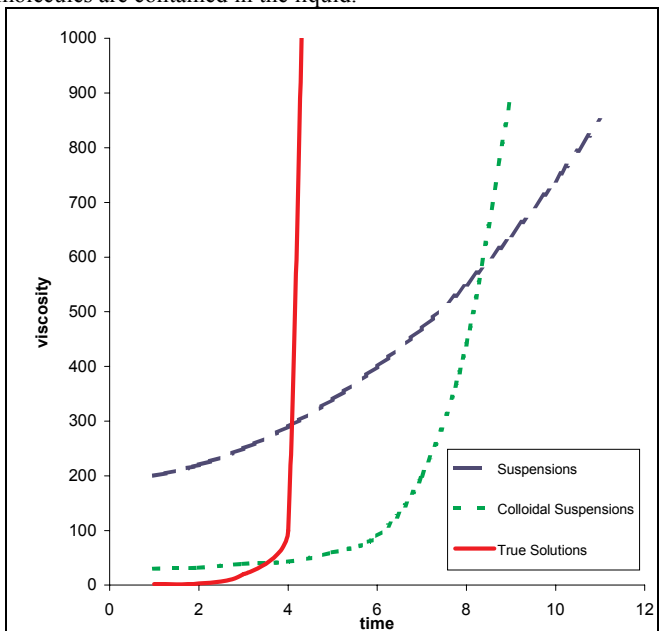


Figure 4.4 Viscosity Development in Time

$v_t (=dv/dx)$ is the shear gradient. *Bingham fluids* have a static yield point which can be considered as cohesion (τ_0), after which linear deformation occurs: $\tau = \tau_0 + \eta_p \cdot v_t$ where η_p is the plastic or apparent viscosity (De Paoli et al, 1992a).

A distinction between grouts can be made based on grout composition and rheology:

1. True solutions;
2. Colloidal solutions;
3. Suspensions.

- Re.1 True solutions have almost no interchange between the dissolved molecules. The dissolved product and the water cannot be separated mechanically. True solutions have a very low viscosity, which remains almost constant until hardening occurs (extremely rapidly). Hardening takes several seconds to about an hour (Figure 4.4). Resins and silica gels resort under this category.
- Re.2 Colloidal is a definition used for particles that are bigger than a molecule and smaller than particles in a suspension ($0,001 \mu\text{m} < d < 0,1 \mu\text{m}$). The viscosity of colloidal solutions varies with the additive used, is low to start with and gradually increases during hardening, which takes several minutes to hours (Figure 4.4). Micro-cements fall into this category.
- Re.3 Suspensions are a mixture of a fluid (water) and a solid, with solid particles having a diameter (d) of $0,1 \mu\text{m}$ to $1 \mu\text{m}$. The viscosity of suspensions drastically increases during hardening and it takes several hours to days (Figure 4.4) for the product to gain sufficient strength. Clay-, bentonite- and cement suspensions are used most frequently.

In addition, for suspensions a qualification can be made based on grout stability, distinguishing:

1. stable suspensions;
2. non-stable suspensions;
3. thixotropic suspensions.

- Re.1 In stable suspensions, the grout will keep flowing as long as the flow caused by the grouting pressure is not exceeded by the retardation of this flow caused by the viscosity. In 2 hours stable suspensions exhibit less than 5 per cent bleeding of clear water at the top of a 1000 ml cylinder with an internal diameter of 60 mm at a temperature of 20°C. For stable suspensions the injection pressure also causes syneresis: the stress independent expulsion of liquid (generally alkaline water) from a set (hardened) gel, accompanied by a contraction of the gel. Syneresis occurs over a period of a few months.
- Re.2 With unstable suspensions the precipitation of the solids fills the pores of the soil and blocks them. The overpressure that is thus created causes further consolidation of the soil.
- Re.3 Fluids that show an increase in apparent viscosity with time are called thixotropic (for instance bentonite suspensions). Thixotropy is common in non-Newtonian grouts. Thixotropy is the property of a material that enables it to stiffen in a relatively short time on standing, but upon agitation or manipulation change to a very soft consistency or to a fluid with high viscosity. This process is fully reversible, i.e. the viscosity of thixotropic fluids decreases with increasing shear rate and returns to its initial value after a time of regeneration. The grout should therefore preferably be fully processed before it starts stiffening.

Grout Types

In engineering practice, a general distinction can be made between the following main grout types:

1. cement grouts;
2. microfine cement grouts;
3. silica gels;
4. resins.

However, it should be noted that in the last three decades many complex grout types have been presented, almost all of which fall into one of the above mentioned categories.

Re.1 Cement Grouts

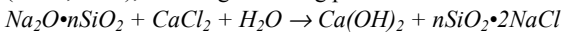
Cement grouts are suspensions with relatively large grain size diameters. The maximum grain size is 0.1 mm and at least 90% of the particles should be < 0.05 mm. The specific surface should be $\geq 3000 \text{ cm}^2/\text{g}$. The grout behaves as a Bingham fluid. Cement grouts with a low wcr^* have high strength but are hard to process and vice versa. Liquefiers increase the processability, making such a grout behave more like a Newton fluid (bleeding decreases, low sedimentation and consistent grout element). Sodium silicate can be used to accelerate hardening (quick set grout).

Re.2 Microfine cement grouts

Microfine cement grouts are colloidal solutions with relatively small grain size diameters. The d_{95} of the cement is reduced considerably by milling the cement and thus further pulverising the solids. The maximum grain size is 0.02mm and at least 90% of the particles should be < 0.016 mm. The specific surface should be $\geq 10000 \text{ cm}^2/\text{g}$. The micro-cement grout behaves like a Newton fluid. The high specific surface makes the strength and the viscosity increase. To reduce viscosity, additives in the form of specially developed liquefiers for micro-cement should be used. Sodium silicate can be used to accelerate the hardening.

Re.3 Silica-gels

These true solutions generally consist of a sodium silicate dissolved in water mixed with an inorganic (sodium aluminate) or an organic (various esters) hardener. The first silica-gel was patented by Joosten (Karol, 1983), and the gel forming process can be described as follows:



The SiO_2 influences the mechanical properties of the gel, a higher silica level results in a stronger gel. The Na_2O is the constituent neutralised to cause gelation. The modern silica-gel grouting processes consist of mixing the silicate with a hardener prior to injection. After the grout has permeated the soil, its components react to form a silica gel matrix, which locks the soil particles together, thus stabilising the soil. Hard-gel (50-60% sodium silicate, 8-10% hardener, 30-42% water) viscosity initially lies in the range of 10 – 200 cP^\dagger . The silica gel behaves like a Newton fluid. The strength of the gel is determined by the silica content and by the type and amount of hardener, which in turn determines the degree of alkali neutralisation. A strong gel requires at least 70% Na_2O neutralisation.

Re. 4 Resins

Many different types of resins exist, which all have in common that they are true solutions. Resin viscosity generally lies in the range of 2 – 10 cP . Resins behave like a Newton fluid. Generally shrinkage is relatively high, resulting in moderate strength properties. Because of their toxicity acryl amide and lignosulfonate resins, like AM-9, have not been used in soil for decades. Other types of resins that are still applied are: PMA (polymethyl acrylates), phenoplasts, aminoplasts and polymers (foaming materials).

Almost all grouts have considerable water content. A verification of the water quality should always be conducted in advance. The pH value is the most important test parameter, because acidity influences the grout setting time. When $6 < \text{pH} < 8$ this influence is negligible. In most circumstances tap water is suitable for application.

4.2.4 Field of Application: Groutability

The groutability of the soil is dependent on the flow properties of the grout and on the soil properties. The grout flow properties for true solutions are usually expressed by describing the development of grout viscosity. The soil parameter that is determinative for the soil's groutability is the coefficient of permeability k (m/s). This coefficient can be determined by using an in situ permeability test or by

* water cement ration

† centiPoise : a measure for the viscosity, water at 20 °C has a viscosity of $1 \text{ cP} = 1 \cdot 10^{-6} \text{ m}^2/\text{s}$

analysing the grain size distribution of the soil. When the soil is suitable to be injected and more or less isotropic, grout will spread equally in all directions when leaving the point of injection.

For suspensions and colloidal solutions, the degree of groutability is often expressed by the groutability ratio (I or GR). The groutability ratio expresses the relationship between the particle size of the grout and the grain size of the soil to be grouted. Three relations are explained here:

1. D_{10}/d_{95} ratio;
2. D_{15}/d_{95} ratio; D_x = soil grain size diameter (x mass % of the soil particles smaller than D);
3. D_{15}/d_{85} ratio; d_y = grout grain size diameter (y mass % of the grout particles smaller than d).

Re.1 A much-used relationship in “the early days” was: $d_{95;grout} \leq \frac{1}{10} D_{10;soil}$. Research by the ACSE (Task Force 27, 1995) has refined this:

$$\text{eqn. 4.1 : } I = \frac{D_{10;soil}}{d_{95;grout}}$$

with:

- $I > 11$ grouting possible;
- $6 < I < 11$ grouting doubtful;
- $I < 6$ grouting impossible.

Re. 2 This relation was published by Mitchell (1970):

$$\text{eqn. 4.2 } I = \frac{D_{15;soil}}{d_{95;grout}}$$

Weaver (1990) has given criteria for using this relation:

- $I > 24$ grouting possible;
- $19 < I < 24$ grouting difficult;
- $11 < I < 19$ grouting doubtful;
- $I < 11$ grouting impossible.

Re. 3 Sherard et al. (1984) and Perbix et al. (1995) give the relation:

$$\text{eqn. 4.3 : } I = \frac{D_{15;soil}}{d_{85;grout}}$$

with (according to Sherard et al.) grouting being possible for $I > 20$ and (according to Perbix et al.):

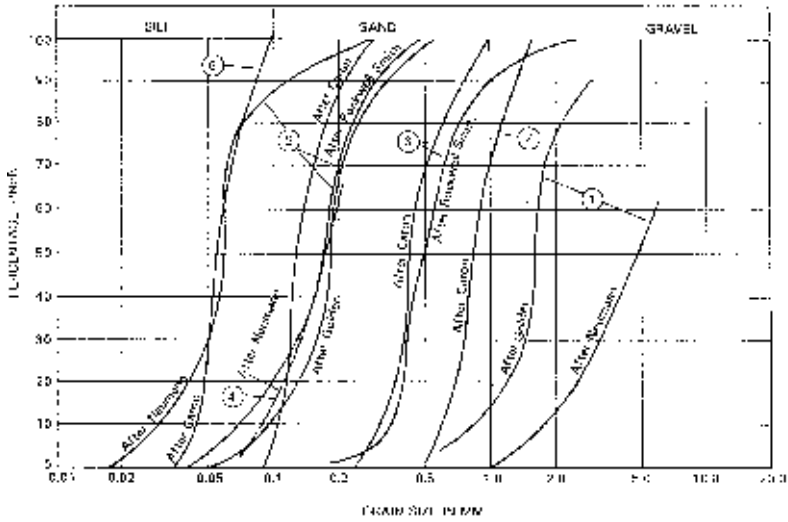
- $I > 24$ grouting possible;
- $11 < I < 24$ grouting doubtful;
- $I < 11$ grouting impossible.

All three relations have a similar character and can well be used for preliminary estimation of the groutability.

However, the relation between the grain size distribution of the soil and the groutability can also be expressed by using a diagram such as that shown in Figure 4.5 and

Figure 4.6, especially when the soil that has to be grouted contains a high percentage of fines. The diagram in Figure 4.5 only shows the lower limits of the grain size distribution; no mention of upper limits to the grain size distribution has been found. This is particularly curious because when the permeability is high and the grout has very low viscosity, it will easily flow away from the injection point because of the different densities of the pore-water and the grout. Groundwater-flow can then also be a disturbing factor. The diagram is especially useful to illustrate the large differences between the limits as indicated by the various researchers.

PERMEATION GROUTING



① Cement ② Clay Cement ③ Clay ④ Joosten Process ⑤ Silicate Gel ⑥ Bitumen-Resin Solution

Figure 4.5 Groutability Based on Grain Size Distribution (Covil, 1991 (after Cambefort, 1964))

The diagram shown in Figure 4.6 is considered representative for the Dutch limits for applying permeation grouting. The grain size distribution of the Amsterdam soil layers is incorporated in the figure.

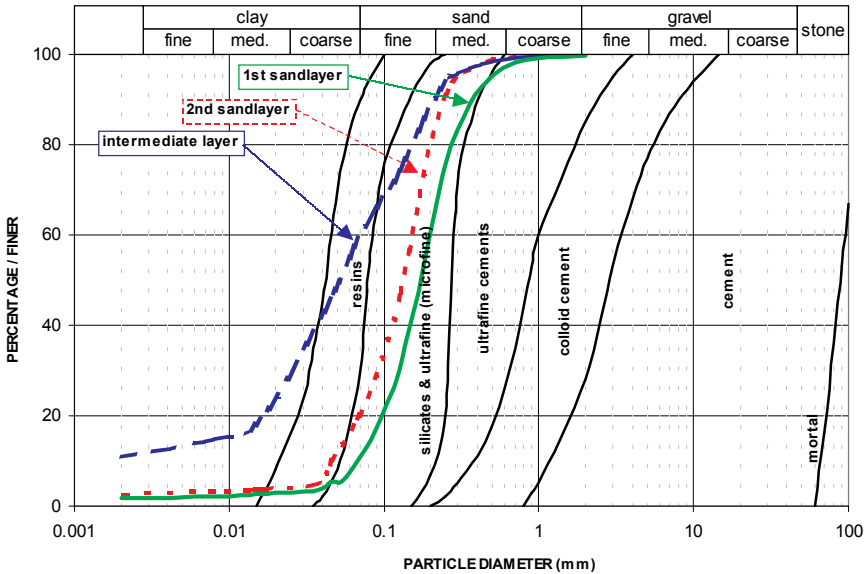


Figure 4.6 Groutability Based on Grain Size Distribution (after Tausch, 1985)

The groutability of the soil is to a lesser extent also influenced by injection pressure, flow rate, gel time and the presence of groundwater. In very fine sand or clay in particular, the presence of groundwater

complicates grouting. Grouting pressure, flow rate and gel time can generally be adjusted to the grout type used and to the soil.

4.2.5 Grouting Pressure

Pumping pressures used for permeation grouting vary in the different soil types. Several rules of thumb apply for the maximum pressure to be used, which all relate to the distance between the point of injection and the surface:

- Europe: $p_{max} = 1$ bar/m;
- US: $p_{max} = 0.22$ bar/m (=1 psi per foot);
- China: $p_{max} = 2$ bar/m.

Other rules of thumb are that the grouting pressure should be approximately 2 to 2.5 times the overburden pressure at injection depth and that the product of grouting pressure (p_{max} ; bar) and grout flow (Q_{max} ; ℓ/min) should preferably not exceed 20:

eqn. 4.1 $p_{max} * Q_{max} \leq 20$.

Note that the big differences in the rules of thumb and the obvious lack of correlation with soil parameters limit their value. However, at all times it is essential to ensure that the grouting pressure does not lead to fracturing (i.e. exceed the limit where the effect will be that the shear strength of the soil is overcome and the soil above the grouted element is lifted). Grouting pressures in soil generally do not exceed 5.0 MPa; normal grout flow is 4 to 10 ℓ/min (i.e. 1 m³ of soil with a 35% pore volume takes ½ - 1½ hours to grout).

4.2.6 Grouting Pattern

When designing a grouted structure much attention should be paid to selecting the right distance between the individual grouting elements, that is the distance between the tubes-à-manchette. The principle of permeation grouting techniques is that by grouting alternate holes, the finer pores are also permeated and because they overlap a better connection between the individual grouted elements is created. In Figure 4.7 an example of the overlap during TAM grouting is shown. Because the Stage 2 grouted element is confined between the two Stage 1 elements, the grout propagates along the Stage 1 elements, thus creating a more or less vertical column instead of an accumulation of spheres.

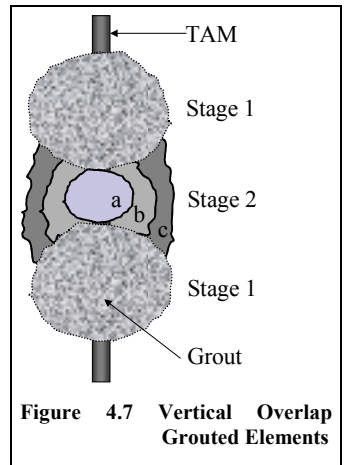


Figure 4.7 Vertical Overlap Grouted Elements

4.3 Modelling Permeation Grouting

4.3.1 General

To examine the influence of permeation grouting on a foundation pile, first it is necessary to understand how the injection process parameters and the initial soil conditions correlate. Some theoretical modelling can demonstrate this.

Aspects that are not considered in these models are:

- the influence of soil heterogeneity and anisotropy; this sometimes causes the grout elements to look like “Christmas trees” rather than spheres or cylinders;
- the occurrence of fractures due to a combination of the influence of soil heterogeneity and anisotropy and not being able to control the grouting pressure adequately; instead of permeation grouting a sort of general soil improvement including fracturing will occur.

It must therefore be realised that permeation grouting is a technique so complex that modelling only serves the purpose of increasing understanding the process. The models are not designed for use in engineering practice.

4.3.2 Empirical Modelling

When the viscosity of the grout is low enough, and the grouting pressures are well controlled, no cracking of the soil will occur. The grout flow can then be modelled by using empirical fluid mechanics laws, like the Hagen - Poiseuille law for laminar flow ($Re < 500$) through a cylindrical body:

$$\text{eqn. 4.4 : } V = \frac{\pi \cdot g \cdot \Delta p \cdot r^4 \cdot t}{8 \cdot L \cdot \nu}$$

with:

V	=	grout-take	(m ³);
Δp	=	pressure-gradient between the extents of the cylinder	(m);
r	=	radius of the cylinder (i.e. pore diameter)	(m);
t	=	time	(s);
L	=	length of the cylinder	(m);
g	=	acceleration of gravity	(m/s ²)
ν	=	kinematic viscosity of the grout	(m ² /s).

This relation suggests that the grout take is highly dependent on the pore diameter. A similar approach to determining the minimum grouting pressure required, has been performed by Gelbert (1972) who determined the critical gradient I_0 (at which grout flow halts) to be:

$$\text{eqn. 4.5 : } I_0 = \frac{8\tau_0}{3r_p \gamma}$$

with:

τ_0	=	initial viscosity, yield point	(kg m ⁻¹ s ⁻²)
γ	=	unit weight of the grout	(N/m ³)
r_p	=	equivalent pore radius	(m)

4.3.3 Analytical Modelling

An analytical approach to analysing spherical grout flow, pressure and time in a porous medium was proposed by Maag (1938) and later on extended by Raffle & Greenwood (1961). It is explained here.

Definition of symbols:

v	=	grout flow velocity	(m/s)
Q	=	Rate of flow	(m ³ /s)
ν^*	=	ratio of the grout viscosity = $\frac{\nu_{grout}}{\nu_{water}}$	(-)
k	=	permeability	(m/s)
i	=	hydraulic gradient	(-)
p	=	net grouting pressure	(N/m ²)
r	=	radius of the grout element	(m)
r_0	=	radius of the injection source	(m)
R	=	radius of the grout element at time t	(m)
t	=	time elapsed since starting grouting	(s)
p_0	=	grouting pressure equalling the ground water level	(N/m ²)
p_I	=	total grouting pressure	(N/m ²)
h	=	required grouting head	(m)
e	=	void ratio	(-)

The grout flow velocity can be expressed by:

$$\text{eqn. 4.6 : } v = \frac{Q}{A_{\text{sphere}}} = \frac{Q}{4\pi r^2}$$

$$\text{eqn. 4.7 : } v = \frac{1}{v^*} ki = -\frac{k}{v^*} \frac{dp}{dr}$$

Combining eqn. 4.6 and eqn. 4.7 and integration from r_0 to R and p_0 to p_1 with $h = p_1 - p_0$, $i = -h/r_0$ and initial condition $Q = vA = ki4\pi r_0^2 / v^*$ gives the grout pressure (h):

$$\text{eqn. 4.8 : } h = \frac{Q}{4\pi k} \left[v^* \left(\frac{1}{r_0} - \frac{1}{R} \right) + \frac{1}{R} \right]$$

Note that in practice the pressure at the pump should be corrected for the pore water pressure and friction losses in the hoses and/or pipes.

The velocity at which the grout element expands can be expressed by:

$$\text{eqn. 4.9 : } \frac{dR}{dt} = \frac{Q}{4\pi R^2 e}$$

Combining eqn. 4.8 and eqn. 4.9 gives:

$$\text{eqn. 4.10 : } \frac{dR}{dt} = \frac{hk}{e} \left(v^* R^2 \left(\frac{1}{r_0} - \frac{1}{R} \right) + R \right)^{-1}$$

By means of the integration of this equation, an expression for the required injection time (t) for creating a grouting element with radius R can be obtained:

$$\text{eqn. 4.11 : } t = \frac{er_0^2}{kh} \left[\frac{v^*}{3} \left(\frac{R^3}{r_0^3} - 1 \right) - \left(\frac{v^* - 1}{2} \right) \left(\frac{R^2}{r_0^2} - 1 \right) \right] \quad (\text{Raffle \& Greenwood, 1961})$$

When the second term between the brackets is neglected the expression simplifies to:

$$\text{eqn. 4.12 : } t = \frac{ev^*(R^3 - r_0^3)}{3khr_0} \quad (\text{Maag, 1938})$$

In Figure 4.8 the relation between the dimensionless parameters R/r_0 and kht/er_0^2 is shown for different values of the ratio of the grout viscosity v .

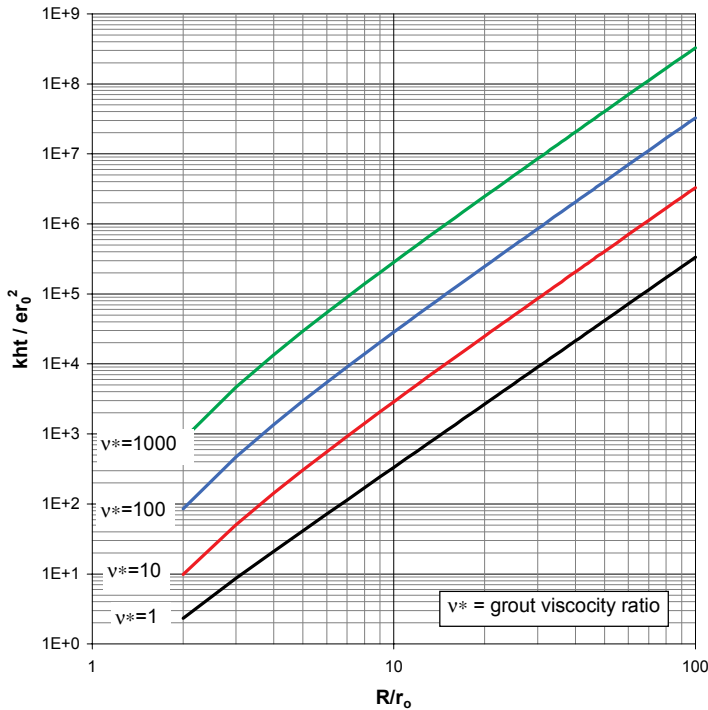


Figure 4.8 Relation between the Dimensionless Parameters R/r_0 and kht/er_0^2 for Different v

4.3.4 Model Applied to the Amsterdam Situation

The Raffle & Greenwood model was applied for the Amsterdam situation to get an indication of the grouting pressures needed and the grouting time. The invariable parameters (obtained from the Noord/Zuidlijn SI Program) used are: $v^* = 10$ (-); $k = 5 \cdot 10^{-5}$ (m/s); $e = 0.5$ (-) and $r = 0.01$ (m). The diameter of the grouted elements that had to be constructed in the test varied between 0.80m and 1.00 m ($0.4 \text{ m} < R < 0.5 \text{ m}$).

In Figure 4.9 the relation between the grouting pressure (h) and the radius of the grouted element (R) is shown for different values of the grout flow (Q). From this figure it can be seen that the necessary grouting pressure will vary between 1.0 MPa and 3.5 MPa.

In Figure 4.10 the relation between the grouting time (t) and the radius of the grouted element (R) is shown for different values of the grouting pressure (h). From this figure it can be seen that the necessary time for grouting pressures between 0.25 MPa and 2.0 MPa, will vary between 15 minutes and 5 hours.

4.3.5 Conclusions

From grouting practice it is known that permeation grouting pressures in soil generally do not exceed 5.0 MPa. Using the Raffle & Greenwood model for grout with a viscosity of 10 cP and a grouting pressure of 5.0 MPa results in an expected grouting time of about 2 hours for a grouted element diameter of circa 1m. Grout flow is then circa 8 ℓ/min. When the viscosity of the grout is doubled to 20 cP, this results in grouting times up to 5 hours. Because these grouting times are unrealistically long, the conclusion is that the models increase the understanding of the grouting process rather than that they can be used for engineering practice.

PERMEATION GROUTING

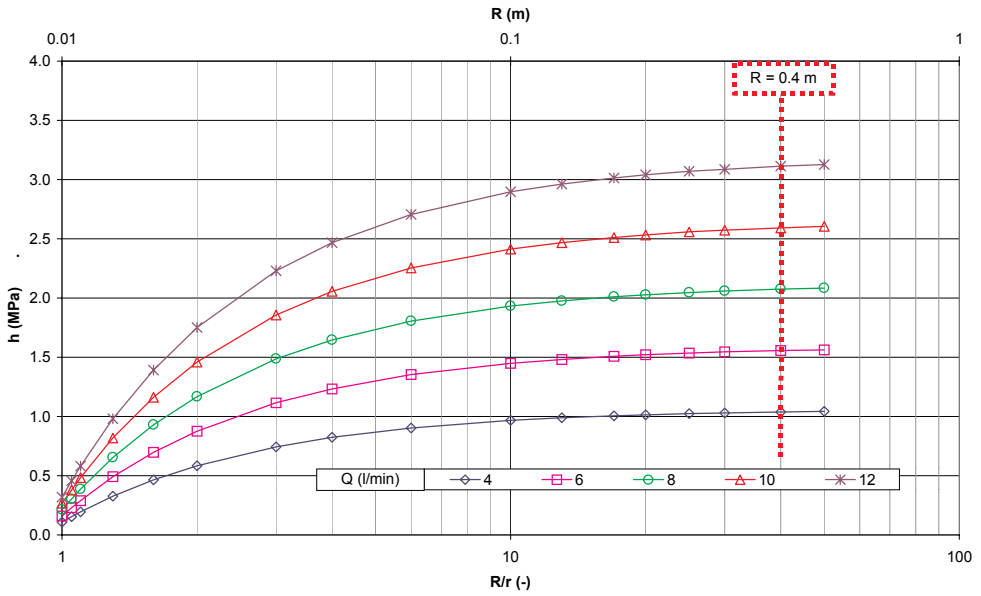


Figure 4.9 Relation between Grouting Pressure and Radius of the Grouted Element

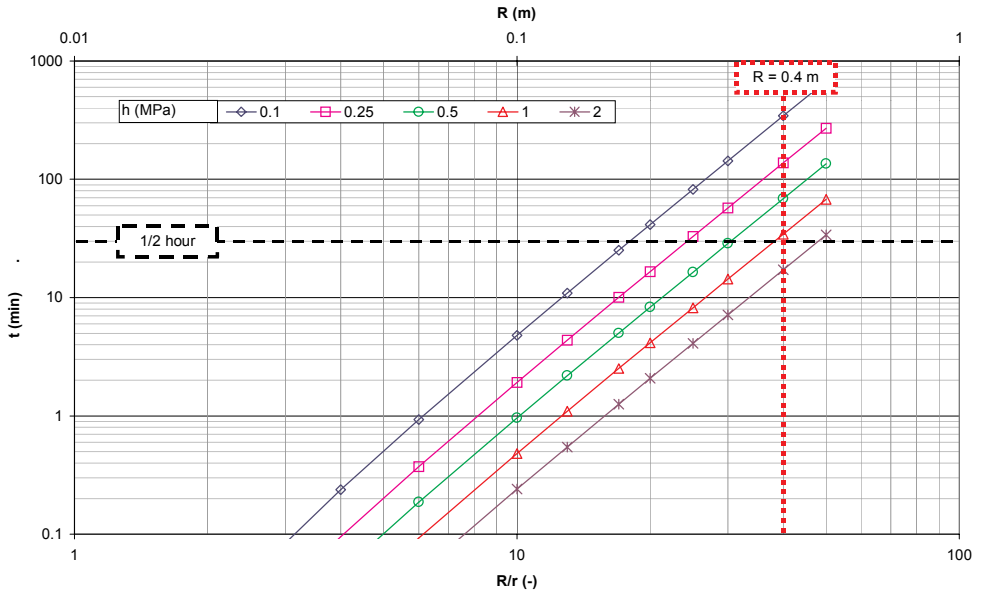


Figure 4.10 Relation between Grouting Time and Radius of the Grouted Element

4.4 Literature References on Grout Strength

It is often overlooked that for good stabilisation **not all** the pores in the soil have to be permeated with grout. This is confirmed by research done by Gularte, Taylor & Borden (1992) and Kutzner (1996). Based on experiments, the latter proposed the relation shown in Figure 4.11. Note that for reducing the soil permeability the percentage of pores in the soil that has to be permeated with grout is much more important.

Krizek (1992) concluded that for over-consolidated, grouted soil the orientation of the sample plays a role when determining the Unconfined Compressive Strength (UCS). The strength of the sample was found to be higher when it was tested perpendicular to the direction of sedimentation.

Few efforts have been made in the field of predicting the strength of grouted samples.

Because soil conditions are neither homogeneous nor isotropic this seems logical. Yonekura & Kaga (1992) have deduced a semi-empirical relation from tests on stabilised sands:

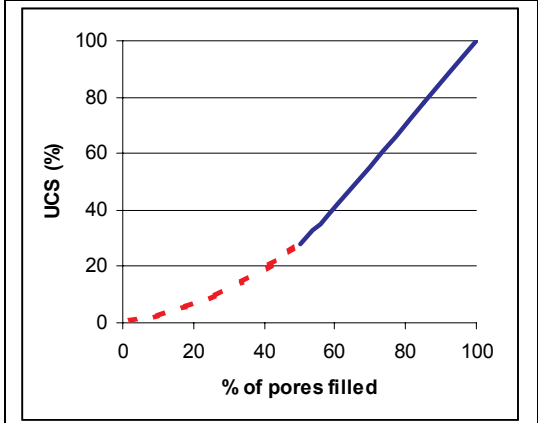


Figure 4.11 Relation Between the Strength (UCS) and the Percentage of Pores Filled (Kutzner, 1996)

eqn. 4.13 : $q_u = 0.098 * [A (10.2 * q_{uh})^m + B]$

with:

- q_u = UCS stabilised sand (MPa)
- q_{uh} = UCS pure silica gel (MPa)
- A, B, m = empirical coefficients, with:

- $A = 43.1 * n * (1 - A_{so}/A_o)$ n = porosity (-)
- $B = 0.003 * A_o$ D_r = relative density (-)
- $m = 0.727 - 0.2D_r$ A_o = specific surface sand (Blaine value) (cm²/g)
- $A_{so} = 213 * \log (A_o/25)$ A_{so} = specific surface sand particles per unit volume of sand (cm²/cm³)

Although apparently good results were obtained with this formula in Japan, it is difficult to understand how the different coefficients (and their dimensions) are linked.

Extensive, mainly laboratory, research was performed by Caron (1963), Warner (1972), Krizek, Liao & Borden (1992) en Vipulanandan & Shenoy (1992) to increase insight into grout strength and behaviour. The most important results are summarised below:

- the soil density has a very limited influence on the strength of the grouted soil;
- samples of mixed soil and grout have a significantly lower strength and E-modulus than samples where the grout is injected into the sample under pressure; the latter is more realistic and therefore preferred;
- continuous dry and wet cycles have a negative effect on grouted soil properties;
- temperature influences the hardening process; natural (at soil temperature) drying of a sample is preferred;
- grouted soil with round grains has moderately better strength properties than grouted soil with grains of a different shape;
- injection under ground water level results in better strength properties than in fine grained soil than in coarse grained soils;

- the load which a sample will resist under continuous stress without continued creep or rupture is significantly less than the ultimate strength of the sample obtained from rapid loading (and can be as low as 20% of the ultimate strength);
- using a sodium silicate in combination with an organic hardener gives significantly better strength properties than using it with a non-organic hardener;
- when testing samples using the Triaxial test, usually the friction angle ϕ' is equal to that of the virgin soil; the cohesion c' increases;
- almost every grout shows at least some reduction in volume when hardening in a *dry* environment; in soil with big pores this should be taken into consideration; in soil with small pores this usually causes no problems.

Mijnsbergen and Reinhardt (1988, 1990) performed extensive research on the use of concrete for offshore applications. One of the main aspects of their study concerned the volumetric behaviour of the concrete when hardening under water. The study showed that the concrete expands when hardening under water. This is an important conclusion for grouting applications under groundwater level. If the grout had reduced in volume during hardening (as it does in dry applications), this might to some extent have resulted in loss of effective soil stresses.

In Table 4.1 an indication is given of the average UCS grout strength in several soil types.

Table 4.1 Indication of Average Unconfined Compressive Strength of Permeation Grouted Soil

Soil type	UCS (MPa)	
	Lower limit	Upper limit
Peat	not groutable	Not groutable
Clay	not groutable	Not groutable
Silt	0.5	4
Sand	1	10
Gravel	2	15

4.5 Amsterdam Groutability Tests

4.5.1 General

This section consists of a summary of the results of the Stage 2 of the Full Scale Injection Test. The full results are incorporated in Van der Stoel (1998b & 1999).

A total of 6 columns and 12 spheres, with an approximate diameter of 1m, were created in different soil layers (Figure 4.12 and Table 4.2). The height of the columns is circa 16 m.

Table 4.2 Soil Layers Tested Using Permeation Grouting

Layer's Name	Depth (m to NAP*)	Description	Permeability (10^{-5} m/s) **	Void Ratio e^{***} (-)**	D_{15} (μm) **
1st sand layer	-12.5 – -15.0	Silty sand	1-5	0.54	55
Intermediate layer	-15.0 – -19.0	Sandy silt	$\ll 0.1$	0.67	8
2nd sand layer (top)	-19.0 – -22.0	Med. Fine sand	5	0.48	80
2nd sand layer (bottom)	-22.0 – -28.5	Med. Fine sand	8	0.67	200

*NAP = Amsterdam Ordnance Datum **average values *** $e = n/(1-n)$

The horizontal permeability of the soil was determined in-situ by using a *Monopool Probe*.

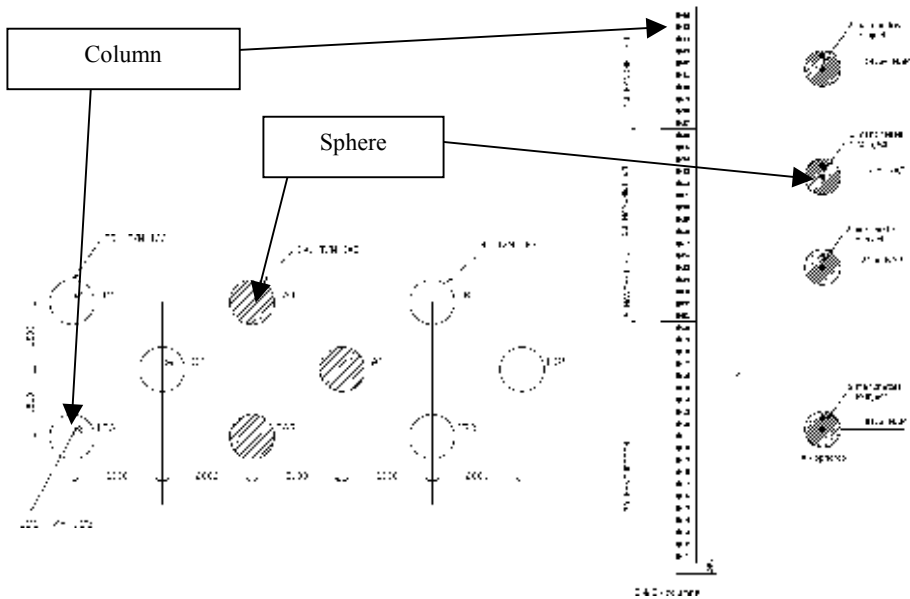


Figure 4.12 Test Set-up of Groutability Test

The columns (B&C) were created to verify the connection between the individual injections. Six TAMs with 46 manchettes were used to create columns B1-B3 and C1-C3. The B columns were investigated by using both electromagnetic and Bore Hole Radar (BHR) measurements. The C columns were investigated by using the electrical resistance method. The spheres (A) were used to determine the shape of a single element in a specific soil layer (sphere or disc?). They were created using a TAM with two manchettes in each layer, so that if one manchette got clogged, the other could be used. Using the groutability limits in Section 4.2.4 and considering the types of soil that have to be grouted in Amsterdam, a 40% silica gel (1), a 60% silica gel (2) and a micro-cement (3) were used in the field test (Table 4.3). Because of low strength properties and high costs, the resins were only used for laboratory test.

Table 4.3 Grout Types used for Testing

Type	Composition	Initial Viscosity (cP)
Silica gel 40v%	40% Crosfield Crystal 0079AG. 52% Water. 8% Hardener R100	7
Silica gel 60v%	60% Crosfield Crystal 0079AG. 30% Water. 10% Hardener R100	13
Micro-cement	25% MICROCEM. 75% Water. 2% ASR Injectionshilfe	(suspension)
Resin 1*	30% AC400. 19.4% Water. 0.25% TEA. 0.24% KFE	2-3
Resin 2*	20 kg A; 18 kg B; 0.6 kg C Sika-Injection 40. 2 kg Water	3-5

An injection container with hydraulic pumps was used to inject 3 TAMs simultaneously. The piston displacement of one pump was 1 litre per stroke. Every 5-10 minutes, a new charge of injection fluid was mixed in the container and pumped through a 40m long hose to the packer. Because of the varying diameter of the TAMs a special large inflatable packer was used.

4.5.2 Injection Pressure and Flow

Throughout the tests, the maximum injection pressure was set to 15 bar and the flow (grout-take) was limited to 10 ℓ/min. Exceeding these limits would most probably crack the soil, i.e. fracturing instead of permeation grouting. In Figure 4.13 the average injection pressure is printed as a function of the depth. The flow was kept constant at 6 – 8 ℓ/min.

Because of the great depth of injection and the pressure and flow restrictions, no problems were encountered concerning breaking out of the injection fluid at the surface. Figure 4.13 clearly shows that the average pressure needed to apply the micro-cement (4.2 bar) is higher than the average pressure needed to inject the 60% Silica gel (3.2 bar) or the 40% Silica gel (2.7 bar). This difference in pressure corresponds with the difference in (apparent) viscosity. The peak at NAP -26m for the 40% silica gel was caused by the gel setting before the grouting was finished.

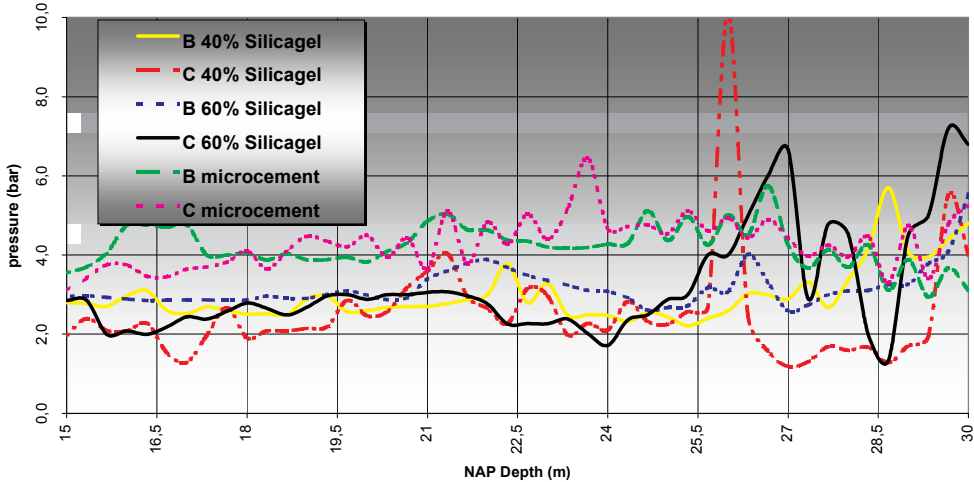


Figure 4.13 Groutability: Injection Pressure and Flow

Since grouting occurred without any problems, it can be concluded that for the Amsterdam soil the following relation between grouting pressure (p_{max} ; bar) and grout flow (Q_{max} ; ℓ/min) may be used :

$$\text{eqn. 4.2} \quad p_{max} * Q_{max} \leq 50$$

This relation allows for about 2.5 times bigger pressure and flow than eqn. 4.1, but the restriction for this particular relation is that it only applies for soil at at least 15 meters depth.

The grouting times and pressures as calculated using the Raffle & Greenwood model (see Section 4.3.4) have proven to give an overestimation for the Amsterdam situation. Based on this model much higher grouting pressures should have occurred, especially for the micro-cement.

4.5.3 Strength of the Samples

It was found that it was very difficult to obtain samples with satisfactory quality from the injection element. Both a light percussion drill and a fluid-flushed rotary coring system was used. The first method, generally used in soft soil, failed at a certain moment because the injected soil was so hard that it was not possible to obtain samples. The second method is also used with jet-grouted elements or rock. When, after sufficient hardening of the injection elements (28 days), the coring was started, the core catcher was only filled with samples to about 20% of the height*, therefore only a limited number of samples could be taken. Both these samples, and also the samples obtained by the laboratory tests, were tested using UCS tests or Triaxial tests. The results of the laboratory tests are shown in Table 4.4.

Table 4.4 shows that the UCS of the samples injected with 40% Silica gel do not generally exceed 0.20 MPa. The samples injected with 60% Silica gel and cement have higher UCS values, but these are still rather low compared to similar test with coarse sands. Fifty percent of the strength reached in the Triaxial test can be considered as an ‘apparent cohesion’. The confining stress σ_3 is chosen as 0.20 MPa

* The cores were apparently not hard enough for this coring system. They were probably damaged because of the high rotational speed of the core catcher.

because this corresponds with an approximate depth of 10-15 m below the surface. The obtained strength of the 1st sand layer samples is still very low; the strength of the 2nd sand layer samples however has reached normal values of 0.8-2.1 MPa. When tests performed on similar sands by Janssen (1999) were compared with these results, it could be concluded that generally samples taken from full scale tests in-situ give much better results than tests performed on samples injected in the laboratory.

Table 4.4 Results of Laboratory UCS Tests on Permeation Grouting Elements

Type of sample		Strength (N/mm ²)			Average E _{mod}
Injection fluid	Layer	UCS Test #1 Ø100 mm	UCS Test #2 Ø100 mm	Triaxial (σ ₃ =0.2 MPa)	MPa
Silica gel 40%	1st s.l.	0.06	0.06	0.06	3
	Intermediate layer	-	-	-	-
	2nd s.l. top	0.1	-	-	15
	2nd s.l. bot.	0.17	0.16	0.86	30
	2nd s.l. bot.	0.23	0.3	0.89	40
	2nd s.l. bot.	0.03	-	-	1
Silica gel 60%	1st s.l.	0.15	0.14	0.1	11
	Intermediate layer	-	-	-	-
	2nd s.l. top	0.54	0.47	0.85	100
	2nd s.l. bot.	1.6	2	2.1	220
Micro-cement	1st s.l.	0.5	0.52	1.2	100
	Intermediate layer	-	-	-	-
	2nd s.l. top	0.95	0.88	1.5	205
	2nd s.l. bot.	-	-	-	-

CPT

As an alternative to the UCS and Triaxial tests, CPT tests were used to determine the difference in cone resistance of the injected layers. The results of these CPT tests show very high cone resistance in the first sand layer. For instance, the 60% Silica gel column shows a CPT value of 70 to 100 MPa in the first sand layer, which normally has a CPT of less than 30 MPa. Deeper layers could not be penetrated because of the high resistance in the top layers.

4.5.4 Geophysical Verification of the Dimensions of the Grouted Elements

The results of the geophysical verification methods are dealt with in Chapter 7. The most important conclusion that could be drawn from the electrical resistance method (see Section 7.4.3), was that for all three columns there was clear evidence of the presence of the injection fluids in the sand layers. The diameter (circa 1.2 m) complied with the designed diameter and the diameter that could be expected based on the volume of grout that was injected (circa 1.1 m).

In the intermediate layer no evidence of the presence of an injection fluid was found. The BHR method showed evidence of the presence of the injection fluids in all layers for all three columns. Considering the high silt content of the intermediate layer, this result is considered to be doubtful. The shape of the grouted spheres could not be determined by any of the geophysical verification methods, because their resolution was not fine enough.

4.5.5 Conclusions

From the groutability test results the subjoined conclusions were drawn.

- The known applicability limits for permeation grouting using a silica gel have proven to be fairly correct for the Amsterdam situation. Based on the geophysical verification methods and the CPTs, the first soil layer that was expected to be difficult to grout* (1st sand layer), consisting of 20% silt, showed satisfactory permeation of injection fluid. The second soil layer that was expected to be difficult to grout* (intermediate layer), consisting of up to 60% silt, showed unsatisfactory permeation of injection fluid. The result in the 1st sand layer was not quite as expected, the result in the 2nd sand layer was. This had some consequences for the design of the Noord/Zuidlijn mitigating measures.
- The results of the micro-cement grouting were better than expected, considering the groutability limits mentioned in 4.2.4. Here the sand layers apparently were also permeated satisfactorily.
- Surprisingly, there was no clear difference in the injection pressures of the different soil layers. This might indicate that not only permeation but also some fracturing occurred. The difference in average injection pressure (Figure 4.13) between injection fluids was expected because of the difference in (apparent) viscosity.
- The grouting times and pressures as calculated using the Raffle & Greenwood model have proven to give an overestimation for the Amsterdam situation.
- The Unconfined Compressive Strength of the samples injected in the laboratory is rather low compared to tests on samples of similar soil injected in the laboratory by Caron (1963), Warner (1972), Krizek, Liao & Borden (1992) en Vipulanandan & Shenoy (1992).
- The results of the CPT test show very high cone resistance in the first sand layer. Deeper layers either could often not be penetrated because of this high resistance, or showed higher resistance.

4.6 Detailed Set-up of Stage 3a

4.6.1 General

The general idea behind permeation grouting below, surrounding or next to a pile toe, is that the grout strengthens the soil. This can basically have two functions.

1. Reduce the sensitivity of the pile to soil movements induced by nearby building activities, for instance by creating a grouted structure near the piles to stabilise the soil before drilling through it with a TBM.
2. Increase the bearing capacity of the pile, for instance for foundation renovation purposes.

In the first case the grouted structure is preferably located at some distance from the piles, in the second the grouted structure is as near to the pile as possible. The aim of this stage of the test is therefore to investigate the influence the TAM installation process and the grouting process and grouting parameters have on:

- pile displacements, pore water pressure and soil stresses;
- the rate of improvement of the bearing capacity of a wooden pile.

The general set-up of the Full Scale Injection Test was discussed in Chapter 3.

In this stage, TAMs were used to create a more-or-less spherical permeation grouting element. During the process of installing the TAMs and during the actual permeation grouting process, vertical displacements of the piles were intensively monitored. The horizontal stresses and the pore pressure were also monitored; the first only in the piles, the latter in both the piles and the soil. The grouted elements were placed at different locations from the piles, to study the influence zone of the permeation grouting. The piezometers in the soil were placed at increasing distance from the grouting points, to monitor the influence of the grouting pressure on the pore pressures.

Figure 4.14 shows the positions of the grout elements and TAMs in relation to the pile positions in plan view. Figure 4.15 and Figure 4.16 show some cross-sections and side views. Table 4.5 gives additional

* Based on the diagram in Figure 4.6

information to that shown on the graphs. Throughout this chapter the graphs can be used to locate the elements used in the test.

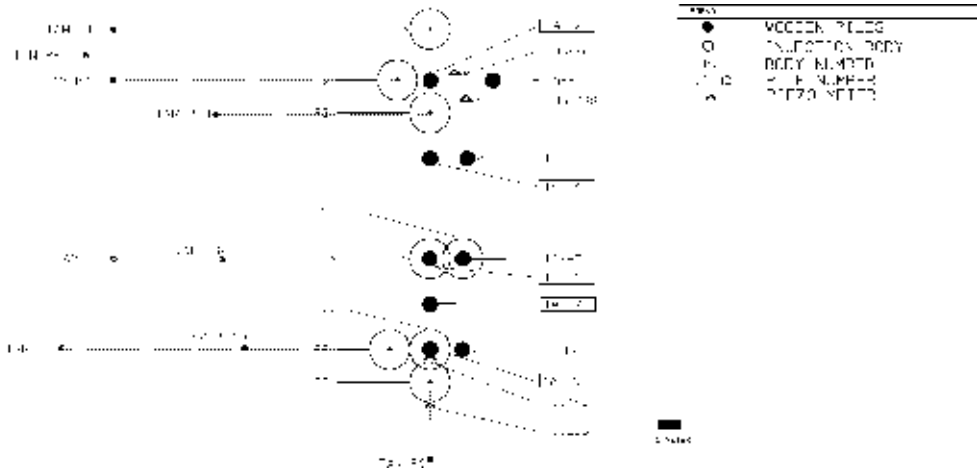


Figure 4.14 Detailed Test Set-up: Plan View of the Piles, TAMs, Piezometers and Grout Elements

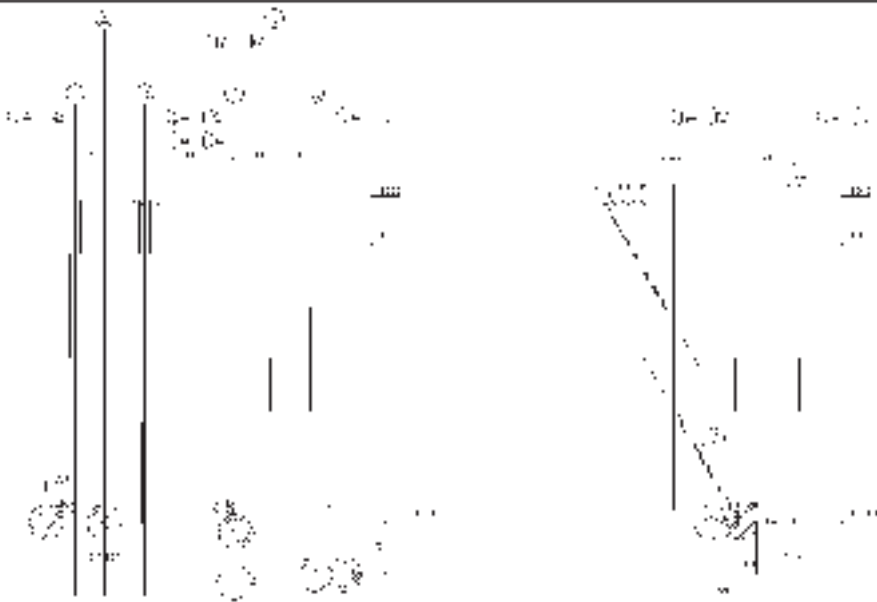


Figure 4.15 Typical Cross Section and Views of Piles, TAMs and Grout Elements

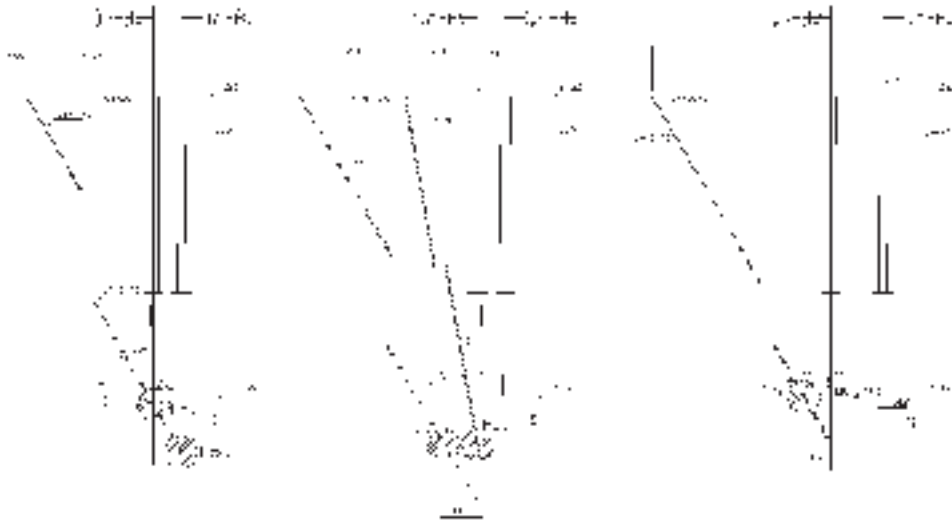


Figure 4.16 Typical Cross Section and Views of Piles, TAMs and Grout Elements

4.6.2 Piles and Monitoring Equipment

Nine wooden piles, coded 1A-H1 to 1A-H9 were used. The top x,y position of all the piles was verified after driving. Some piles were supplied with piezometers and SMS. The location of the monitoring equipment is illustrated in Figure 4.14. As already explained in Chapter 3, pile displacement was monitored using both jointmeters and the automatic levelling system. Because here the piles were located under the ballast-frame, the pile positions could not be measured directly at the piles (the targets would not be visible for the total station). Connecting jointmeters on each individual pile to a reference frame solved the problem. Because the reference frame itself was susceptible to movement as it was placed on the surface and influenced by temperature, it was monitored by using targets. A correction for temperature and surface measurements could then be made whenever necessary.

4.6.3 TAMs and Grout Elements

All the grout elements were installed by using TAMs. In Table 4.5 the position in relation to the pile and the TAM that was used to create the grout elements is given for all grout elements. TAMs P2 and P5 were used to create two grout elements, TAMs PF2, PF4, PF6 and PF10 were also used for fracturing during compensation grouting Stage 3C.

Table 4.5 Grout Elements and Accompanying TAM Code

Injection element code	Injected by TAM	Position relative to pile	Stage 3A	Stage 3C
P1	P1	Next to pile toe	x	
P2A	PF2	Next to pile toe	x	x
P2B	PF2	Beneath pile toe	x	x
P3	P3	Next to pile toe	x	
-	PF4	Beneath pile toe		x
P5A	P5	Surrounding pile toe	x	
P5B	P5	Beneath pile toe	x	
P6	PF6	Beneath pile toe	x	x
P8	P8	Beneath and next to pile toe	x	
P9	P9	Beneath and next to pile toe	x	
P10	PF10	Beneath pile toe	x	x

PERMEATION GROUTING

In Table 4.6 the grouting characteristics are displayed. This includes installation times, maximum pressure during injection, the total injected volume of grout and the sleeve through which the injection took place.

For the TAMs two different types of tube were used. The TAMs used for *both* permeation grouting and compensation grouting fracturing (PF-type) were made of steel, with a 101 mm outer diameter and variable distances between the manchettes. The TAMs used for permeation grouting *only* (P-type) were made out of PVC, with a 50 mm outer diameter and 350mm between the manchettes.

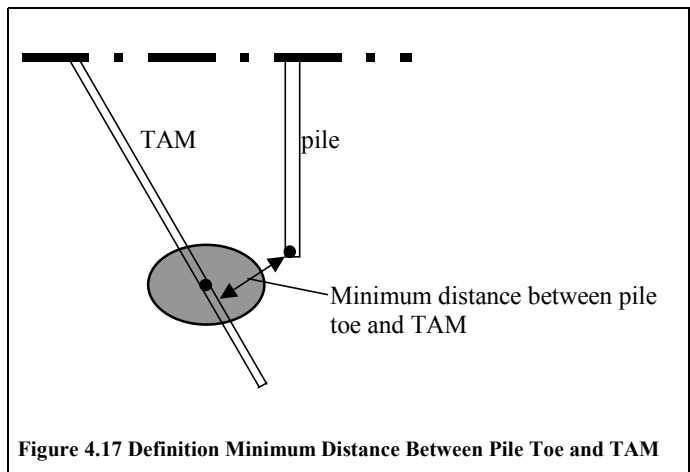
The TAMs were installed by using 150 mm diameter, water assisted rotary-flushed borings without using a casing. The TAMs were lowered manually into the borehole and fixed in place by means of a bentonite-cement sleeve grout.

Table 4.6 Permeation Grouting Characteristics

Grout element	Reported injection time			Maximum pressure (bar)	Injected volume (litre)	Location injection sleeve <i>Distance to bottom end of TAM (m)</i>
	Start	end	duration (h)			
P2	14-9-99 13:00	14-9-99 13:15	0:15	2.0	147	1.95
P5B	14-9-99 14:35	14-9-99 14:46	0:11	2.0	154	2.10
P8	14-9-99 15:00	14-9-99 15:14	0:14	1.0	112	1.05
P3	14-9-99 15:22	14-9-99 15:38	0:16	1.5	121	1.05
P5A	14-9-99 15:47	14-9-99 15:57	0:10	2.0	115	1.05
P10	14-9-99 16:04	14-9-99 16:20	0:16	1.0	121	0.50
P2A	14-9-99 16:27	14-9-99 16:43	0:16	1.5	118	0.50
P9	14-9-99 16:49	14-9-99 17:03	0:14	3.0	119	1.05
P4	13-10-99 20:35	13-10-99 20:52	0:17	0.2	100	0.50
P6	13-10-99 20:58	13-10-99 21:12	0:14	1.4	100	0.50
P2B	13-10-99 21:16	13-10-99 21:31	0:15	1.0	100	1.00

To create the grout elements a silica gel was used that consisted of 50v% Crosfield Crystal Type 0317*, 9v% R100 hardener and 41v% water. The hardening time of this silica gel was about 35 minutes. Note that although the grout elements are presented as being spherical in the figures, the actual shape depends on the local soil characteristics. Because of the depth at which the grout elements were created the actual shapes could not be verified.

Two types of shape can be assumed for the grouted volume: a spherical or an ellipsoidal shaped grout element (Figure 4.18). The difference between the horizontal and vertical permeability of the soil makes the ellipsoidal shape more likely. The injected volumes listed in Table 4.6 were used to determine the extents of the different grouted elements and the minimal distance between the grouted element and the TAM (as defined in Figure 4.17; for more information see APPENDIX XI).



* A specially modified silicate with better grouting and strength properties

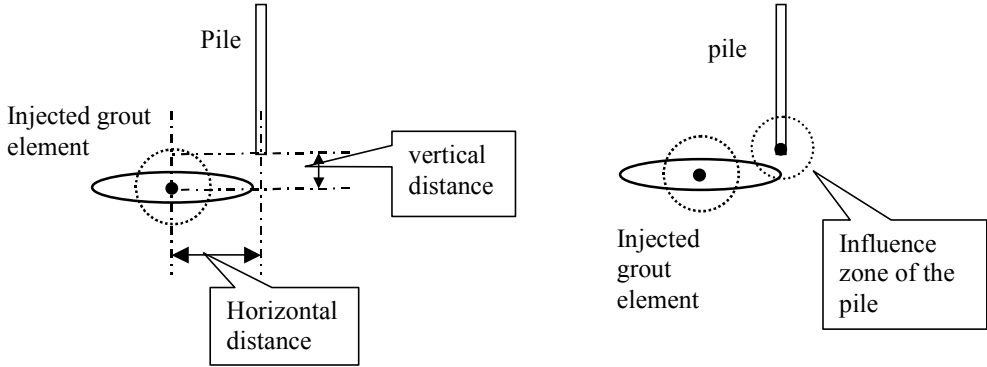


Figure 4.18 Visualisation of the Grouted Element and the Influence Zone of the Pile

4.7 Results of TAM Installation Test

4.7.1 General

In this section the influence of TAM installation on the piles and the soil is discussed. The observations concerning the installation of the TAMs for compensation grouting Stage 3C are also included. For a detailed description of Stage 3C reference should be made to Chapter 6.

4.7.2 Pile Displacement

As an example, Figure 4.19 shows all monitoring instruments near pile 1A-H5. Figure 4.20 shows the displacements of the jointmeters on all nine piles during installation of about half of the TAMs. The installation of the other TAMs showed no significant displacement at all and is not displayed.

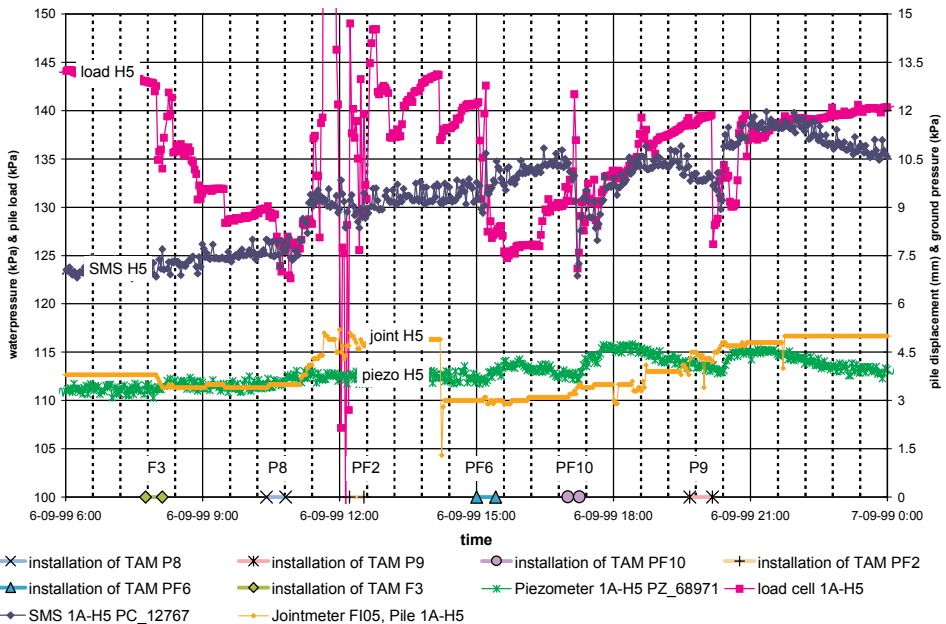


Figure 4.19 Monitoring Data of Pile 1A-H5 during TAM Installation

PERMEATION GROUTING

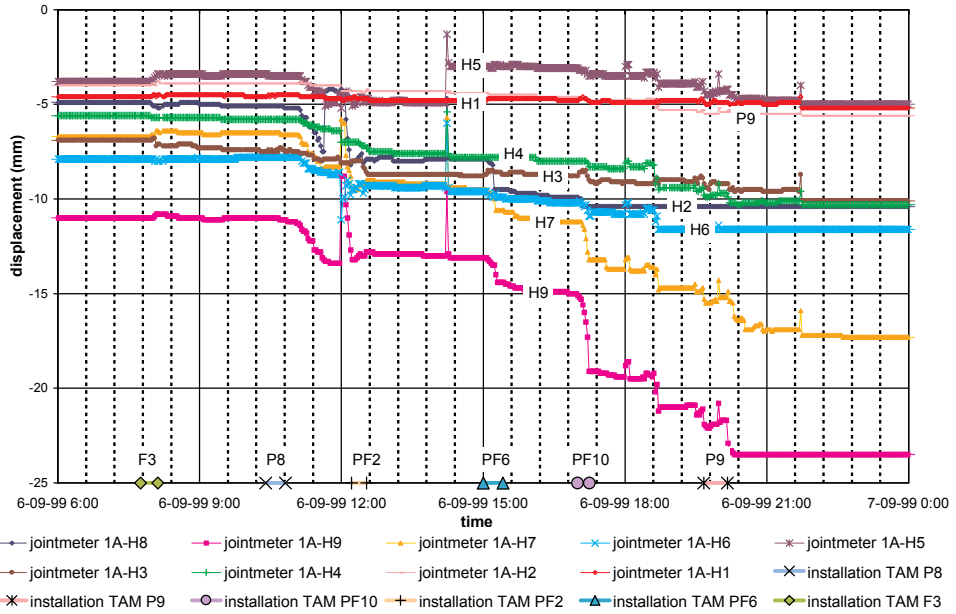


Figure 4.20 Jointmeter Readings during TAM Installation

From Figure 4.20 it can be seen that Piles 1A-H7 and 1A-H9 show the largest displacement during TAM installation. The other piles show no significant response. The big displacement of piles H7 and H9 is more thoroughly examined in Figure 4.21.

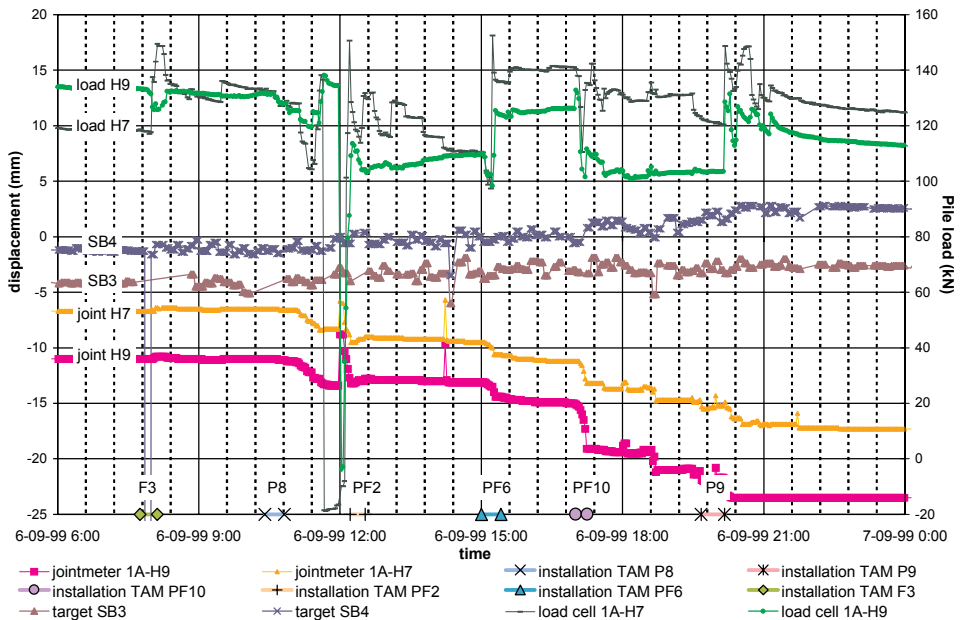


Figure 4.21 Load and Displacement of Piles 1A-H7 and 1A-H9 during TAM Installation

From Figure 4.21 it can be observed that settlement caused by the TAM installation results in an expected pressure drop in the pile loads. For pile H9 the settlements can be explained by the proximity

of this pile to the TAMs and the relative low ultimate bearing capacity (see Section 3.10.3). Pile H7 however is located at a much larger distance from the TAMs and has a normal ultimate bearing capacity. Therefore its settlement can not be explained from TAM installation. The reaction of both piles to the installation of TAM PF6 is also peculiar because of the large distance between the TAM and these piles. A possible explanation might be the relative large pile load adjustment that took place at that time. Because the position of the TAMs that cause the pile settlement is very near to the pile toes that settle, it seems logical to examine the influence the distance between the TAM and the pile has on the settlement more closely. This is done in the next subsection.

4.7.3 Correlation of Pile Displacement - Minimum Distance between TAM & Pile

The influence of TAM installation on the pile can be presented as a relation between the minimum distance between TAM & pile and the vertical displacement of this pile during TAM installation. In Figure 4.22 a scatter plot of this relation is presented. In APPENDIX XII two more specific plots, making a distinction per pile and per TAM are presented.

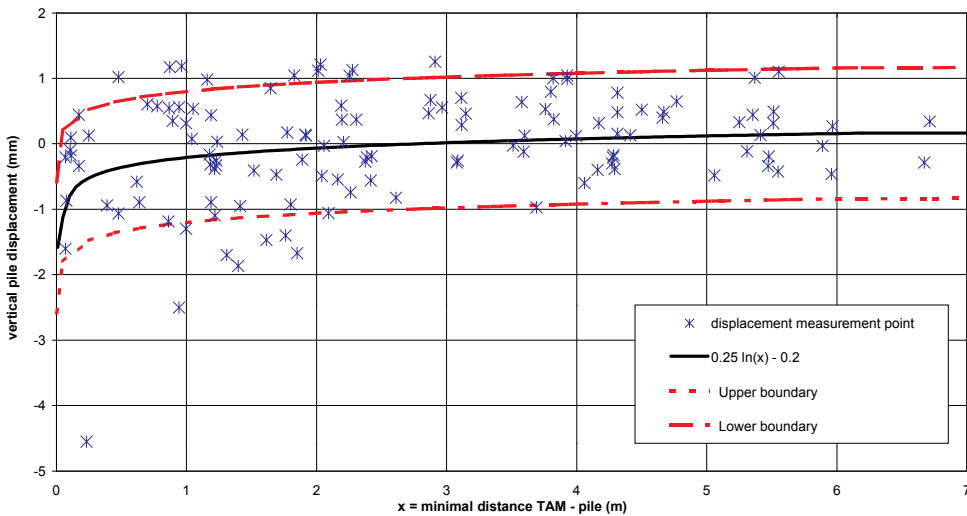


Figure 4.22 Pile Reaction During Ø 150mm, Rotary Flushed Borings without Casing (TAM Installation)

The points with the biggest displacement refer to piles 1A-H7 and H9. As could be seen in Figure 4.21 the jointmeter readings of these piles are quite high, even after correction for measurement frame movement (SB3 & SB4). This correction introduces some noise in the data, sometimes indicating pile heave where the jointmeter only gives a slight response. Therefore all readings between -1mm and +1mm are considered to lie within the accuracy limits of the measurement system.

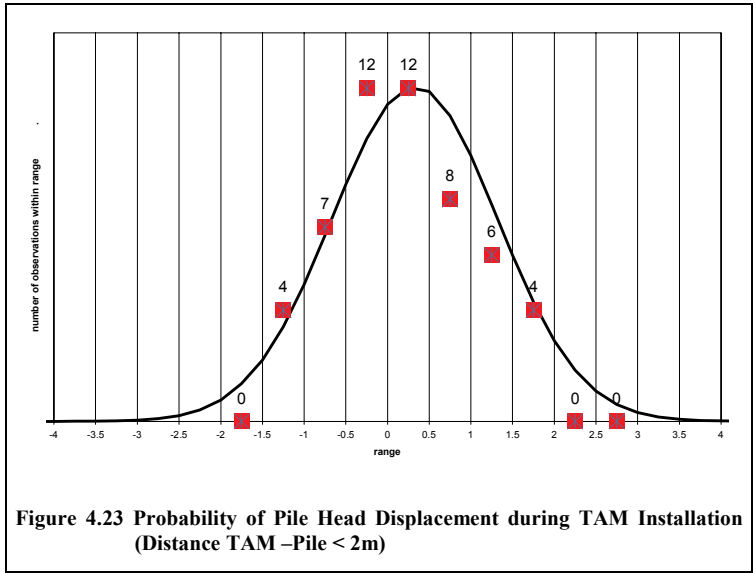
It is concluded that there is no significant influence of TAM installation when the minimal distance between a TAM and a wooden pile exceeds 2 m. Because the influence increases to a certain extent within these 2 meter, an exponential relation was deduced from the data:

eqn. 4.3 $s = 0.25 \ln(x) - 0.2$

where:

- s = the vertical displacement (mm)
- x = the minimal distance between TAM and pile (m)

In Figure 4.23 all the observation points with a minimal distance pile/TAM of less than 2 m are shown in a bar chart. For illustrative purposes a probability density curve is drawn on the same graph. The normal distribution of the pile movements indicates that the displacements seem to be influenced mainly by measurement errors.



4.7.4 Pore Water Pressures & Effective Stress

Most of the piezometers show a response to the TAM installation. Depending on the distance between the TAM and the piezometer, the response varies between 0 kPa (no response) and 8 kPa. The magnitude of the response is influenced by two factors: the distance between the injection point and the piezometer and the differences in permeability of the soil. The first reason is rather obvious, the greater the distance the more pressure energy is lost along this path. The latter factor was more clearly observed during Stage 3C. From these observations it could be concluded that the piezometers that were placed in the upper part of the sand layer reacted with a lower magnitude than the ones that were placed somewhat deeper. As the upper part of the first sand layer is classified having a higher silt content, the difference in response is most probably caused by permeability differences. In Figure 4.24 the results of monitoring the piezometers and SMS during the installation of the TAMs are presented. The figure gives a good indication on the decrease in excess pore pressures with time. After approximately two hours most of the excess pore pressures have dissipated. In the figure both total stresses and pore water pressures are presented during TAM installation for pile 1A-H5. The effective stress readings (total stresses) are to some extent consistent with the pore water pressure readings; both show a slight increase during TAM installation.

The conclusion that can be drawn from the results of the monitoring, is that only insignificant changes (<10kPa) in water and soil pressures occur during TAM installation. Because the changes are so small, examining the correlation with the TAM distance was considered to be neither worthwhile, nor feasible.

PERMEATION GROUTING

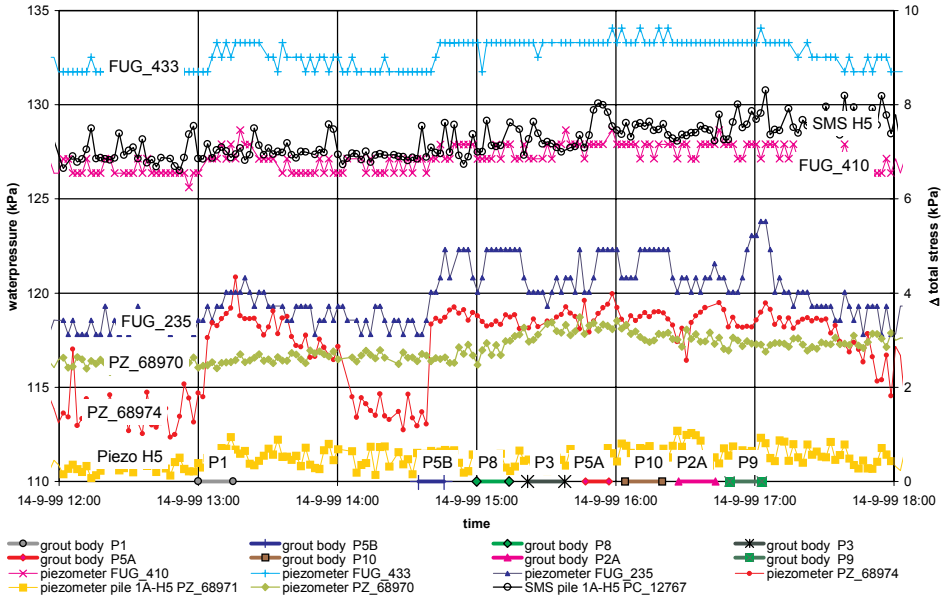


Figure 4.25 Piezometer and SMS Readings during Permeation Grouting

4.8.3 Bearing Capacity

The bearing capacity of the nine wooden piles was determined both before and after permeation grouting. The results of these pile load tests are shown in APPENDIX VIII. As an example the test for pile H5 is shown in Figure 4.26.

When comparing tests #1 and #2 (before) with test #4 (after)* some conclusions can be drawn:

1. the load-settlement behaviour of piles H3, H5, H7 and H8 is about the same as before grouting;
2. the load-settlement behaviour of piles H1, H2, H4, H6 and H9 is significantly stiffer than before grouting when $F > 0.5 * F_{ubc}$;
3. the ultimate bearing capacity of piles H3, H4, H5, H7 and H8 did not significantly change ($\Delta F \leq \pm 10\%$) after grouting;
4. after grouting the ultimate bearing capacity of piles H1, H2, H6 and H9 changed by an unknown %, +20%, +36% and +35% respectively; test #4 on pile H1 had to be stopped because the pile head did not move at all, so no increase of F_{ubc} could be recorded, although most probably it exceeded +50%.

To study the influence zone of the permeation grouting the results from the bearing capacity tests were compared with the position of the grout elements relative to the piles (Figure 4.14 to Figure 4.16). It has emerged that the piles that show an increase in bearing capacity are all surrounded by permeation grouting elements (H2, H9) or have a permeation grouting element directly at their toes (H6). Pile H1 also shows an increase, although it could not be brought to its failure load. When the grout elements near H1 were being created probably some fracturing occurred just under the pile toe. The hard grout lens that formed under the pile could not be broken.

* Test #3 was only conducted on the piles of stage 3B

PERMEATION GROUTING

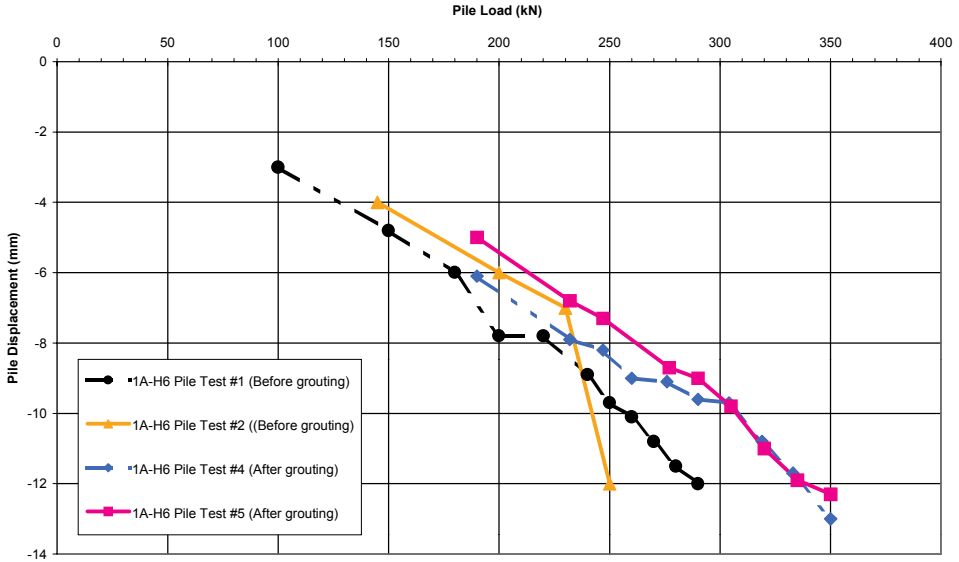


Figure 4.26 Example of Pile Load Test: Wooden Pile 1A-H6

Regarding the use of permeation grouting to create a grouted structure to reduce the sensitivity of the pile to soil movements induced by nearby building activities, the most important conclusion that can be drawn from the tests is that the bearing capacity of the piles will certainly not decrease owing to the permeation grouting activities. Because, when conducted properly, permeation grouting leaves the soil grain structure intact, this seems a logical result.

Regarding the purpose to increase the bearing capacity of the pile, for instance for foundation renovation purposes, it can be concluded that by permeation grouting close to or at pile toe level, the bearing capacity and stiffness of the piles can be considerably increased. A quantitative relationship between the increase in bearing capacity of the piles and the position of the grouted elements could not be given, because of the different configurations of grouted elements used in the test. It is however clear that when the grouted element is located closer to the pile and more elements are grouted near the piles, the positive effect on the bearing capacity increases.

4.9 Conclusions and Recommendations

From the literature references on permeation grouting and analysis of the results of the Amsterdam tests, it can be concluded that permeation grouting is a technique so complex that modelling only serves the purposes of increasing understanding of the process. The models are not designed for use in engineering practice. The grouting times and pressures as calculated using the Raffle & Greenwood model have proven to give an overestimation for the Amsterdam situation. A rule of thumb that is considered to be a valuable practical tool in designing and controlling the grouting works for the Amsterdam situation, when grouting at 15 meter or deeper, is that the product of grouting pressure (p_{max} ; bar) and grout flow (Q_{max} ; ℓ/min) should preferably not exceed 50:

$$\text{eqn. 4.2} \quad p_{max} * Q_{max} \leq 50$$

From the groutability test it could be concluded that the known applicability limits for permeation grouting using a silica gel, have proved fairly correct for the Amsterdam situation. Based on the positive results of the geophysical verification methods and the high CPT values that were found after grouting,

the 1st sand layer, consisting of 20% silt, showed satisfactory permeation of injection fluid. The intermediate layer, consisting of up to 60% silt, showed unsatisfactory permeation of injection fluid. The results of the micro-cement grouting were better than expected, considering the groutability limits mentioned in 4.2.4. Surprisingly, there was no clear difference in injection pressure between the different soil layers for any of the grouts used in the tests, which might indicate that only partial permeation took place.

When installing the tubes-à-manchette using an uncased, rotary flush boring, generally only insignificant changes (<10kPa) in water and soil pressures occur. Two out of nine piles showed relatively large settlements. The settlement of one these piles could be attributed to the close proximity of several TAMs, the settlement of the other pile could not directly be attributed to TAM installation. Regarding pile displacements, there are no significant installation effects when the minimal distance between a TAM and a wooden pile exceeds 2 m. When this distance is less than 2 m and the pile is maintained under a constant working load, the relation between the vertical displacement of the pile (s ; mm) and the minimal distance between TAM and pile (x ; m) was found to be:

$$\text{eqn. 4.3 } s = 0.25 \cdot \ln(x) - 0.2$$

The pile reactions resulting from the actual grouting process were insignificant. From the readings it could be concluded that the influence of grouting on pile displacements and total stresses and pore water pressures is negligible. This result corresponds to the non-disturbing character of the grouting process when properly conducted.

When using permeation grouting for foundation protection, to create a grouted structure to reduce the sensitivity of the pile to soil movements induced by nearby building activities, the bearing capacity of the piles will certainly not decrease owing to the permeation grouting activities, when these activities are conducted properly.

When permeation grouting is used for foundation renovation, close to or at pile toe level, the bearing capacity and stiffness of the piles can be considerably increased. When the grouted element is located closer to the pile and more elements are grouted near the piles, the positive effect on the bearing capacity can increase considerably (up to 36% in this test).

Regarding the long-term behaviour, it could be concluded that 2 weeks after grouting the piles showed no signs of consolidation effects whatsoever. There is also no need for concern about possible creep effects and a subsequent loss of effective soil stresses, because the material is more likely to expand than to shrink.

The concern that may arise when thinking of using permeation grouting for foundation renovation purposes, is that limited pile settlement can occur when installing the TAM close to the toes of the existing foundation piles. It should, however, be clear that during the test, the pile loads were kept at a constant level, whilst when permeation grouting is used for foundation renovation purposes, the pile load of the pile thus treated will be redistributed to the other piles. It is therefore recommended that the work should be carefully phased, so that the settlement due to TAM installation will be minimised. When this requirement is met with, grouting where it is most effective, i.e. near the pile toes, is feasible and can be very effective as a foundation renovation system. In Chapter 8 the practical aspects of using permeation grouting for foundation renovation will be more closely examined

Chapter 5 JET GROUTING

5.1 Introduction

Jet grouting is a technique that is frequently used in underground construction to create grouted soil structures for the purpose of soil stabilisation or reduction of soil permeability. The technique involves eroding the soil with a high energy grout jet (Figure 5.1). The result of the process is a so-called jet grouted column, a soil – cement column with better strength, stiffness and permeability properties than the original soil. To indicate the possibilities and extent of the use of jet grouting, first an introduction to the technique describing the history is given, after which main characteristics and fields of application of the different jet grouting methods are explained. The proposed method for assessing the influence jet grouting has on pile foundations is also presented. Because the jet grouting process is an eroding process, it induces changes in the

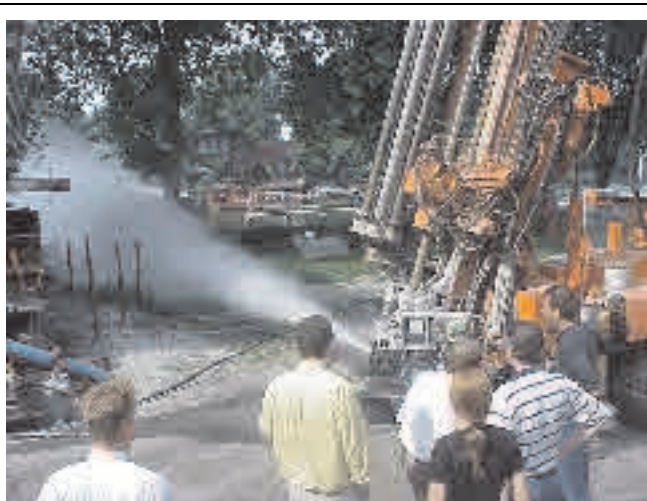


Figure 5.1 Jet Grouting: High Pressure Cutting with Water (Shown at Surface Level)

soil. Since, at present very little is known about the effect of jet grouting on local soil conditions and especially on pile foundations, the Full Scale Injection Test was conducted. The general set-up of this full-scale test was explained in Chapter 3. This chapter deals with the jet grouting stage (3B) of the test.

When investigating the effects of jet grouting on the local soil conditions and nearby foundations, differential displacements, total stresses and pore water pressures must be considered. The main part of this chapter discusses the effects of jet grouting on pile foundations, considering three aspects in particular:

- the effects of jet grouting for foundation protection;
- the effects of jet grouting when creating pile extensions for foundation renovation;
- the strength and stiffness parameters of the jet grouting material itself.

An effort is made to correlate several strength and stiffness parameters of the soil that has been treated by jet grouting.

In jet grouting terminology, several different definitions are often used for what is basically the same concept. To avoid misunderstanding, in this thesis the terminology suggested in the European Code on Jet Grouting: prEN 12716 has been used.

5.2 Jet Grouting Process

5.2.1 History

Jet grouting, also known as *Very High Pressure (VHP) Grouting* or, in German, *Hohe Druck Injektion (HDI)*, was first applied around 1950 by Cementation Co. in Pakistan (Lunardi, 1997). From 1965 onward, further development was carried out by the Yamakado brothers in Japan (Ichise, 1974). In the seventies two jet grouting concepts were developed simultaneously. The first method developed by Nakanishi N.I.T. (Nakanishi, 1974) was named *Chemical Churning Pile* or *CCP jet grouting*. As the chemical or cement grout was being injected at ultra high pressures through 1-2mm diameter nozzles located at the bottom of a single drill rod, the rod was pulled and rotated, thus creating a soil-cement column. The second method, named *jet grouting* by its creator *Yahiro* (1973), is based on cutting, replacing and cementing the soil, typically by using three concentric rods supplying water, air and cement grout.

In Japan, many subsequent modifications of the jet grouting system have since appeared. The most important was the use of an air-encapsulated cement grout, creating the so called *Jumbo Special Grout (JSG)* (Ichise, 1974). The JSG is capable of providing columns with diameters 1,5 – 2 times larger than the *CCP Columns*.

Following the initial development in Japan, jet grouting was introduced and further optimised in the 1980s in Germany (Company: *Keller*), France (Company: *Soletanche-Bachy*), Brazil (Company: *Novatecna*) and especially Italy (Company: *Rodio and C. and Pacchiosi*). The most recent optimisation of the jet grouting process concerns a system called the *X-jet (Cross-jet)* system. This system, which is capable of obtaining greater jet grouted column diameters at greater accuracy, was developed in Japan by the *Chemical Grouting Company* and licensed for Europe by *Keller*. The system is based on using two jets, which maintain high cutting energy until they cross (see Figure 5.2). Relevant information on this process has not yet been published.



Figure 5.2 X-Jet

5.2.2 Definitions, Process and Equipment

Jet grouting is a process involving disaggregation of a soil and its mixing with and partial replacement by a cementing agent. The disaggregation of the soil is achieved by a high-energy jet.

Before explaining the process some definitions are given:

- the *rig* is a rotary rig able to automatically regulate the rotation and translation of the jet grouting string and monitor.
- the *string* is used to convey the grouting materials down-hole to the required depth.
- the *monitor* (Figure 5.3) is a device attached to the end of the jet grouting string, comprising a drill bit and nozzles.
- a *nozzle* (Figure 5.3) is a device especially manufactured and fitted into the monitor, which is designed to transform a high pressure fluid flow in the string into a high speed jet directed at the soil.

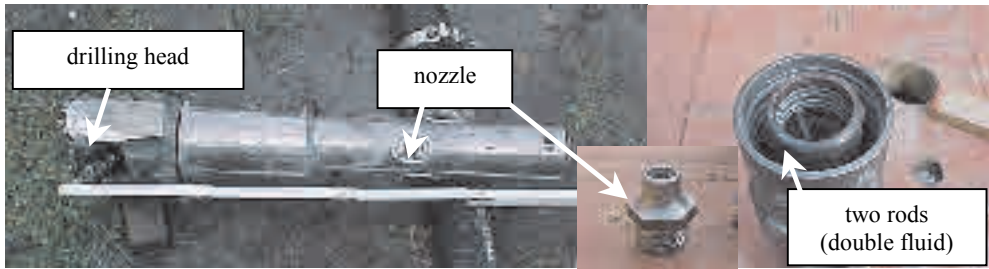


Figure 5.3 Monitor Used at the Test

The nozzle should be designed in such a way that the jetted fluid remains very compact (i.e. a small cross section) for as long as possible. This is because diverging of the jet strongly reduces the jetting effectively and accuracy to obtain the designed column diameter.

Figure 5.4 shows a schematic representation of the jet grouting process. The jet grouting string and monitor are first drilled to the required depth by the rig, after which they are pulled and rotated whilst jetting a water-cement grout under high pressure from the monitor.

The soil is eroded, partly mixed with the cement grout and partly pushed to the surface along the string. This effluent that comes to the surface during jet grouting is called *spoil*. The mixture that remains in the soil hardens and forms a jet grouted column. Creating multiple columns next to each other creates a jet grouted element or structure (see Section 5.2.3 and 5.2.4).

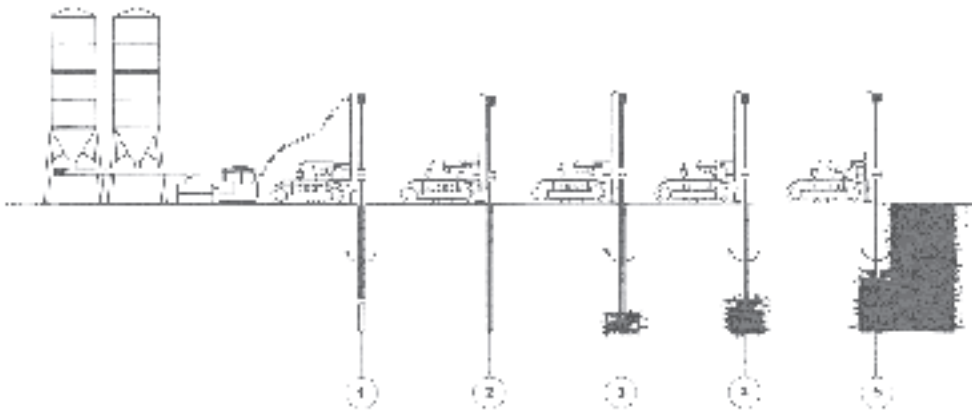


Figure 5.4 Jet Grouting Process

As was noted in Section 5.2.1, several different jet grouting systems are available, permitting jet grouting to be used in a variety of types of deposits and the creation of various diameter elements.

The main jet grouting systems that can be distinguished are:

- the single fluid system;
- the double fluid (air) system;
- the double fluid (water) system;
- the triple fluid system.

Each of these systems is explained in the following text and the accompanying figures.

JET GROUTING

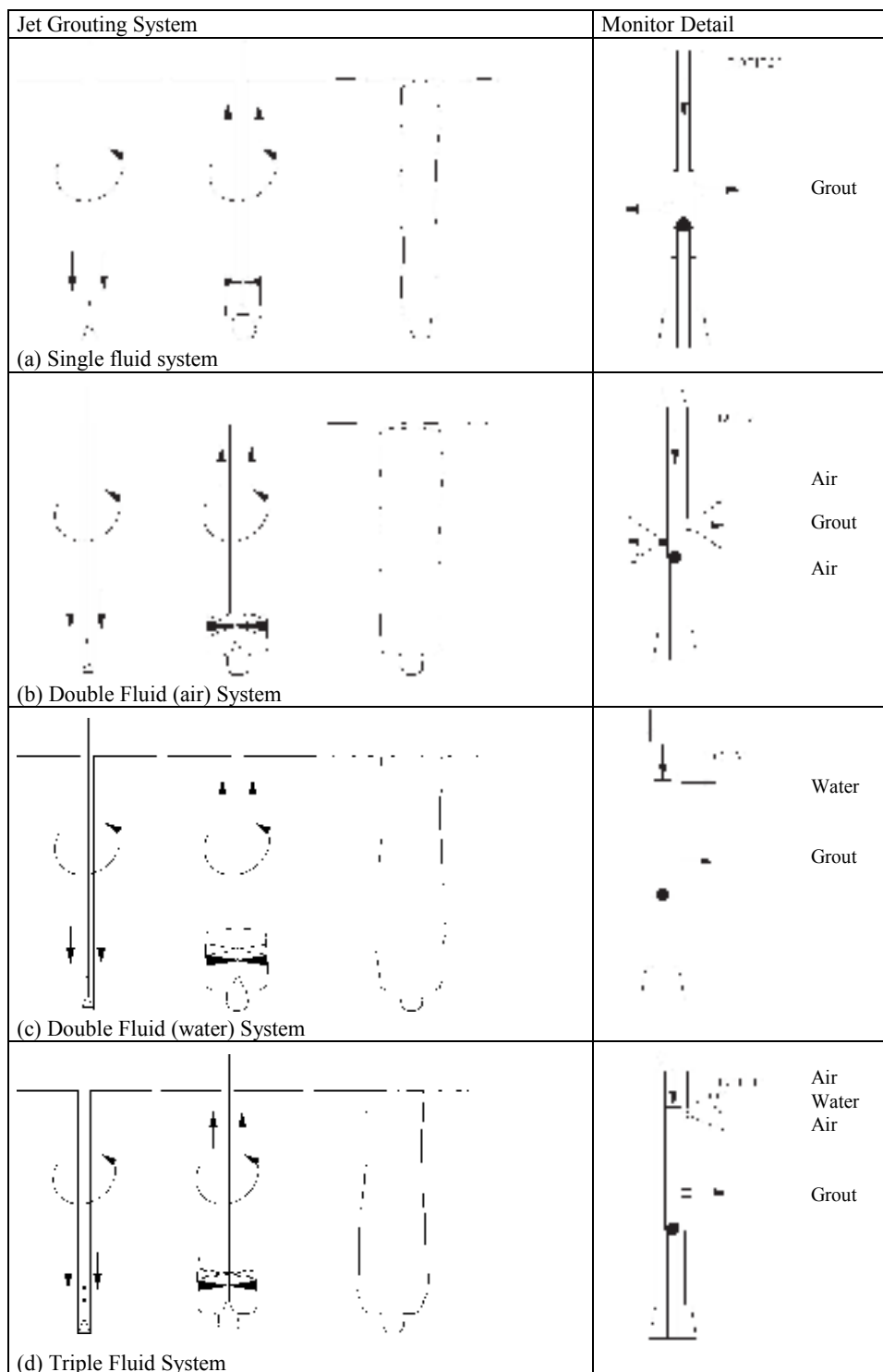


Figure 5.5 Jet Grouting Systems: Principle Layout and Monitor Detail

The **single fluid system** is a jet grouting process in which the disaggregation and cementation of the soil are obtained by using a high energy jet of a single fluid, usually a cement grout (Figure 5.5a). One or more circular nozzles* are used to allow the jetting of grout. For the high pressure supply of the cement mix only one rod is used.

The **double fluid air system** is a jet grouting process in which the disaggregation and the cementation of the soil are obtained by using one fluid (usually a cement grout) assisted by an air jet shroud as a second “fluid” (Figure 5.5b). One or more double nozzles* are used to allow the simultaneous jetting of air and grout. The air nozzle is an annulus around the circular nozzle for grout. Two rods are used, separately conveying the two fluids (air and cement mix or water and cement mix respectively; Figure 5.3 right).

The **double fluid water system** is a jet grouting process in which the disaggregation of the soil is obtained by using a high energy water jet and the cementing is simultaneously obtained by a separate grout jet (Figure 5.5c). One or more nozzles* are used for high pressure jetting of water and one or more deeper nozzles for jetting or grouting of cement mix.

The **triple fluid system** is a jet grouting process in which the disaggregation of the soil is obtained by using a high energy water jet assisted by an air jet shroud, and the cementing is simultaneously obtained by a separate grout jet (Figure 5.5d). In special cases the water can be replaced by other appropriate liquids or suspensions. One or more double nozzles are used to allow the simultaneous jetting of air and water and one or more simple nozzles located at a deeper level are used to allow the grout injection. Three rods are used to supply the high pressure water, the compressed air and the pressure cement mix.

Pre-jetting[†] is optionally used in cohesive soil layers. The jet grouting of an element is then facilitated by a preliminary disaggregation phase with a water jet only (single fluid system) or a water and air jet (double fluid system).

The equipment has to be able to perform the jet grouting operation by assuring the translation and rotation displacement of the string at the designed speed. It is also necessary to ensure that the string is supplied with the fluids coming from the plant, at the required pressure and rate of flow.

The principle components of a jet grouting system are illustrated in Figure 5.6. Different mixing and grouting plants are required for each jet grouting process. For all cement and other materials storage, a colloidal mixing plant, agitator tanks and a high pressure grout pump are required. The plant may also include bentonite hydration facilities, an air compressor and a high pressure water pump. From the figure it can be seen that the jet grouting plant

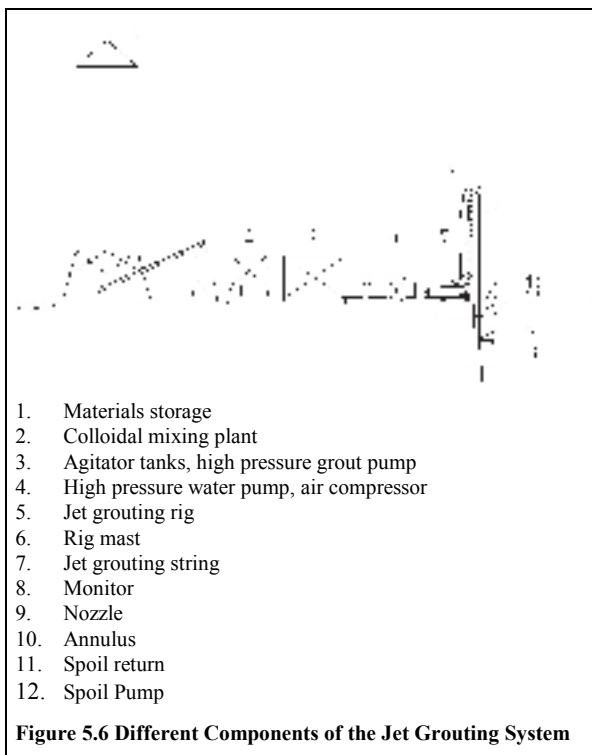


Figure 5.6 Different Components of the Jet Grouting System

* located at the same level or at different levels, with constant mutual staggered angles

† also known as pre-cutting, prélavage or pre-washing

occupies considerable space.

The length of the string and the height of the rig's mast, should preferably not be shorter than the length of the designed jet grouted element. If large depths are involved or there are access limitations, in order to limit the need to interrupt the jet grouting operation the string should be divided into a minimum number of elements. This is necessary because interruption results in an increase in the spoil quantities, the risk of discontinuity of the element and a decrease in quality of the element

5.2.3 Jet Grouting Elements

A jet grouted element is a volume of soil treated through a single drilled hole. The most common types of jet grouted elements are the:

- jet grouted column, a cylindrical jet grouted element;
- jet grouted panel, a plane jet grouted element.

Examples are shown in Figure 5.7. The elements are either created in a *fresh in fresh* sequence or in a primary-secondary sequence as illustrated in Figure 5.8. With the *fresh in fresh* sequence of work the jet grouting elements are constructed successively without waiting for the grout to harden in the overlapping elements. With the *primary-secondary* sequence of work, the execution of an overlapping element cannot commence before a specified hardening time has elapsed or before a pre-determined strength of the adjacent previously constructed elements has been achieved.

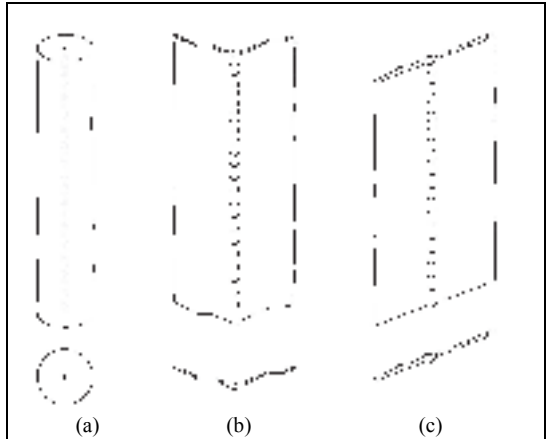


Figure 5.7 Jet Grouted Column (a) and Jet Grouted Panel (b,c)

5.2.4 Jet Grouting Structures

A structure can be created from different arrangements of jet grouted elements. The most common are a jet grouted:

- a) Diaphragm: a wall obtained by making interlocked elements;
- b) Slab: a horizontal structure formed by interlocked elements;
- c) Canopy: an arch formed by interlocked horizontal or sub-horizontal elements;
- d) Block: a three-dimensional structure formed by interlocked elements.

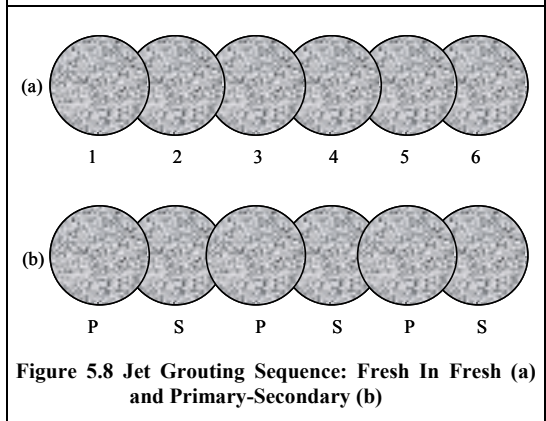


Figure 5.8 Jet Grouting Sequence: Fresh In Fresh (a) and Primary-Secondary (b)

Structures a, b and c are illustrated in Figure 5.9. Interlocking can be full or partial. When jet grouting is used to create stability, partial interlocking is often sufficient. If jet grouting is used to create a low permeability barrier, the elements should interlock completely. This is however not reviewed in this thesis.

5.2.5 Field of Application

Jet grouting can be used for different purposes in either temporary or permanent works, for example:

- to provide foundations for new structures;
- to underpin existing foundations;
- to create low permeability barriers;
- to create retaining or supporting structures;
- to complement other geotechnical works (for instance temporary stabilisation);
- to reinforce a soil mass.

This study focuses only on the first two aspects. An illustration of jet grouting used for underpinning of a pile foundation is shown in Section 2.7.3. To give an indication of the strength that can be obtained when jet grouting soil, in the next sub-section a table of grout strengths based on project references is presented.

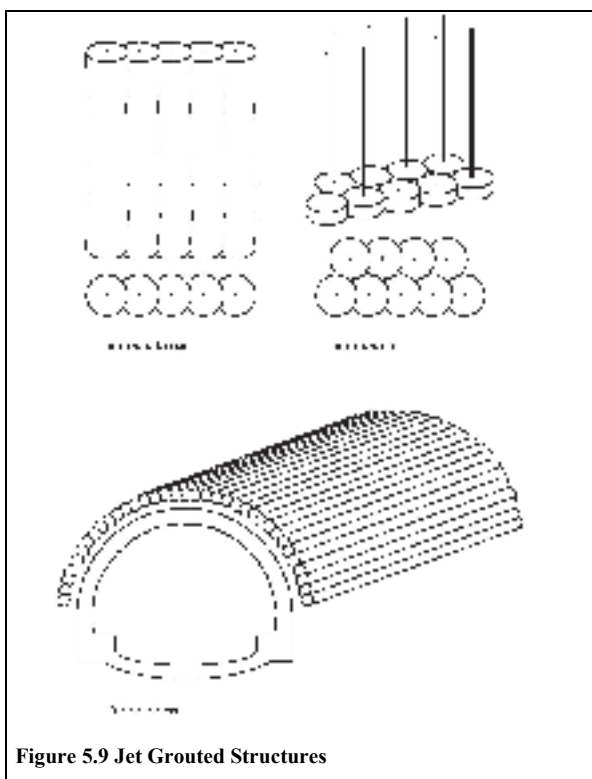


Figure 5.9 Jet Grouted Structures

5.2.6 Grout Strength

Information concerning the strength of the jet grouted columns given in scientific publications often lacks information on jet grouting process parameters. Therefore predictions of the strength by using the graphs or relations given in such publications should be made with care.

Rodio (Kauschinger et al., 1992^{*}) presents a highly simplified model (eqn. 5.1) for predicting the wcr of samples taken from a jet grouted column created in moist sandy gravel soil, using the unconfined compressive strength of the sample. The wcr is then used to calculate the jet grouted column diameter. The relationship, which is based on a series of test columns, only takes into account the UCS, but the authors report obtaining satisfactory results for the tested columns.

$$\text{eqn. 5.1: } wcr_{ejected} = \frac{\sqrt{f_c}}{7.4}$$

where:

$wcr_{ejected}$ water cement ratio of the spoil;

f_c unconfined compressive strength of samples taken from the jet grouted column (kg/cm^2).

In 5.6.2 Rodio's relationship is used to examine the correlation between the wcr and the UCS in the Amsterdam test.

From the published information on projects where the strength of the jet grouted columns was recorded, it is possible to derive an indication of the average grout strength in several soil types, as shown in Table 4.1.

^{*} Kauschinger refers to internal Rodio report (which could not be obtained)

Table 5.1 Typical Average Unconfined Compressive Strength of Jet Grouted Soil

Soil type	UCS (MPa)	
	Lower limit	Upper limit
Peat	1	6
Clay	3	7
Silt	5	15
Sand	10	40
Gravel	10	40

5.2.7 Jet Grouting Parameters

Commonly during jet grouting the following parameters are monitored:

- pressure of the fluid(s);
- flow rate of the fluid(s);
- grout composition;
- translation and rotation speed of the jet grouting string.

The fluid pressure and flow rate are commonly measured as pump pressure before entering the jet grouting string. The working parameters usually adopted for the different jet grouting systems fall within the ranges shown in Table 5.2.

Table 5.2 Ranges of Jet Grouting Parameters (from prEN 12761)

<i>Working parameters</i>	Single fluid	Double fluid (air)	Double fluid (water)	Triple fluid
<i>Grout pressure (MPa)</i>	30 – 50	30 – 50	>2	>2
<i>Grout flow rate (ℓ/min)</i>	50 – 450	50 – 450	50 – 200	50 – 200
<i>Water pressure (MPa)</i>	not applicable	not applicable	30 – 60	30 – 60
<i>Water flow rate (ℓ/min)</i>	not applicable	not applicable	50 – 150	50 – 150
<i>Air pressure (MPa)</i>	not applicable	0.2 – 1.7	not applicable	0.2 – 1.7
<i>Air flow rate (ℓ/min)</i>	not applicable	3 – 12	not applicable	3 – 12

Lower limits of grout and water pressure down to 10 MPa have also been adopted in particular cases, such as small diameter jet grouted columns in very loose soils. The most recently developed pumping equipment allows pressures of the disaggregating fluid (water or grout) up to 70 MPa and flow rates up to 650 ℓ/min.

Because of the increasing use of jet grouting in deep foundation technology, much effort has recently been put into finding a tool to measure the inclination of the jet grouting string. This is considered separately in the next section.

To gain insight into how some principal jet grouting parameters interrelate, in Figure 5.10 an example is shown of the working diagram of a high pressure grout pump as presented by De Vleeshauer and Maertens (1999). If the flow rate, the water cement ratio and the grouting pressure are known, the proper nozzle diameter for the appropriate pump can be determined from the diagram. In the example shown in the figure, a flow rate of 150 ℓ/min, a water cement ratio of 0.9 and a grouting pressure of 400 bar, leads to the determination of a nozzle diameter of 2.5 mm when using 2 nozzles.

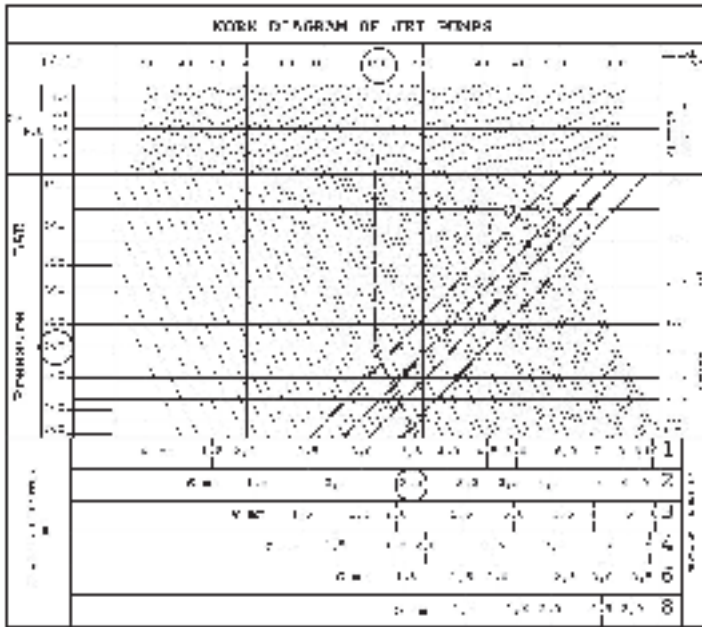


Figure 5.10 Example of Work Diagram of Jet Grouting Pumps (De Vleeshauwer and Maertens, 1999)

5.2.8 Horizontal Position of the Jet Grouted Column

To determine the horizontal position of the jet grouted column at a certain depth, the vertical inclination has to be verified. Basically there are three methods to measure this position, these being:

1. the use of an inclinometer tube in the freshly grouted column;
2. the use of an inclinometer inside the jet grouting string after drilling the string;
3. the integration of an inclinometer in the jet grouting string measurement during grouting.

The first method can only be used when the jet grouted column is still accessible (i.e. fluid enough), which is often not the case. Another problem is that the inclinometer tube may tend to assume a vertical position even when the column is inclined.

The second method works well but its most important disadvantages are that it requires a costly pause in the jet grouting process and that the drilling has already been carried out when the measurements are conducted. This method was used in the Full Scale Injection Test.

The third method originated in the last decade. In the ideal situation the data of the inclinometer measurement can be read online and corrections to the position of the jet grouting string can be immediately made. Several jet grouting companies are now simultaneously developing and testing this kind of equipment (see Chapter 10).

Normal accuracy for jet grouting in soil is $\pm 0.5\%$ for drilling up to 15 meters and $\pm 1.0\%$ for drilling up to 30 meters of depth.

The horizontal position of the column is one of the aspects that determine the zone of influence of a jet grouted column and therefore the influence jet grouting has on a pile foundation. An overview of all aspects is given in the next section.

5.3 Assessing the Influence of Jet Grouting on Pile Foundations

5.3.1 Introduction

To assess the influence of jet grouting on pile foundations the diameter, strength and stiffness of the jet-grouted element have to be known. The diameter of the element is important because it determines the range of influence of the jet grouting process. The strength and stiffness of the grouted element determine its behaviour as a part of the foundation (renovation) or the soil mass (foundation protection). One of the biggest complications for those trying to understand the jet grouting process is that there are so many interrelating parameters that modelling the process is very complex. Few attempts have been made to model jet grouting numerically, only a few theoretical models have been presented and although many jet grouting contractors have their own models, these are not generally available.

In the text some theoretical models for diameter prediction and strength are explained, followed by a conclusion considering the feasibility of modelling the influence of jet grouting on pile foundations.

5.3.2 Assessing the Jet Grouting Process

Before assessing the influence jet grouting has on pile foundations, the jet grouting process itself has to be closer looked at. Jet grouting can ideally be assessed by describing five different stages of the process:

1. drilling the monitor to depth;
2. pre-cutting the soil (optional for cohesive soil layers);
3. jetting the soil;
4. pre-set condition of the grouted soil*;
5. set condition of the grouted soil.

The drilling, pre-cutting and jetting stages are all of a dynamic nature. Several aspects play a role here, the most important of which are the influence of the soil heterogeneity and the large number of jet grouting parameters that influence the result. Quantitative modelling of the influence of these parameters is very complex. However, because they determine the diameter of the jet grouted column, and thus indirectly the distance between the foundation pile and the column, they are important.

The spoil return flow deserves special consideration, since when the return flow is blocked, a large pressure build up can occur. This may lead to heave and ultimately even to a possible blow-out and should therefore be prevented.

During *drilling the monitor to depth* a borehole with a small diameter is created. As was discussed in Section 4.7, the effect of the formation of such a borehole on the surrounding soil is limited. Sometimes a little cement and/or betonite is added to the process-water to prevent the borehole from collapsing.

The stage in which *pre-cutting of the soil* is applied is optional for cohesive soil. Because the soil is being eroded and mixed with water, the unit weight of this mixture is temporarily lower than that of the intact surrounding soil. The stiffness and strength of this mixture also tend to zero. However, because of the cohesive nature of the surrounding soil, combined with the lateral pressure performed by the mixture, the element will not instantly collapse. Nevertheless, it is advisable that jetting follows fairly quickly after pre-cutting has taken place. Often drilling and pre-cutting are combined, by using the double water jet system.

During the *jetting stage* the soil is eroded and mixed with water and cement. Because of the high unit weight of cement, the unit weight of the grout/soil mixture in cohesive soil is usually equal to or greater than that of the surrounding soil. However, because of the semi-fluid state of the element its stiffness and strength will be lower than those of the soil. Problems with the stability of a nearby foundation may occur when the jetting takes place close to this foundation.

The temporary *pre-set stage* is significant because the complete grouted element is in a liquid state in this stage and therefore the soil or the stability of a nearby foundation may be influenced. When the soil

* i.e. the condition before the grouted soil has reached its full hardness

is normally consolidated, the lateral pressure performed by the mixture is usually sufficient to compensate the lateral effective stress acting on the element:

eqn. 5.2 $\gamma_{grout} \cdot h \geq K_0 \cdot \sigma'_v + u$

where:

γ_{grout}	=	unit weight of the grout mixture	(kN/m ³)
h	=	height of the grout mixture column	(m)
K_0	=	lateral stress ratio	(-)
σ'_v	=	effective vertical stress	(kN/m ²)
u	=	pore water pressure	(kN/m ²)

For over-consolidated soil or soil close to the base of displacement piles, the lateral stress ratio (K) will be higher than K_0 and thus problems might occur concerning the soil stability. As the stiffness and strength of the element develop only gradually with the hydration process, whether or not a nearby foundation is capable of temporarily withstanding a unfavourable change of soil properties in the area of the element, is an important issue.

The *set stage* does not negatively influence the stability of a foundation. Any inherent instability that was going to occur would have occurred in the previous stages. In the set stage, however, usually a load is applied to the jet grouted column and both the stability of the jet grouted column itself and that of the foundation adjoining the jet grouted column should then be verified.

5.3.3 Modelling Jet Grouting

Currently when it is necessary to make predictions to assess the effect of creating jet grouted columns, the most common approach is to estimate the required diameter on the basis of practical experience. In other words, the soil properties are assessed and practical experience is used to estimate jet grouting parameters that will result in the desired jet grouted column diameter.

Kanematsu (1980) presents relationships between nozzle diameter (d) and the maximum jet grouted column diameter (D). The length of the zone before the jet becomes unfocused and discontinuous and cavitation effects start to occur (R_a), is about 300 times the nozzle diameter: $R_a = 300 \cdot d$. The diameter of the column is approximately equal to twice this length: $D = 2 \cdot R_a$.

Kauschinger et al. (1992) present a relation based on the mass balance approach:

eqn. 5.3 :
$$D = \sqrt{\frac{W_t^c}{\frac{\pi}{4} H \gamma_t^c}}$$

Where:

W_t^c	Weight of the soil, water and cement in the column
H	Height of the column (section)
γ_t^c	Unit weight of the column

The accumulated weight W_t^c should be calculated from the balance between the *measured* weight of the in-situ, injected and the ejected soil:

eqn. 5.4: $W_t^c = W_{cement}^c + W_{water}^c + W_{soil}^c + W_{air}^c$

where:

W_{cement}^c	Weight of the cement in the column	W_{soil}^c	Weight of the soil in the column
W_{water}^c	Weight of the water in the column	W_{air}^c	Weight of the air in the column

The difficulty with this theoretical approach is that it is based on the assumption that the jet grouted column is homogeneous, that no fracturing occurs, that there is no drainage of water during consolidation of the jet grouted column and that it is difficult to determine the weight parameters in the column.

JET GROUTING

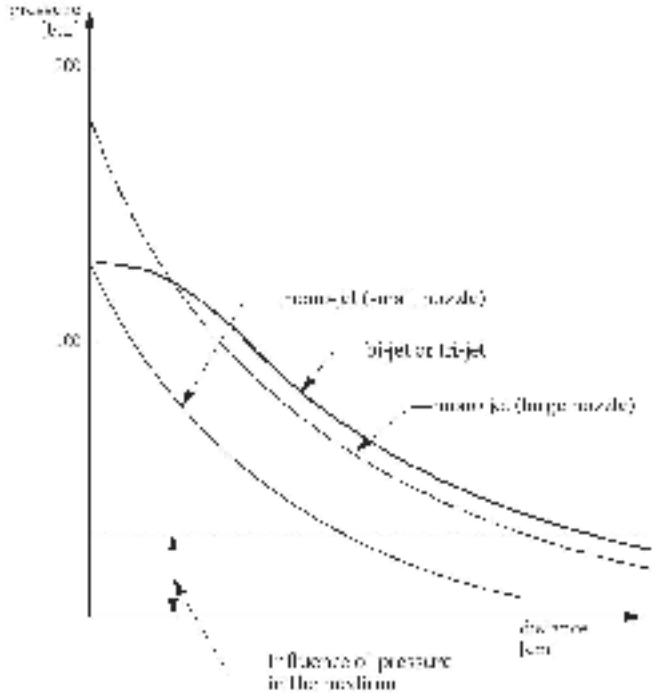


Figure 5.11 Relation Jet Grouting Pressure - Penetration Distance (De Vleeshauer and Maertens, 1999)

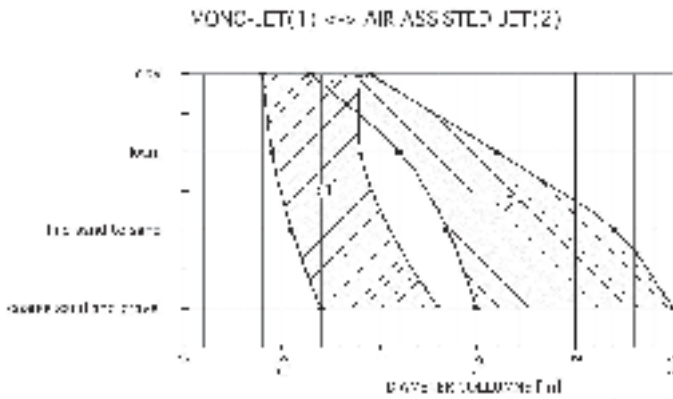


Figure 5.12 Indication of Jet Grouting Column Diameters (De Vleeshauer and Maertens, 1999)

Table 5.3 Results of 3D-FEM Calculations for Jet Grouted Columns near Concrete Pile

Stage	Distance from pile (m)	Column diameter (m)	Measured Settlement (mm)	3D-FEM settlement (mm)
1	1.00	1	0.5-3.0	0.23
	0.33	1		0.58
2	1.00	2		0.21
	0.33	2		0.73

To be able to predict the diameter of jet grouted columns, De Vleeshauer and Maertens (1999) conducted tests at Leuven University concerning the pressure development of the jet. In these tests pressures of a water jet in a water basin were measured. Selected results are shown in Figure 5.13. Note that while a good indication of the pressure drop at different grouting pressures was obtained from the results, only a constant nozzle diameter was investigated and the soil properties were not taken into account. The radius of the area of influence that is obtained from the figures gives an indication of the maximum jet grouted column diameter that can be obtained for different grouting pressures (Figure 5.11).

A substantial amount of data concerning the diameter of jet grouted columns has been published. Because this data often lacks information on several grouting and soil parameters, predictions of the diameter based on the graphs or relations given in these publications should be made with care. A summary of column diameters realised in several soil types is shown in Figure 5.12 (De Vleeshauer and Maertens, 1999). Data from Covil (1991) has been verified to comply with this graph.

FEM

The results of Finite Element Method (FEM) calculations to analyse the influence of the jet grouting on pile foundations are summarised by Van Zanten, Kay and Van der Stoel (2001). The conclusions that could be drawn from the 2D FEM calculations was that the limitations of 2D modelling resulted in too much restrictions for an accurate model to be created. The 3D FEM predictions showed displacements of the foundation pile similar to the ones found in the test (Table 5.3). Because of the many schematisations that had to be made during modelling, the principal contribution of the FEM calculations is that they provide a rough estimate of likely pile settlements. Because the pile settlements are relatively small, the practical value of these calculations is limited.

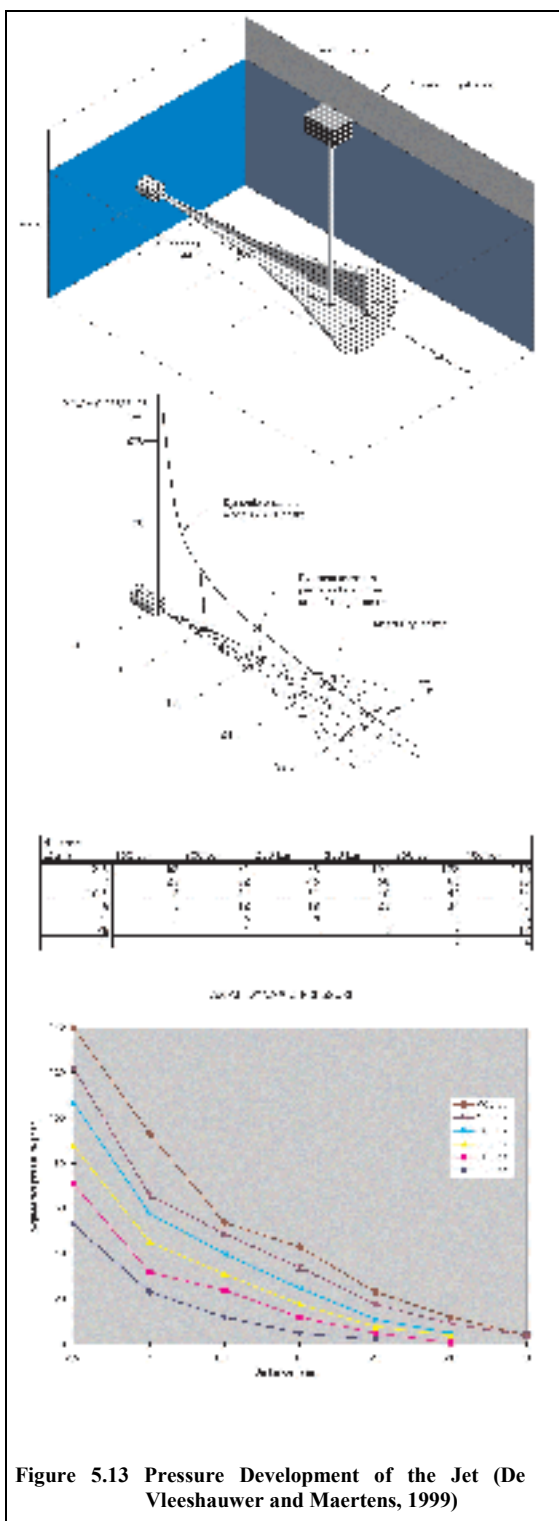


Figure 5.13 Pressure Development of the Jet (De Vleeshauer and Maertens, 1999)

5.3.4 Conclusions

Using the above considerations it is concluded that the zone of influence of a jet grouted column, and therefore the influence jet grouting has on a pile foundation, is dependent on the:

1. jet grouting process parameters;
2. soil parameters;
3. position of the jet grouted column;
4. foundation pile characteristics.

The first two items together determine the diameter of the jet grouted column.

- Re.1 The *jet grouting process parameters* depend on a number of factors such as the pre-cutting pressure, the jetting pressure, the flow rate, the nozzle diameter, the uplift and rotational speed of the monitor and the number of nozzles. All these jet grouting process parameters can in turn be specified by making distinctions between the water, air and grouting pressures, flow rate(s) and nozzle diameter(s).
- Re.2 The *soil parameters* can be expressed as a function of grain size distribution, cohesion, initial stresses and pore water pressure in the soil layer that is to be grouted.
- Re.3 The *position of the column* is influenced by the co-ordinates of the starting/drilling point and the inclination of the drilling direction.
- Re.4 The *influence of the pile characteristics* is characterised by the safety factor of the pile, the percentage of shaft bearing capacity and end bearing capacity, the shape of the pile and the pile surface.

Because the foundation pile characteristics can be assessed by careful research and the position of the column can be controlled by careful positioning the jet grouting rig and string, they have a significantly smaller influence than the jet grouting process and the soil parameters.

Although some parameters will have a much greater influence than others and although many parameters are interrelated, the complexity of the relationships between the parameters is probably the reason for the lack of reliable models for predicting the influence of jet grouting on pile foundations. It is not expected that in the near future (<10 years) reliable models to predict this influence will become available. This, combined with the fact that experience of jet grouting near or under pile foundations is very limited, justifies devising tests that can be used to provide a proper risk assessment. In Amsterdam therefore a full scale test was performed, the detailed set-up of which will be discussed in the next section.

5.4 Details of Jet Grouting Test Set-up

5.4.1 General

Because of the difficulties encountered when trying to make reliable jet grouting diameter and strength predictions in Amsterdam, it was decided that full scale testing was necessary. In this way the jet grouting process and the influence jet grouting has on pile foundations could be studied. For general information concerning the organisation, aims and general set-up of the Full Scale Injection Test reference may be made to Chapter 3. This section deals specifically with the test set-up for stage 3B.

Throughout the text some figures are needed from which the position of the grouted columns relative to the piles and monitoring equipment can be derived:

- Figure 5.15 shows a plan view of columns A, B, C and D, which were created next to the piles to study the influence of jet grouting for foundation protection (see Figure 2.17).
- Figure 5.16 shows a cross section of columns A, B, C, D, X1 and X2 and the piles.
- Figure 5.15 shows a plan view of columns E, F, W1, W2 and W3, which were created under pile toes, to create pile extensions for foundation renovation purposes (see Figure 2.15). The upper position of these columns is indicated by *u* and the lower position by *l*. Columns X1 and X2, which were created with a different water cement ratio, are also shown in this figure.
- Figure 5.17 shows cross sections of columns E, F and W1-W3 and the piles they extend.

The design philosophy for the test was to create the jet grouted columns A-F sequentially, leaving enough time between each procedure to study the time dependant effects of grouting each column. Column A, located furthest from the piles and expected to have very little influence on the piles, was therefore created first. Column B was located very close to the piles and was expected to influence the piles significantly. The three wooden and concrete piles were located at an increasing distance from column B, thus creating an opportunity to measure the extent of the influence of grouting as a function of the distance.

Inclined drilling was necessary for columns E, F, W1, W2 and W3 because of the position of the ballast frame*.

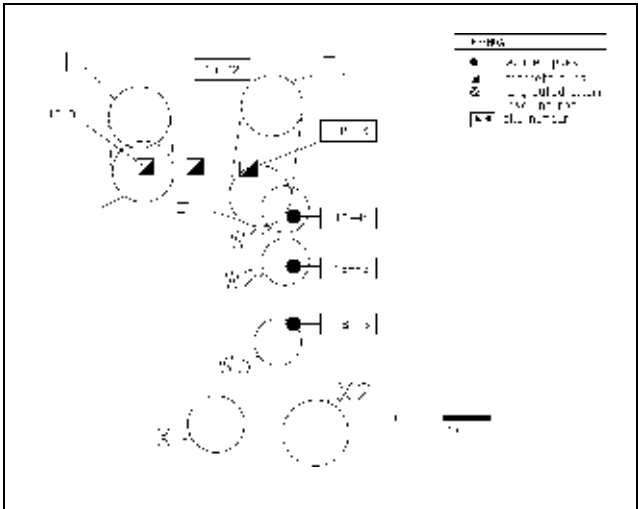


Figure 5.14 Details of Jet Grouting for Foundation Renovation: Columns E,F, W1, W2, W3 and with Alternative *wcr* for Columns X1 & X2

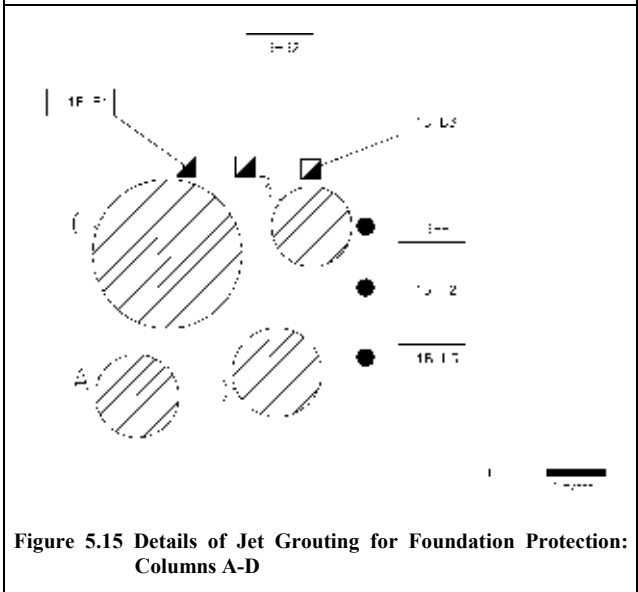


Figure 5.15 Details of Jet Grouting for Foundation Protection: Columns A-D

* Note that when using Jet Grouting for foundation renovation inclined drilling may also be necessary to reach the pile from outside the structure

JET GROUTING

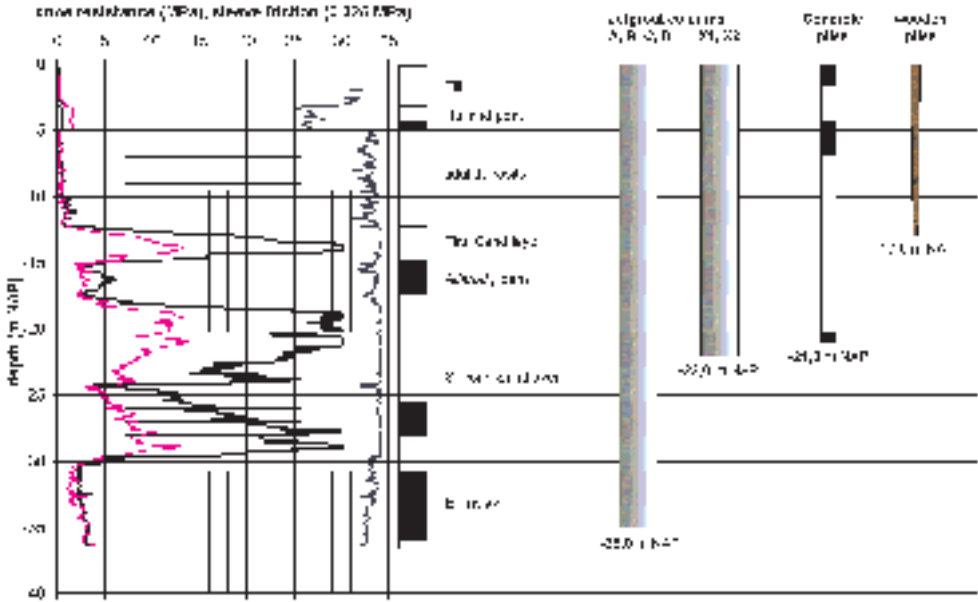


Figure 5.16 Detailed Test Set-Up: Cross Section of Columns A, B, C, D, X1 and X2 and Piles

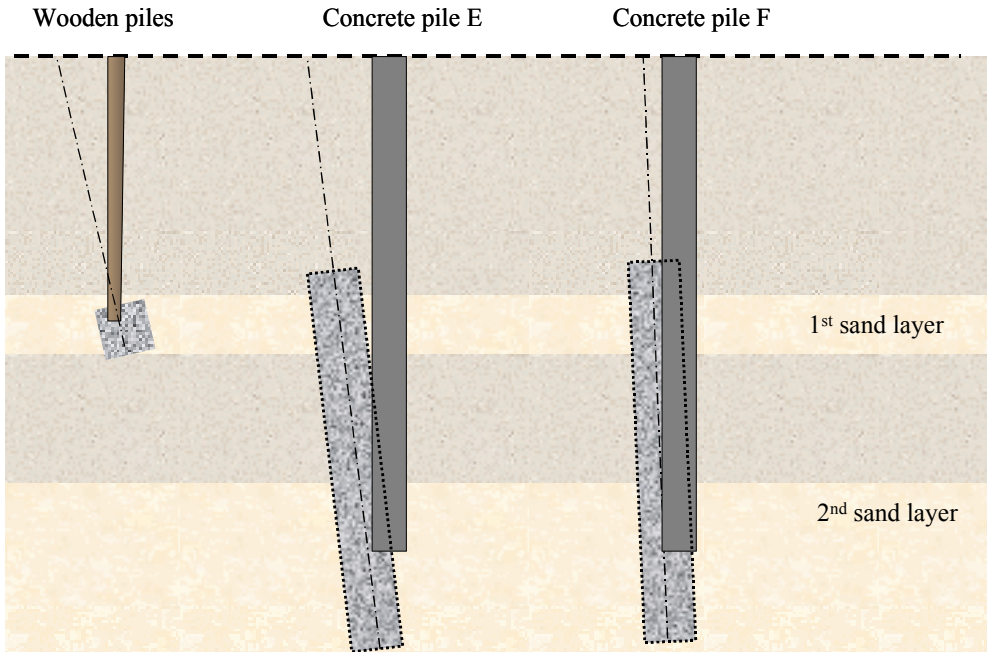


Figure 5.17 Cross Section of Jet Grouting for Foundation Renovation: Pile Extension Columns E, F and W

5.4.2 Piles

Three wooden piles 1B-H1, 1B-H2 and 1B-H3, and three concrete piles 1B-B1, 1B-B2 and 1B-B3 were installed. The top x,y position of all the piles was verified after driving. The x,y,z position of the concrete piles was checked by inclinometer measurements, from which it could be derived that the piles were installed as good as vertically.

The wooden and concrete piles were supplied with piezometers and stress cells (SMS). The SMS and piezometers that functioned after installation were located in the toes of piles 1B-B1, 1B-B3 and 1B-H3 and the middle of piles 1B-B1, 1B-B2 and 1B-B3. The pile heads were all individually monitored using both targets and jointmeters (see Section 3.4).

5.4.3 Jet Grouted Columns

The dimensions of the jet grouted columns are given in Table 5.4. Note that the diameters of the columns, as shown in Figure 5.15 differ from the designed diameter. The diameter of the columns was determined using excavations (see Section 5.11) and geophysical investigation methods (see Chapter 7). The verticality of the jet grouted columns was checked in 2 directions using inclinometer measurements in the string after drilling and before jetting. The maximum deviation from the designed drilling angle was 0.35 m (approximately 1 %).

Table 5.4 Dimensions of the Jet Grouted Columns.

Column	Designed diameter \varnothing_d (m)	Realised diameter \varnothing_r (m)	Grouting		<i>wcr</i>
			From NAP (m)	To	
A, B	1.0	1.45 , 1.40	-35	-2	1.0
C,D	2.0	2.60 , 1.55	-35	-2	1.0
E, F	1.0	- , -	-22	-10	1.0
X1	1.0	1.20	-22	-2	0.8
X2	1.0	1.40	-22	-2	1.2
W1,2,3	1.0	- , - , -	-13.5	-11.5	1.0

Various process procedures were employed during the creation of the jet-grouted columns. They are mentioned below.

For columns *A, B, C, D, X1*, and *X2* :

1. Drilling until the monitor reached the required cutting depth.
2. Pre-cutting the clay layer with water by lifting the monitor until the sand layer is reached.
3. Bringing the monitor back down to the required jetting depth.
4. Jetting the clay layer and sand layer until the next clay layer is reached and repeat from step 2.

For columns *E* and *F* :

1. Drilling until the monitor has reached NAP -22 m.
2. Jetting from NAP -22 m to -17 m; followed by an overnight rest period.
3. Next day re-drilling to NAP -17.5 m and jetting from NAP -17 m to -10 m.

For columns *W1, W2* and *W3* :

1. Drilling until the monitor has reached NAP -13,5 m.
2. Jetting from NAP -13,5 m to -11,5 m.

5.4.4 Monitoring Equipment

Surface and subsurface soil displacements were measured in all three co-ordinate directions using a combination of levelling points, extensometers and inclinometers (Figure 5.19).

Surface levelling points were used to measure vertical surface displacement. To monitor the displacement beacons TS 7 to TS 12 were installed at increasing distance from the jet grouted columns. They were monitored with the aid of targets attached to the pole of the beacon.

Vertical displacements from ground level to NAP -15m and -25m were monitored by using *extensometers* EX1 and EX2. The surface position was also monitored using the automatic theodolite and a target. The change in distance between ground level and the extensometer anchors at various depths was then monitored and used to calculate the absolute vertical displacement profile.

Inclinometers INCL1 and INCL2 were used to measure the horizontal displacement profile at a depth of NAP +0.5 to NAP -30m. The inclinometers were monitored only before and after grouting. The position of the top of the inclinometers was continuously monitored with the aid of targets mounted on the inclinometer on surface level.

In addition to soil displacements, pore water pressures were also monitored, using *piezometers* installed in the soil at different distances from the jet grouted columns. Three piezometers, FUG_432, FUG_437 and FUG_451, were installed at NAP -12.5 m (Figure 5.19).

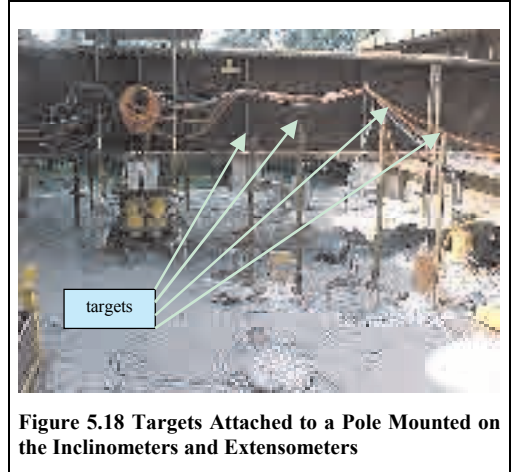


Figure 5.18 Targets Attached to a Pole Mounted on the Inclinometers and Extensometers

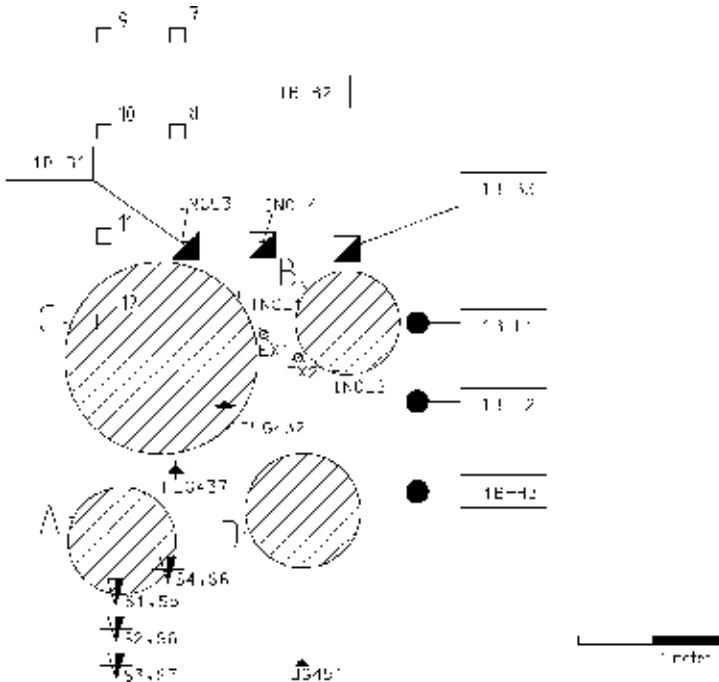


Figure 5.19 Position of the Inclinometers, CPTs, Extensometers, Beacons and Piezometers in the Soil

5.5 Jet Grouting Process Parameters

For all jet grouted columns, with exception of columns E and F, pre-cutting by means of water-jetting was used in the cohesive soil-layers. The purpose of the pre-cutting was to facilitate the formation of a column with sufficient diameter and to increase the strength and stiffness of the column. The design parameters of the jet grouting process are set out in Table 5.5.

Table 5.5 Average Process Parameters used for Jetting the Columns.

Column	Jet System	Ø design (m)	Grouting From To NAP (m)		wcr (-)	Lift speed pre-cutting (sec/2cm)(10 ⁻³ m/s)		Lift speed grouting (sec/2cm)
A, B	Single	1	-35	-2	1.0	5	4.00	6
E, F	Single	1	-22	-10	1.0	--		6
C	Double	2	-35	-2	1.0	8	2.50	12
D	Single	2	-35	-2	1.0	7	2.86	13
X1	Single	1	-22	-2	0.8	4	5.00	6
X2	Single	1	-22	-2	1.2	4	5.00	6

Column	Nozzle Diameter (mm)	Water Flow Rate (l/s)	Pre-cutting Pressure (MPa)	Grout Flow Rate (l/s)	Grouting Pressure (MPa)
A, B	4.0	3.15	20	2.60	40
E, F	4.0	-	20	2.60	40
C	5.0	4.92	40	4.07	40
D	5.0	4.92	40	4.28	45
X1	4.0	2.53	20	2.53	40
Column	4.0	2.63	20	2.63	40

- Note that the string is withdrawn in 2 cm steps, therefore the lift speed is also given in *sec/2cm*.
- The rotation speed of the nozzles is the same for all columns: 6-8 r/min.
- The air pressure used with column C amounted 6 bar during pre-cutting and 8 bar during grouting, both with a flow rate of 75 l/min.
- Hoogoven cement class III/B 42,5 LH HS and Amsterdam tap water were used for the water-cement mixture.
- The weight of cement used per grouted volume of 1 m³ was 750 kg in sand layers and 1300-1400 kg in clay layers
- The jet grouting rig used for the test weighed 15.000 kg; the pump used was capable of generating a maximum grouting pressure of 80 MPa.

5.6 Grout Quality

5.6.1 General

To test the quality of the grout, core drilling of columns A, B, C, D, X1 and X2 was carried out over the full length of these columns. The core drilling was carried out for the designed 1m diameter and 2m diameter columns at approximately 0.20m and 0.40m from the centre of the jet grouted column, as shown in Figure 5.21. Eccentric drilling was used as there was concern that drilling along the centre line of the jet grouted columns might not give representative samples.

The grout samples were tested at least 28 days after jet grouting to assure significant maturity of the grout (APPENDIX V). Regarding the core drilling, it was assumed that in 10 days the strength of the grout would be sufficient to carry out the drilling. In APPENDIX V, A.Table 4 the hardening time of the different grout columns is given. After drilling, the grout cores were kept in a water basin until the tests were conducted (Figure 5.22).

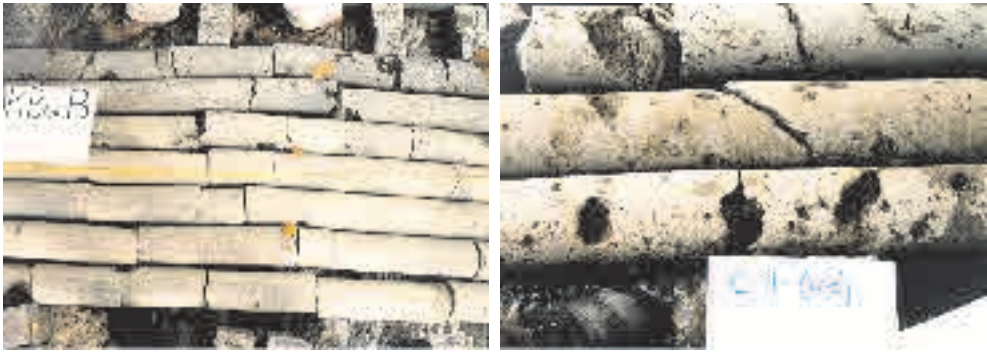


Figure 5.20 Cores taken from Jet Grouted Sand Column B (left) and Jet Grouted Peat Column C (right)

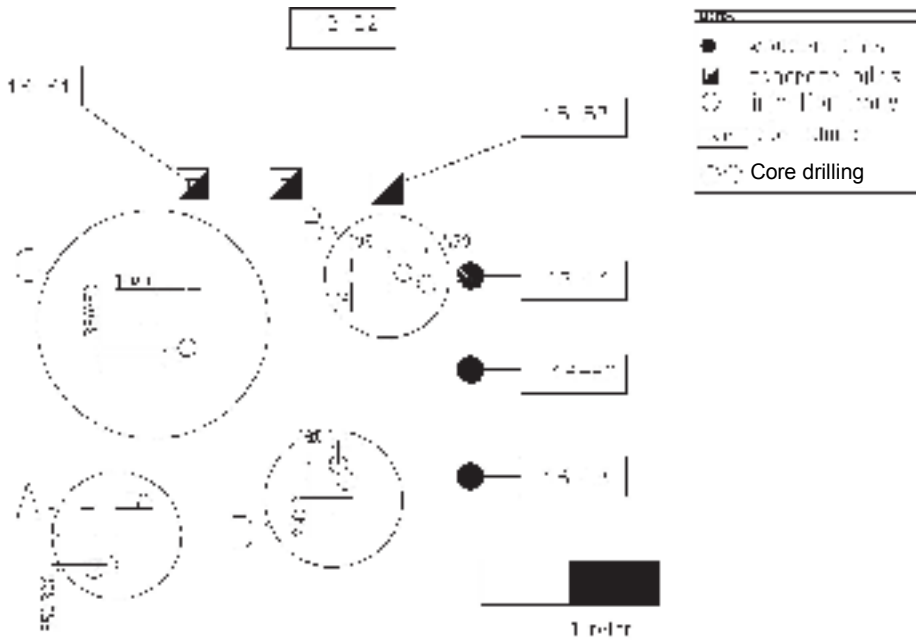


Figure 5.21 Position of the Cores taken from Columns A – D

The verticality of the core drilling was checked by using an inclinometer. The maximum deviation was shown to be 0.35 m ($\approx 1\%$ of the column height). A total of 294 samples were taken from the drilled cores (Figure 5.20), of which 177 samples were used to determine compressive strength, 93 samples to determine tensile strength and 24 samples to determine shear strength.

In the following sections the results of the analysis of the strength and stiffness parameters is presented. Because the number of jet grouting cores that were obtained per layer was limited, some decisions had to be made about which columns and layers could be combined in the analysis. It was decided that the results of columns A, B and D could be combined because of the similarity in the grouting process, but that column C was not comparable with those columns because of the air used in the grouting process. Columns A and B are fully comparable, but for D a different withdrawal speed, flow rate and grouting pressure was used.

It was recognised that combining the columns would probably lead to higher standard deviations for the strength and stiffness parameters. These effects are discussed in the next sub-sections. Van der Stoel (2001) gives a complete overview of all the test results.



Figure 5.22 Storage in Water Basin of Cores from Jet Grouted Columns

5.6.2 Unconfined Compressive Strength

Unconfined Compressive Strength (UCS) tests (in accordance with DIN 18136) were used to determine the compressive strength of the grout. Table 5.6 gives an overview of the main results.

Table 5.6 Average and Standard Deviation UCS (f_c ; MPa)

layer #	system	Single Jet			Single Jet			Single Jet			Double Jet			Single Jet		
	wcr	0.8			1.0			1.2			1.0			1.0		
	column	X1			A,B			X2			C			A,B,D		
	layer	Category 1			Category 2			Category 3			Category 4			Category 5		
	n	mean	sd	n	mean	sd	n	mean	sd	n	mean	sd	n	mean	sd	
1	Peat layer	3	5.5	2.3	3	2.4	0.1	3	1.7	0.4	4	2.3	0.8	6	2.6	0.3
2	Upper clay layer	6	5.4	1.0	12	3.4	1.0	6	3.0	0.7	0	-	-	12	3.3	1.0
3	Lower clay layer	4	13.9	10.2	12	11.8	8.9	4	3.4	2.5	3	3.3	0.4	15	9.9	8.8
4	1st sand layer	4	7.9	3.6	12	19.6	12.6	4	4.4	3.0	4	2.9	0.9	15	17.1	12.4
5	Intermediate layer	4	11.1	1.9	6	12.9	8.3	4	8.6	1.7	4	7.3	1.0	9	15.4	9.0
6	Upper 2nd sand layer	5	33.1	16.4	4	14.6	3.9	4	23.0	13.2	4	8.9	1.4	7	14.6	3.9
7	Lower 2nd sand layer	-	-	-	12	22.3	12.9	-	-	-	6	8.2	2.7	18	19.8	12.4
8	Eemclay layer	-	-	-	10	14.7	7.4	-	-	-	5	5.6	1.1	15	12.6	6.7

The standard deviations of the UCS values per grouted soil layer are relatively large. This is due to the sensitivity of the jet grouting material properties to the in situ mixing process and to a minor extent of the location to the core in the column. The results from column A, which were extraordinarily favourable, also contributed to the high standard deviations of the reviewed test results. The variation coefficient lies between 0.02 and 0.89.

Samples from the same boring that were taken in the same layer and close to each other (i.e. within 0.5 m) often show much smaller deviations in strength than samples taken further apart. Figure 5.23 presents the UCS related to the depth the sample was taken and thus shows a relation between the grout strength and the grouted soil layer. Using Figure 5.23 and the figure, an analysis can be made.

- The large scatter in the results is caused by the fact that the clear boundary between the relatively thin soil layers disappears due to the jet grouting process (the boundary fades due to the eroding process). In the analysis however, the boundaries of the soil are used to distinguish different jet

grouted layers and therefore in the boundary areas the largest variation in strength parameters originate. Figure 5.23 shows that at the boundary the soil material of each original layer influences not only the strength of that layer when it is grouted but also of the adjacent layer that are grouted

- On average, column C shows lower UCS values than the other columns, which can be explained by the use of air during the jet grouting process.
- The UCS of the grouted Holocene layers was not influenced by the different parameters used for column D.

The only apparent explanation for the higher strength properties of column A is that the grouting process was performed differently because it was the first column to be created.

The rapid drop in UCS near the bottom of the columns can be explained by the relatively high soil content at the lower end of the columns as a result of sedimentation of clay lumps.

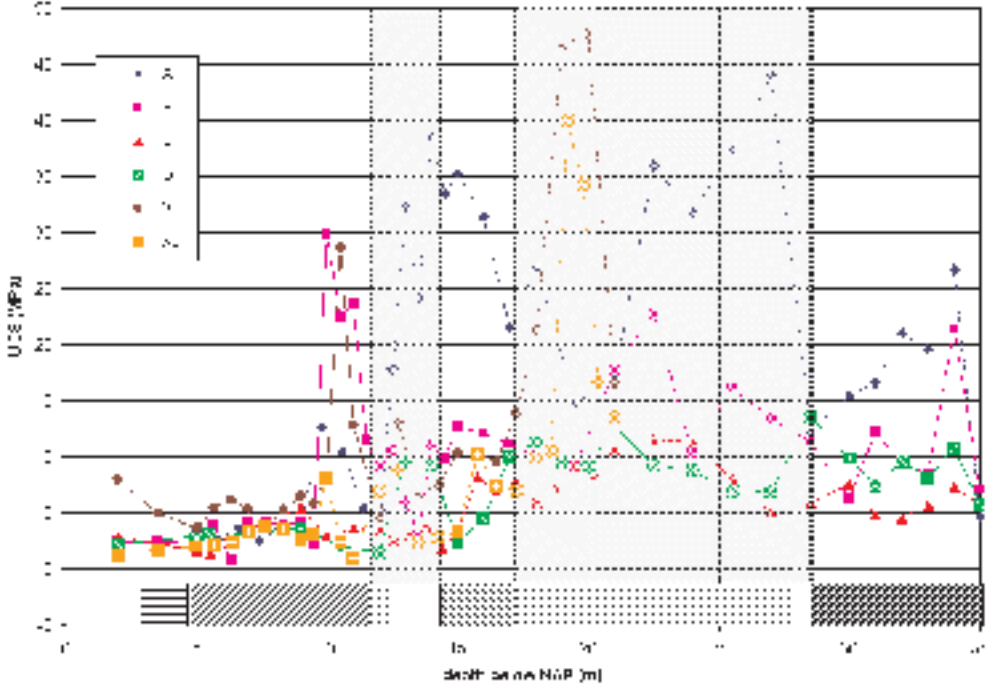


Figure 5.23 UCS Related to NAP Depth (m)

For the test, in general the lower *wcr* results in significantly better strength properties; the higher *wcr* results in significantly lower strength properties. Therefore the relation between the water-cement ratio and the compressive strength was also examined. In Figure 5.24 and Figure 5.25 this relation is shown for the clay layers and the sand layers respectively. For the sand layers the results comply fairly well with the relation between the *wcr* and f_c as presented by Rodio for spoil samples (see Section 5.2.6). Therefore this relation was used to deduce a similar relation for the Amsterdam sand and clay layers, for $0.6 < wcr < 1.4$:

eqn. 5.5 $f_c = 7 + 8.1 (wcr)^2$ (Jet grouted sand)

eqn. 5.6 $f_c = 2 + 3.6 (wcr)^2$ (Jet grouted clay)

where:

wcr = water cement ratio (-)

f_c = compressive strength (MPa)

JET GROUTING

It is important to realise that these relations can only give a rough estimate, because many jet grouting parameters that also influence the strength are not incorporated in the relation. For similar grouting processes the relation can however be a useful rule of thumb.

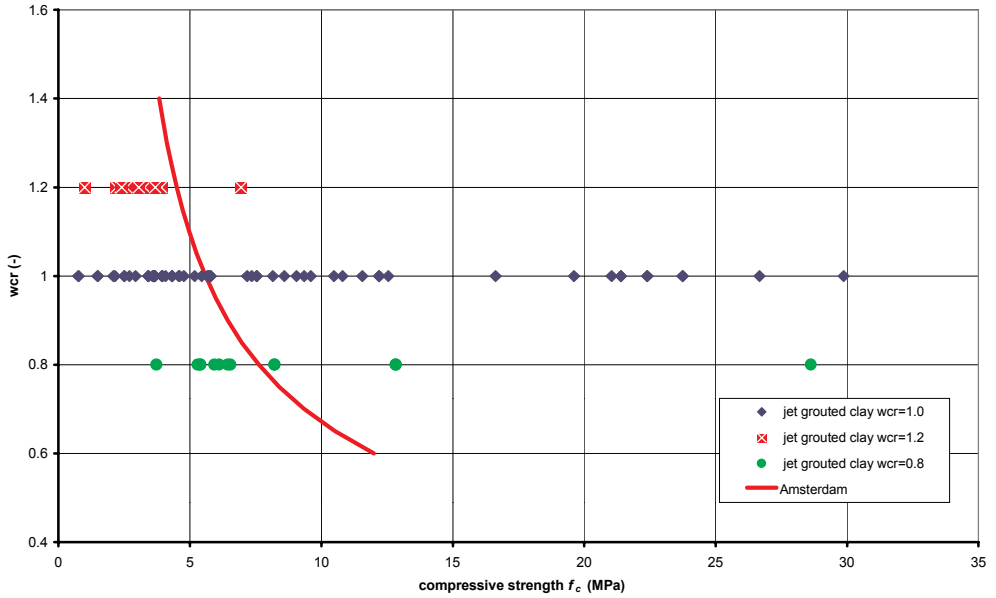


Figure 5.24 Relation between Water Cement Ratio wcr and Compressive Strength f_u for Clay Layers

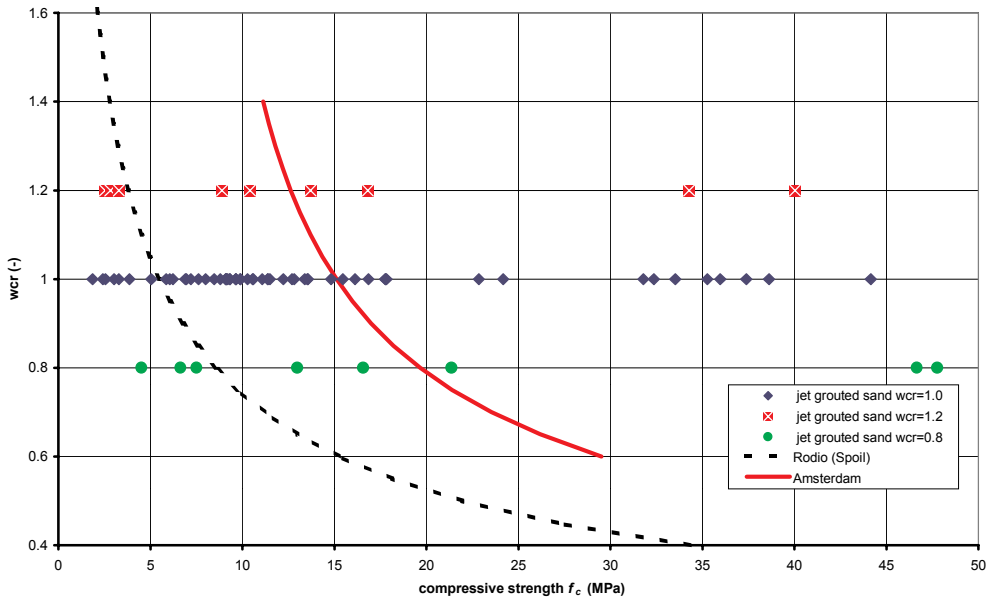


Figure 5.25 Relation between Water Cement Ratio wcr and Compressive Strength f_u for Sand Layers

5.6.3 Tensile Strength

To determine the tensile strength of the grout, the Brazilian Split Test (BST) was used. For concrete the tensile strength obtained by a BST is generally considered to overestimate the direct tensile strength by 5-12 %. For mortar there is a comparable underestimation (Neville, 1997). The main results of the BST are shown in Table 5.7 for reasons already given in Section 5.6.2, the variation coefficient lies between 0.06 and 0.98.

Table 5.7 Average and Standard Deviation Tensile Strength ($f_{ct,sp}$; MPa)

layer #	system	Single Jet			Single Jet			Single Jet			Double Jet			Single Jet		
	wcr	0.8			1.0			1.2			1.0			1.0		
	column	X1			A,B			X2			C			A,B,D		
	layer	Category 1			Category 2			Category 3			Category 4			Category 5		
	n	mean	sd	n	mean	sd	n	mean	sd	n	mean	sd	n	mean	sd	
1	Peat layer															
2	Upper clay layer															
3	Lower clay layer															
4	1st sand layer															
5	Intermediate layer															
6	Upper 2nd sand layer															
7	Lower 2nd sand layer															
8	Eemclay layer															

A relation between the strength and stiffness parameters of the jet grouted material can be extremely helpful in the design process. Therefore the relation between the compressive strength f_c and the tensile strength $f_{ct,sp}$ of the grout were examined. In Figure 5.26 and Figure 5.27, the test results for the sand (#4, 5 and 6) and clay (#2, 3 and 8) layers are displayed. It should be noted that more UCS-tests; BS-tests were made, so sometimes multiple compressive strength f_c values are compared with a single tensile strength $f_{ct,sp}$ value.

For concrete, a number of empirical formulae connecting f_c and $f_{ct,sp}$ were suggested, many of them of the type: $f_{ct,sp} = k (f_c)^n$ (Neville, 1997). Because of the similarities between jet grouted material and concrete this relation was applied to the test data, resulting in expressions eqn. 5.7 and eqn. 5.8:

eqn. 5.7 $f_{ct,sp} = 0.3 (f_c)^{3/5}$ (Jet grouted sand)

eqn. 5.8 $f_{ct,sp} = 0.4 (f_c)^{3/10}$ (Jet grouted clay)

where:

- $f_{ct,sp}$ = tensile strength (MPa)
- f_c = compressive strength (MPa)

The relations apply for a water-cement ratio of 1.0. The correlation for the sand layers is considered to be moderate ($R^2=0.6$); for the clay layers the correlation is considered to be weak ($R^2=0.2$).

5.6.4 Young's Modulus

The Secant or Young's modulus is defined in DIN 18136 as:

eqn. 5.9 $E = \frac{\sigma_{70} - \sigma_{30}}{\epsilon_{70} - \epsilon_{30}}$

where ϵ and σ are respectively the stress and strain at either 30% or 70% of the failure stress during testing of the sample. The main results concerning the Young's moduli determined from the UCS test results are given in Table 5.8. The variation coefficient lies between 0.11 and 0.76 for reasons already given in Section 5.6.2.

JET GROUTING

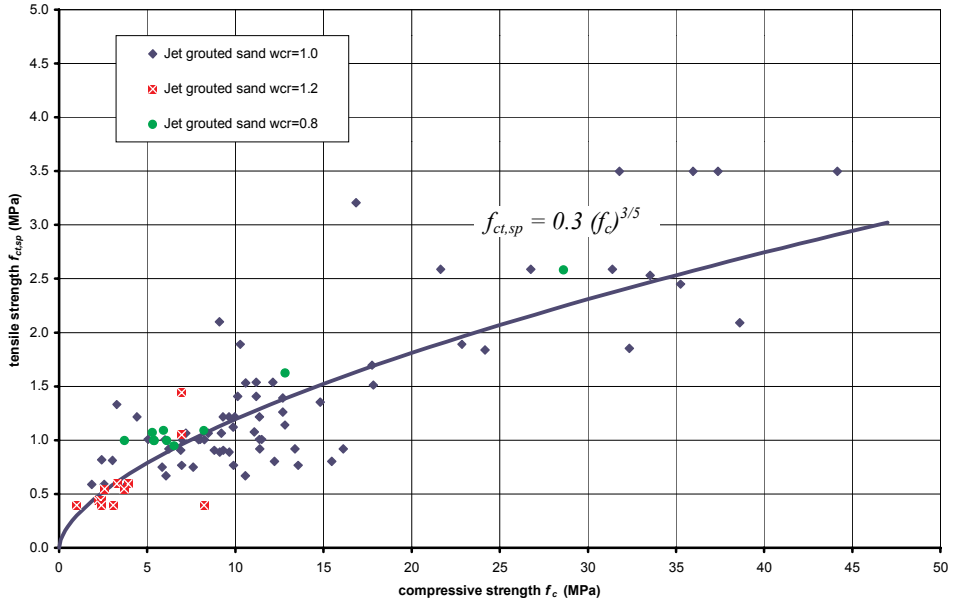


Figure 5.26 Tensile Strength $f_{ct,sp}$ vs. Compressive Strength f_c for Jet Grouted Sand Layers

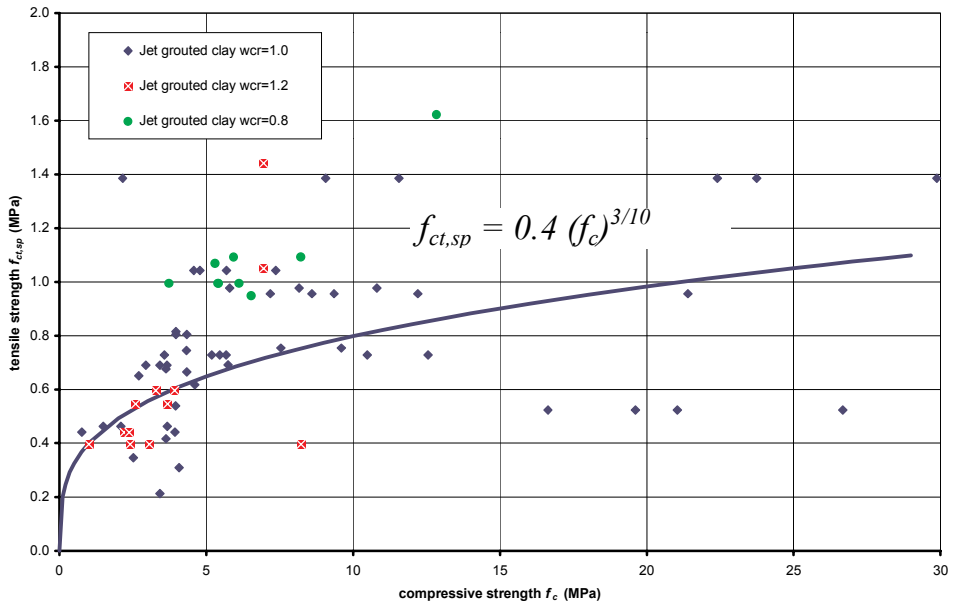


Figure 5.27 Tensile Strength $f_{ct,sp}$ vs. Compressive Strength f_c for Jet Grouted Clay Layers

Table 5.8 Average and Standard Deviation Young’s Modulus (E_{cm} ; MPa)

layer #	system	Single Jet			Single Jet			Single Jet			Double Jet			Single Jet		
	wcr	0.8			1.0			1.2			1.0			1.0		
	column	X1			A,B			X2			C			A,B,D		
	layer	Category 1			Category 2			Category 3			Category 4			Category 5		
		n	mean	sd	n	mean	sd	n	mean	sd	n	mean	sd	n	mean	sd
1	Peat layer	3	1365	745	3	633	184	3	490	71	4	374	41	6	662	123
2	Upper clay layer	6	2050	702	12	1197	914	6	982	473	0	-	-	12	1096	837
3	Lower clay layer	4	3391	1839	12	2623	1166	4	1194	886	3	933	230	15	2335	1193
4	1st sand layer	4	2830	934	12	3449	1249	4	1330	746	4	924	335	15	3427	1164
5	Intermediate layer	4	3412	971	6	2551	1007	4	2264	399	4	1737	399	9	2913	991
6	Upper 2nd sand layer	5	5222	1622	4	2812	381	4	3565	1418	4	2479	577	7	2812	381
7	Lower 2nd sand layer	-	-	-	12	3528	1369	-	-	-	6	2237	565	18	3399	1259
8	Eemclay layer	-	-	-	10	2687	673	-	-	-	5	1532	427	15	2775	632

Because a relation between the strength and stiffness parameters of the jet grouted material can be extremely helpful in the design process, the relation between the compressive strength f_c and the Young’s Modulus E_{cm} of the grout have been examined. Figure 5.28 and Figure 5.29 show the test results for the sand layers and for the clay layers in terms of f_c and $f_{ct,sp}$. Here also an empirical formula of the type: $E_{cm} = k (f_c)^n$ is used, resulting in expressions eqn. 5.10 and eqn. 5.11:

eqn. 5.10 $E_{cm} = 800 (f_c)^{1/2}$ **(Jet grouted sand)**

eqn. 5.11 $E_{cm} = 500 (f_c)^{2/3}$ **(Jet grouted clay)**

where:

E_{cm} = Young’s modulus at 30 –70% of the failure compression strength (MPa)

f_c = compressive strength (MPa)

The relations apply for a water-cement ratio of 1.0. The correlation for the sand layers ($R^2=0.6$) and clay layers ($R^2=0.5$) is considered to be moderate. Because the number of tests resulting in high compressive strength is significantly lower than the number of tests resulting in low compressive strengths, the expressions for E_{cm} and $f_{ct,sp}$ are more sensitive to variations with higher values of f_c .

5.6.5 Shear Strength

The shear strength of the grout was determined by using Triaxial Tests. These tests are not commonly conducted on grout samples, but can be performed because the parameters that result from the test (c' and ϕ') are necessary for FEM analysis. One of the purposes of the Full Scale Injection Test was to explore the possibilities of using Triaxial Testing for grouts.

In total 26 samples were tested at a cell pressure of 0.5 MPa. The shear strength c' and the friction angle ϕ' were determined by combining the results with the UCS tests and drawing Mohr’s Circles (Table 5.9).

Table 5.9 Average Friction Angle and Shear Strength of the Grout

Layer		Number of samples	ϕ' (°)		c' (MPa)		f_c (MPa)	
#	Name		N	mean	S.D.	mean	S.D.	mean
2	Upper clay layer	5	38.7	16.3	0.9	0.7	3.0	2.1
3	Lower clay layer	11	39.5	10.7	1.7	2.0	7.2	8.4
5	Intermediate layer	1	42.1	--	2.5	--	10.9	-
6	2nd sand layer	6	34.0	19.6	2.8	1.8	10.9	3.6
8	Eemclay layer	4	26.5	21.0	3.6	1.8	11.2	7.0

When the C_u values in this table are compared with the f_c values of Table 5.6 and considering the large scatter, it can be concluded that the results are of the same magnitude. The standard deviation of the

JET GROUTING

parameters c' and ϕ' is also high, which can be partly attributed to the fact that only a small number of Triaxial tests were conducted in each layer. The test method was also shown to be sensitive to the irregularities in the grout.

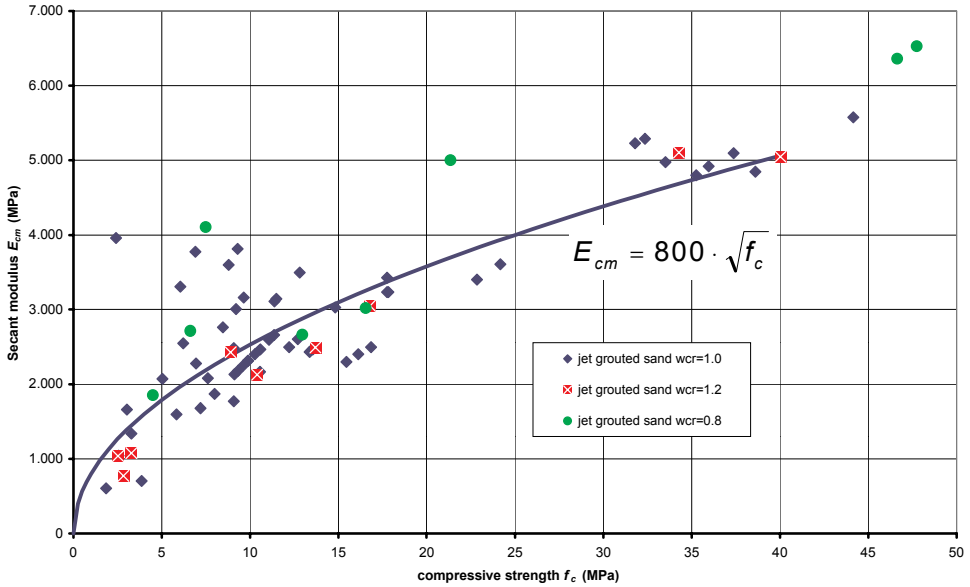


Figure 5.28 Young's Modulus E_{cm} vs. Compressive Strength f_c for Jet Grouted Sand Layers

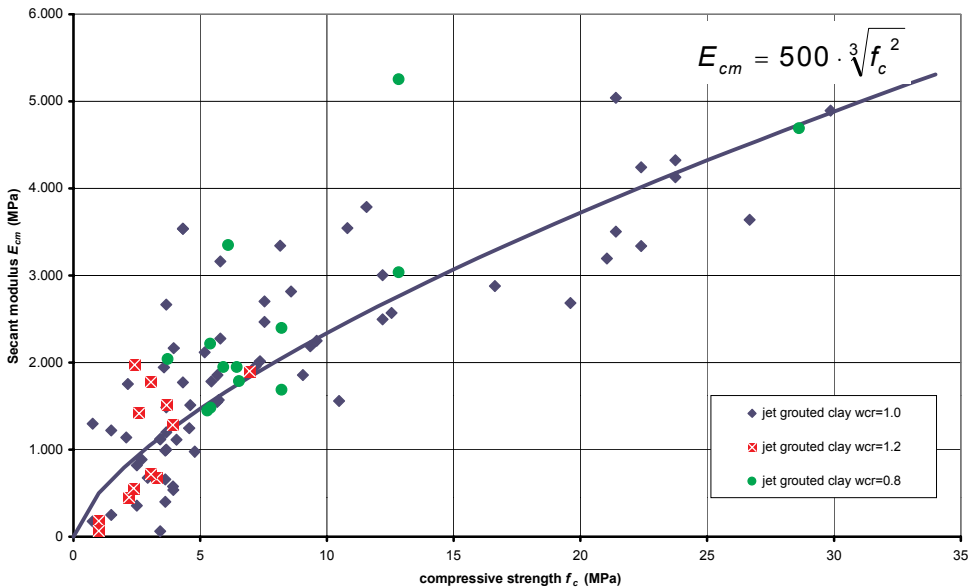


Figure 5.29 Young's Modulus E_{cm} vs. Compressive Strength f_c for Jet Grouted Clay Layers

5.6.6 Relations between Grout and Spoil Parameters

When there is a relation between soil parameters and grout parameters, a prediction of the grout strength can be made during the design process, based on the soil parameters and the jet grouting process parameters. Therefore here the mass density and compressive strength of the grout are compared to the mass density and compressive strength of the spoil.

Mass Density Soil – Mass Density Grout

The determination of the mass density of the grout was carried out on site using the (UCS, BST and Triaxial) samples. In the graph both the mean for columns A, B and D and the mean for all columns is given. The differences are all less than 2 %, unlike those of the first sand layer (6%).

A relationship between the mass density of the soil and that of the grout would be useful, because an estimate of the strength and stiffness properties of the jet grouted column could then be made using the mass density. In Table 5.10 and Figure 5.30 a comparison is made between the mass density of the soil and of the grout. For the grout the average mass density of columns A, B, C and D is used ($w_{cr} = 1.0$). No mass density was available for soil layers 1,2 and 3.

It can be concluded that, with the exception of the first sand layer, there seems to be no significant difference between mass density of the soil and the grout. Because of the lower mass density of the grout (apr. 1500 kg/m³), in sand layers this can only be explained if relatively more water than soil particles is replaced by the grout.

Table 5.10 Comparison Mass Density Soil versus Grouted Soil (kg/m³)

Layer #	Layer name	Grout (A,B,C,D)	Soil (in situ)	Relation Grout/Soil
4	1st sand layer	1806	2000	90%
5	Intermediate layer	1870	1870	100%
6	Upper 2nd sand layer	1856	1900	98%
7	Lower 2nd sand layer	1853	1840	101%
8	Eemclay layer	1710	1660	103%

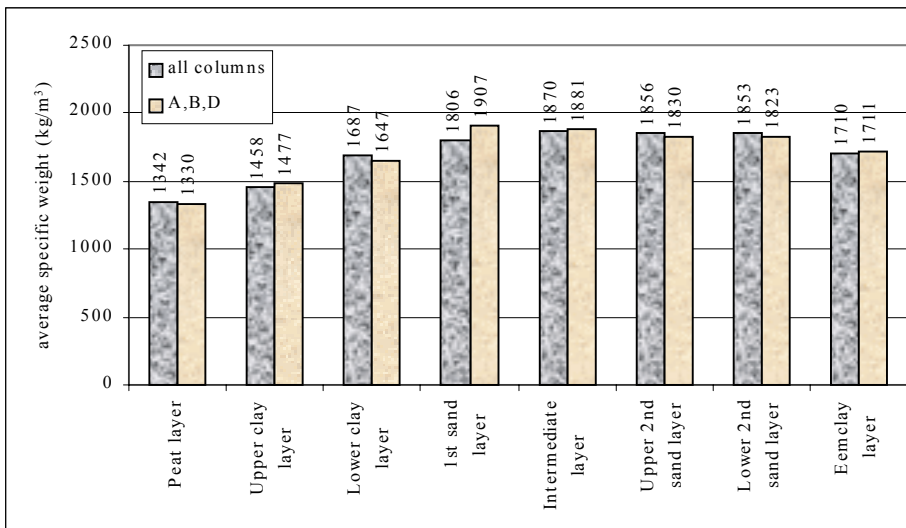


Figure 5.30 Mass Density of the Jet Grouted Soil Layers

Compressive Strength Spoil – Compressive Strength Grout

When a relation between the compressive strength of the spoil $f_{c:spoil}$ and the compressive strength of the grout f_c exists, during grouting a prediction of the grout strength based on the spoil strength can be made. Jet grouting process parameters can then be adjusted during the progression of the work. Spoil samples can be taken during the grouting process and tested some days afterwards.

To examine the possible strength correlation, UCS tests were performed on spoil samples from columns A, B, C and D and were compared with the UCS test results of the cores.

It is necessary to take into account that between the grouting of a certain soil layer and the arrival of the spoil at the surface some time elapses. This largely depends on the depth of the monitor and the lift speed of the monitor.

In Table 5.11 a comparison is given between the average compressive strength of the spoil samples and the average compressive strength of the cores (for column A, B, C and D, *age*>28 days). It can be concluded that for the non-cohesive soil layers (#4, 5, 6, 7) there is an indication of a proportional relation between the strength of the spoil and the strength of the cores. The strength of the grout is always higher than the spoil strength. For the cohesive soil layers the relation is not so clear. The lower grout strength may be influenced by the presence of discontinuities in the grouted column. The number of samples was however considered to be too small for any conclusions to be drawn.

Table 5.11 Compressive Strength Grout vs. Spoil

E_{mod} (kN/m ²)	Layer	Average Compressive Strength f_c (MPa)		Number of spoil samples	Factor Grout/Spoil (-)
		Grout	Spoil		
	#				
	Peat layer	2.0	--	0	--
	Upper clay layer	2.5	16.0	2	0.2
	Lower clay layer	8.0	12.1	2	0.7
	<i>1st sand layer</i>	<i>14.0</i>	<i>12.9</i>	<i>6</i>	<i>1.1</i>
	<i>Intermediate layer</i>	<i>12.5</i>	<i>10.3</i>	<i>3</i>	<i>1.2</i>
	<i>Upper 2nd sand layer</i>	<i>15.0</i>	<i>15.6</i>	<i>8</i>	<i>1.0</i>
	<i>Lower 2nd sand layer</i>	<i>17.0</i>	<i>13.5</i>	<i>16</i>	<i>1.3</i>
	Eemclay layer	10.0	3.2	8	3.1

5.6.7 Conclusions

Drilling cores from the jet grouted columns could be performed without significant problems. Only a small percentage (about 2%) of the cores crumbled and therefore could not be used in laboratory tests. The cores could be drilled over a large depth without exceeding the prescribed 1% horizontal deviation limit. Therefore core drilling is a reliable method to investigate the jet grout material quality parameters.

Although satisfactory strength and stiffness parameters were obtained, with average values complying with the upper segment of reviewed literature values given in Table 5.1 on page 76, the variation coefficient of the UCS, tensile strength and Young’s modulus were high. The large scatter in these parameters was mainly due to the influence of the heterogeneity of the soil. Figure 5.23 shows that at the boundary between the original soil layers, the soil material on both sides of the original boundary influences the strength and stiffness parameters of the grouted soil.

Using the test results some rules of thumb have been introduced for jet grouting in sand and clay layers. A summary is shown in Table 5.15 in the conclusions of this chapter. In almost all cases the positive effect of using a higher cement content on the strength and stiffness parameters was confirmed. The jet grouted column created by using the double system shows lower average strength and stiffness parameters, which could be expected because of the air used in the process.

For the non-cohesive soil layers the strength of the grout was always found to be higher than the spoil strength. For the cohesive soil layers this relation was not so clear. With the exception of the first sand

layer, no significant difference was found between the mass density of the soil and that of the grout. Because of the lower mass density of the grout (apr. 1500 kg/m³), in sand layers this can only be explained if relatively more water than soil particles is replaced by the grout.

Despite the limited number of Triaxial tests that were conducted, it can be concluded that this test method is sensitive to the irregularities in the grout sample and therefore not very suitable to obtain grout parameters.

5.7 Jet Grouting for Foundation Protection

5.7.1 Pile Displacement

In this section the reaction of the various monitoring equipment during jet grouting columns A to D, which were all installed next to the foundation piles is analysed. The analysis includes the vertical displacement of the pile, the ground and pore water pressures and the vertical and horizontal soil displacement.

A graph in which the pile load and jointmeter readings are plotted has been made for both pile-types (i.e. wooden and concrete piles) and during the installation of the jet grouted columns. Here graphs containing the readings of the most important monitoring tools for column B are presented as an example in Figure 5.31 to Figure 5.33. The complete graphs are given in Van der Stoel (2001).

From Figure 5.31 it can clearly be seen that shortly before **drilling** column B (9-8; 13:20) all pile loads were adjusted, which however has nothing to do with jet grouting effects. After this adjustment and during drilling only changes smaller than 1.5 mm appeared in pile displacement. The fluctuations in pile load are a result of making a correction for the redistribution of loads between all piles of the ballast frame.

During **jetting** only small displacements (<2mm) of the wooden piles occurred. In Figure 5.32 a close up of Figure 5.31 for jetting column B, located closest to the piles, is presented. In the figure it is indicated each time the pile load is adjusted as a correction for the redistribution of loads and the relaxation that occurs as a result of pile settlement. During grouting column B, a 1 – 2 mm settlement of the wooden piles and concrete piles (Figure 5.33) occurred. The correlation between the displacement caused by drilling and jetting columns A-D and the distance between the pile and the edge of the column is further discussed in Section 5.9.

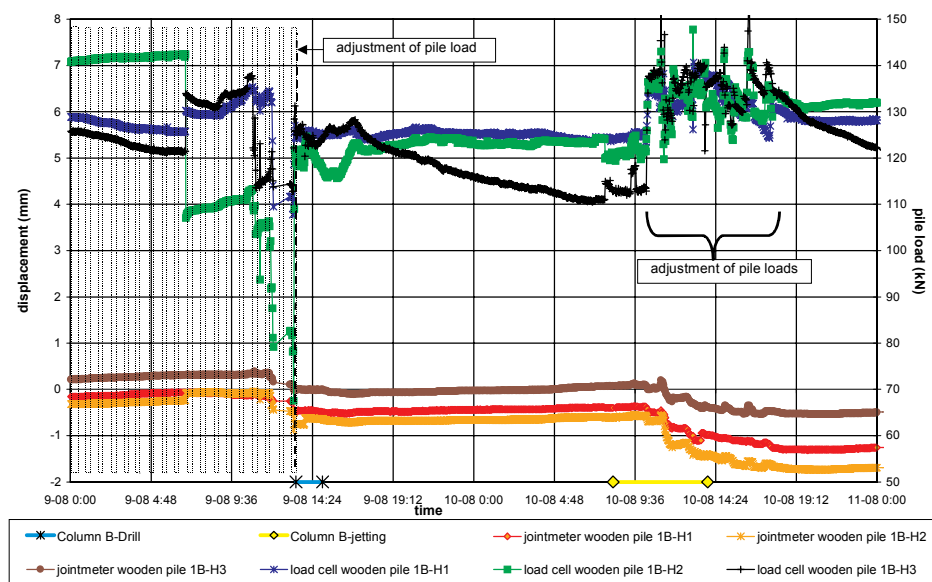


Figure 5.31 Displacement of Wooden Piles during Jet Grouting Column B

JET GROUTING

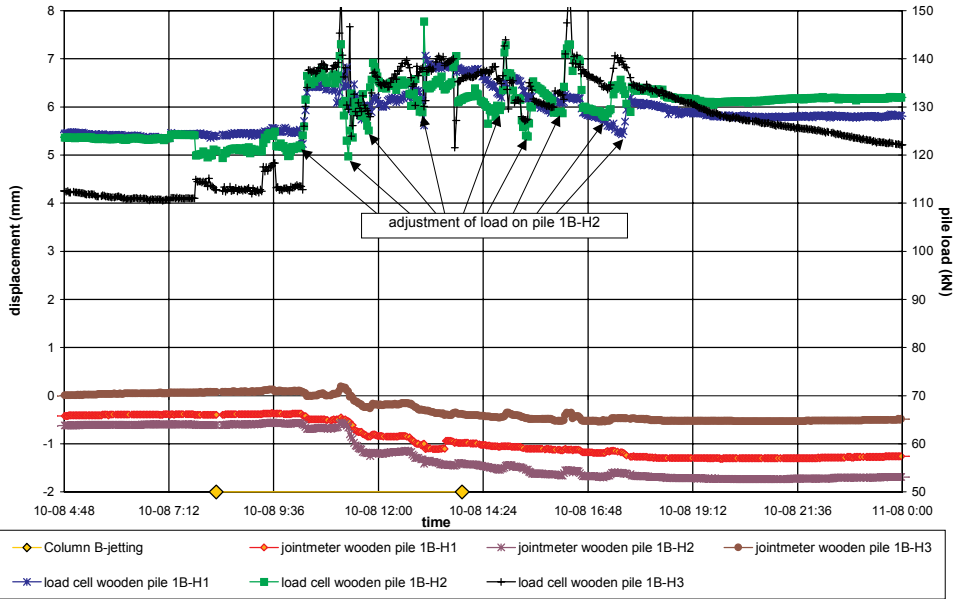


Figure 5.32 Close up of Displacement of Wooden Piles during Jetting Column B

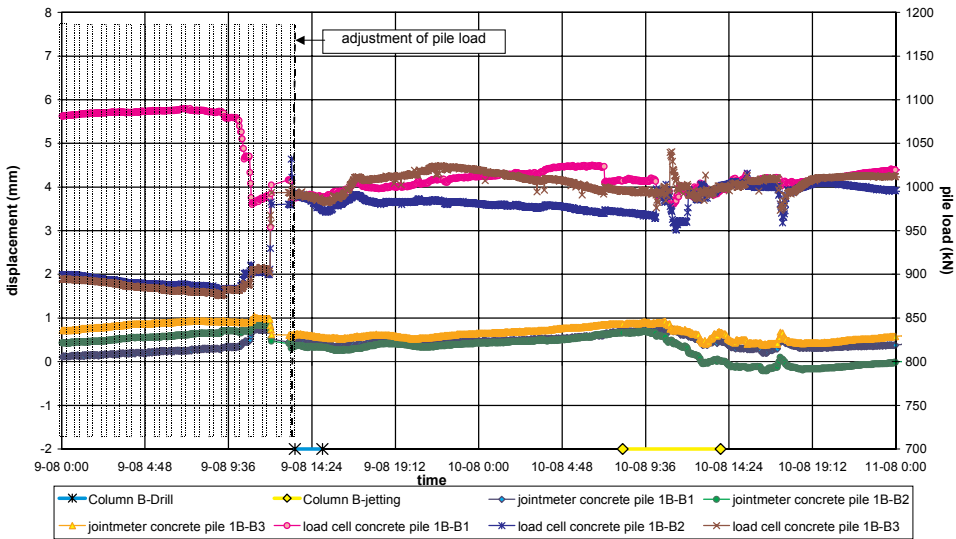


Figure 5.33 Displacement of Concrete Piles during Jet Grouting Installation (Column B)

During the last part of grouting column C (shallow grouting) a blow-out occurred (Figure 3.13, page 34). This blowout was caused by large lumps of peat blocking the jet grouting annulus. The spoil flow was thus obstructed resulting in a pressure build up which ultimately led to a large soil movement near the jet grouting rig. As a result of this soil movement much of the monitoring equipment was disturbed and could not be used for some hours.

Between jet grouting activities no significant additional pile displacement occurred. The period after jet grouting was also analysed to quantify the consolidation and creep effects. Based on this analysis it was

concluded that time/consolidation effects resulting from jet grouting next to piles do not lead to additional settlement of the pile.

The horizontal displacement of the piles was limited to a maximum of about 20 mm towards the jet grouted columns at a depth of NAP -6m. At surface level and at NAP -12 m and deeper levels the horizontal displacement was insignificant.

5.7.2 Pore Water Pressure

In Van der Stoel (2001) all graphs of the piezometer readings during the different grouting stages are presented for each piezometer individually. It could be deduced from these graphs that generally the readings show a peak when jet grouting is at the level of the piezometer. The jetting peaks are generally higher than the drilling peaks. The peaks seem logical considering the high cutting and jetting pressures used when jet grouting the soil. In Figure 5.34 an example for column B is plotted. From the graph it can be recognised that when the monitor reaches the level of the piezometer, the pore water pressure starts to increase. The dip in the increase that can be seen in this figure is not representative for the other graphs. A likely explanation for the temporary pressure decrease might be that the grouting was stopped for a short while*. The total increment in pore water pressure varies for each column and is plotted in Figure 5.38. For most of the piezometers the excess pore water pressures dissipate within 1-2 hours.

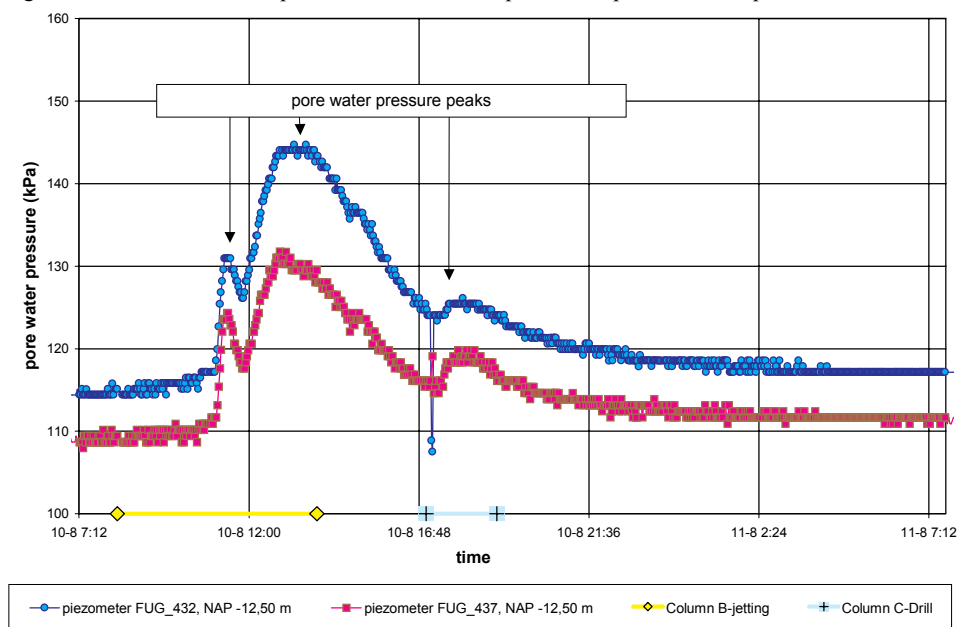


Figure 5.34 Piezometer during Jet Grouting Column B

In Figure 5.35, Figure 5.36 and Figure 5.37 the most important piezometer readings are summarised. Jet grouting usually causes a limited (10-50 kPa) increase in pore water pressure, but the fluctuations of FUG_432 and FUG_437 (Figure 5.35) are remarkable. Considering their position (Figure 5.19) most fluctuations can be explained by the likelihood that they were hit by the jet during the grouting process. However, the extreme fluctuations (to +550 kPa) that occur in FUG_437 just before drilling column D can not be explained as being anything other than measurement errors. Piezometers FUG_451 and FUG_433 are located at circa 4 m and 10 m from the jet grouting site and therefore show a much decreased response to the grouting activities.

* the log shows maintenance has to be performed that day, but the exact time is not shown

JET GROUTING

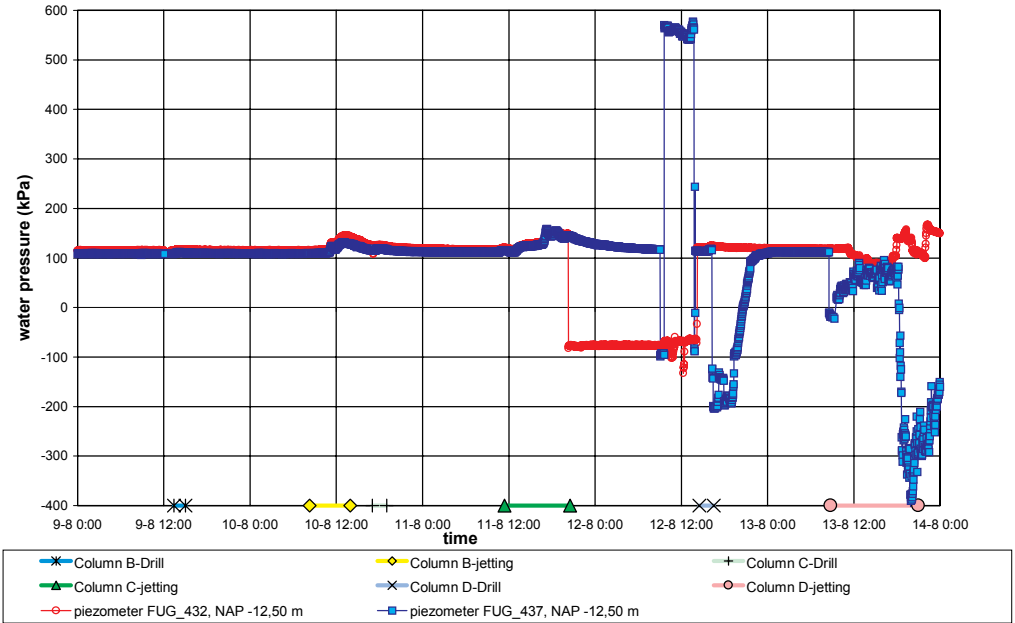


Figure 5.35 Piezometers in the Soil During Jet Grouted Columns B, C and D

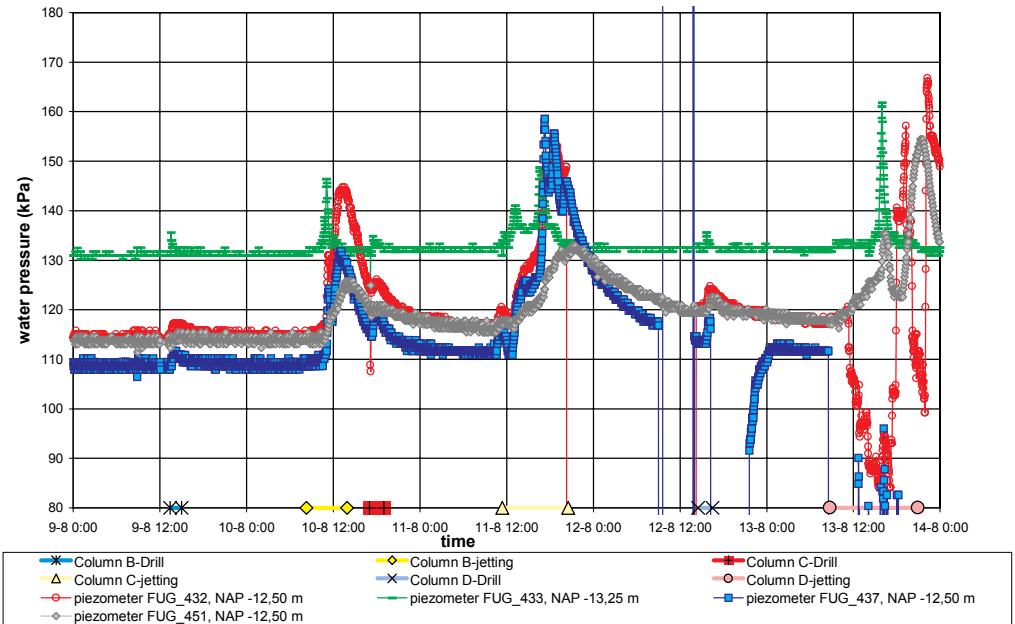
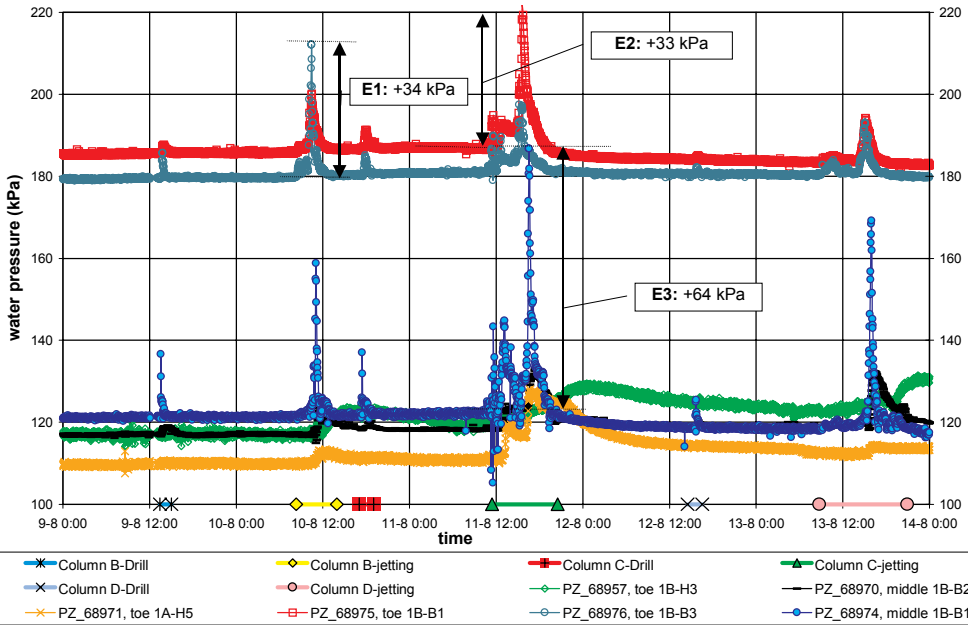


Figure 5.36 Close Up of Piezometers in the Soil during Jet Grouting Columns B,C and D

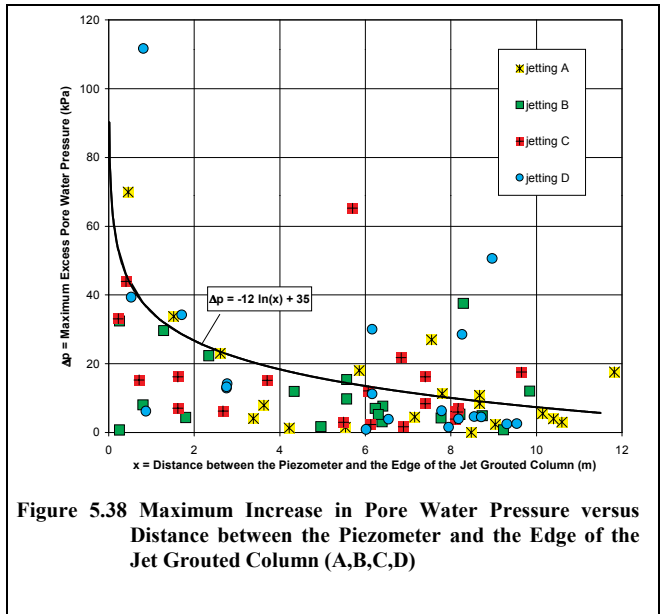


In Figure 5.37 it can clearly be seen that the piezometer that is closest to the monitor responds most strongly to the jet grouting. For example E1 shows an increase in pore pressure for the toe of B3 of 34 kPa at the moment column B is jetted. The increase for the toe of B1 is then only 18 kPa. When column C is jetted, the toe of B3 only shows a 17 kPa increase, whilst the toe of B1 then shows a 33 kPa increase (E2 = +33 kPa).

To further examine this relation, in Figure 5.38 the maximum excess pore water pressure (Δp ; kPa) is plotted against the distance between the edge of the jet grouted columns and the piezometer (x ; m). It can clearly be seen that the influence of jet grouting pressure diminishes with distance. In eqn. 5.12 this relation has been expressed:

eqn. 5.12: $\Delta p = -12 \cdot \ln(x) + 35$

From the figure it can also be concluded that at about 2 times the column diameter the influence on the pore pressure has diminished to about 0.5% of the jetting pressure. Curve fitting the data points shows the degree of correlation can be considered moderate (R=0.6, with R=1.0 being a perfect fit).



5.7.3 Total Stress and Effective Stress

The Stress Monitoring Stations (SMS) on the piles are orientated towards columns A-D, measure total horizontal stress and are considered to give relative readings rather than an absolute value (further details were given in Section 3.9.4). For columns A and D, both located at several meters from the piles, the change in total stress was limited. For grouting columns B and C, that were located much closer (Figure 5.19), the changes were significant (>20 kPa). A correlation between jet grouting and ground- and water pressure changes can be recognised. The changes generally occur when the jet grouting monitor is at SMS level. Analogous to the piezometers, it can be recognised that the SMS in the pile that is located closest to the grouting shows the strongest response (i.e. the SMS in B3 to grouting B, the SMS in B1 to grouting F).

In Figure 5.39 a summary of the SMS readings is given. When this figure is compared with Figure 5.37, it can be concluded that locally large changes occur in effective horizontal stress, because of the decrease in total horizontal stress and the simultaneous increase in pore water pressure. Examples E1, E2 and E3 illustrated in the figures and in Table 5.12 demonstrate this phenomenon. The variation in effective horizontal stress suggests that, depending on the value of K_0 , it might temporarily become negative. Since this cannot be the case, the most probable event is that the SMS readings are not reliable for these big pressure changes. It is, however, plausible that the effective stresses because of the jet grouting process temporarily reduce to zero.

Table 5.12 Calculation of Effective Stress Change from Total Stress and Pore Water Pressure Change

Example	Position	$\Delta\sigma_h^{total}$	Δu	$\Delta\sigma_h'$
E1	toe pile B3	-80	+34	-114
E2	toe pile B1	-150	+33	-183
E3	middle pile B1	-120	+64	-184

The use of air during the construction of column C caused a major drop in total stress for the two SMS in pile B1. However there were no pile displacements, and the stress changes did not seem to influence the piles in any other way. Even in the long run the local disturbance did not to affect the position of the pile.

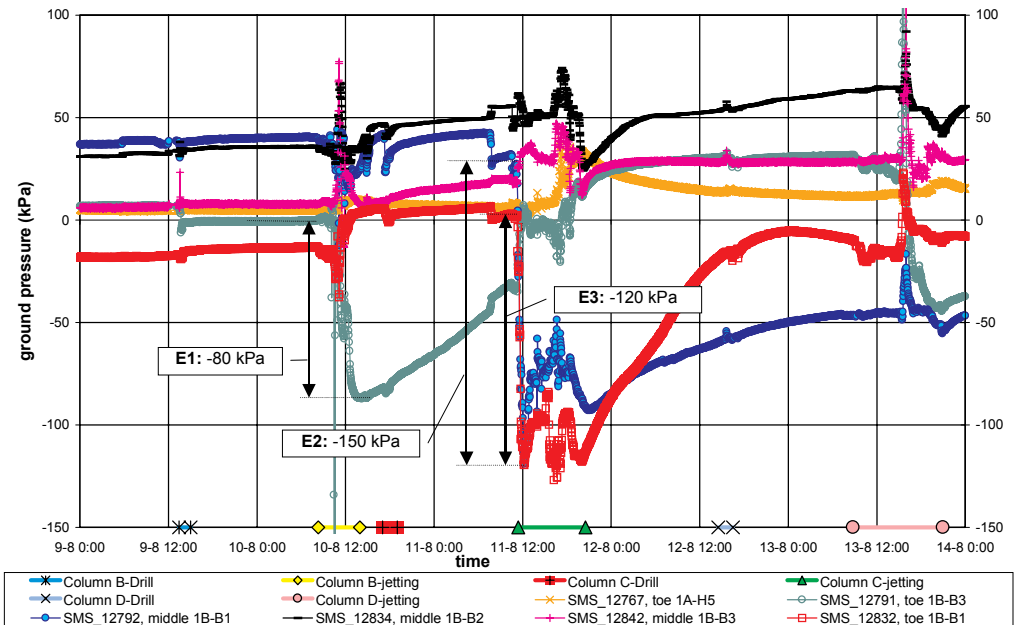


Figure 5.39 SMS in the Piles During Grouting Columns B, C and D

When the changes in total stress, pore water pressure and effective stress are compared with the pile settlements, it can be concluded that there is a relation between the stress changes and pile settlement. Although the reduction of the effective stress may locally affect the foundation piles, the settlement as a result of these pressure decreases remained limited to several mm (see Section 5.9). This might be partially explained by the fact that only on one side of the pile shaft and near the pile toe were the stresses reduced.

5.7.4 Soil Movement

Vertical movement

Extensometers and beacons, as described in Chapter 3, were used to monitor soil movement. The extensometer readings at each depth were corrected using the accompanying target readings at surface level (see Figure 5.18). An overview of the extensometer readings is presented in Van der Stoel (2001). The most important extensometer readings are presented in Figure 5.40.

During **drilling** of the columns only small (<2mm) displacements were observed. An exception is made for the drilling of column C where a heave of over 10 mm was measured just before drilling commenced. The only plausible explanation for this “heave” is that the positioning of the jet grouting rig close to the extensometer caused the soil to settle, resulting in shortening of the extensometer cables and thus an apparent heave.

No changes were observed to have resulted from **jetting** columns A and D (their distance from the piles exceeds 0.5 m). Figure 5.40 shows that the extensometer readings during jetting columns B and C did not give consistent results. Extensometer 2 shows a heave of 14-18 mm due to jetting column B and 4-5 mm due to jetting column C. Extensometer 1 shows small (<5mm) movements due to jetting column B and 5-8 mm settlement due to jetting column C. A possible explanation for the heave of extensometer 2 might be that it was located so close to column B (Figure 5.19) that, owing to the larger diameter of this column, the jet was initially located under the anchors of extensometer 2. When jetting in upward direction, the pressure pushed these anchors up. This explains why the deepest anchor moves upwards first. Extensometer 1 was located about 0.5 m further from the edge of the column and therefore might only have reacted to the changes in effective stress in the soil.

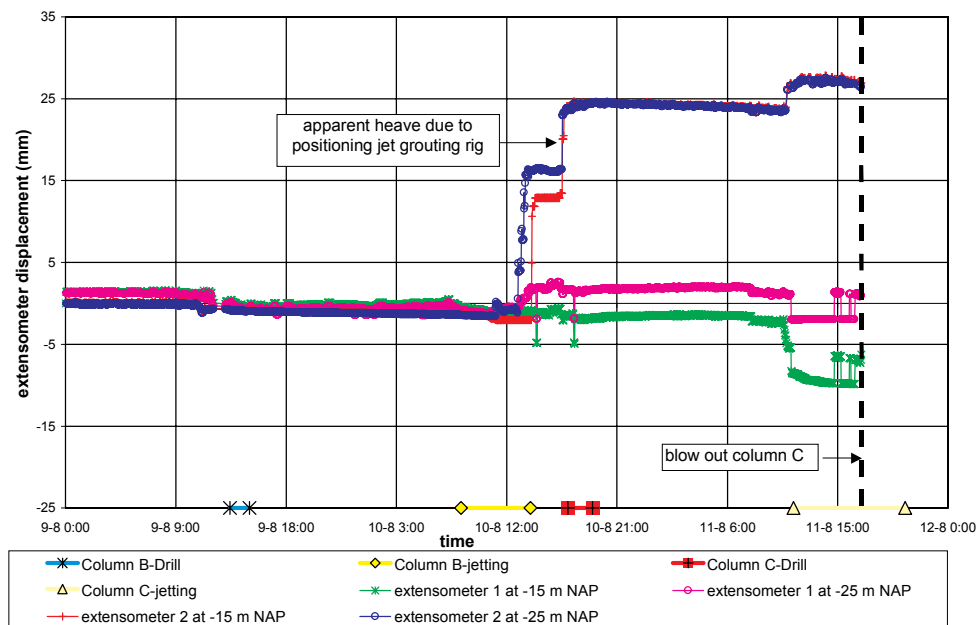


Figure 5.40 Extensometer Displacement during Jet Grouting Columns B and C

JET GROUTING

In Figure 5.41 the displacement of the surface levelling points is presented. The surface levelling points moved insignificantly (<1.5 mm) due to the grouting of the columns.

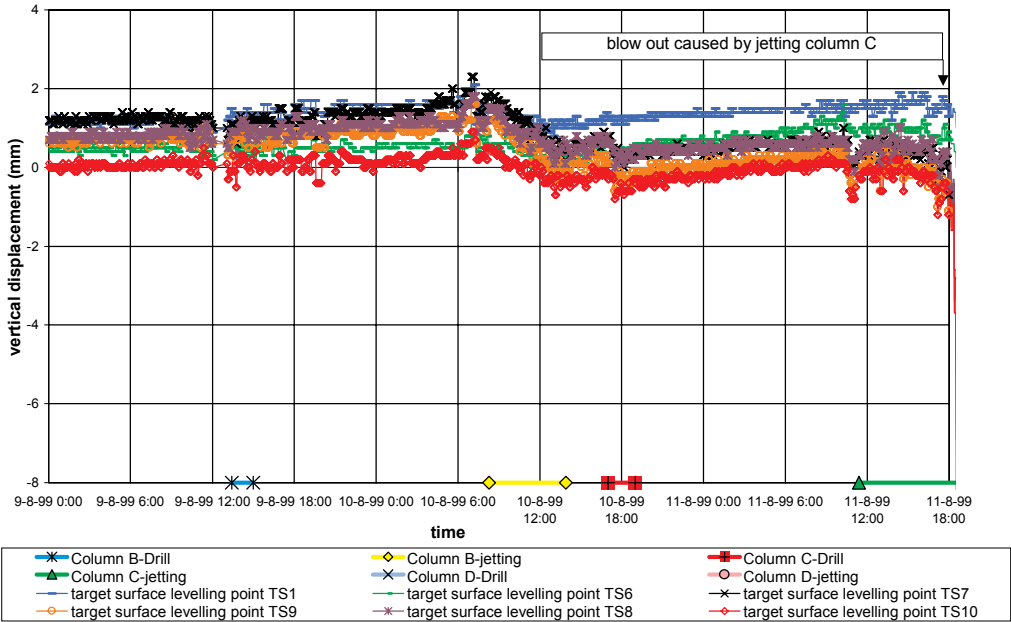


Figure 5.41 Surface Levelling Point Displacement during Jet Grouting Columns A,B,C,D

Horizontal movements

Owing to the blow-out caused by jet grouted column C inclinometer INCL1 was damaged and the positioning and orientation of inclinometer INCL2 was affected. Therefore no exact measurements results can be presented here.

5.7.5 Bearing Capacity

The bearing capacity of the wooden piles was determined both before and after jet grouting columns A, B, C and D. The results of these pile load tests are shown in APPENDIX VIII: A. Figure 25 and A. Figure 29 to A. Figure 31. In Figure 5.42 the pile load test on pile 1B-H1 is presented as an example. From comparisons of tests #1 and #2 (before) with test #3 (after) two conclusions can be drawn:

- After grouting the piles exhibit an initial ($F < 0.8 * F_{ubc}$) stiffer reaction; when the pile load approaches F_{ubc} the pile reacts less stiffly.
- The ultimate bearing capacity of the piles after grouting is somewhat higher than before grouting ($F_{ubc;3} \approx 1,1 * F_{ubc;1/2}$).

The initial stiffer behaviour and the slightly higher ultimate bearing capacity can be explained by the increase in lateral pressure due to the grouting. Because the increase in ultimate bearing capacity is limited the conclusion is drawn that jet grouting next to wooden piles in soft alluvial soils does not lead to a reduction in their bearing capacity.

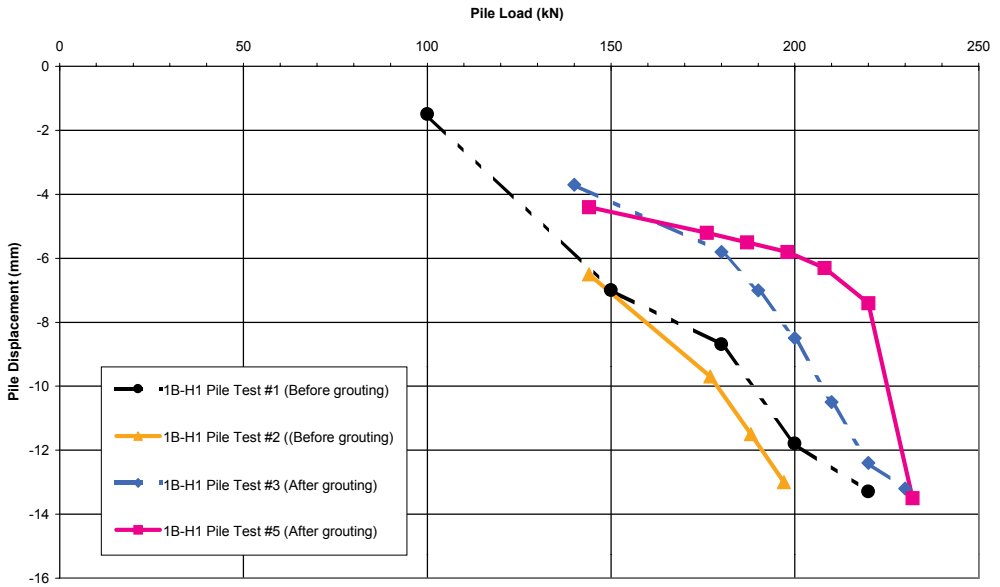


Figure 5.42 Example of Pile Load Test: Wooden Pile 1B-H1

5.7.6 Conclusions on Jet Grouting for Foundation Protection

The conclusions in this subsection apply to jet grouting situations where the horizontal distance between the pile and the edge of the jet grouted column is 0.5 m or more. This is typical of the application of jet grouting for foundation protection.

With regard to pile displacement, it could be concluded that no significant changes appeared in pile load or pile displacement (<1.5mm) during drilling and that during jetting the pile settlement remained limited to 2 mm for each column. Neither the distance between the pile and the jet-grouted column nor the diameter of the column seemed to influence the pile displacement. No significant additional pile displacements occurred between jet grouting activities and consolidation effects did not lead to additional settlement of the pile. When blockage in the spoil return flow occurred during the installation of a jet-grouted column, this resulted in a blowout leading to large displacements.

Because of the high cutting and jetting pressures used, jet grouting generally caused an increase in pore water pressure (Δp ; kPa). Although some scatter was found in the results, a relation of a logarithmic nature with the distance between the edge of the jet grouted columns and the piezometer (x ; m) was found, expressed by eqn. 5.12 : $\Delta p = -12 \cdot \ln(x) + 35$.

At about twice the jet grouted column diameter the change in pore water pressure was reduced to 0.5% of the jetting pressure. A significant (>20 kPa) decrease in total stress was recorded when grouting close (<2m) to the SMS in the pile; because of the decrease in total stress and the simultaneous increase in pore water pressure, the biggest changes occur in effective stress. It is plausible that the effective horizontal stresses are temporarily strongly reduced when grouting at 0.5 m from the pile and SMS.

The impact of the soil movements during jet grouting for foundation protection is expected to be limited because the displacements in the soil that is very close (<0.5 m) to the edge of the columns is marginal. More specifically, the drilling stage leads to vertical soil displacements smaller than 0.5 mm. When jetting at over 0.5 m from the extensometers no vertical soil displacements occurred.

An important argument for using jet grouting for foundation protection is that the grouting did not negatively influence the bearing capacity and stiffness of the wooden piles.

5.8 Results of Jet Grouting for Foundation Renovation

5.8.1 Pile Displacement

General

In this section the influence on the foundation piles of creating pile extensions by jet grouting columns E, F, W1, W2 and W3 is analysed. Creating pile extensions by jet grouting may be performed for foundation renovation purposes. In the subsequent subsections the reaction of the various monitoring equipment during jet grouting is analysed and discussed. This includes the vertical displacement of the pile, the ground and pore water pressures and the vertical and horizontal soil displacements.

Column E was created under concrete pile B3, column F under concrete pile B1 and columns W1, W2 and W3 under wooden piles H1, H2 and H3 respectively (Figure 5.15).

Analyses of grouting under Concrete Piles (E, F)

Figure 5.43 shows the vertical displacement of the concrete piles as a result of grouting columns E and F. In Figure 5.44 a close up of this figure is presented. During the jet grouting of column E only small pile settlements (<4mm) occur, while during jetting the bottom of column F large settlements occurred. The difference can be explained by the fact that column F is completely located under the toe of pile B1 whilst column E is located more next to pile B3 than under it (see Figure 5.17). At the moment the monitor reaches the pile toe level of B1 the soil around the pile toe is totally liquefied. The settlement due to the loss in pile toe resistance can be observed from the figures. The jointmeter on pile B1 shows a 38 mm settlement, after which the range of the jointmeter was exceeded. This was only noticed after about 20 minutes, and it was then corrected* (-14mm), but by that time the displacements had stabilised. Therefore at least 14+50=64 mm pile displacement had occurred.

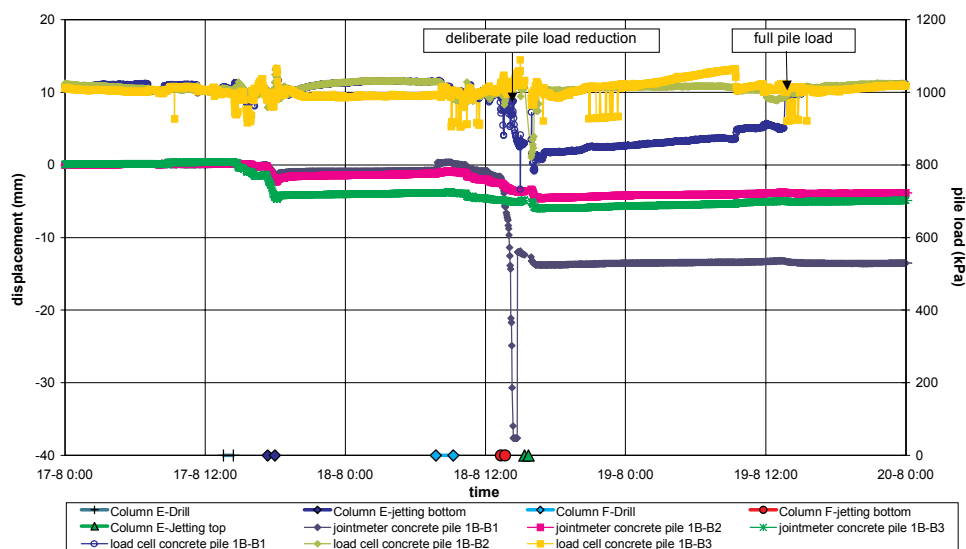


Figure 5.43 Displacement of Concrete Piles during Jet Grouting Columns E and F

Because the displacements of pile B1 were ongoing, the decision was made to stop adjusting the pile load on B1 (18-8-1999; 14.30h) and determine at what load the displacement would cease. When the load was reduced from 1000 kN to about 800 kN, displacement ceased. According to the calculations in Section 3.10.2, the pile shaft should be capable of developing 1575 kN positive shaft friction. Because these calculations included shaft friction at the pile toe, where the soil has been eroded by the grouting, a new calculation was made for the maximum positive shaft friction. According to this calculation, the positive shaft friction without the shaft friction in the 2nd sand layer (NAP -17m and deeper) amounts to 828 kN, which agrees very well with the 800 kN found in the test. After 24 hours, pile B1 was again fully loaded. By then the jet grouted column had hardened and was able to withstand this load without pile B1 showing any displacements.

In Figure 5.45 it can be seen that the vertical displacement of the wooden piles as a result of grouting columns E and F is very small. Moreover, these displacements were only of a temporary nature. The same applies to the displacements that occurred just after jetting the top of column E. The reason for these displacements is that hydro fracturing of the soil occurred because (project to the project log) at both times the spoil flow was temporarily blocked.

The jointmeters on piles 1B-H1 and 1B-H2 (closest to column E) both showed a 2 mm settlement during jetting the bottom of column E. However, this settlement is permanent and cannot be explained

* the jointmeter was adjusted by placing a 50 mm cube between the pile and the needle of the jointmeter

JET GROUTING

by any fracturing occurring. Since the settlements started before grouting commenced, the only possible explanation is that moving the jet grouting rig caused the small extra settlements.

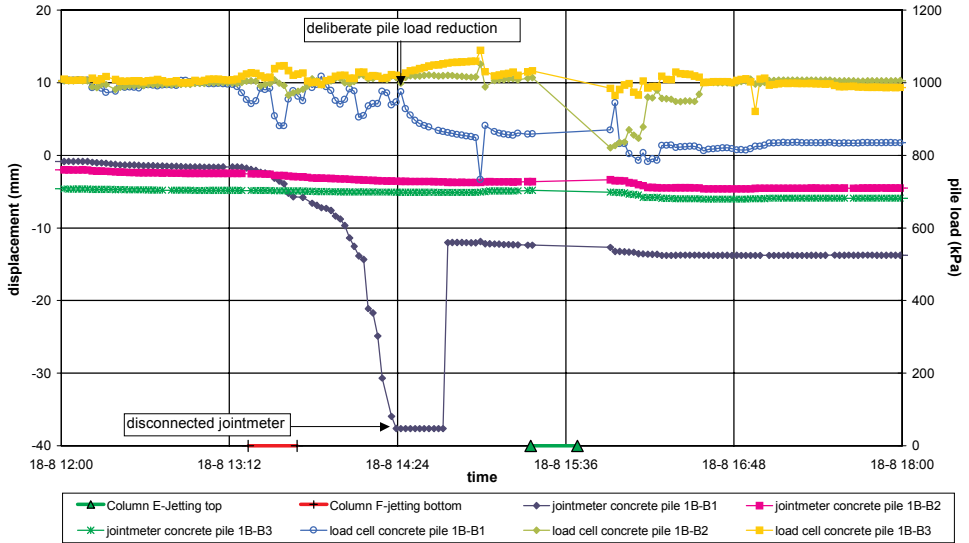


Figure 5.44 Displacement of Concrete Piles during Jet Grouting Column F (close up)

The most plausible explanation for the decrease in pile load of piles H1 and H3, that occurred after jetting the bottom of column E, is that small* vertical pile displacements caused some relaxation in the load cell. Because these displacements are not observed and because pile H2 does not seem to be affected by the same phenomenon, no plausible explanation could be found. The correlation between the distance between the pile and the grout jet is examined in Section 5.9.

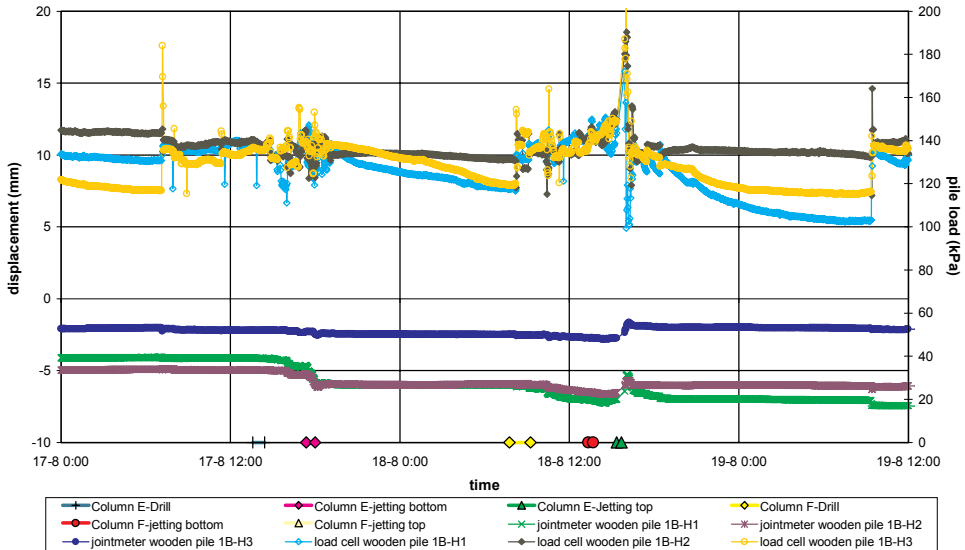


Figure 5.45 Displacement of Wooden Piles during Jet Grouting Columns E and F

* in order to get a 30 kN load reduction, the elastic deformation of the wooden pile has to amount to 1.0-1.5 mm

Analyses of grouting under Wooden Piles (W1, W2, W3)

In Figure 5.46 the wooden pile displacements due to jet grouting columns W1 and W3 are shown; the pile displacements caused by jet grouted column W2 are illustrated in Figure 5.47. From Figure 5.46 it can be seen that during the grouting of column W1 the jointmeter on H1 showed hardly any displacement. The jointmeter on H2 showed a 2 mm overall settlement, but no direct influence of the jet grouting. For jet grouted column W3, the jointmeter showed a 2-3 mm settlement due to the drilling. It is remarkable that such limited displacements, occur due to the grouting of columns W1 and W2. It was expected that because the soil near the pile toe was eroded, the piles would have showed extensive settlements once the monitor had reached pile toe level. The only possible explanation seems to be that the columns were not grouted near the pile toe. The position of the jet grouting string was however measured after drilling, and from Figure 5.15 it can be seen that all columns are located under the pile toe. Only column W3 is partly located next to pile H3 instead of under it. Because this still does not explain the absence of pile movement, no plausible explanation for the observed phenomena can be given.

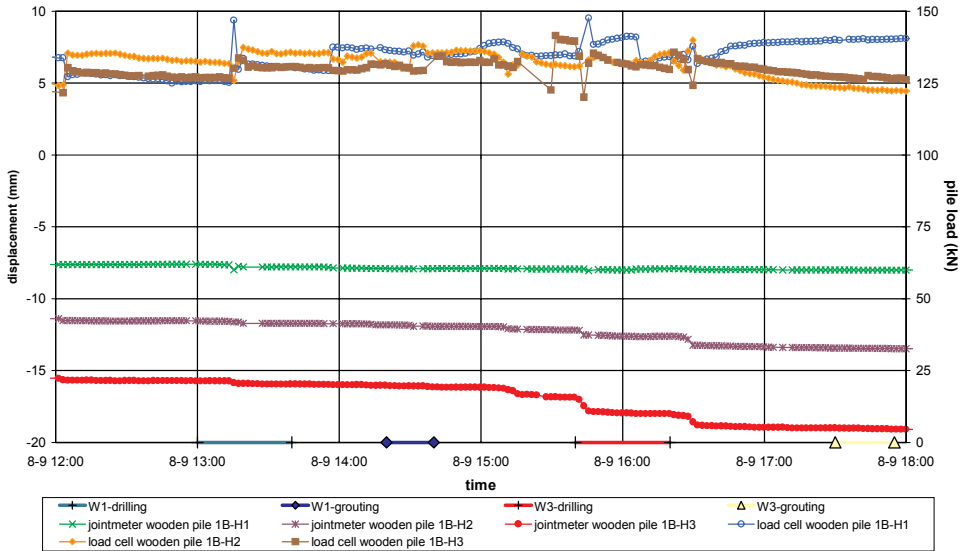


Figure 5.46 Displacement of Wooden Piles during Jet Grouted Columns W1 and W3

Figure 5.47 shows that the grouting activities on column W2 did not cause any vertical movement of pile H1. The jointmeter on pile H2 showed a 7-8 mm settlement of the pile. The jointmeter on pile H3 showed a 10 mm pile settlement. For both, about half of the displacements seemed to have been caused during the last stage of drilling column W2 and the other half due to grouting column W2. The 7-8 mm pile settlement of H2 due to the jetting was expected although it is considered to be rather limited. The settlement of H2 due to the drilling can be explained by the fact that the drilling bit actually hit the pile during drilling, so the soil at the pile toe was considerably disturbed. The settlement of pile H3 could only be explained by the occurrence of a grout fracture that reached the pile toe level of H3. This assumption is proven by the fact that H3 is not encapsulated by grout on the side adjacent to H2. Nevertheless, this does not explain the settlement of H3 during the drilling of W2. The only explanation that remains is that the fracture already originated during drilling column W2. This is however also not very plausible.

JET GROUTING

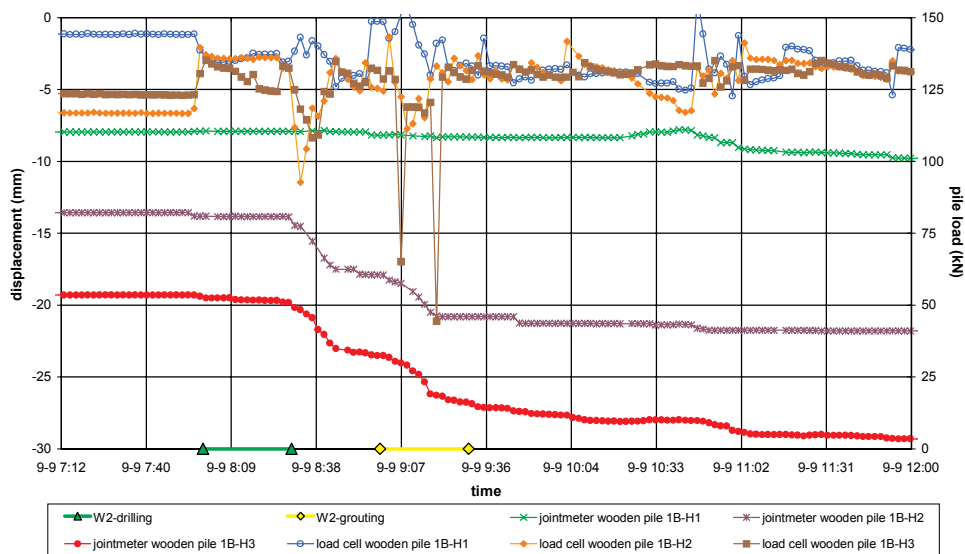


Figure 5.47 Displacement of Wooden Piles during Jet Grouting Column W2

The displacements of the concrete piles caused by jet grouted columns W1, W2 and W3 were insignificant, as could be expected because they are located several meters from the wooden piles, their pile toes are located about 8 meters deeper and two concrete piles already had a grouted extension. The correlation between the distance between the pile and the grout jet is examined in Section 5.9.

5.8.2 Total Stress, Pore Water Pressure and Effective Stress

Analyses of Creating Concrete Pile Extensions (E, F)

Figure 5.48 shows the results of total stress and pore water pressure measurements from the SMS and piezometers in the piles as a result of grouting columns E and F. Except for the piezometer in the middle of B3, none of the piezometers in the piles showed any response to the grouting (and therefore they are not displayed in the graphs). This is especially remarkable because the piezometer and SMS in the middle of B3 show a corresponding reaction to jetting the top of column E, so the other piles might be expected to behave in a similar way.

In Figure 5.49 a close up of Figure 5.48 is presented, containing monitoring equipment within the range: -100 kPa to $+100$ kPa. From this figure it can be seen that the total stress in the middle of pile B1 decreases as a result of drilling column F, because the drilling bit is within 1 m of that SMS during drilling. The relaxation as a result of the drilling causes a 60 kPa stress reduction on the SMS.

Both figures show that the response of the SMS to the grouting was generally limited (<20 kPa). A clear exception could be seen for the total stress measured at the toes of B1 and B3 during drilling columns F and E respectively. Figure 5.48 shows a decrease of total stress at the pile toes of 240 kPa respectively 350 kPa. These total stress decreases correspond approximately with a total local loss of the calculated vertical pressure at the pile toe. When comparing these graphs with the pile displacement graphs in the previous sub-section, it becomes clear that a total stress decrease bigger than 20 kPa always resulted in pile settlements. However no coherent relation between the total stress change and the pile settlement could be detected. The decrease in total stress as a result of the drilling of column F is for instance about equal to the decrease due to the jetting of the bottom of column F. The settlements however, are of a completely different magnitude: 1-2 mm as a result of drilling, over 38 mm settlement as a result of jetting. The same reasoning applies for jet grouting column E.

JET GROUTING

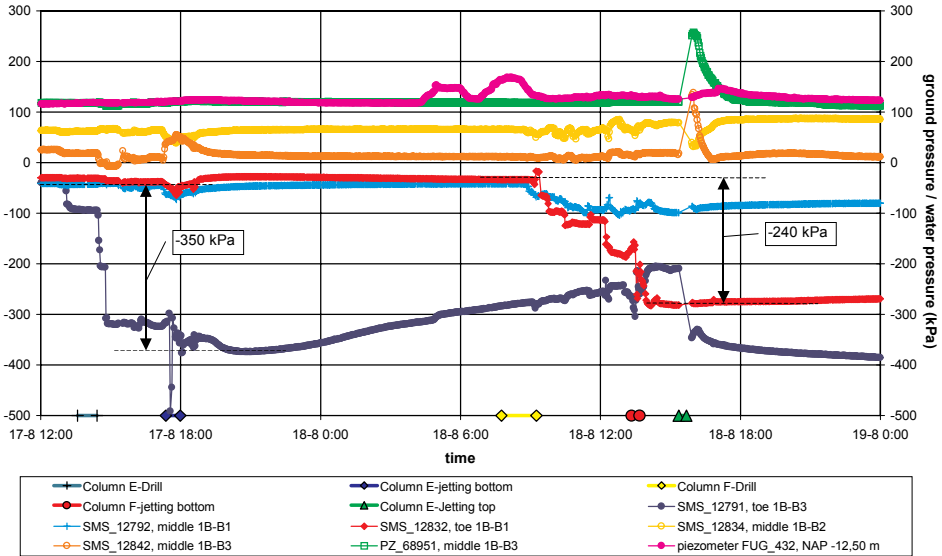


Figure 5.48 Piezometers and SMS during Jet Grouting Columns E and F

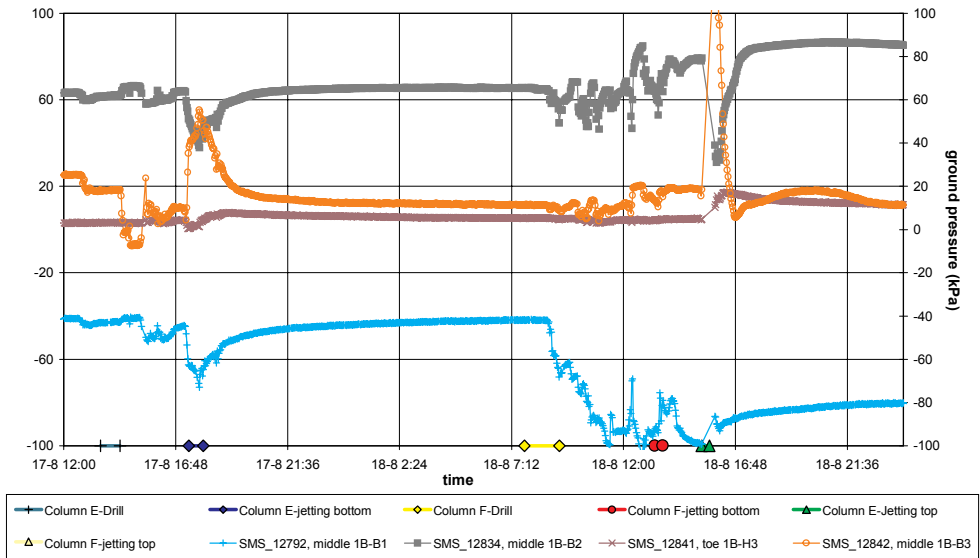


Figure 5.49 SMS during Jet Grouting Columns E and F (close up)

Analyses of Creating Wooden Pile Extensions (W1, W2, W3)

In Van der Stoel (2001) all the SMS and piezometer readings are presented. Figure 5.50 shows a close up of the soil and pore water pressures of the relevant SMS and piezometers as a result of grouting column W2. The effects are limited to a temporary 25 kPa rise. There is not much difference between the excess pore pressure in the toe of wooden pile H3 and in the middle of the concrete piles. This can

be explained by the fact that the SMS are all located in the 1st sand layer. Therefore the recorded rise in total stress is about equal to the excess pore pressure due to grouting, as can be seen from the figure. Since the grouting of columns W1 and W3 shows a similar trend, it is remarkable that only grouting W2 resulted in pile settlements bigger than 1mm. When the figure is compared with the pile settlements during grouting as presented in Figure 5.47, it can be seen that when the stress gradient is highest, the pile also shows the biggest settlement rate. Right after the stress peak, the settlement decreases. This confirms that there is a relation between the total stress and pile displacements (see Section 5.7.3)

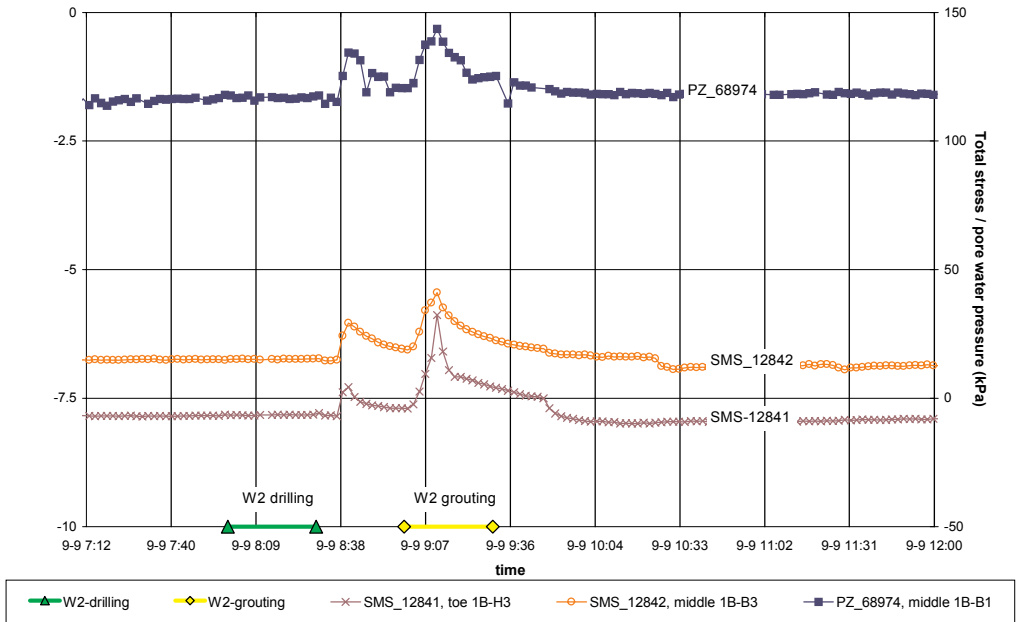


Figure 5.50 Piezometers and SMS during Jet Grouting Column W2 (close up)

5.8.3 Soil Movement

The surface displacements during the grouting of columns W1 and W3 were negligible. Just after finishing grouting column W2, however, some fluctuations were evident. These were totally compensated 36 hours later. These fluctuations were attributed to the jet grouting rig being moved away from the site, which led to a decompression of the peat layer. The surface displacements during the grouting of columns E and F could not be monitored as the beacons had to be removed temporarily to create space for the jet grouting rig.

5.8.4 Bearing Capacity

Concrete piles

The bearing capacity of the concrete piles was determined both before and after jet grouted columns E and F. APPENDIX VIII (A.Figure 26 - A.Figure 28) shows the results of these pile load test. When comparing tests #1 and #2 (before) with test #5 (after) some conclusions can be drawn:

1. piles B1 and B3 reacted significantly more stiffly due to the grouting of columns F and E respectively;
2. pile B2 was not affected by the grouting of columns E and F; the ultimate bearing capacity and stiffness did not change.

No pile load tests (#3) were conducted on the concrete piles after grouting columns A to D (or before grouting columns E and F). The effect on piles B1 and B3 might therefore have been influenced by the grouting of columns A – D. However, as B2 seemed unaffected it was assumed that this effect was negligible. This was also confirmed by the following findings.

In Figure 5.51 the test results of pile B1 are shown. In this figure pile deformation is shown by assuming the pile was only subjected to elastic deformations ($E_c=30.000 \text{ N/mm}^2$). The measured deformations were smaller than the calculated elastic deformations, because in reality some of the load on the pile was reduced by positive skin friction. Based on the test results of test #5 on pile B1 and B3 the apparent Young's Modulus of the concrete (E_c) was calculated. For B1 this resulted in $E_c \approx 41.000 \text{ N/mm}^2$ and for B3 in $E_c \approx 31.000 \text{ N/mm}^2$. The stiffer behaviour of B1 seemed logical because column F was centred under the pile toe (whilst column E was created next to pile B3).

Based on these results it was concluded that owing to the creation of jet grouted pile extensions, the piles barely settled any more when they were re-loaded, 1 day after grouting. Safety aspects prevented loading the pile above 4300 kN, therefore it was not possible to study the behaviour of the pile during failure. When comparing the load – settlement curves before and after grouting however, it is clear that the grouted piles in test #5 showed no sign of reaching their ultimate bearing capacity. It seems logical to assume the ultimate bearing capacity will be much higher than the value obtained without jet grouting.

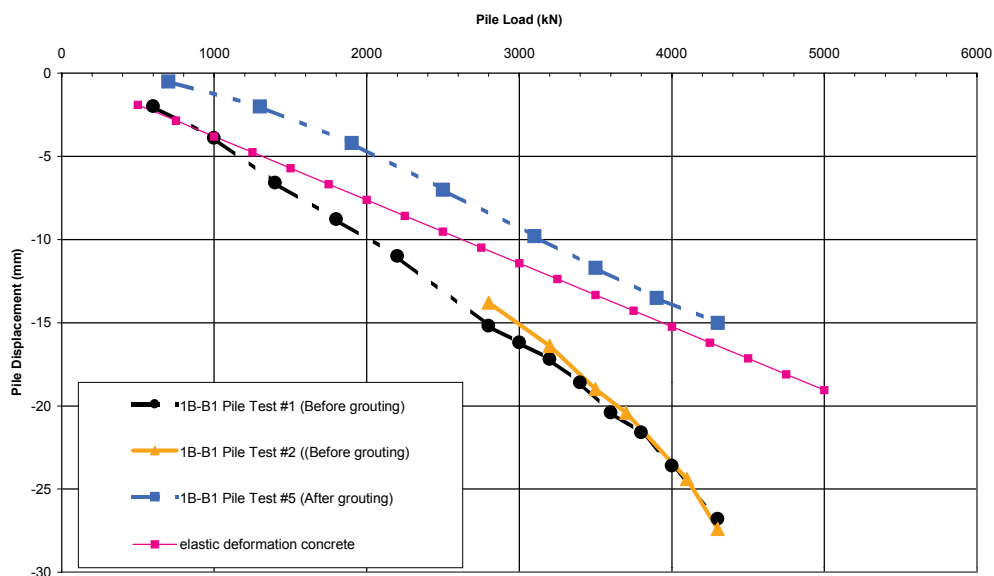


Figure 5.51 Test Results of Pile B1 and Elastic Deformation of a Concrete Pile with $E_c=30.000 \text{ N/mm}^2$

Wooden piles

The bearing capacity of the wooden piles was determined both before and after the jet grouting of columns A, B, C and D and columns W1, W2 and W3. The results of these pile load tests are shown in APPENDIX VIII (A.Figure 26, A.Figure 29 - A.Figure 31).

Comparing test #3 (after A – D and before W1 – W3) with test #5 (after W1 – W3) shows that no consistent difference was detected. In test #5 the initial reaction of pile H1 was stiffer than that in test #3, pile H2 however reacted less stiffly. Pile H3 already shows ongoing settlement at 100kN. Because of the settlements that occurred during grouting the toes of wooden piles H2 and H3, it was expected that the ultimate bearing capacity of these piles would have increased as a result of the grout at their pile toe. These wooden piles, unlike the grouted concrete piles, however show no sign of an increased

bearing capacity. The increased bearing capacity of pile H1 is not surprising, considering that grouting activities did result in a jet grouted column at its toe.

5.8.5 Conclusions on Jet Grouting for Foundation Renovation

The conclusions in this subsection apply to situations where jet grouting is used to create pile extensions for foundation renovation. This application is characterized by the fact that the jet grouted column approaches the area within 0.5 m of the pile toe.

With regard to the pile displacements, it could be concluded that when creating the extensions for the concrete piles, these were limited when grouting next to the pile (4 mm) and unacceptably large when jetting under the pile (≥ 64 mm). In the latter case, reducing the pile load to a force equal to the calculated shaft friction resulted in pile displacements ceasing and when the pile was reloaded after 24 hours no significant pile displacement occurred. A minor blockage in the spoil return flow during the installation of one of the concrete pile extensions led to a minor fracturing incident, which resulted in 1-2 mm pile heave of some of the wooden piles.

No reliable trend in pile displacements was detected during the creation of the extensions for the wooden piles. One of these pile extensions caused no pile settlement at all and for another both the pile to be extended and an adjacent pile showed equal settlement of about 7 to 8 mm.

Consolidation effects did not cause any significant additional pile displacement of either the extended concrete piles or the extended wooden piles.

Regarding the change in total stresses caused by jet grouting the pile extensions, it can be concluded that the response of the SMS to the grouting was generally limited. A clear exception can be made for the SMS located in the toes of the concrete piles. The total stress decreases in these piles correspond approximately with a total local loss of the lateral pressure at the pile toe. Although no coherent relation between the total stress change and the pile settlement could be detected, it can be concluded that a total stress decrease bigger than 20 kPa always resulted in pile settlement.

The creation of the jet grouted pile extensions for the wooden piles did not result in any consistent difference in the bearing capacity. It was expected that the wooden piles that showed settlements during grouting would have a considerably higher bearing capacity owing to the hardened grout at their toe. However, no increase was measured during the load tests, which could only be explained by the absence of grout. When the extended concrete piles were subjected to the load test the deformations were almost exclusively limited to elastic deformations of the piles themselves. Because loading above 4300 kN was not possible (because of safety aspects) it was not possible to study the pile behaviour during failure. However, when comparing the load – settlement curves before and after grouting, it is clear that after the hardening of the extensions the grouted concrete piles showed no signs of having reached their ultimate bearing capacity.

5.9 Correlation Pile Displacement - Distance

To analyse the influence of the distance between the pile and the jet grouted columns on the displacement of a pile, a scatter plot was made. In Figure 5.52 the horizontal distance between a pile and the outside of the jet grouted column (columns A-D) or the vertical distance between the monitor and the pile toe (columns E,F and W1-W3) is plotted against pile settlement. A distinction was also made between the drilling stage and the jetting stage. The area between -0.5 mm and $+0.5$ mm is considered to lie within the accuracy of the measurement system.

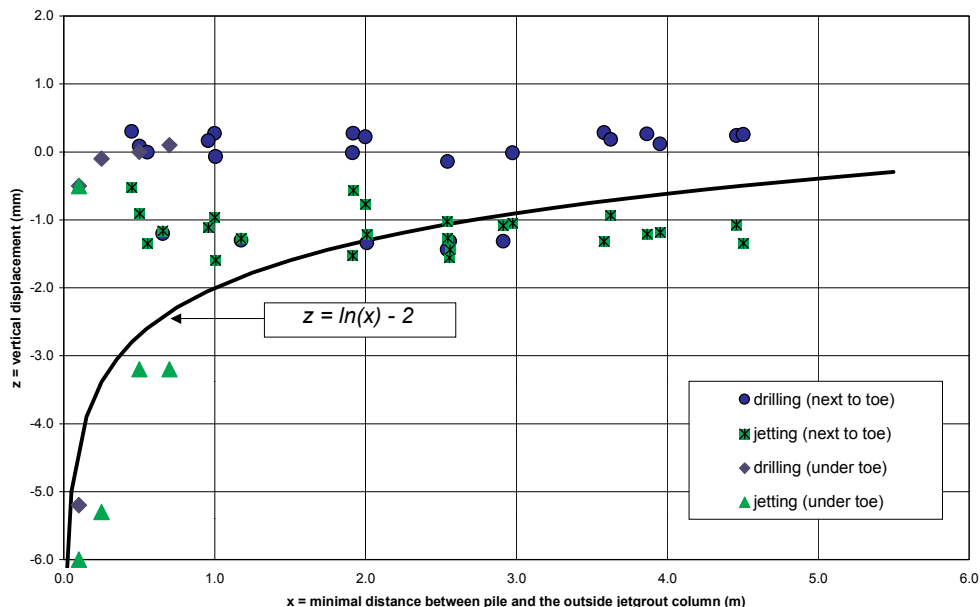


Figure 5.52 Pile Settlement versus Distance Pile - Outside Jet Grouted Column

From Figure 5.52 it can be concluded that drilling at a horizontal distance of up to 0.5 m from the pile usually had no significant (<1.5 mm) influence on the pile. For the jetting it can be concluded that pile settlement remained limited to 2 mm for each column.

When grouting closer to the pile toe than 0.5 m the pile toe, the pile displacements increase exponentially, especially when grouting just below pile toe level. Using the test data a rule of , for the relation between the pile settlement (z ; mm) and distance between the pile and the edge of the jet grouted column (x ; m) is presented:

$$\text{eqn. 5.13 } z = \ln(x) - 2$$

When comparing the settlement graphs with the jet grouting parameters, it could be concluded for the concrete piles that as long as the vertical distance between the monitor and the pile toe exceeded circa 4 times the pile diameter ($4D$) no significant pile displacements occurred. However, when this distance was smaller than circa $4D$ the pile started to settle. This complies with the NEN6743 design theory that states that the pile derives its bearing capacity from an area within $4D$ below the pile toe.

It is remarkable that when the horizontal distance between the pile and the edge of the jet grouted column stay the same, the diameter of the column does not seem to influence the pile displacement. This probably has to do with the limited extra volume of soil the pile derives its bearing capacity from that is disturbed when jet grouting a larger diameter column. This is shown graphically in Figure 5.53.

For the situation as displayed in Figure 5.53, the column diameter is 2.5 m instead of 1.5 m. The extra volume of the “ $4D$ - $8D$ zone” of the pile that is disturbed by jetting the larger diameter is less than 1%. This explains the limited difference in displacement response to the jet grouting.

5.10 Influence of Jet Grouting on CPT

Before and after* the jet grouting of column A, four Dutch Cone Penetration Tests (CPTs) were conducted in order to investigate to what extent the total stresses changed. An overview of all results of the CPTs is given in Van der Stoel (2001). Table 5.13 gives an overview the average change in cone resistance before and after jet grouting, for each soil layer. The distance mentioned is that between the edge of the column and the centre of the CPT. The locations of the CPTs are shown in Figure 5.19 and Figure 5.54.

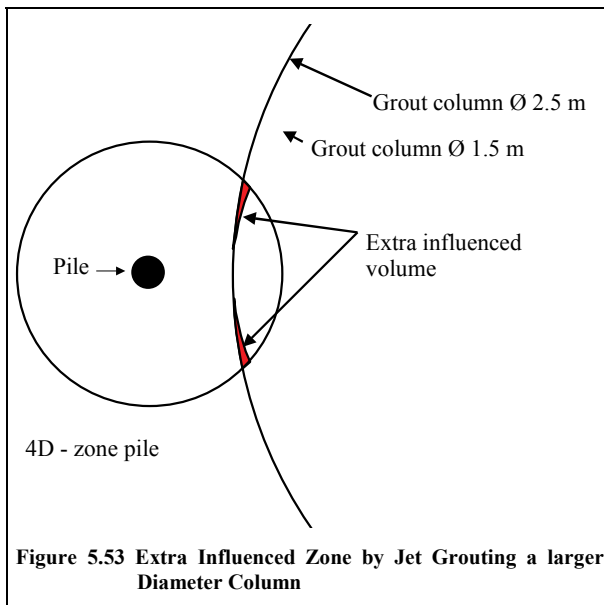


Figure 5.53 Extra Influenced Zone by Jet Grouting a larger Diameter Column

Since the CPTs were carried out at increasing distances from the edge of the jet grouted column, a systematic development of the cone resistance for the various soil layers was sought. In Figure 5.54 the relationships of Table 5.13 are illustrated graphically. Because two CPTs were carried out closest to column A, two combinations were examined, # 1,2,3 and # 4,2,3. From Figure 5.54 it can be seen that the combinations #1,2,3 and #4,2,3 differ significantly. Although #1 is at almost the same distance from column A as #4, for the 2nd sand layer #1 showed an increase of 30% in cone resistance whilst #4 showed a decrease of 20%. An explanation for the one peak value found with CPT #1 could be that it was made just outside the jet grouted column. In the 2nd sand layer this zone contained some grout from the column which had possibly penetrated the soil making it stiffer. Most of the other CPTs showed a small (<20%) decrease in cone resistance, except for #1 in the 1st sand layer. The relative large decrease that was found here was expected based on the fact that this layer is over-consolidated (see Section 5.3.2). The reason why the other CPT in the 1st sand layer (#4) did not decrease is unknown. The proposed zone of influence reaches about ½ the column diameter from the edge of the column.

Table 5.13 Changing CPT value due to Jet Grouting (CPT after/CPT before * 100%)

Combination	CPTs	1 st sand layer		2 nd sand layer		Eemclay layer	
		distance	change	distance	change	distance	change
#		(m)	(%)	(m)	(%)	(m)	(%)
1	S1,S5	0.27	93.3	0.27	129.0	0.29	89.0
2	S2,S6	0.77	73.1	0.77	92.0	0.79	99.7
3	S3,S7	1.27	78.0	1.27	58.2	1.29	97.7
4	S4,S8	0.23	29.7	0.19	80.6	0.09	98.6

The conclusion is that based on these test results, it is not possible to deduce an unambiguous relation for the change of cone resistance due to the jet grouting. Because 3 of the 4 relations showed a decrease in cone resistance, it may be surmised that it is likely that the cone resistance would decrease to some extent due to the jet grouting process, which also complies with the extensometer displacements, the total stress readings and the pile settlements. However, it does not comply with the unchanged bearing capacity of the piles after grouting for foundation protection.

* 70 days before and 117 days after

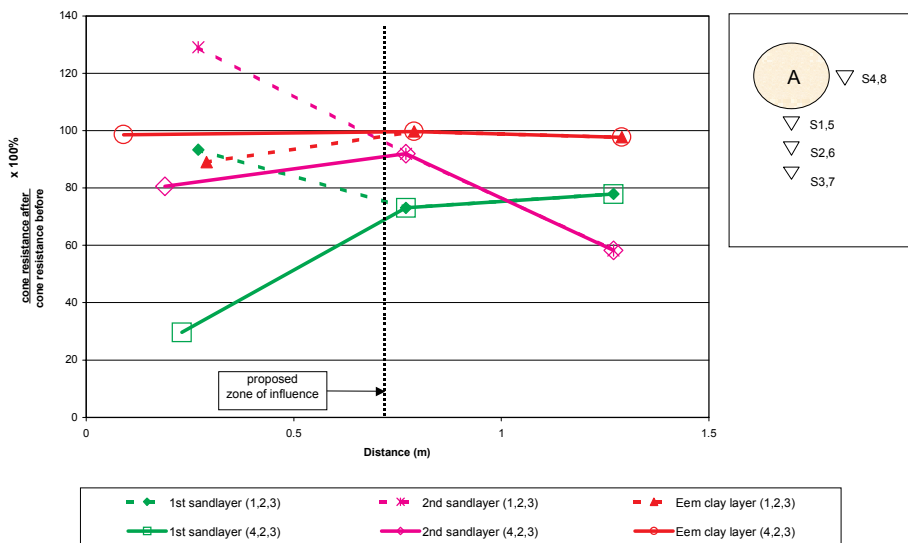


Figure 5.54 Reduction of Cone Resistance as Function of the Distance from the Column

5.11 Diameter Determination by Excavation

To determine the in situ diameter of the jet grouted columns and validate the results of the geophysical methods, the top 5 meters of the jet grouting site were excavated (in a sheet piled building pit). The validation of the geophysical methods is not further discussed here, but outlined separately in Chapter 7. It should be noted that the analysis of the diameter in this sub-section only applies to the diameter in the Holocene top layers, because only this layer was excavated. The results of the geophysical methods however justify the assumption of a similar trend in diameter for the deeper layers.

Figure 5.55 (left) shows an inclined view (note the three concrete piles) and a top view of column A (right). At this stage the wooden piles had already been removed. In between columns B and C some soil is still visible. All the columns were inspected and the average diameter was measured. From the figure that it can immediately be seen the average diameter of columns A, B, C and X1 exceeds the designed diameter. The diameter of column D was smaller than the intended diameter (Table 5.14).

The columns were approximately circular in cross-section, with the exception of column C, which had a somewhat square shape for which no explanation could be found.

The reason the actual column diameter differed from the designed diameter must be sought in the fact that a reliable model for predicting the diameter and experience of using jet grouting in Amsterdam soil was lacking until the test was performed.*

When comparing the diameters obtained with records from the literature (see Section 5.3.3), it can be concluded that the diameters obtained in sand for all columns except column C lie within the usual (1.0-1.5m) diameter range. The diameters obtained in cohesive soil are larger than expected. Column C shows a diameter that is 1.5-2 times larger than usual diameters obtained in cohesive soil. This has to do with the combination of using air in the pre-cutting stage and in the jetting stage, the low lifting speed of the monitor and the large grout flow rate compared to that of columns made in similar soil for other projects.

* to be able to assess the influence of jet grouting parameters, it is common practice for contractors to make a series of trial columns before starting large scale jet grouting projects



Figure 5.55 View of Excavated Site (left) ; Top View of Column A (right)

For all columns but column D, the jet grouting parameters that were used resulted in the diameter being exceeded. For the cohesive soil layers, the exceeding of the diameter is most probably caused by the positive effect of pre-cutting these layers. In general, the conclusion is that for these columns a lower pressure or a higher withdrawal rate could have been used. The halved withdrawal rate and doubled higher cutting pressure and grout flow rate that were used for column D were expected by the contractor to result in a doubled diameter. According to Coomber (1985) a change in withdrawal rate from 10 cm/min to 20 cm/min should result in an increase in the diameter for medium dense sands (grouted at 20 MPa) of 0.6 m to 0.8 m and for loose clayey silts (grouted at 40 MPa) of 1.2 m to 1.5m, or respectively 33% and 25%. If a similar increase is applied on the Amsterdam columns, the diameter of column D should be: $\varnothing_D = 1.25 * \varnothing_A = 1.25 * 1.45 = 1.81\text{m}$. This does not agree with the measured diameter of column D (1.55m). Although this was not observed during excavation, it is remarkable that both geophysical measurements do show a larger diameter for column D (see Figure 7.7). Because further excavation was not possible, the extent to which the changed parameters for column D resulted in a different diameter at larger depths remains unknown. The result of using air in the grouting process for column C clearly increased the column diameter.

Table 5.14 Average Measured Diameter (Excavation)

Column	Designed diameter (m)	Realised diameter (m)
A	1.0	1.45
B	1.0	1.40
C	2.0	2.60
D	2.0	1.55
X1	1.0	1.40
X2	1.0	1.20

5.12 Conclusions on Jet Grouting for Pile Foundation Improvement

To assess the influence of jet grouting on pile foundations, it is necessary to know the jet grouting diameter (which is determined by the process and soil parameters), the position of the jet grouted column and the foundation pile characteristics. Some parameters have a much greater influence than others and many parameters are interrelated, but the complexity of the relationships between the parameters is probably the reason for the lack of reliable models for predicting the influence of jet grouting on pile foundations. It is not expected that reliable models to predict this influence will become available in the near future (<10 years).

Because of the limitations of modelling, the influence of jet grouting on pile foundations was examined by using the results of a full-scale test performed in Amsterdam. A distinction was made between foundation protection and foundation renovation. When jet grouting for foundation protection, the horizontal distance between the pile and the edge of the jet grouted column was 0.5 m or further. When jet grouting to create pile extensions for foundation protection, the jet grouted column approaches the area within 0.5 m of the pile toe.

From Figure 5.52 it could be concluded that drilling at a horizontal distance of up to 0.5 m from the pile usually had no significant (<1.5 mm) influence on the pile. For the jetting it could be concluded that pile settlement remained limited to 2 mm for each column. Neither the distance between the pile and the jet grouted column nor the diameter of the column seemed to influence the pile displacement. When grouting closer to the pile toe than 0.5 m, the pile displacements increased exponentially, especially when grouting just below pile toe level. For concrete piles the pile displacements showed limited displacements when grouting was done next to the pile (4 mm) and unacceptably large displacements when jetting was in progress under the pile (≥ 64 mm). In the latter case, reducing the pile load to a force equal to the calculated shaft friction resulted in the pile displacements ceasing. No reliable trend in pile displacements could be found for the wooden piles. Using the test data, a rule of thumb was found for the relation between the pile settlement (z ; mm) and distance between the pile and the edge of the jet grouted column (x ; m):

$$\text{eqn. 5.13} \quad z = \ln(x) - 2$$

Comparisons between the settlement and the jet grouting parameters when creating pile extensions for the concrete piles led to the conclusion that no significant pile displacements occur as long as the vertical distance between the monitor and the pile toe exceeds circa 4 times the pile diameter (4D)

However, when this distance is smaller than circa 4D the piles started to settle. This complies with the NEN6743 design theory that states that the pile derives its bearing capacity from an area within 4D from the pile toe. The consolidation effects did not result in any significant additional pile displacement in either the concrete pile extensions or the wooden pile extensions

Because of the high cutting and jetting pressures used, jet grouting generally caused an increase in pore water pressure (Δp ; kPa). A relation with the distance between the edge of the jet grouted columns and the piezometer (x ; m) was found, expressed by:

$$\text{eqn. 5.12} : \Delta p = -12 \cdot \ln(x) + 35$$

At about twice the jet grouted column diameter the change in pore water pressure was reduced to 0.5% of the jetting pressure. A significant (>20 kPa) decrease in total stress was recorded when grouting close (<2m) to the SMS in the pile; because of the decrease in total stress and the simultaneous increase in pore water pressure, the biggest changes occur in effective stress. It is plausible that the effective horizontal stresses are temporarily strongly reduced when grouting at 0.5 m from the pile and SMS.

After grouting for foundation protection, neither the bearing capacity nor the stiffness of the wooden piles was negatively influenced by the grouting, which is an important argument for using jet grouting for foundation protection. After grouting for foundation renovation, the bearing capacity of two of the

wooden piles (that showed settlement during grouting) did not show a higher bearing capacity. This can only be explained by the absence of grout at their toes. When the extended concrete piles were subjected to the load test, the deformations were almost exclusively limited to elastic deformations of the piles themselves and showed no sign of reaching their ultimate bearing capacity.

It has not been possible to deduce an unambiguous relation for the change in cone resistance caused by the jet grouting. Because 3 of the 4 relations showed a decrease in cone resistance, it may be surmised that it is likely that to some extent the decrease in cone resistance is due to the jet grouting process. This agrees with the displacements measured by the extensometer, the total stress readings and the pile settlement. However it does not explain the unchanged bearing capacity of the wooden piles after grouting for foundation protection.

From the samples obtained from the jet grouting columns after the grouting process, it could be deduced that although satisfactory strength and stiffness parameters were achieved, the variation coefficient of the UCS, the tensile strength and the Young's modulus were high. The large scatter in these parameters was mainly caused by the influence of the heterogeneity of the soil. Some empirical relations were derived from the test results. These are shown in Table 5.15.

Table 5.15 Empirical Relations for the Relation between Various Grout Parameters

Relation	Grouted Sand Layers	Grouted Clay Layers
Tensile Strength $f_{ct,sp}$ and UCS f_c	$f_{ct,sp} = 0.3 (f_c)^{3/5}$	$f_{ct,sp} = 0.4 (f_c)^{3/10}$
Young's Modulus E_{cm} and UCS f_c	$E_{cm} = 800 (f_c)^{1/2}$	$E_{cm} = 500 (f_c)^{2/3}$
UCS f_c and Water-Cement Ratio wcr *	$f_c = 7 + 8.1 (wcr)^2$	$f_c = 2 + 3.6 /wcr)^2$

* *Applicable for $0.6 < wcr < 1.4$*

In almost all cases the positive effect of using a lower wcr on the strength and stiffness parameters was confirmed. The jet grouted column created by using the triple system shows significantly lower strength and stiffness parameters, which could be expected by the effects of the air used in the process. For the non-cohesive soil layers the strength of the grout was always found to be higher than the spoil strength. For the cohesive soil layers this relation was less clear.

When comparing the jet grouting column diameters that were obtained with records from the literature, it can be concluded that the diameters obtained for all columns, except the column created with the double jet system, for sand lie within the usual (1.0-1.5m) diameter range. For the cohesive layers the diameters are bigger than could be expected. The reason why the actual column diameters differed from the designed diameters may be that the estimates of the jet grouting parameters made by the contractor were incorrect. Because contractors base their predictions on experience, and they had no experience of using jet grouting in Amsterdam soil until the test was performed, this is not very surprising.

5.13 Recommendations and Future Perspectives

Because of the wide scatter that is generally found when analysing jet grouting data, it is advisable that adequate risk assessments should be made. Until a database containing the relation between the jet grouting process and soil parameters on the one hand and the column diameter and grout strength and stiffness parameters on the other hand is available, it is highly recommended that trial columns should be made before the actual project is started. Depending on the type of project, the test program and the function of the jet grouted structure, the use of material factors of 2 to 3 is recommended.

Because of the destructive effect of blowouts that was encountered in this project and in others, the significance of careful monitoring of the jet grouting process is emphasised. Blockage of the spoil return flow by a clogged annulus is the main cause of blowouts, so two measures to counter this are recommended. Firstly, the return flow should be constantly monitored (which in most cases is already common practice). Secondly, the pressure at the monitor should be monitored, for instance by integrating stress cells into the monitor. In this way the process can be automatically stopped when the pressure exceeds a predetermined limit.

Recommendations concerning the use of geophysical methods to monitor the diameter of a jet grouted column are given in Chapter 7.

The suitability of jet grouting for foundation renovation applications is discussed in Chapter 8.

Chapter 6 COMPACTION GROUTING

6.1 Introduction

Compaction grouting is a compensation grouting technique that can be used to compensate for settlements and/or effective stresses relaxation induced by underground construction activities (see Section 2.7). The other compensation grouting technique, fracturing, is only suitable for settlement compensation and is therefore not dealt with in this Chapter.

During the compaction grouting process, very stiff grout with low mobility (Figure 6.1) is injected into the soil at high pressure. The grout should remain a mass in the vicinity of the injection point and should not fracture the soil or enter the pores. Compaction grouting changes the properties of the soil, making it stiffer and stronger. The effect of compaction will be highest in loosely packed, non-cohesive soil. In cohesive soil, consolidation effects

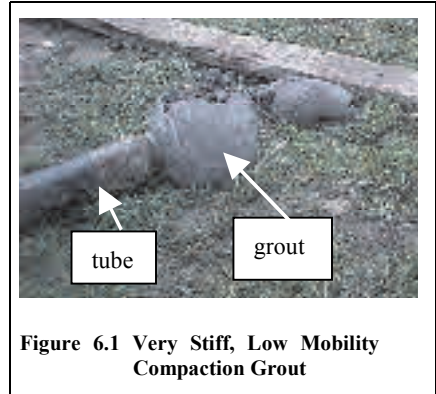


Figure 6.1 Very Stiff, Low Mobility Compaction Grout

will also play a role. Because little is known about the effect of compaction grouting on pile foundations, a test was conducted. The general set-up of this Full-Scale Injection Test was explained in Chapter 3. This chapter deals with compaction grouting Stage 3C of the test.

Compaction grouting is the newest of the grouting techniques considered in this thesis. First, the history, main characteristics and fields of application of the compaction grouting system are outlined. Subsequently some models that describe compaction grouting are discussed. To determine the effects of compaction grouting on the soil and the pile foundations, the differential displacements of the soil and piles, the bearing capacity of the piles and the influence on the total soil stresses and the pore water pressures are considered.

6.2 Compaction Grouting Technique

6.2.1 History

Compaction grouting originated in the USA (California) in the 1950s. The first publication, on the compaction grouting procedure, describes a theoretical model of radial densification of the soil based on a spherical injected mass (Graf, 1969). The first Dutch application of compaction grouting was the lifting of a pneumatic caissons that subsided 30mm owing to a flooding accident (Gelderloos et al., 1969). The caisson was returned to its original position by pumping concrete in the underground channel that originated under it owing to the flooding. Brown and Warner (1973) were the first to conduct tests examining the actual grouting mechanism. These tests included injections and the excavation of grouted elements. Since then many different tests have been conducted to examine the grouting procedure, including measurements of lateral forces, CPTs before and after grouting and the monitoring of structures.

The first application of compaction grouting to control ground movements and to prevent possible damage to structures* during tunnelling was made during the construction of the Bolton Hill Tunnel (Baker, Cording & MacPherson, 1983). Grouting and monitoring were successfully used to compensate settlements caused by a 5.8 m diameter steel-lined TBM tunnel in very dense sand and gravel. Since this successful application, compaction grouting has been extensively used for soil densification and tunnelling projects, mainly in the United States. The technique was first used on a large scale in Europe

* 40 structures, principally two to five stories high with brick bearing walls and shallow foundations

during the construction of the new London Metro connections, like the Jubilee Line Extension and the Docklands Light Rail.

Compaction grouting can also be used for soil densification. Baker (1985) describes the use of compaction grouting to compact in-situ liquefiable soils below two existing dam embankments. Boulanger & Hayden (1995) describe the use of compaction grouting combined with dynamic compaction to densify deep, loose fill deposits.

Over the last 10 years the important influence of the properties of the grout on the grouting results has been increasingly recognized. This has led to some developments, which are discussed in the next subsection.

6.2.2 Compaction Grout

There are many different opinions on the definition of an acceptable composition for compaction grout. Compaction grout has often been described as a “zero slump” grout. However the definition of slump is not often mentioned*. The Geotechnical Engineering Division of the ASCE (Warner, 1992) defined compaction grout as:

“Grout injected with less than 1 inch (25 mm) slump, normally a soil-cement with sufficient silt size to provide plasticity together with sufficient sand size to develop internal friction. The grout generally does not enter the soil pores but remains in a homogeneous mass that gives controlled displacements to compact loose soils, gives controlled displacements of structures or both.”.

From the examined literature (Warner 1972, 1978, 1992, 1997, Warner et al. 1974, 1992 and Bandimere, 1997) it can be concluded that the mobility of the grout is more important than the slump. The grout has to remain mobile until it has reached the intended destination, after which it will preferably become immobile and have adequate internal friction properties. Grouts that are too mobile may result in fracturing of the soil and subsequent loss of control of the grouting process. The effectiveness of compaction grouting will cease and the density of the overlying soils may even be reduced (Warner, 1992).

The slump, the mobility and the pumping characteristics are not directly related. Grouts with high slump characteristics may have low mobility and vice versa. Therefore it would be wise to replace stipulations relating to slump with stipulations relating to mobility.

The gradation of the aggregate in the grout mix, the silt/cement (fines) content and the water content are the three dominant factors that determine the rheological properties of the grout. Warner (Warner 1972, 1978, 1992, 1997 and Warner et al. 1974, 1992) carried out extensive research in this field. Bandimere (1997) has combined this research with the evidence gained from the experience of the biggest grouting contractor in the USA, which has resulted in Figure 6.2.

In recent decades developments in pumping equipment have permitted the use of increasingly coarse aggregate material (see Section 4.2.2). Bandimere (1997) mentions that limestone aggregates require far smaller silt content than mineralogical aggregates and, as a result, give greater grout strengths and better control. The use of poorly graded or angular aggregate material results in a low mobility grout, irrespective of slump (Warner, 1992).

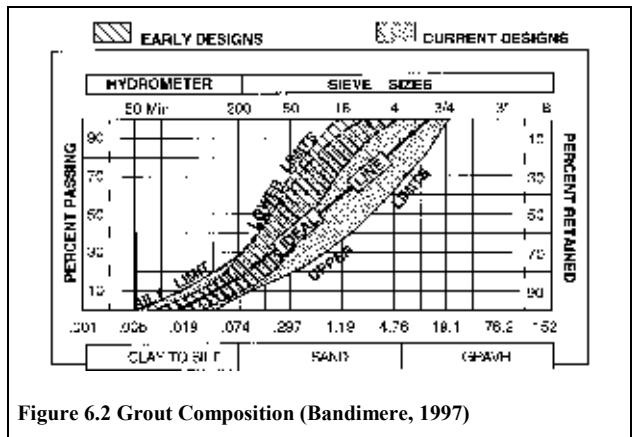


Figure 6.2 Grout Composition (Bandimere, 1997)

* usually the slump using is measured using Abram’s cone or a resembling method

The *silt/cement content* determines the pumping characteristics of the grout and the ability to filter the water when the grout leaves the grouting tube. Excessive quantities of fine materials in the mixture result in hydraulic fracturing of the soil, it is difficult to determine the silt/cement content in situ because a hydrometer is needed to do this. The cement content determines the strength of the grout. When grouting for compaction purposes only, little or no cement is needed because the grout strength does not have to exceed the soil strength. Borden & Ivanetich (1997) give more specific information on the influence of the fines content.

The filtration of the *water* from the grout will result in a loss of plasticity and thus a reduction in pumpability, while an excessive quantity of water will result in hydraulic fracturing of the soil.

It has become clear from the above that the pumping characteristics of the grout play an important role in the effectiveness of the method. As a consequence, the grouting equipment, which will be dealt with in the next sub-section, also plays an important role in the process. The influence the grout composition has on the maximum pumping pressure is discussed in Sub-Section 6.2.4.

6.2.3 Grouting Equipment

Compaction grouting equipment usually comprises a drilling rig (which may be combined with a crane to pull the grout tubes), an injection unit and grout tubes.

The *drilling rig* that is used to install the grout pipes, which are usually made of steel, is similar to the rig used for permeation grouting (Chapter 4) or jet grouting (Chapter 5). The *grout pipes* are installed by means of rotary flush drilling which optionally can be cased. Casing may be preferred when grouting horizontally and/or under foundations. Casings typically have a 50 mm diameter, although casings up to 150 mm are used (Bandimere, 1997). To accommodate a single pass insertion the drilling rig is usually also used for grouting. When a long extraction of the tube is necessary, it is necessary to use a crane with long pulling capacity.

The *injection unit* consists of a grout mixer and a pump. Because of the high shear that has to be overcome to mix the grout, the *grout mixer* used must be a batch pug or screw mixer. Preferably equipment capable of recording the quantities of the added grout components should be used. Because of the risk of fracturing the soil when too much water is added, the use of an automatic water pump provided with a water-meter is especially recommended. The *pump* that is used must be able to displace grouts with low mobility and low slump at pressures up to 15 MPa and grouting rates of 0.1 m³/min. Ideally, it should be possible to change the rate of displacement without interrupting the pumping process. When a piston pump is used the quantity of grout injected can be assessed by counting the pump strokes. More specific information on grouting equipment can be found in Müller and Bruce (2000).

6.2.4 Grouting Pressure and Pumping Rate

The maximum grouting/pumping pressure and pumping rate that can be used are highly dependent on the type of grout and the composition of the soil formation being grouted. When compaction is the only goal, surface or structural disturbance due to heave must either be kept within set limits or prevented. Other restrictions concern consolidation effects due to grouting and grout break out or blow out.

The grouting or pumping rate must be rigidly controlled and according to Warner (1997) should not exceed 0.06 m³/min. Graf (1992) indicates 0.085 m³/min as an upper limit and 0.02 m³/min as an average value for the grouting rate. Bandimere (1997) indicates a maximum pumping rate of 0.1 m³/min at a maximum pressure at the pump of 10 MPa. For sensitive works a much lower pumping rate will often be advisable.

Warner and Brown (1974) indicate that *pressures at the injection point* will vary from 0.35 MPa to 1.7 MPa when injecting within about 1.5 m from the surface to 3.5 MPa when working at 6 m or deeper. Sometimes pressures up to 7 MPa are needed to initiate the grouting. Note that line losses are high because of the high internal friction of the material. Warner and Brown (1974) indicate a line loss of 0.07 MPa per m² of hose (for 38 mm hose). Essler et al. (2000) indicate that the grouting pressure should be equal to $6C_u + \sigma_h$ (where: C_u = in-situ shear stress; σ_h = horizontal overburden stress), resulting in compaction grouting pressures varying from 1.5 MPa (at 15 m depth) to 1.8 MPa (at 30 m

depth). According to Essler et al. this limit is based on the failure of a pile. In Figure 6.7 among other limits for the grouting pressure the Warner & Brown and Essler et al. limits are displayed graphically. In addition to these practical considerations, in the next section some theoretical models for compaction grouting are discussed.

6.3 Field of Application

Compaction grouting is mainly used in soil stabilization or tunnelling projects. It can be used in all types of soils, although it should be noted that as a result of the increase in pore water pressure, consolidation effects might occur in cohesive soils. Much information can be found on the application of compaction grouting to compensate for settlements of shallow foundations induced by tunnelling. However, the information on compaction grouting to compensate for the settlements of pile foundations as well as for increasing the bearing capacity of pile foundations is very limited. In addition to the reviewed literature in Section 6.2 the methods of compaction grouting pile foundations will be discussed combined, with the reviewed literature on grouting near foundations.

Compensation grouting has been used extensively for the compensation of settlements, mostly induced by tunnelling activities, of structures with a shallow foundation. Mair et al. (1994) and Harris et al. (1994) report elaborately on compensation grouting undertaken between the tunnels and overlying structures. The authors report on the observational method used, performance of the instrumentation, the specified requirements for compensation grouting and a summary of the grouting operations. Compensation grouting proved to be successful in limiting the settlements and distortion caused by the construction of 8.25 m diameter tunnels, of the Victory Arch and WCL tunnels. Maximum settlements were limited to 10-14 mm with rotations less than 1/1000.

Soga et al. (2001) have presented the results of extensive grout injection tests performed at the University of Cambridge. Various grouts were injected into both normally and over consolidated clay to observe the fracturing pattern and measure the compensation efficiency. Centrifuge testing was also performed to allow to investigate boundary value problems and the effects of grouting on tunnel lining deformation. Numerical modelling was performed using the finite element analysis of case studies (field and centrifuge tests) and the local modelling of grout injection. The results show that clays with a higher OCR show higher grout efficiency, as do balloon expansion of the grout and close spacing of the injection points. The results of the centrifuge tests (also Bolton (1996) et al.) show that injections should not be made too far ahead of the face if they are to be effective in preventing subsidence above the face of the tunnel. The effects of settlements induced by the dissipation of excess pore pressures caused by compaction grouting are also shown. The results on the numerical models have not yet been published.

Scherer and Gay (2000) present case histories on the use of compaction grouting to densify loose, liquefiable soil. although this specific topic is beyond the scope of this research programs, the authors present some SPT results showing doubled N-values after grouting.

Compaction grouting can be performed top-down, bottom-up or by using a combination of these approaches. For stabilization applications an allowance is made for a minimal heave of the structure, in which case the bottom-up method is used. For shallow applications and the correction of the position (heave) of a structure the top-down method is more appropriate. From a practical point of view, top-down grouting is not efficient, because after each injection it is necessary to re-drill the grouting tube through the grouted element. When first stabilizing deeper soil layers it is possible to use a combination of the methods, by first following the bottom-up procedure and then introducing the load of the structure top-down* (Bandimere, 1997).

Compaction grouting can also be used close to pile toes in order to increase the pile bearing capacity or to create a grout body to compensate for soil settlements as a result of TBM tunnelling. The general idea behind compaction grouting below, surrounding or next to a pile toe, is that the grout stiffens the soil, thus reducing the sensitivity of the pile to soil movements. In Figure 6.3 (*left*) the bottom-up method is

* therefore still some drilling is required, although much less than when working completely top down

illustrated for grouting near a foundation pile. Figure 6.3 (right) illustrates the top-down method. In both illustrations the left pile is grouted from one side only, whilst the right pile is grouted from both sides. Grouting from both sides has the advantage of providing a controlled increase in the lateral stresses on both sides of the pile. When the pile is somewhat flexible it is not necessary to grout at both sides because the lateral displacement of the pile will increase the soil stresses on the “shadow” side of the pile (see Figure 6.4). This lateral displacement is dependent on the distance between the grouted element and the pile and on the pile diameter and pile material and will be in the order of 0.05m.

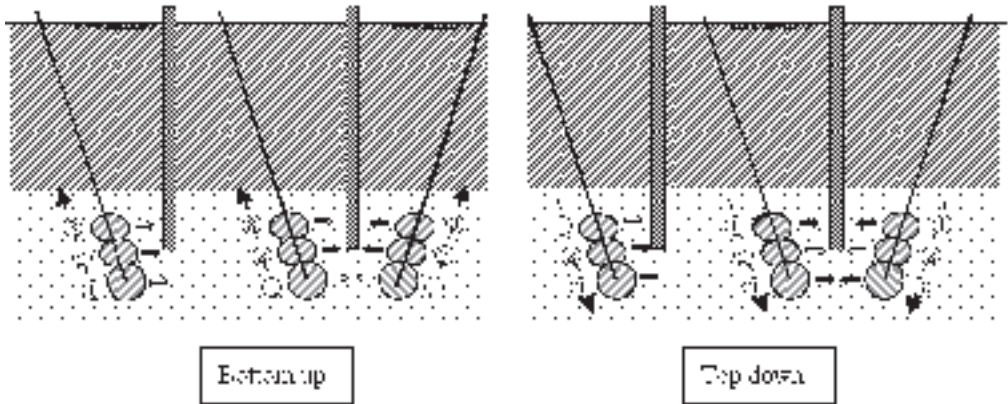


Figure 6.3 Bottom Up (left) and Top Down (right) Grouting of a Foundation Pile

Essler et al. (2000) report that performing compensation grouting in close proximity to pile foundations needs careful consideration. Whether or not the pile can be moved depends on the relative position of the pile and the compensation grouting zone. If the compensation grouting zone is below the pile toes then the piles will move during compensation grouting as the upward force is below the pile. An example is given of compensation grouting carried out in very soft clays above end-bearing piles. The skin friction support will then be small and the ground will move relative to the piles. Essler et al. also indicate that dissipation of pore pressure when carrying out compensation grouting in clays needs careful consideration. It is indicated that pore pressure dissipation in soft clays will result in some long term settlement following tunnelling and will probably require return visits to the site to inject grout to correct for this settlement.

Faught (1997) reports on the use of compaction grouting near the tips of sheet piles to improve the density of sandy silt and gravelly sand strata near these tips. The grouting was performed in primary and secondary stages. Based on the lower grout take during the secondary stage, the author concludes that the grouting was successful. No results of CPT or density measurements are presented however, nor were consolidation effects considered, making the conclusions seem premature.

Van Weele (1993) gives an example of compensation grouting a factory in Rotterdam. The existing end-bearing wooden pile foundation settled as a result of oscillated piles that were installed next to it. To stop these settlements

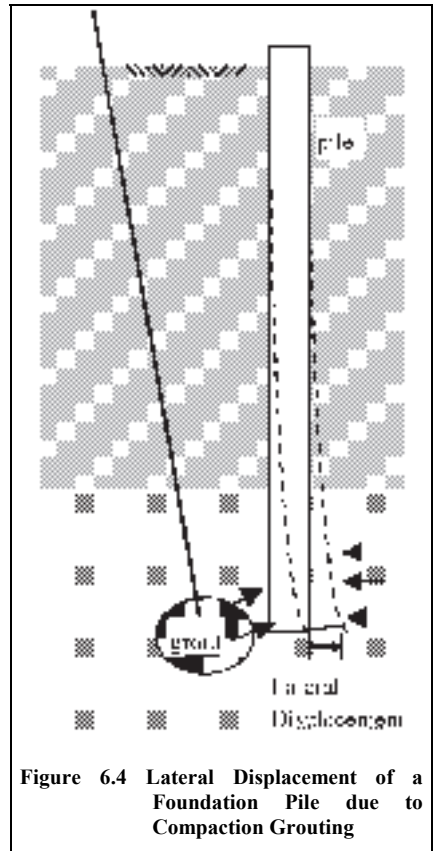


Figure 6.4 Lateral Displacement of a Foundation Pile due to Compaction Grouting

a cement-bentonite mixture was injected adjacent to the pile shafts to compensate for the reduction in effective stresses/cone resistance. The soil below the piles was fractured using a cement-bentonite mixture to heave the complete structure, including the foundation. The author reports that of the 30mm settlement that occurred as a result of the installation of the oscillated piles, 10 mm could be compensated and that additional 20 mm heave would have been possible to undo all settlements. No information on the change in bearing capacity was given.

In Figure 6.5 the densification of soil and the possible soil movements are illustrated. When compaction grouting is used for soil densification, the lateral displacement of the soil should result in densification and an increase in lateral stresses. However, with increasing pressure the soil will also show signs of vertical displacement, which in most cases will be limited. When compaction grouting is used for densification purposes, careful control of the compaction grouting program should result in an optimum stress increase at minimum lift. More information on the modelling the mechanisms of compaction grouting is given in the next section.

6.4 Modelling Compaction Grouting

6.4.1 Compaction Grouting Models

Models are either used to determine the possible radius of the compaction-grouted element, the grouting time or the maximum grouting pressure. These parameters are mainly assessed by determining the resistance of the soil, the surface area of the element and the grouting pressure at the element. The soil resistance is determined by calculating the weight of the inverted cone of soil above the element and the shear strength along this cone. Most models incorporate one or more of the above factors. Although Boulanger and Hayden (1995) concluded “the mechanisms of compaction grouting are not well understood presently”, there have been many efforts to try to model compaction grouting.

In this study, models were sought to determine the maximum grouting pressure and the lateral stress increase or increase in cone resistance due to the grouting. Some compaction grouting models are summarized here.

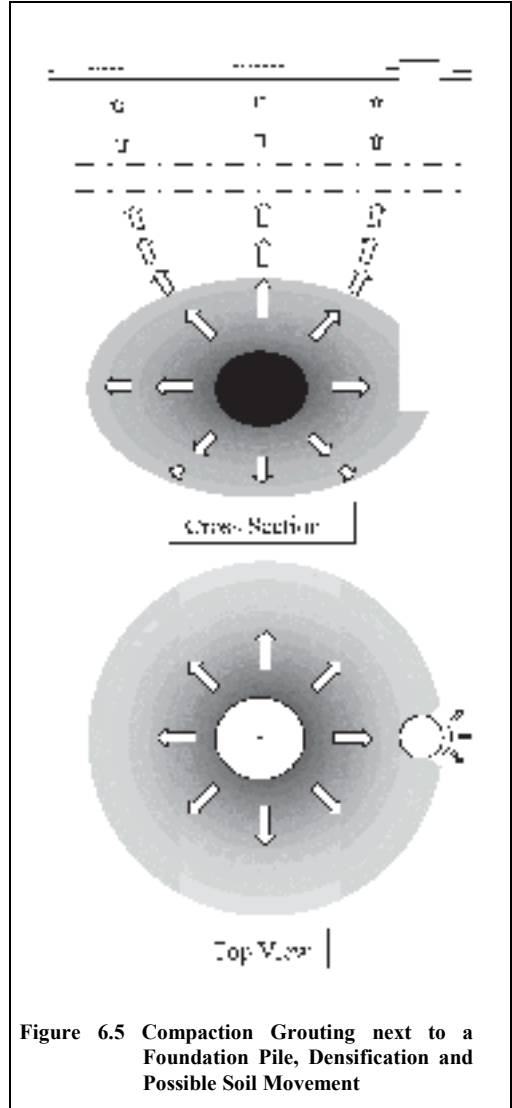


Figure 6.5 Compaction Grouting next to a Foundation Pile, Densification and Possible Soil Movement

Al-Alusi (1997) presented a model based on a volume-mass balance of the grouted soil. When the injected grout volume and the radius of influence of the injection are known, the increased Young’s Modulus of the grouted soil can be calculated. The difficulty of applying this theory for practical purposes is that the influence radius of the grouting is unknown (and in fact one of the parameters that should be determined using a model).

Mace and Martin (1996) have tried to model the expansion of a grout bulb and the soil response by using numerical methods. However the verification of these models proved to be very difficult and therefore these models could not be used to successfully model the grouting process. Kudella (1994) tried to do the same, using small scale model tests, a field test and mathematical models. The conclusions was that the mechanisms of soil fracturing and compaction are very sensitive to all kinds of subsoil inhomogeneities. Moreover, Kudella concluded that although it may be possible to assign a most likely spreading mechanism to each combination of soil and grout mechanisms, a reliable prediction of grout spreading and improvement effect seemed unrealistic at that time.

Schmertman & Henry (1992) present a design theory for compaction grouting based on shear enhancement along grouted columns caused by lateral stress and density increases. The lateral stress due to grouting is defined as:

eqn. 6.1 $K = K_0 + \alpha (K_g - K_0)$

where:

- K = σ_h / σ_v
- K_0 = K before grouting
- K_g = K after grouting (determined from in-situ pressure meter test)
- α = coefficient between 0 and 1

Laboratory tests are needed to determine the coefficients used in the equation. Because the authors also indicate that K_g will vary from 1.5 to 10, and that α should fall between 0 and 1 this model is considered to be impracticable to use.

Wong (1974) has assumed that when the grouting pressure is essentially uniform throughout the grouted element, a first order approximation (eqn. 6.2) can predict the maximum grouting pressures for the process. The model is based on the uplift of a truncated cone above the grouted element. The potential conical shear failure surface will be inclined at an angle θ of about 60° with the horizontal. (equivalent to application of the Mohr-Coulomb failure criterion to any point along the conical surface).

eqn. 6.2
$$p_u = \gamma h \frac{\left(\frac{h}{a}\right)^2 + 3\left(\frac{h}{a}\right)\tan\theta + 3\tan^2\theta}{3\tan^2\theta} \left[1 + \frac{2(1 - \sin\phi)\cos(\pi - \theta + \phi)}{\cos\phi\cos\theta} \right]$$

where:

- p_u = maximum allowable grouting pressure (MPa);
- h = depth of centre of grouted element below the ground surface (m);
- a = radius of spherical grouted element (m);
- γ = total soil bulk density (kN/m³);
- ϕ = internal friction angle of the soil (rad);
- θ = the potential conical shear failure surface angle = $\pi/4 + \phi/2$ (rad)

A fundamental approach to cavity expansion, which can be used to model compaction grouting, is given by Vesić (1972). The approach is based on distinguishing a plastic and an elastic zone generated by the grouting. Vesić combines the differential equation for spherical cavity expansion and the condition of rupture according to Mohr, to obtain the ultimate pressure p_u . At this pressure, the cavity will have a radius R_u , and the plastic zone will extend to a radius R_p . Beyond this radius the soil mass remains in a state of elastic equilibrium. In Figure 6.6 the expansion of a cavity is shown.

For a spherical grout element, the radial stress σ_r can be expressed as:

eqn. 6.3
$$\sigma_r = (p_u + c \cot\phi) \left(\frac{R_u}{r}\right)^{4 \sin\phi / (1 + \sin\phi)} - c \cot\phi$$

where:

p_u	=	the ultimate pressure	(MPa)
c	=	cohesion	(MPa)
ϕ	=	angle of shearing resistance	(°)
R_p	=	radius of the plastic zone around the cavity	(m)
R_u	=	radius of the cavity at p_u	(m)
r	=	distance to the centre of the cavity	(m)

According to Vesić (1972), the ultimate cavity pressure can be computed by using eqn. 6.4*:

$$\text{eqn. 6.4 } p_u = 0.314(cF_c + qF_q)$$

where q is the isotropic effective stress (MPa) and F_q and F_c are dimensionless factors:

$$\text{eqn. 6.5 } F_q = \frac{3(1 + \sin \phi)}{3 - \sin \phi} (I_{rr})^{4 \sin \phi / [3(1 + \sin \phi)]}$$

$$\text{eqn. 6.6 } F_c = (F_q - 1) \cot \phi$$

I_{rr} may be termed the reduced rigidity index:

$$\text{eqn. 6.7 } I_{rr} = \frac{I_r}{1 + I_r \Delta} = \left(\frac{R_p}{R_u} \right)^3$$

where:

Δ	=	average volumetric strain (-)
I_r	=	rigidity index (-)

I_r represents the ratio of the soils shear modulus (G) to its initial strength ($s = c + q \tan \phi$):

$$\text{eqn. 6.8 } I_r = 0.305 \frac{E}{2(1 + \nu)(c + q \tan \phi)} = 0.305 \frac{G}{s}$$

where:

E	=	Young's Modulus	(MPa)
ν	=	Poisson's ratio	(-)

The main disadvantage of the Vesić model is that no boundaries are included in the model. This will result in high pressures near the surface, which will be shown in the next sub-section.

Most of the models have been used to make predictions for the compaction-grouting test that was performed in Amsterdam. It may be concluded that all models are very sensitive to the parameters used and that assumptions concerning the homogeneity or isotropy of the material very much influence the results. Because, however, the models are useful to provide insight into the compaction grouting mechanisms, some calculations are incorporated in the next subsection.

6.4.2 Modelling Compaction Grouting in Amsterdam

The Wong and Vesić formulae were used to predict the maximum possible grouting pressure to be used during the compaction grouting trial in Amsterdam. To be able to use these models some

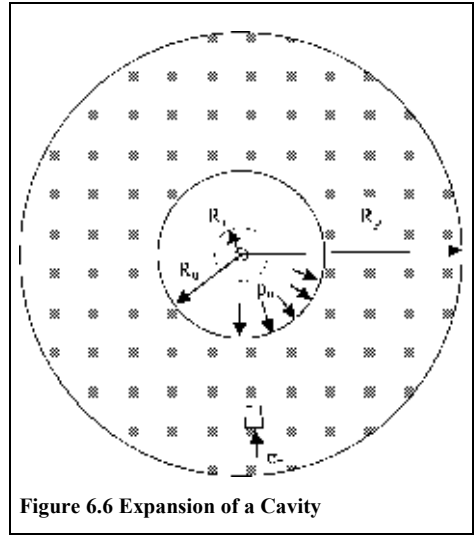


Figure 6.6 Expansion of a Cavity

* The factor 0.314 in eqn. 6.8 and eqn. 6.4 is used to compensate for the depth given in feet (/0.305 for conversion to m) and the pressure in tons per sq ft (*0.0958 for conversion to MPa) in the original formulae.

schematisations of the soil profile and an estimation of soil parameters had to be made. For both models the soil has to be modelled as a homogenous medium. The following parameters were used:

- for the Wong model: $a = 0.4 \text{ m}$; $\gamma = 20 \text{ kN/m}^3$ and $\phi = 30^\circ$;
- for the Vesić model: $c = 0 \text{ MPa}$; $\phi = 30^\circ$; $\gamma = 20 \text{ kN/m}^3$; $\Delta = 0.01$; $E = 70 \text{ MPa}$; $\nu = 0.3$.

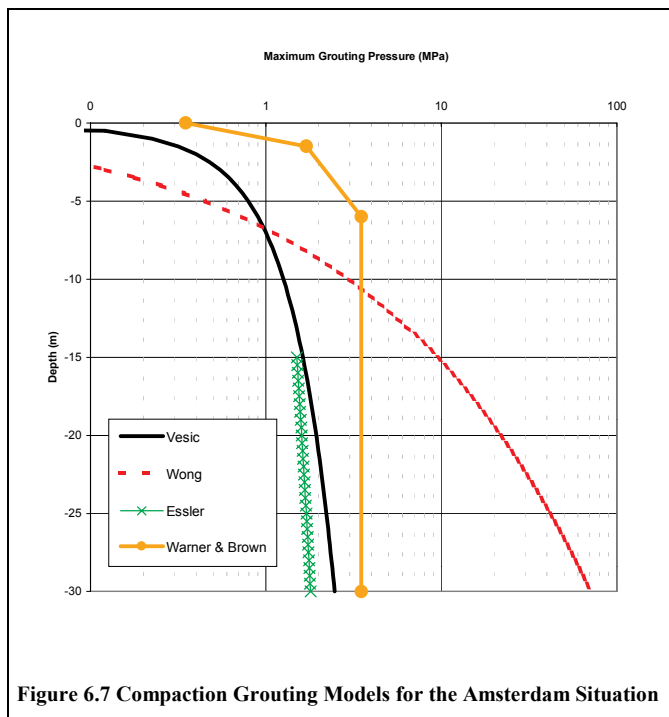
Figure 6.7 shows the results of the predictions. In this figure the limits from grouting practice, as mentioned in Section 6.2.4, are also indicated. It is immediately apparent that at depths of 10 m or more, the practical limits are much lower than the values that are considered theoretically possible. This relates on one hand to the schematisations used in the theoretical models, and on the other hand to the safety factors that are incorporated in the practical limits (because they have to apply to a random soil type).

Because the maximum pressure is the Wong model is determined by the uplift of a truncated cone above the grouted element, at large depths ($>10\text{m}$) this criterion is no longer considered to be reliable. Using the Vesić model results in high allowable grouting pressures at limited depth ($<2\text{m}$).

This is not considered accurate, because the risk of fractures and blow out occurring will then be normative. The Vesić criterion however shows a good resemblance to the Essler et al. limit, which seems logical because both limits are based on local failure. Because of the length of the piles, compaction grouting for pile foundations is always performed at a depth of circa 5 meters or more. Considering this and also its resemblance to the practical limits, the Vesić criterion is considered to give a safe criterion for the maximum grouting pressure at 2m depth and more.

Because of the differences in maximum grouting pressure indicated by the models and the limits from grouting practice, 2-dimensional Finite Element Method (FEM) calculations were made in addition to using PLAXIS. It should be noted that the purpose of the FEM calculations is not to model the actual situation. The complexity of modelling the foundation piles in the soft, stratified soil, the modelling of the grouting process and the 2D character of the calculation prevent such a prediction. The FEM analysis is therefore used only to get an indication of the possible grouting pressure, the soil displacements and the effective stress changes.

The main imperfection of this model is that the 2D situation underestimates the maximum pressure that can be used during the grouting process. However, because the tunnelling option was used to model the grouting process, it was not possible to make a 3D calculation. The complete results may be found in Everaars & Van der Stoel (2000); only the most important points of departure, boundary conditions and results are mentioned here.



The Amsterdam soil was modelled using the PLAXIS non-linear hardening soil model. The soil parameters are shown in Table 6.1. The compaction grouting element was modelled using a tunnel element with an initial radius of 0.10 m, and a flexible lining, located at 17 m depth in a 17 m high, 20 m wide axi-symmetric mesh (Figure 6.8). By gradually increasing the pore water pressure inside the tunnel (grouting) element in accordance with a *phreatic line* calculation, the element was “inflated”.

Table 6.1 Parameters used for PLAXIS 2D-FEM Calculations

Parameter	Value	Dimension
γ_{sat}	19.0	kN/m ³
c'	0	kPa
ϕ'	28 – 47	°
Ψ	0 – 17	°
k_v	$10^{-3} - 10^{-5}$	M/s
ν	0.2	-
K_η	0.4	-
<i>POP</i>	0	kPa
<i>OCR</i>	1	-
Hardening-Soil model		
p_{ref}	100	kPa
$E'_{50:ref}$	24,600 – 49,400	kPa
$E_{oed:ref}$	19,200 – 58,500	kPa
$E_{ur:ref}$	61,500 – 364,000	kPa
M	0.5	-

The calculations showed that for an element created in a homogeneous sand layer, the soil collapsed at a grouting pressure (water pressure inside the tunnel) of 1.4 MPa. The relative shear stresses at the moment the soil collapses are displayed in Figure 6.9 (*left*). From this figure it can be seen that the shear stress are close to the tunnel/grouted element are exceeded. In Figure 6.9 (*right*) a close up of the mesh in which the plastic points are displayed is given. From this figure it can be concluded that plastic point occur within 0.35 m of the edge of the tunnel/grouted element.

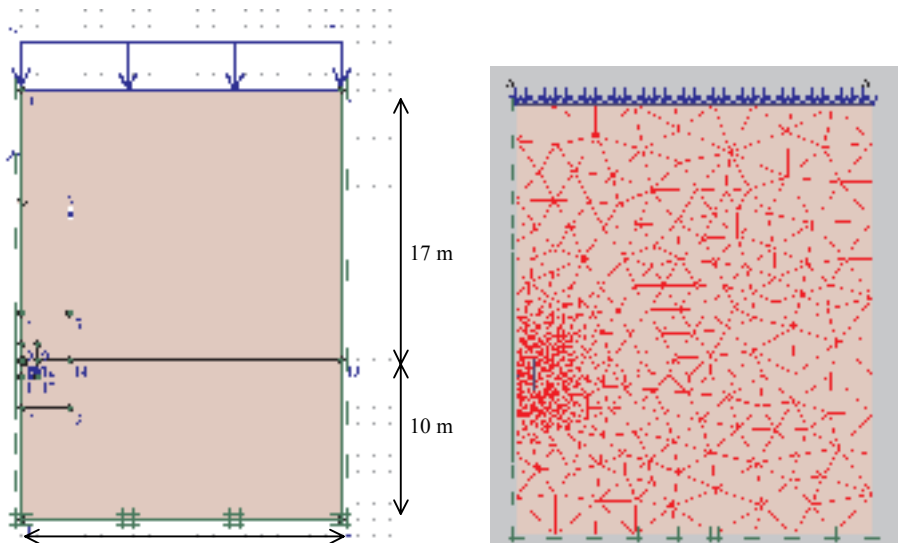


Figure 6.8 Geometry (*left*) and Mesh (*right*)

For this specific situation, the horizontal and vertical effective stresses at a horizontal cross section in the grouting point (line 3-13 in Figure 6.8 *left*) are displayed in Figure 6.10. From this figure it can be seen that owing to the grouting the horizontal stresses up to a distance of 5 meters increase considerably (>125%). The decreases in vertical effective stresses are caused by the failure mechanism (uplift of a cone) that occurs.

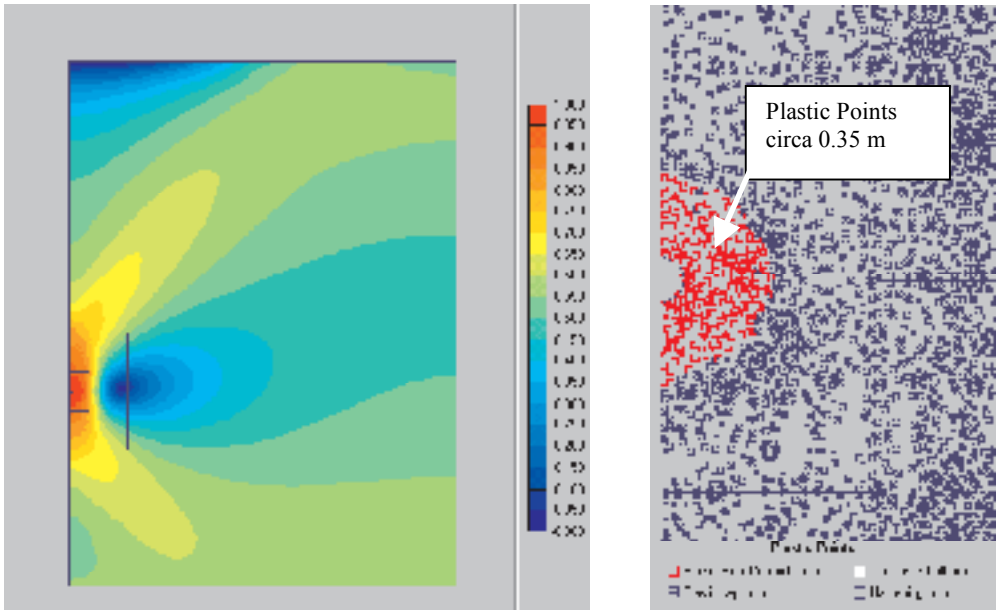


Figure 6.9 Relative Shear Stress at Failure (*left*) and Plastic Points (*right*)

The total displacements at this cross section are displayed in Figure 6.11. The displacements are especially large (5-56mm) within 1 meter of the grouting point (which has then increased in radius from 0.1 m to 0.16m).

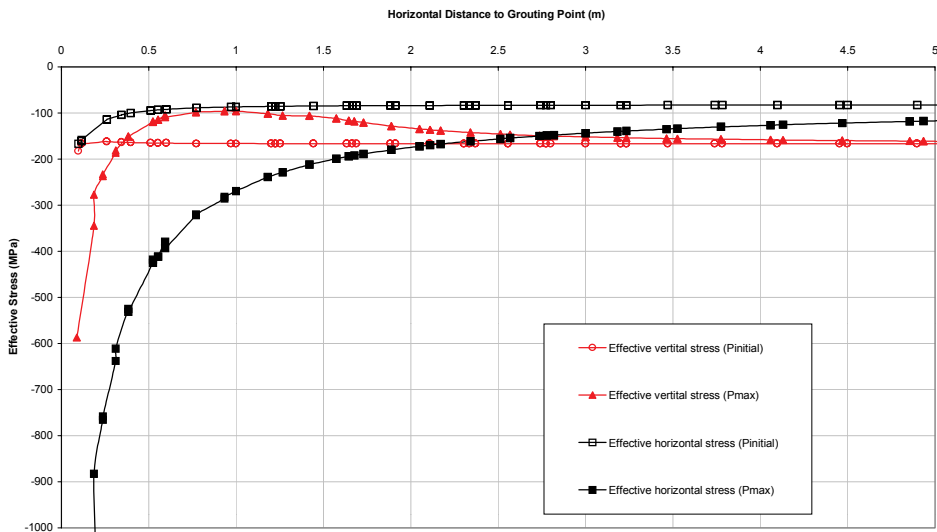


Figure 6.10 Effective Stresses next to a Compaction Grouting Element

The FEM calculations have given a good indication of the influence of compaction grouting on the soil surrounding the injection point. The deformation of the tunnel (grouted element) is considered to be small considering the volumes grouted in similar soil in practice. This however probably has to do with

the 2D schematisation. A positive result of the calculations is that the failure mechanism and an indication of the plastic zone and deformations around the tunnel/grouted element could be obtained.

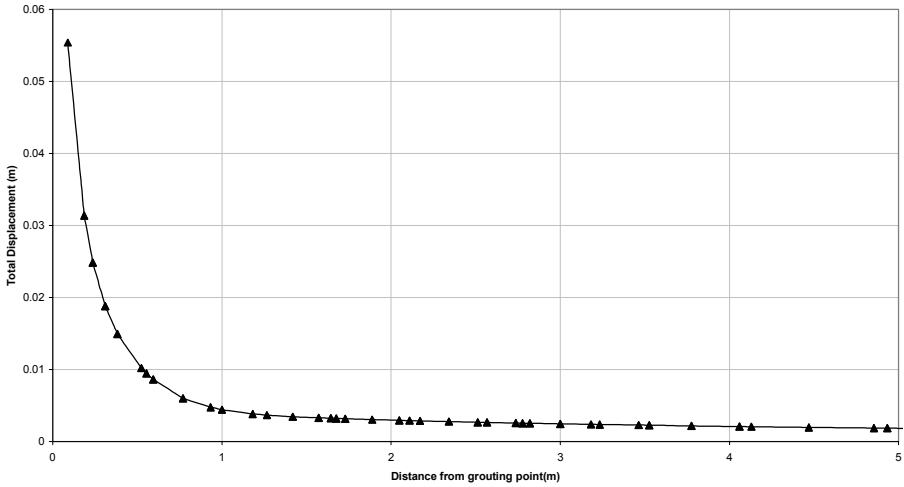


Figure 6.11 Total Displacements next to a Compaction Grouting Element

When the results of the FEM calculations are compared with the results shown in Figure 6.7, at first sight the results seem to comply fairly well with grouting pressure limit given by Essler et al. ($p_u=1.5$ MPa). However It should be considered that both this limit and the limit obtained from the FEM calculation underestimate the actual pressure limit. The first because safety is included in this relation, the latter because the 2D schematisation underestimates the capacity of 3D reality.

Considering the 2D character of the FEM calculations, for the Amsterdam situation it was decided to maintain a compaction grouting pressure limit of 2.5 MPa at the injection point for grouting at approximately 15 meters depth. Considering a possible friction loss in the system (hoses and grout tube) of 0.07 MPa/m (see Section 6.2.4) and a system length of about 25 meter, a pressure limit of 4.0 MPa at the pump was used. In the next section the detailed test set-up will be explained, after which the test results will be outlined and a comparison will be made between the results obtained from the predictions and the results from the test.

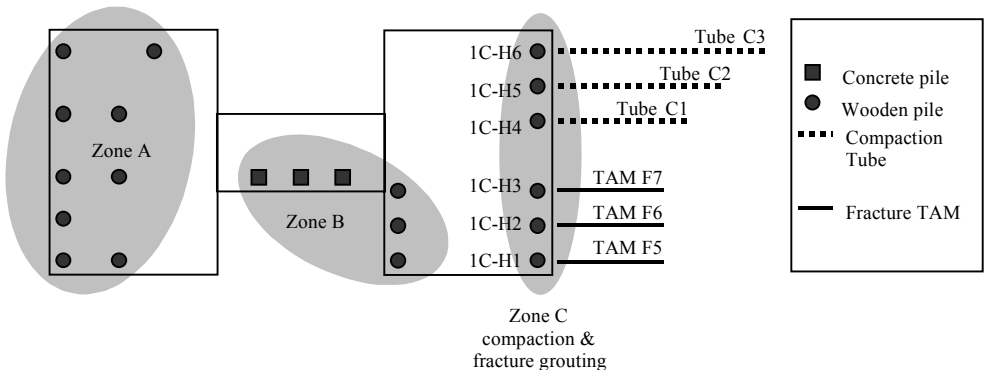


Figure 6.12 General Plan View of the Piles and Tubes

6.5 Detailed Test Set-up

6.5.1 General

The general set-up of the Full Scale Injection Test was discussed in Chapter 3. The aim of this stage of the test is to investigate the influence of compaction grouting on:

- pile displacements, pore water pressure and soil stresses;
- the bearing capacity of a wooden pile.

Steel tubes were used to inject grout and thus create a more-or-less cylindrical compaction grouting body. During the installation of the tubes and during the actual compaction grouting process, vertical displacements of the piles were closely monitored. The horizontal total stress and the pore water pressure were also monitored; the former only in the piles, the latter in both the piles and the soil. The tubes were placed at different angles of inclination in order to study installation effects of the compaction grouting tubes. The piezometers in the soil were placed at increasing distances from the grouting points, to monitor the influence of the grouting pressure.

In this stage of the test also some experiments on fracturing the soil under the pile toes were conducted. The results of these experiments are not included in this thesis, as fracturing is not expected to improve the bearing capacity of the piles. Because, however, the piles used for the fracturing lie within the compaction grouting range and because fracturing was conducted *after* compaction grouting, the response of these piles was also observed in the analysis. Figure 6.12 shows a general plan view of the position of the tubes in relation to the pile positions. In Figure 6.13 a typical cross-section is shown.

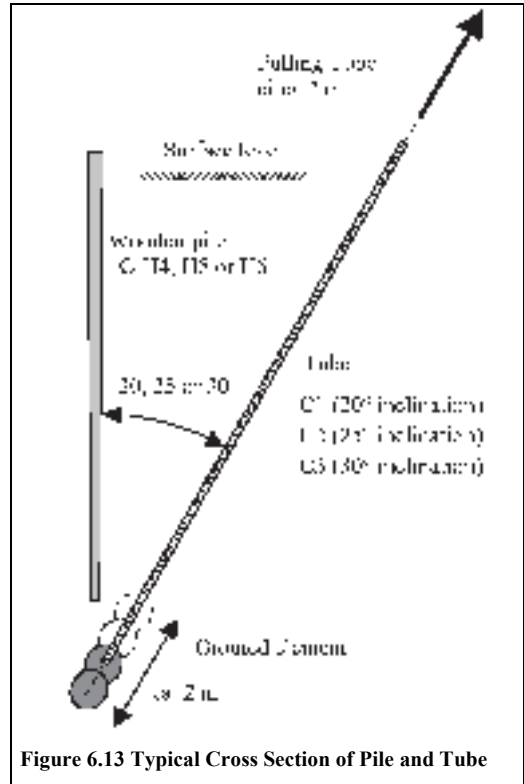


Figure 6.13 Typical Cross Section of Pile and Tube

6.5.2 Piles and Monitoring Equipment

Three wooden piles, coded 1C-H4 to 1C-H6 were used to study the effect of compaction grouting and three wooden piles, coded 1C-H1 to 1C-H3 were used to study the effect of fracturing. The top x,y position of all the piles was verified after driving. All piles were supplied with piezometers and SMS. However because none of the piezometers integrated in the piles functioned properly and only the SMS in pile 1C-H2 functioned properly, two additional piezometers were installed in the first sand layer, between the piles (WM30 & WM31). The location of the monitoring equipment is illustrated in Figure 6.14. The grouting centre of gravity that is shown in the figure is further explained in 6.7.2. Additional information on the monitoring equipment is given in Table 6.2.

To monitor the surface displacements, both beacons (ZB9-ZB14) and in addition two reference targets (SB5-SB6) were used. As was explained in Chapter 3, pile displacement was monitored by using both joint meters and the automatic levelling system. The joint meters were connected to each individual pile by using a reference frame (Figure 6.15). Because, being placed on the surface the reference frame itself was susceptible to movement and the readings of this frame were also influenced by temperature, it was monitored by using targets SB5 and SB6. In this way a correction for temperature and surface measurements was made whenever necessary.

COMPACTION GROUTING

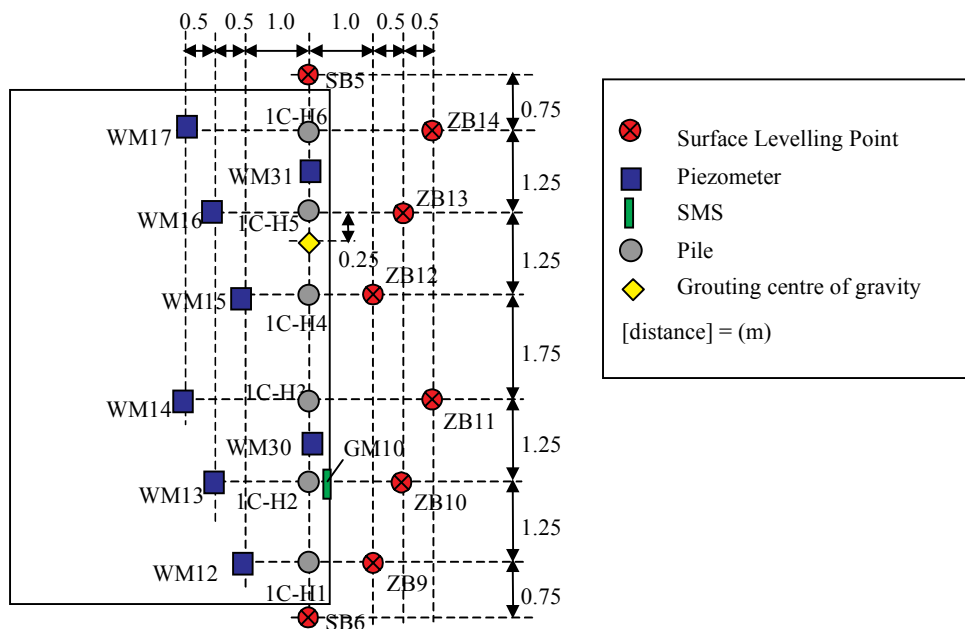


Figure 6.14 Detailed Test Set-up: Plan View of the Monitoring Equipment

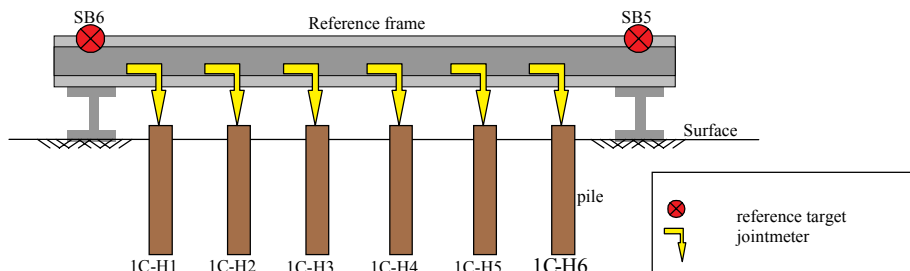


Figure 6.15 Typical Cross Section of Piles and Reference Frame

Table 6.2 Piezometers

Piezometer	Adjoining Pile	Distance from axis pile row (m)	Depth NAP (m)
WM12*	IC-H1	1.0	-12.3
WM13	IC-H2	1.5	-11.7
WM30	Between IC-H2 and H3	0	-14.6
WM14*	IC-H3	2.0	-11.7
WM15	IC-H4	1.0	-11.7
WM16	IC-H5	1.5	-11.7
WM31	Between IC-H5 and H6	0	-14.1
WM17	IC-H6	2.0	-11.7

* not functioning

6.5.3 Grout Composition

In Table 6.3 the grout composition is shown. Note that very little cement was used because the strength of the compaction grouting body was not required to exceed the strength of the surrounding soil.

Table 6.3 Compaction Grout Composition

Component	Quantity	Mass %
Sand 0-4 mm	540 kg	24
Sand 0-1 mm	1000 kg	43
Cement	50 kg	2
Fly ash < 80µm	470 kg	10
Water	250 litre	3
Retarder (ligno-sulphamate)	2 litre	0.1

6.5.4 Compaction Grouting Wooden Piles in the 1st Sand Layer

The principle on which the desired effect of compaction grout injections used in the test is based is shown in Figure 6.16 (left). By injecting the grout a little below and beside the 4D-8D area of the pile, the sand is compacted and densified. The lateral effective stresses and cone resistance near the pile toe are increased, which should result in a higher end bearing capacity. A side effect of the compaction grouting might be that the pile is lifted several millimetres (Figure 6.16 right) because of difficulties in controlling the grouting process. Another problem was formed by the small thickness of the 1st sand layer. Because of the risk of grout being injected into the cohesive layers above and below this layer, a risk of consolidation effects occurring in these layers was identified.

Because it was not possible to predict what the pile response would be, it was decided that the pile heave should not exceed 10 mm and the maximum grouting pressure should not exceed 2.5 MPa (see Section 6.4.2).

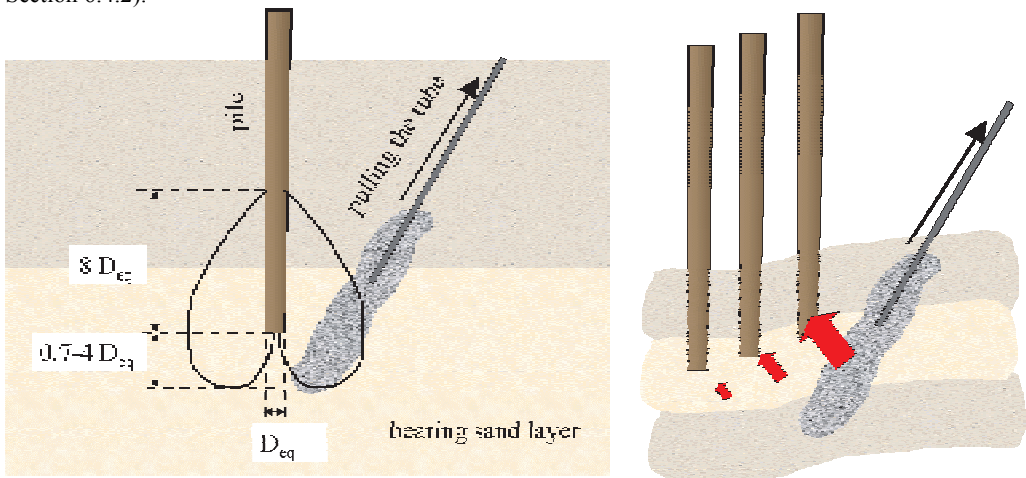


Figure 6.16 Position of the Grouted Element (left) and Causing of the Heave (right)

6.5.5 Grouting the Elements

The steel tubes used for compaction grouting had an outer diameter of 114.3 mm and an inner diameter of 101.7 mm and were installed in a borehole created by using 150 mm diameter, rotary-flushed borings without using a casing. They were lowered into the borehole manually and fixed in place by means of a bentonite-cement sleeve grout*. For use in compaction grouting these steel tubes they were equipped

* Only little cement was used, because the tube cannot be pulled when the sleeve is too hard

COMPACTION GROUTING

with a special removable plug at their lower ends (Figure 6.17). When the grouting process starts the plug is blown from the tube by using a high pressure.



Figure 6.17 Attachment of a Removable Plug at the Bottom End of the Tube



Figure 6.18 Installation of the Tubes

The grouting rig was used for installing the tubes and for pulling them during the grouting operation (Figure 6.18 & Figure 6.19).

The tube was connected by a special hose to a concrete mixer filled with grout. A manometer and printer were used to record the grouting pressure. The objective of the grouting procedure is to ensure that after each with the next stroke of the pump the soil should become more densified and therefore be even harder to compact the next stroke. After a series of pump strokes the pressure will rise above the acceptable limit (either for the pump or for the soil) and the tube must be raised for circa 0.5 m. The procedure is then repeated until the tube has been raised circa 2 meters.

The general data concerning the compaction grouting installation and grouting operation are shown in Table 6.4. The pressure fluctuations during grouting were significant and are therefore not incorporated in the table, but treated separately:

- *Grouted Element C3 at pile 1C-H6*: This tube was pulled 4 times, each time the maximum pressure reached 4 MPa before pulling. The tube was pulled circa 0.5 m each time; a total of 22 piston strokes* were injected.
- *Grouted Element C2 at pile 1C-H5*: This tube was pulled 4 times. The first time, after 14 strokes, the pressure had reached 1.8 MPa and cement bentonite (from the sleeve) escaped at the surface (see Figure 6.20). The tube was pulled 0.5 meters, after which grouting resumed without problems. The pressure no longer exceeded 1.5 MPa and the tube was pulled 3 more times (again 0.5 m at a time).
- *Grouted Element C3 at pile 1C-H3*: This tube was pulled 5 times. The first time, after 20 strokes, the pressure had reached 1.2 MPa. Pulling the tube the 1st, 3rd and 5th time did not result in a pressure decrease, although the 2nd and 4th pulls did do so. The pressure did not exceed 1.5 MPa.

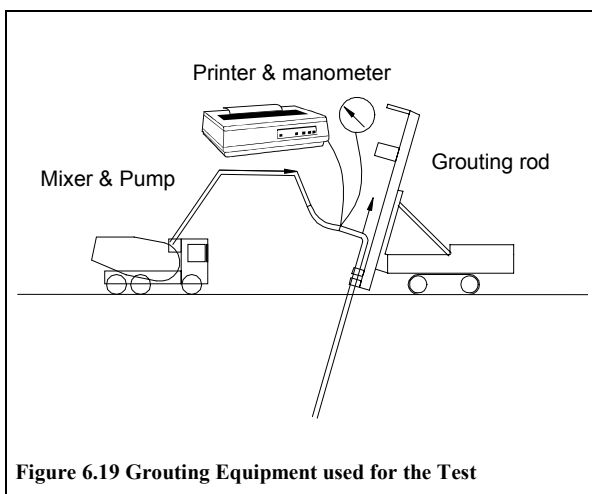


Figure 6.19 Grouting Equipment used for the Test

Table 6.4 Tube Installation and Grouting Data

Activity		Tube		
		C1	C2	C3
Installation	Date	12-10-1999	12-10-1999	08-10-1999
	Time	13:00 – 15:00	09:00 – 11:00	10:00 – 12:00
	Designed install. angle	20	25	30
	Realized install. angle	19.7	24.2	28.5
	Bottom level Tube (m)	NAP – 16.52	NAP – 15.99	NAP – 15.84
Grouting	Date	14-10-1999	14-10-1999	14-10-1999
	Time	09:55 – 10:20	09:00 – 09:20	08:20 – 08:50
	Strokes of grout pump	109	77	22
	Grouted volume (m ³)	2.666	1.883	0.538
	Maximum pressure stroke 1 (MPa)	4.0	1.8	1.2
	Maximum pressure stroke 2 (MPa)	4.0	1.5	1.5
	Maximum pressure stroke 3 (MPa)	4.0	1.5	1.5
	Maximum pressure stroke 4 (MPa)	4.0	1.5	1.5
Maximum pressure stroke 5 (MPa)	-	-	1.5	

During grouting of the elements the maximum pressure of 4.0 MPa was not exceeded. During the first injection the maximum pressure reached 4.0 MPa, but at that point the pump was no longer able to displace the grout. Because the break out during the second injection concerned some sleeve bentonite-cement grout, it can be concluded that the maximum pressure of 4.0 MPa is sufficient to prevent blow-out. In the next section the effects of tube installation on the piles and soil will be discussed. The subsequent section deals with the effects of the grouting.

* 1 stroke equals approximately 25 litres



Figure 6.20 Cement Bentonite Sleeve Grout Backflow at Surface Level

6.6 Results of Tube Installation

The displacements of the piles as well as the changes in pore water pressure and total stress as a result of the tube installation were relatively insignificant. Based on the results of the installation of the permeation grouting TAMs (see Section 4.7), which although smaller in diameter were located much closer to the piles, this was expected. The pile displacements resulting from compaction grouting tube installation are shown in Table 6.5. The implications of installing tubes or TAMs close to piles were already dealt with in Section 4.7 and are not further explained here.

Table 6.5 Vertical Displacements (mm) due to Compaction Grouting Tube Installation

Installation Tube	date	1C-H1	1C-H2	1C-H3	1C-H4	1C-H5	1C-H6
C3	08-10-99	0	0	0	0	0	0
C2 and C1	12-10-99	0	-0.5	-0.5	-0.5	0	-0.5

6.7 Results of Compaction Grouting

6.7.1 Introduction

In this section the pile displacements as a result of compaction grouting as well as the effects compaction grouting had on total stress, pore water pressure and pile bearing capacity are presented. The graphs incorporated in this chapter show the most important measurements parameters in time. A complete overview of all graphs, showing the readings of each monitoring tool individually in time, can be found in Achterbosch (2001).

6.7.2 Pile Displacement

The vertical pile displacements during compaction grouting, as monitored by the joint meters, are shown in Figure 6.21, Figure 6.22 and Figure 6.23. The figures are first discussed in broad outlines before they are more thoroughly analysed.

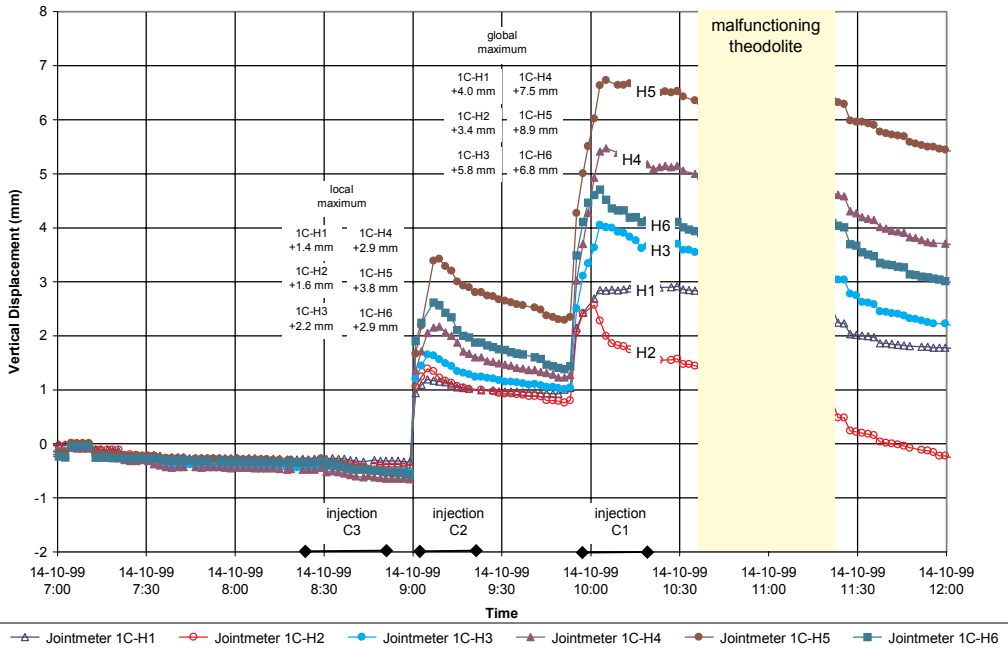


Figure 6.21 Displacement of the Piles During Grouting

From Figure 6.21 it can be seen that the displacements caused by the first injection (C3) are insignificant. The effect of the second injection (C2) is most significant on piles H5 (closest to C2) and H4 & H6 (adjoining pile H5). The displacements caused by the last injection (C1) caused the biggest pile heaves on all piles. Immediately after the last injection the piles start to settle. From Figure 6.22 it can be seen that the piles stopped settling on the 16th at around 12:00 hrs.

A problem when trying to analyse the consolidation effects of the compaction grouting, is that the contribution of each individual injection to the pile settlements cannot be recognized. Therefore, using the grouted volumes, the position of the *grouting centre of gravity* (as indicated in Figure 6.14) was calculated. This grouting centre of gravity is only used during the analyses to assess the influence of the distance between the grouting centre of gravity and the pile *after* grouting. During grouting each injection is looked at individually.

COMPACTION GROUTING

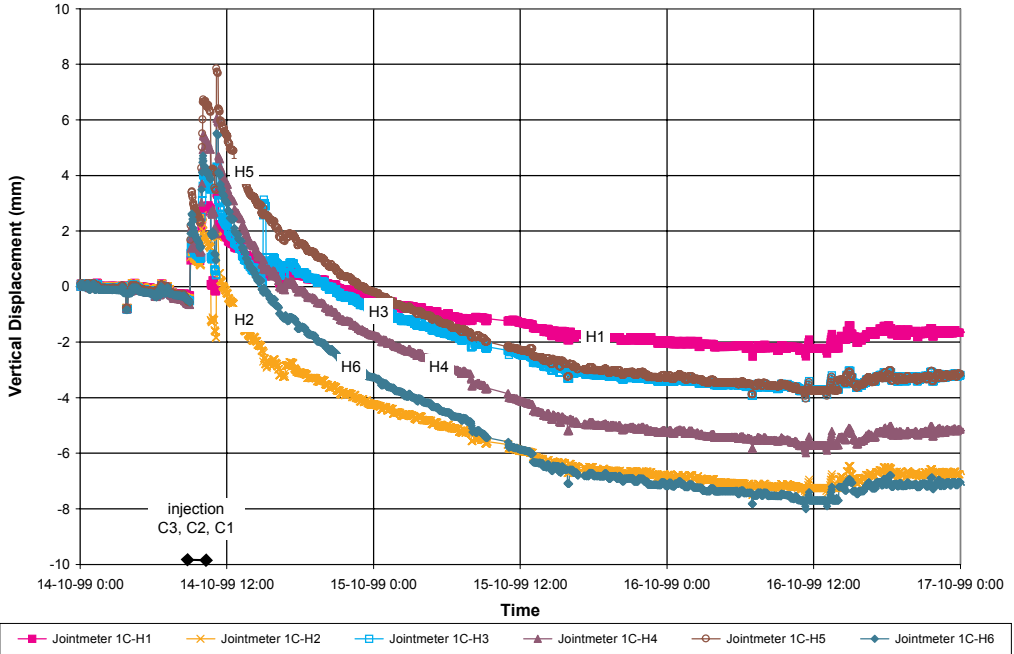


Figure 6.22 Vertical Displacements due to Grouting

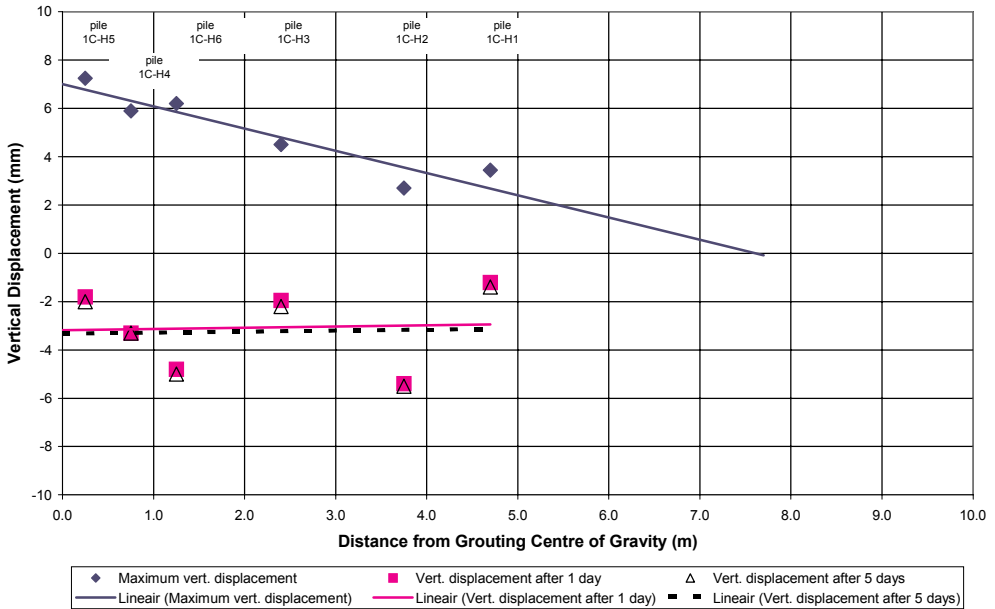


Figure 6.23 Displacement of the Piles in Relation to Distance from the Grouting Centre of Gravity

In Figure 6.23 the pile settlement as a function of the distance between the piles and the grouting centre of gravity and a linear average of these readings are shown. It is clear that after 5 days the pile settlements do not differ significantly from the pile settlements after 2 days. It can also be concluded

that, on average, the piles that are closest to the centre of gravity initially show the largest heave. The settlement below the initial readings is limited to 6 mm.

The vertical pile displacements caused by the first injection (C3) have been insignificant. The effect of the second injection (C2) and the last injection (C1) caused all piles to heave. Immediately after the last two injections the piles start to settle. On average, the piles that are closest to the grouting centre of gravity initially show the largest heave. After 5 days the pile settlements do not differ significantly from the pile settlements after 2 days and are limited to 6 mm. It is remarkable that pile H2 shows 8.5 mm settlement, although it is located at over 3.5 m distance from the grouting centre of gravity. The only possible explanation is that a grout fracture very locally disturbed the soil near the toe of this pile. This assumption may be conformed by the fact that the bearing capacity of this pile was reduced after grouting, although this could also have been caused by the fracturing that was performed under this pile (after the compaction grouting had finished, but before the pile load test).

When comparing the individual injections, it is obvious that the grout volume injected for the first injection (C3, $V=0.54\text{m}^3$) is about 3 to 5 times smaller than the grout volumes used during the second (C2, $V=1.88\text{m}^3$) and last (C1, $V=2.67\text{m}^3$) injection. Because the piles do not significantly heave during first injection C3 or settle directly afterwards, it was concluded that this injection did not contribute to the vertical pile displacements. Because the injection pressures during grouting C3 were the highest of all injections, there must have been significant compaction of the soil. This assumption that the soil is compacted due to the grouting is confirmed by estimating the ratio of the volume of soil heaved and the grouted volume. For injecting C3 this ratio would be infinitely large, because no soil was heaved. To estimate the overall result therefore the effect of the total grouted volume V_{grout} (5.1 m^3) and heave were used. The volume of the heave at pile toe level ($V_{heave} = \frac{1}{3} * \pi * 7.5^2 * 0.007 = 0.4\text{ m}^3$) is calculated using Figure 6.23, assuming ground heave is equal to pile heave and using the linear relation for the vertical displacement of the piles. The compaction ratio, defined here as V_{grout}/V_{heave} , then amounts to 12.4. Because it is expected that the soil is partly pushed between the piles (which is conformed by the calculations of soil heave in Section 6.7.3) the actual compaction ratio will be lower. However there can be no doubt that compaction does occur.

When comparing the test results with the results of the FEM calculation, it should be considered that no exact comparison can be made, because the FEM analysis was only used to get an *indication* of the possible grouting pressure, the soil displacements and the effective stress changes. The only conclusion that can therefore be drawn considering the pile displacements, is that the indicative FEM calculations also showed upward displacements above and next to the injection point. Although the displacements are of the same magnitude (5-10mm), the injected volumes are of a completely different order and therefore cannot be compared. The settlement that occurs after the grouting has finished was not found in the FEM calculations, which relates to the fact that no clay layers, but only a homogeneous sand layer was incorporated in the FEM model. prediction. The excess pore pressures induced by the grouting will not cause significant consolidation of this sand layer.

Considering the pile settlements after installation, it seems likely from the settlement pattern that consolidation effects have caused the pile settlements. Therefore, in the sub-section 6.7.4 the consolidation effects are more accurately looked at using the piezometer and SMS readings. First, in the next sub-section the surface displacements are examined.

6.7.3 Surface Displacements

From Figure 6.24 it can be recognized that the soil surface displacements, as measured by the surface levelling points, are analogous to the vertical pile displacements. During the grouting process the grouting rig temporarily interrupted the monitoring of the surface levelling points. However, although the effects of the individual injections cannot be determined precisely, the reaction of SB5 and ZB14 indicates that again the displacements caused by the last injection (C1) are most significant.

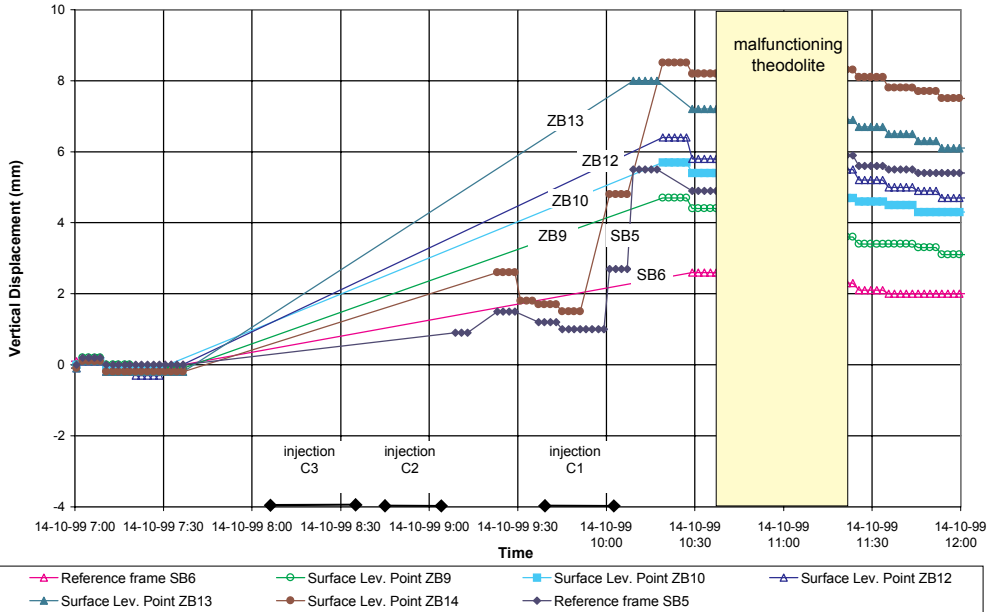


Figure 6.24 Surface Levelling Point during Grouting

From Figure 6.25 it can be seen that, again analogous to the vertical pile displacements and in accordance with the piezometer readings, about 2 days after compaction grouting the surface displacements have stabilized (16-10 12:00*). Here only half of the surface levelling points have settled more than they were lifted by the compaction grouting, the other half returned to their original level.

In Figure 6.26 the surface displacement as a function of the distance between the surface levelling points and the grouting centre of gravity and a linear average of these readings are shown. It can be concluded that, on average, the surface levelling points that are closest to the centre of gravity initially show the largest heave. The settlement below the initial readings is limited to 2 mm.

On average, the *surface levelling points* that are closest to the centre of gravity of the grouted body initially show the largest heave. As is the case of the vertical pile displacements and in accordance with the piezometer readings, about 2 days after compaction grouting the surface displacements have stabilized. They are limited to 2 mm.

Using Figure 6.26, the volume of the heave at surface level is calculated: $V_{heave} = \frac{1}{3} * \pi * 10^2 * 0.01 = 1.0 \text{ m}^3$. The compaction ratio, defined here as V_{grout} / V_{heave} , then amounts to 4.9. This is smaller than for the piles, which can be expected due to the larger distance from the grouting points.

* the jump just after 12:00 is caused by a monitoring error

COMPACTION GROUTING

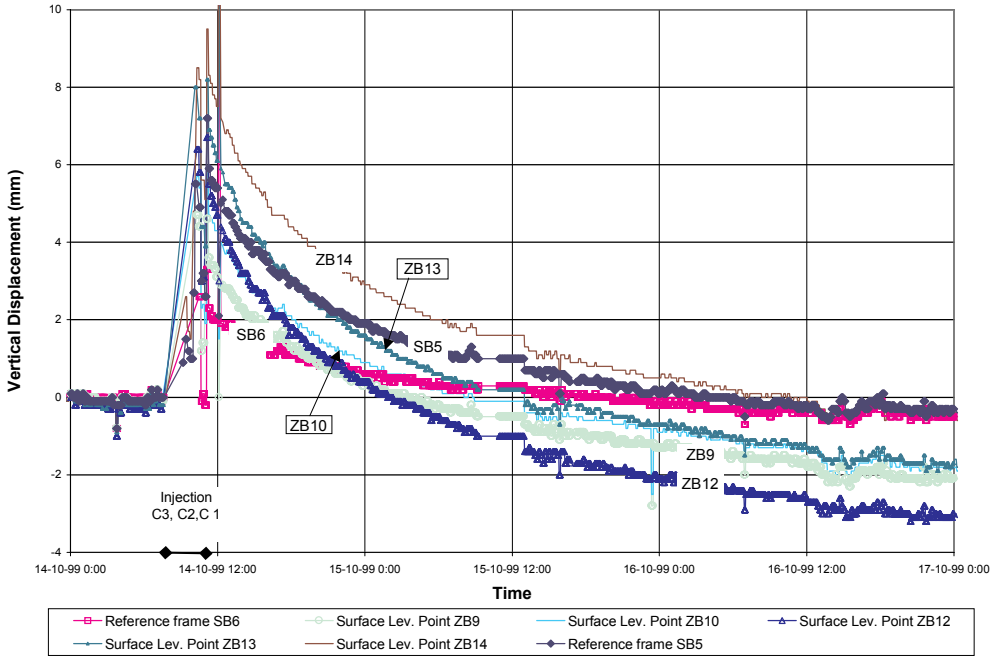


Figure 6.25 Surface Levelling Point during and 2.5 Days after Grouting

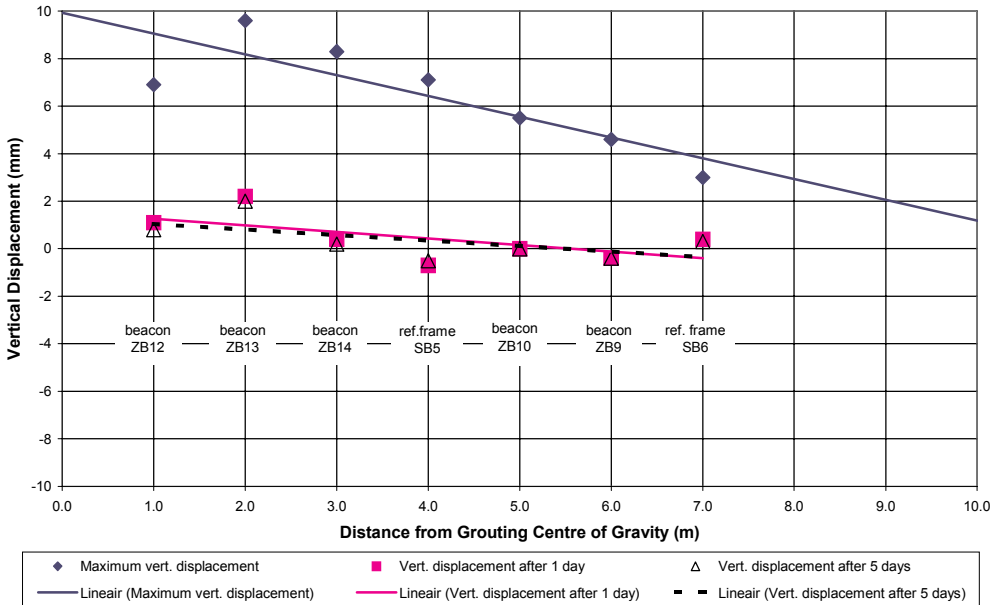


Figure 6.26 Surface Levelling Points: Maximum, after 1 Day and after 5 Days

6.7.4 Pore Water Pressure & Total Stress

The response of the piezometers during grouting is shown in Figure 6.27. It is clear that owing to the grouting the pore water pressures in the soil increase considerably. Usually it is the piezometer closest to the point of injection that gives the most significant reaction to the grouting. When the grouting starts the pressures show a sharp rise; when grouting stops the excess pore pressure quickly decreases in the sand layers (WM30,31) and slowly dissipates in the clay layers (WM13,15,16,17). The excess pore pressures had dissipated to 5% on the 16th around 12:00 (see Figure 6.28), which is the same time that the piles stopped settling.

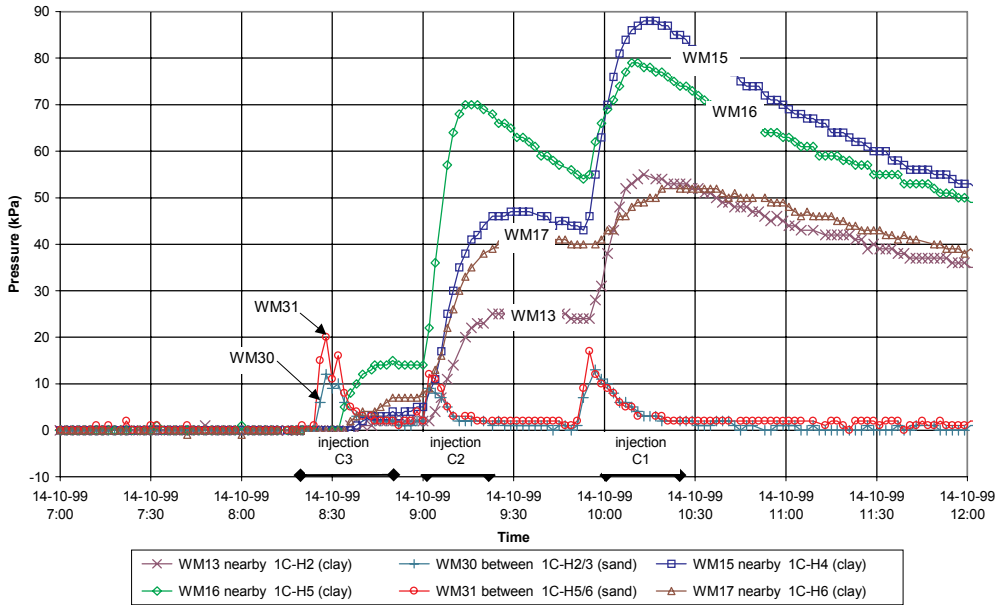


Figure 6.27 Piezometer Readings during Compaction Grouting

In Figure 6.29 the maximum pressure changes as a function of the distance between the injection point and the piezometer are given. Here, as in Figure 6.27, it is obvious that the pore water pressure changes caused by grouting C1 are the most significant.

There is no apparent relation between the increase in excess pore pressures and the grouting pressures. For instance, during grouting C3 the highest pumping pressure of the three injections was reached (4 MPa) whilst the response of the piezometers (at most +20kPa) was smallest. Figure 6.27 shows that the two piezometers in the sand demonstrate identical reactions to all three injections. The piezometers in the clay layer above the first sand layer, however, show a much more significant reaction to grouting C2 and C1. Considering the volumes of grout that were injected during grouting elements C2 and C1, this seems an indication that these piezometers reacted to compression of this clay layer, caused by the large volumes of grout that were injected during grouting C2 and C1.

To examine this assumption, indicative settlement calculations were made using Terzaghi's logarithmic settlement equation and the excess pore pressures in the clay layer during grouting. These calculations showed that the magnitude of the settlements of the clay layer agreed with the measured settlements. The calculations however did not explain why the piles ($s_{max}=6mm$) settled more than the surface ($s_{max}=2mm$). Apparently the pile settlement was not exclusively caused by consolidation of the clay layer. Local consolidation of the silty sand layer that is located under the pile toe must have also played a part in this process, causing the remaining 3-4mm settlement. Because of the limited thickness of the 1st sand layer and the large volumes of grout injected during grouting C2 and C1, this assumption of

COMPACTION GROUTING

local consolidation seems plausible. The fact that the bottom of the grouting tubes inadvertently had inadvertently been positioned 1 meter too deep, causing the grouted element to be located partially (for about 1 meter) in the silty sand layer under the first sand layer, may have also contributed to these settlements.

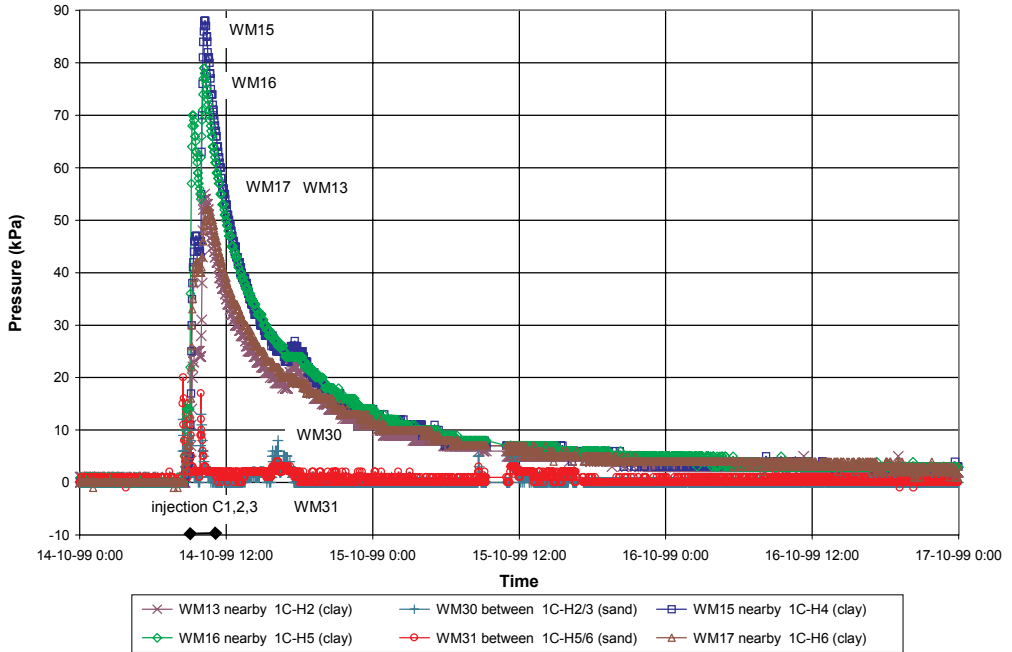


Figure 6.28 Piezometer Readings after Compaction Grouting

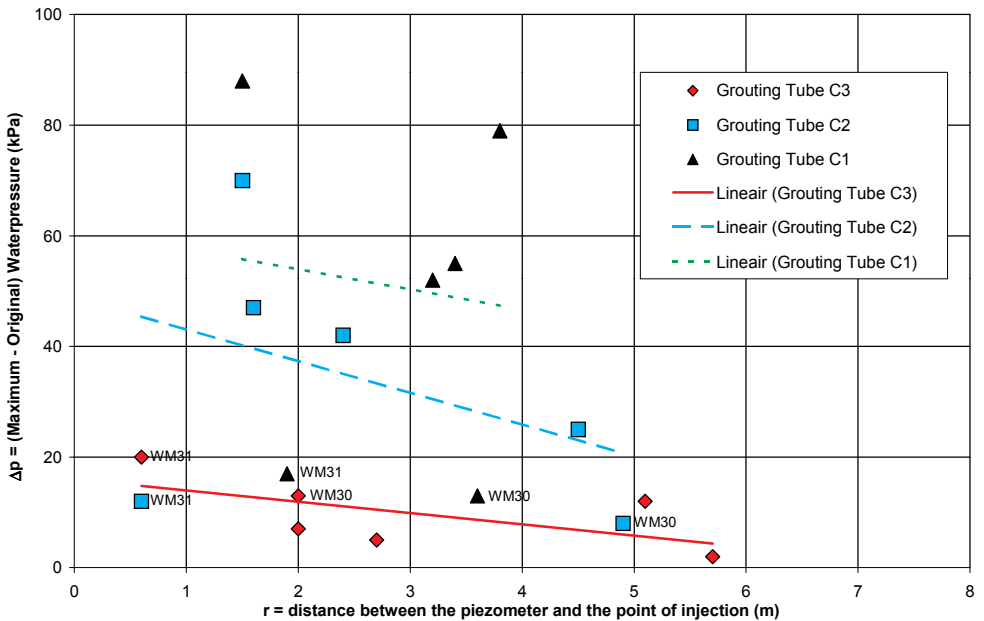


Figure 6.29 Maximum Piezometer Readings as a Function of Distance to the Point of Injection

COMPACTION GROUTING

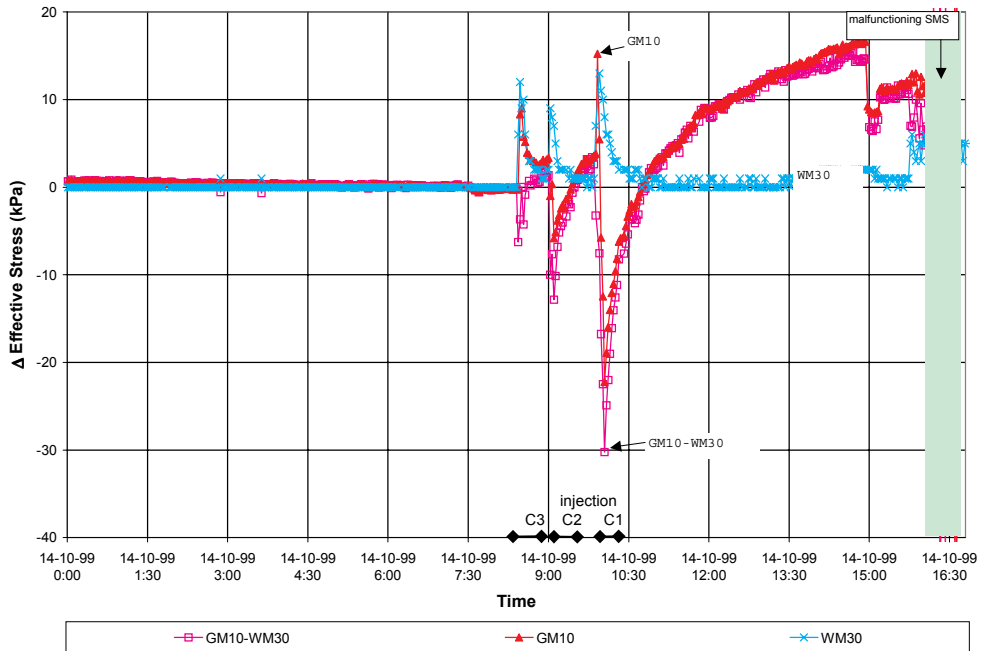


Figure 6.30 Reconstruction of the Horizontal Effective Stresses

Because *GM10* in pile H2 (see Figure 6.14) was the only properly functioning SMS, a reconstruction of the horizontal effective stresses could only be made using this SMS. Therefore the total stress changes measured by *GM10* were combined with excess pore pressures of the nearest piezometer in the sand layer (*WM30*) to reconstruct the effective stresses, as shown in Figure 6.30. From the readings it can be concluded that the influence of grouting on the horizontal effective stresses is small for first injection C3 (at circa 5.5 m) and small for second injection C2 (at circa 4.3 m). Third injection C1 (at circa 3 m), however, causes the horizontal effective decrease 25 kPa. It is likely that this decrease is caused by the uplift of the pile due to the grouting. As already concluded in 6.7.2, pile H2 shows divergent settlement which is probably caused by a grout fracture. Just after grouting the effective stresses start increasing. In the afternoon the effective stress rise has increased to 15 kPa, after which the SMS started malfunctioning (for unknown reasons) No readings were obtained after that.

The effective stresses could only be deduced from the readings of one SMS and therefore no hard conclusions can be drawn from these readings. The reduction of the effective stress for this particular pile seems logical, considering 3.5 m distance from the grouting centre of gravity and the heave of the pile.

When the readings are compared with the FEM predictions in Section 6.4.2 it can be concluded that the horizontal radius of the influence of the grouting proved to be smaller in the test than in the FEM model, even though the injected volumes were much bigger than those modelled in the FEM calculations. A possible explanation might be the absence of the soft soil layers in the FEM model.

6.7.5 CPTs

After compaction grouting, 9 CPTs were conducted near piles H4, H5 and H6 to monitor the effect of the compaction grouting on the cone resistance q_c . In Figure 6.31 the locations of the CPTs are shown. It should be noted that the exact positions of the CPTs might not be those indicated on the drawing, because inadvertently no CPT inclination measurements were made.

In Table 6.6 the average and maximum CPT values before and after compaction grouting are shown, to investigate whether the cone resistance had increased, as Scherer and Gay (see Section 6.3) had found*. The average CPT value was calculated over the top 1.5 m of the 1st sand layer, because for some CPTs no data was available at a deeper level. CPTs 5 and 6 were not conducted. CPTs 4 and 8 had to be stopped before reaching the full depth because the cone resistance increased to the maximum allowable value. This was probably because the cone hit a grout element.

Because the piles had already been removed when the CPTs were conducted, for the CPTs 1,2,3,7 and 9 only CPT values *below* pile toe level have been compared. It can be seen that most maximum CPT values have fallen by between 10% and 20%, while it was anticipated that compaction grouting would increase the effective stresses. However, the average CPT values over the top 1.5 m of the first sand layer show no significant change. Moreover, because CPTs 1-4 were located at a significant distance from the reference CPT, the differences between the CPTs taken at different locations of the test site are of the same magnitude and because a different type of cone was used for the CPTs after grouting, the only conclusion that can be drawn is that the CPT values have not changed significantly.

Because after grouting most CPTs were located a significant distance from the reference CPT, the differences between the reference CPTs taken at different locations on the test site are of the same magnitude as the differences before and after grouting. Moreover, because a different type of cone was used for the CPTs after grouting, the only conclusion that can be drawn is that the CPT values have not changed significantly.

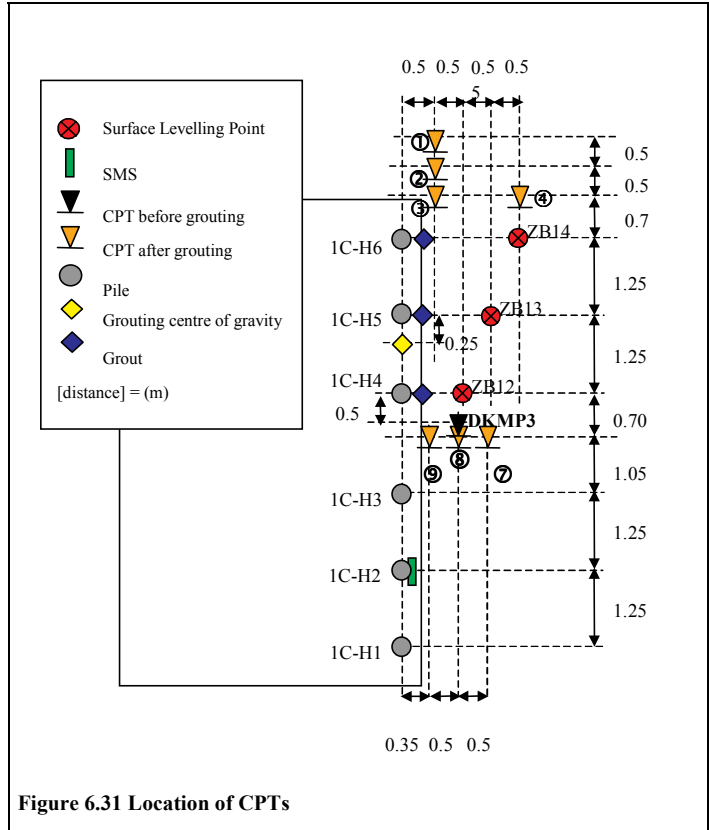


Figure 6.31 Location of CPTs

* although Scherer and Gay examined loose, liquefiable sands

COMPACTION GROUTING

Table 6.6 Maximum CPT Values Before and After Compaction Grouting

CPT carried out:	Before Grouting	After Grouting							
CPT id# (-)	DKMP3	9	8*	7		3	2	1	4*
nearest grouted element (-)	C1	C1	C1	C1		C3	C3	C3	C3
nearest pile (-)	1C-H4	1C-H4	1C-H4	1C-H4		1C-H6	1C-H6	1C-H6	1C-H6
distance between pile and grouting point (m)	1.0	0.8	1.1	1.5		0.9	1.3	1.8	2.1
level top 1 st sand layer (m NAP)	-12.8	-13.0	NA	-12.7		-12.8	-12.8	-12.6	NA
level bottom 1 st sand layer (m NAP)	-15.8	NA	NA	NA		-15.8	-16.0	-16.0	NA
level $q_{c,max}$ (m NAP)	-14.2	-14.8	-11.4*	-14.1		-14.5	-14.6	-14.2	-11.8*
$q_{c,max}$ (MPa)	36	38	>100*	29		30	29	32	>100*
Average q_c %	100	101	-	98		99	97	102	-
$\delta q_{c,max}$ (MPa)	-	+2	-	-7		-6	-7	-4	-

6.7.6 Bearing Capacity

The bearing capacity of the three* wooden piles was determined both before and after compaction grouting. The results of these pile load tests are shown in A.Figure 32 to A.Figure 35 in APPENDIX X. As an example the test for pile H6 is shown in Figure 6.32.

Comparisons between tests #1 and #2 (before) and test #5 (after)[†] lead to the following conclusions:

1. the load-settlement behaviour of all piles is significantly stiffer than it was before grouting;
2. after grouting the ultimate bearing capacity of piles H4, H5 and H6 changed by +19%, an unknown % and +35% respectively; test #5 on pile H5 was stopped prematurely (-6.5 mm at 180 kN), so no increase of F_{ubc} could be recorded, although it most probably exceeded +50%.

The most important conclusion that can be drawn from the tests is that the bearing capacity of piles H5 and H6 has considerably increased (at least +35%).

Assuming that the increase of 35% in the bearing capacity of grouted pile H6 is only caused by injection C3, this is another indication of compaction of the soil occurring. Although both other piles also showed a significant increase in bearing capacity, the undesirable large pile displacements caused by the large grout volumes during the creating of their grout elements annul this positive effect.

* Piles 1C-H1, H2 and H3 were also influenced by the fracturing which was performed after the compaction grouting and are therefore not included in this analysis; the bearing capacity of these piles however did not change significantly

[†] Test #3 and Test #4 were not conducted on the 3C piles

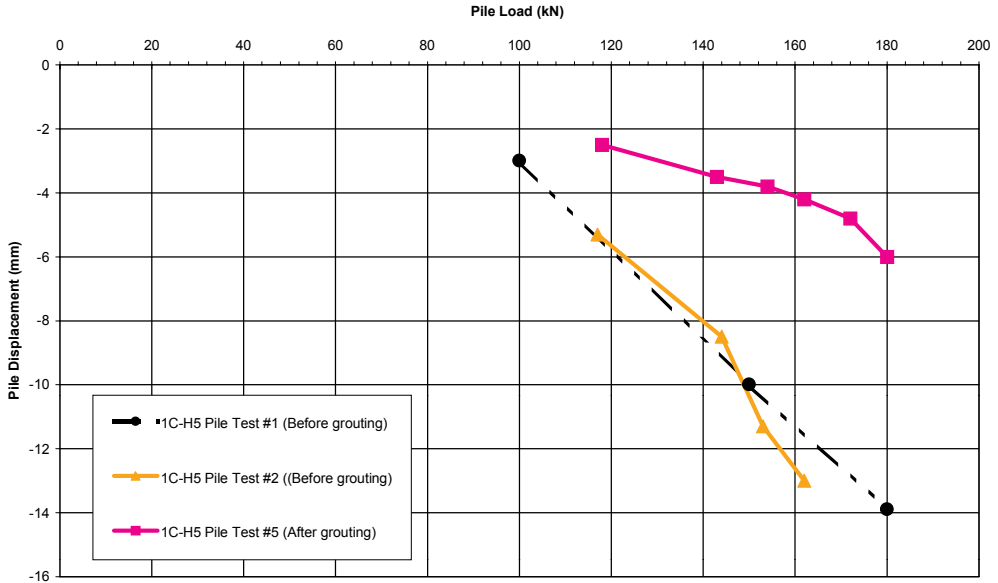


Figure 6.32 Example of Pile Load Test: Wooden Pile 1C-H5

6.8 Conclusions

The models used to make predictions for the maximum grouting pressure to be used during the Amsterdam compaction grouting test are useful in that they provide insight into the compaction grouting mechanisms. However, they proved to be sensitive to the parameters used and to the assumptions concerning the homogeneity or isotropy of the material. The predictions made by using these models have been compared with limits from grouting practice (See Figure 6.7). At 12 m depth or deeper, the practical limits for the maximum grouting pressure are much lower than the values that are considered possible theoretically.

In addition to the use of the formulae and the practical limits, PLAXIS was used to make 2-dimensional indicative FEM calculations. The FEM analysis was only used to provide an *indication* of the maximum possible grouting pressure, the soil displacements and the effective stress changes. The conclusions that can be drawn are that the indicative FEM calculations underestimated the possible grouting pressure which, based on the limitations of the model, could be expected.

Compared to the test results, the FEM calculations also showed upward displacements above and next to the injection point. Although the injected volumes were much bigger than those modelled the radius of the horizontal influence of the grouting proved to be smaller in the test than in the model. A possible explanation for this might be the absence of the soft soil layers in the model.

Based on the predictions, it was decided that a compaction grouting pressure limit of 2.5 MPa should be maintained at the injection point, which considering friction loss in the system, amounts to a pressure limit of 4.0 MPa at the pump. During grouting of the elements in the test this maximum pressure was not exceeded and was sufficient to prevent blowouts.

The principle on which the desired effect of compaction grouting for foundation renovation is based, is that the soil is compacted by injecting the grout a little below and next to the 4D-8D area of the pile. This should lead to an increase in cone resistance and effective stresses near the pile toe and therefore to

an increased bearing capacity of the pile. The pile may also be lifted several millimetres, which is not necessarily desirable.

During the test, compaction grouting subsequently caused the piles to heave (+3.4 mm to +7.5 mm) and settle (1.5 mm to -5.5 mm). The soil surface displacements were analogous to the vertical pile displacements. Generally the points closest to the injection point showed the largest displacement. It was concluded that the heave of the piles was caused by the large volumes of grout that were injected; the settlements were a result of the consolidation of two different soil layers.

In the first place, the clay layer above the 1st sand layer consolidated. Indicative settlement calculations showed that the magnitude of the settlement of this layer was the same as the measured settlement at the surface, but only contributed to 1/3 of the pile settlement.

In the second place, the remaining 2/3 of the pile settlement was caused by local consolidation of the silty sand layer located under the pile toe that was caused by the limited thickness of 1st sand layer and the large volumes of grout injected. The fact that the bottom of the grouting tubes had been inadvertently positioned too deeply may also have contributed to these settlements. Correct installation would still have caused some local consolidation under the pile toes, but the effects of this would have been more limited.

During grouting the pore water pressures in the soil increased considerably; the piezometer closest to the point of injection gives the most significant reaction to the grouting. No apparent relation between the increase in excess pore pressures and the grouting pressures was found. Excess pore pressures had dissipated to 5% after circa 1 day, which was the time that the piles stopped settling.

The assumption the compaction of the soil is caused by the grouting was confirmed by calculations of the *compaction ratio*: the ratio between the volume of soil heaved and the grouted volume. Because calculations indicated that the soil is partly pushed between the piles, the actual compaction ratio of the soil at pile toe level will be lower than the ratio calculated based on pile heave.

The most important conclusion that could be drawn from the test is that compaction grouting near a pile toe can considerably (at least 35%) increase the bearing capacity, which agrees with the calculations of the compaction ratio. Moreover, the load-settlement behaviour of all piles significantly stiffened. For one of the piles the bearing capacity increased 35% without any significant pile displacements as a result of the grouting. Therefore it seems plausible that compaction grouting can be an effective method for foundation renovation.

6.9 Recommendations and Future Perspective

The most important recommendations that follow from these tests are that the volume of the grouted element should be carefully controlled and that it is necessary to ensure that the installation procedure is accurate. Moreover, for piles at 12m depth, the grouted volume should be injected at approximately 0.5 m horizontally from the pile toe and vertically within the 4D-8D area of the pile. The diameter of the grouted element should not exceed 0.6 m (assuming a cylindrical shape) and the grouting pressures should not exceed 2.5 MPa at the injection point. These measures should be complied with to prevent the settlement that may occur as a result of the consolidation of the cohesive layers above and below the bearing stratum (1st sand layer).

Because the small space between the piles complicated observation of the effects of each injection individually, it is recommended that to permit observation of consolidation phenomena more research should be carried out with piles at a greater distance from each other and more time between individual injections. A larger number of piles, different types of grout and grouted elements at varying distances should help to optimise this method.

Chapter 7 GROUTING VERIFICATION METHODS

7.1 Introduction

The position and shape of a grouted element plays a very important role in its effectiveness. A major concern when using grouting is the fact that a reliable verification of the exact position and shape of the grouted element is still difficult to obtain. This is a result of the depth of the grouted element or of a small working site. Because grouting, and especially jet grouting, cannot be controlled precisely, quality control is essential. During the last ten years many efforts have been made to develop detection systems to determine the position and geometry of grouted material. The position is often determined by using inclinometer measurements. The geometry for all grouting methods can be determined by using *geophysical detection methods*, of which there are various types. In this chapter the basic principles will be explained of geophysical detection methods using:

- electrical resistance;
- electromagnetism;
- acoustics;
- borehole radar (BHR).

For jet grouting, *umbrella* measurements and *hydrophone* measurements can also be used.

The applicability of these methods as a verification tool for determining the position and shape of grouted elements is discussed using the results of the Full Scale Injection Test. Amongst the aspects considered are: the aim of the test, characterisation of the electrical resistance and BHR measurement equipment used, the monitoring program and the results of the test program. To conclude this chapter some future prospects for using geophysical detection systems for grouting verification purposes are given.

It was decided that for the Full Scale Test the resolution of the position measurements should be smaller than 0.01 m, the resolution for the geometry measurements should be smaller than 0.10 m.

7.2 Determining the Position of a Grouted Element

The position of a grouted element should always be measured in two ways (see also Section 5.2.8). First the position where either the TAM or the jet-grouting rod enters the soil is recorded, for example by using a total station. After the determination of the x , y , z position, the horizontal inclination of the axis of the grouted element can be determined at regular intervals from the top to the bottom by using an inclinometer.

For permeation grouting and compensation grouting the position of the TAMs can be determined by using a regular inclinometer and an inclinometer casing that is temporarily positioned in the TAM. Special attention should be paid to the orientation of the guide grooves in the inclinometer casing.

The same inclinometer system can be used for jet grouting (Stein, 2000), but as an alternative the optical systems may be used. These systems, of which one called Minibore was also used at the Full Scale Injection Test, measure the bending of the measuring rods in the borehole or jet grouting string (www.reflex.se).

The disadvantage of the above mentioned inclinometer systems is that they determine the position of the jet grouting string (or TAM) after drilling (or installing). When the position proves to be incorrect, there is no alternative but reinstallation, which has considerable time and cost consequences. Research has been conducted on the use of gyroscopes and infrared connections to permit online measurement of the inclination (Evers, 2000).

7.3 Determining the Geometry of a Grouted Element

Umbrella measurements or *spider measurements* have been successfully used in jet grouted sand layers, but no successful results have been obtained in jet grouted cohesive soil. The measurements are performed by lowering a steel device resembling an inverse umbrella in the centre of a not yet hardened jet grouting column. Depending on the type of umbrella, one or more arms are used. The arms can be manually or hydraulically extended until they reach the interface between grouted and virgin soil. A device on the surface records the extension of the arms and thus the column diameter.

The principle of the *electrical resistance method* is based on measurements of the resistance levels in the soil. This resistance level is measured by using electrodes located at regular intervals* that alternately inject a current into the ground or measure the potential difference. When electrodes at varying distances from each other are used the penetration of the current changes and an image of the specific resistance as a function of the penetration depth are obtained. The interface between grouted soil and virgin soil is shown by a change in this specific resistance. The geometry of the grouted element can be determined from this change. By decreasing the distance between the electrodes the resolution can be increased, although simultaneously the penetration depth is reduced.

The *electromagnetic method* uses transmitting spools to introduce circular currents in the soil. The electrical resistance of the soil influences the magnitude of the circular currents and the secondary magnetic field that is introduced. By measuring the strength of the secondary field using receiving spools the geometry of the grouted element can be measured. The transmitting and receiving spools are combined in a probe that can be lowered down a drilled log in the hardened element.

Borehole radar (BHR) is a non-destructive geophysical electromagnetic (EM) method for subsurface mapping. The method is based on the propagation of EM waves in the subsurface. The principle of a BHR measurement is based on measuring the travel time of an EM wave between radiation, reflection and reception. The measured travel time multiplied by the propagation velocity of the EM wave in the medium represents the distance between the antennas and the reflector.

The BHR principle can be applied for geometrical mapping of grouted elements. A transmitter radar antenna is placed in the centre of the element and radiates an EM wave. This EM wave propagates through the grout and is reflected at the interface of grouted soil and virgin soil. The reflected wave is received by a receiver radar antenna that is fixed above the transmitter antenna. The measured travel time of the EM wave is then converted to an element diameter. Measurements at different depths provide the geometry of the element.

Acoustic reflection is based on the measurement of acoustic signals transmitted by a vibrator in the drilling log. Reflection of this signal will occur at the interface zone of grouted soil and virgin soil and is detected by acoustic recorders in the same log. Using the propagation speed and the reflection time of these signals the position of the transition can be determined.

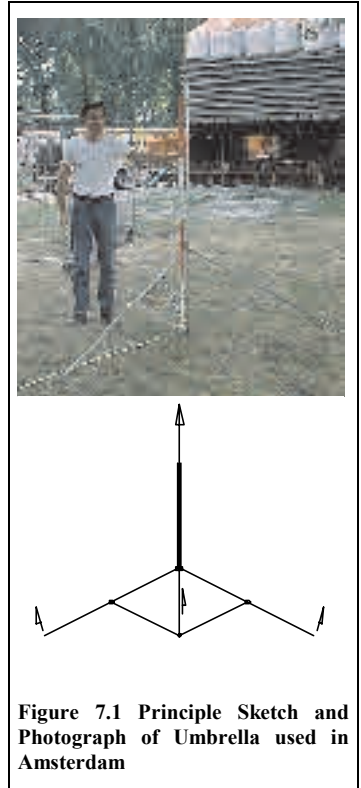


Figure 7.1 Principle Sketch and Photograph of Umbrella used in Amsterdam

* integrated on a TAM or in a separate cable attached to the TAM

Acoustic tomography is also based on measurement of acoustic signals transmitted by a vibrator in the drilling log, but now the reflection is detected by acoustic recorders in a different log. The position of the vibrator is varied and for each recorder the reflection time is recorded. The position of the transition zone is determined from the variations in propagation speed of the signals.

A special application of the acoustic tomography method is the *Hydrophone* method (Jörger, 2000). This method uses a water-filled steel pipe (\varnothing 40mm) in which a hydrophone is maintained at jet grouting monitor depth (within 200 mm of each other). When the cutting jet passes the hydrophone, the jet signal is converted into an analogue electrical signal. The waveform of the signal is used to estimate the column diameter. By using an array of hydrophones at varying radial distances from the drill rod, the geometry of the grouted columns can be constructed. This system requires the verticality of both the jet grouted column as the steel pipes to be known exactly and requires the installation of multiple pipes and hydrophones for each column. Interpretation of the results requires some experience. The hydrophone measurements were not considered applicable for the measuring the jet grout columns of Full Scale Injection Test because of the large depth of these columns.

7.4 Results of the Full Scale Injection Test

7.4.1 General

Because the grouted elements needed for pile foundation improvement in general, and for the Noord/Zuidlijn project in particular, need to be created at great depth (i.e. 10 m to 30 m below ground surface), verification of their position and geometry by means of excavation would be impractical and moreover lead to high costs. For this reason in Stage 1 of the Full Scale Injection Test research was conducted to select suitable geophysical detection methods for determining the geometry of permeation grouting elements. In Stage 2 suitable methods from Stage 1 and BHR were used in Amsterdam soil to make large-scale measurements of permeation grouting bodies. In Stage 3 these methods were used to measure the geometry of jet grouted columns.

7.4.2 Stage 1: Determining Suitable Geophysical Detection Methods

In a shallow building pit in Utrecht (where excavation was required in any case), electrical resistance, electromagnetic and acoustic tomography & transmission measurements* were used to measure the geometry of four different permeation-grouting bodies. These bodies had a designed diameter of 1m and were circa 4m high and were created at a shallow depth (Figure 7.2). The TAMs for the electrical resistance method were equipped with special rings to measure the electrical resistance. For the other methods special large diameter (\varnothing 67 mm) TAMs were used, so a probe could be lowered inside the TAM. After the measurements had been conducted the grouted elements

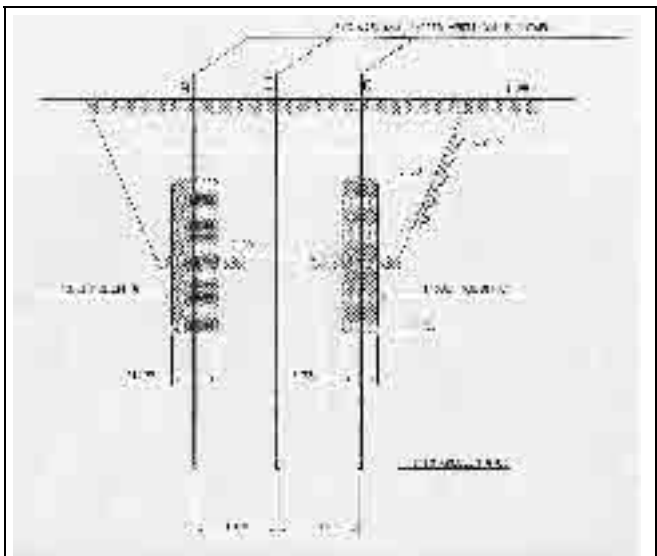


Figure 7.2 Test Set-up Stage 1

* Bore Hole Radar was not used, because an antenna which could reach the desired measurement resolution, would only fit into a Tube à Manchette with a 200 mm inner-diameter, which was bigger than that used TAM diameter (\varnothing 67mm).

were excavated and their shapes were measured.

The results of the test (Hopman, Van der Stoel & V. Dalssen, 1999) showed, that when the electrical resistance method was used the geometry of the grouted element could be determined with satisfactory (<0.10 m) accuracy (Figure 7.3 left). The electromagnetic method showed usable information concerning the shape, but inaccurate information concerning the diameter. Line A and line C in Figure 7.3 (right) represent the maximum and minimum measured diameter. Evaluation of the results was conducted by comparing the results of the geophysical measurements with measurements from excavation of the elements.

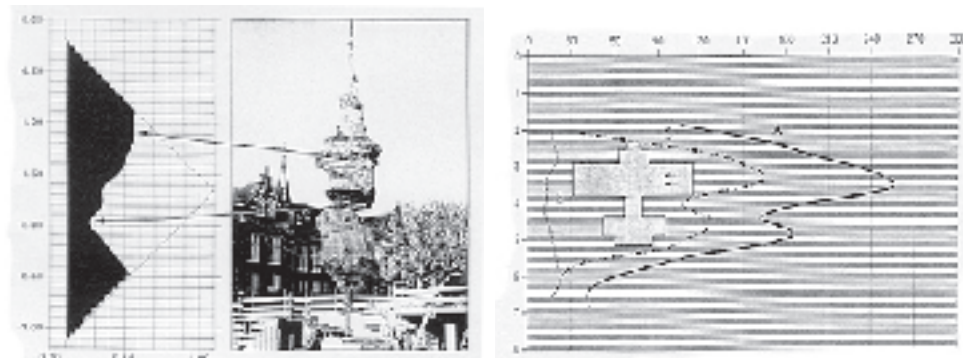


Figure 7.3 Results of Electrical Resistance (left) Electromagnetic Measurements (right)

Because both methods only present a 2D, axial-symmetric image of the body, they are somewhat limited. Regrettably comparison of the electrical resistance method and the electromagnetic method could not be conducted. Because the steel rings and cables of the electrical resistance method disturb the electromagnetic method no grouted body could be measured y using both methods.

7.4.3 Stage 2: Measuring the Geometry of Permeation Grouting Bodies

Based on the results of Stage 1, the electrical resistance method was used in stage 2 to obtain an impression of the shape of the grouted elements. During Stage 1 it was found that attaching the steel rings for the electrical resistance method was a very labour-intensive process. Therefore, in Stage 2 a specially prepared cable was used, which was attached to the TAM. During the preparation of Stage 2, the ground radar applications developing company T&A Radar claimed that they had developed a BHR system that was able to enter a Ø 67-mm TAM, without violating the measurement resolution restriction ($\leq 0.11\text{m}$). Based upon tests conducted elsewhere with this BHR system, it was decided to incorporate it in Stage 2. Figure 4.12 on page 54 shows the test set-up of Stage 2.

An example of the *electrical resistance measurement* is shown in Figure 7.4. The solid line represents the minimum diameter, the dotted line represents the maximum

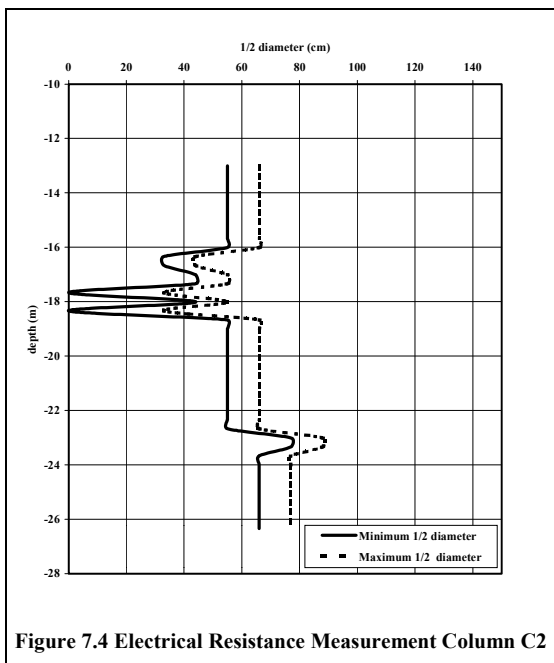


Figure 7.4 Electrical Resistance Measurement Column C2

diameter. The resolution is 0.11m and when the diameter was smaller than 0,33 m it could not be measured. All measured columns show one or more grooves between NAP -15 and NAP -19 m, where the silty Intermediate layer is found. This corresponded to the expectations of poor groutability for this layer. The good groutability of the 2nd sand layer was confirmed by the absence of irregularities in measured column diameter.

The shape of the other columns was measured by using the *BHR* and in principle it should have been the same, since the same type of injection fluid was used in what should have been identical soil. The BHR measurements show a diameter of the columns similar to that measured when using the electrical resistance measurement, however no discontinuities were visible there. The reason for this dissimilarity is not evident, but most probably is something to do with the low contrast between the grouted soil and the virgin soil.

7.4.4 Stage 3: Measuring the Geometry of Jet Grouted Columns

In Stage 3 of the Full Scale Injection Test the geometry of four jet grouted columns was measured by using electrical resistance measurements and BHR. Although an effort was also made to use umbrella measurements to measure the column diameter, these did not succeed because the cohesive soil prevented an effective use of the umbrella. Figure 5.15 on page 83 shows the test set-up of stage 3.

For the *electrical resistance measurements*, first calibration measurements were taken in the virgin soil. After these measurements, columns A and D were measured by inserting PVC tubing into the fresh grout and lowering measuring equipment in this tube. Column A was measured 4 hours after grouting (up to 8,5 m deep) and measured again after 11 days. A typical increase in the resistance of column A after hardening could be noted (0,5-7 Ω m before, 40-60 Ω m after). Column D was measured 12 hours after grouting, after re-drilling a log in the centre hole of the jet grouted column. A specially developed finite difference numerical (iterative calculation) program was used for data interpretation. This program compares the calibration measurements with the measurements obtained after grouting. Figure 7.6 and Figure 7.7 show the interpreted diameters of columns A and D respectively.

For the *BHR measurements* conducted at the Full Scale Injection Test, modified equipment was used. The standard system consists of a radar system that maps the subsurface between two boreholes. This cross-hole survey BHR configuration uses the transmitter and receiver antenna in separate boreholes. For mapping the jet grouted column geometry this configuration was not considered useful, so a single-hole measurements using a two-dimensional BHR system, which applies both the antennas in the same borehole, was developed by T&A Radar. For this purpose system modifications were required with respect to radiated antenna power, electronic circuit of the antenna, antenna power supply, antenna cabling and antenna housing.

The BHR survey was conducted in six fresh jet grouted columns and in two hardened columns. The “fresh measurements” were conducted immediately after the production of the column by connecting the antenna housing in which both the radar antennas are fixed onto the jet-grouting rod. The antennas were lowered as deeply as possible into the centre of the fresh grout column. Because of the relatively short curing time of the grout, it was not possible to measure an entire column at once, but only the top 10 to 20 meters. Attempts were made to map one entire column by jetting the column in three stages and conducting BHR measurements after each stage. Unfortunately this did not succeed for the deepest stage (NAP -25 m to NAP -35 m).

To obtain samples from the columns, 35 m long, cores were taken by drilling and sampling (Section 5.6). In two hardened columns measurements were conducted by manually lowering the radar antennas in the boreholes thus created. The main disadvantage of this type of measurement is that a borehole must be specially created for this purpose. In this case another disadvantage was that the boreholes in the cured columns were not central, so the interpreted column diameter from the BHR measurements underestimates the real diameter.

Figure 7.5 shows a characteristic processed image of BHR measurement in a jet grouted column. The depth is shown on the vertical axis, the travel time of the radar signal on the horizontal axes. The dotted line marks the event that represents a change in the received radar signal caused by the presence of the antennas inside the column. Without a priori information this is interpreted as transition from the grouted column to the virgin soil. Measurements were conducted in columns A, B, C, D, X1 and X2. The interpreted diameters of these columns are shown in Figure 7.6 through Figure 7.11. The distance from the antennae to the reflector, interpreted as column diameter is shown on the vertical axis, the depth on the horizontal axis.

After all measurements had been conducted the top 4.5 meters of jet grouted columns A, B, C, D, X1 and X2 were carefully excavated. In Section 5.11 the results of the excavation can be found. The measurements of the column geometry are incorporated in Figure 7.6 to Figure 7.11.

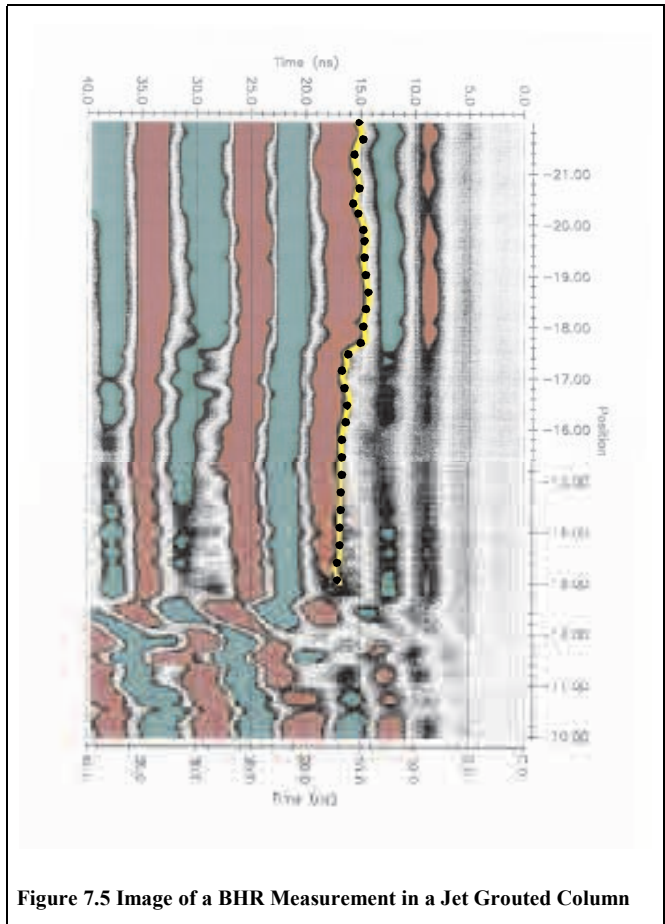


Figure 7.5 Image of a BHR Measurement in a Jet Grouted Column

The electrical resistance measurement gives satisfactory results for column A; the results for column D, however, do not fit the excavation curve (overestimation). The ‘dip’ in the D curve at NAP –4m remains unexplained.

In five of the jet grouted columns the BHR underestimates the column diameter by between 20 cm and 100 cm. Only with column D is the diameter overestimated. The height of the column can easily be mapped, because the transition grout-soil at the top column is marked by a clear signal anomaly in BHR data.

The deviations in diameter can be explained by a number of factors. Firstly, the geophysical conditions inside a grouted column are hard material (conductive soil, conductive grout, BHR measurements below the water table, slight geophysical contrast between grout and virgin soil) but not too hard, because the received signal does show events due to grout presence. Secondly there are several hypotheses for the underestimation of the column diameter, for example, the irregular column geometry (not a perfect cylinder but a rough shaped column) and the necessarily decentralised BHR measurements. For column B, as an example, a correction was made for a 20 cm eccentricity of the borehole (assuming the minimum diameter was measured), as shown in Figure 7.8. This correction led to a much better result for the hardened jet grouted column.

GROUTING VERIFICATION METHODS

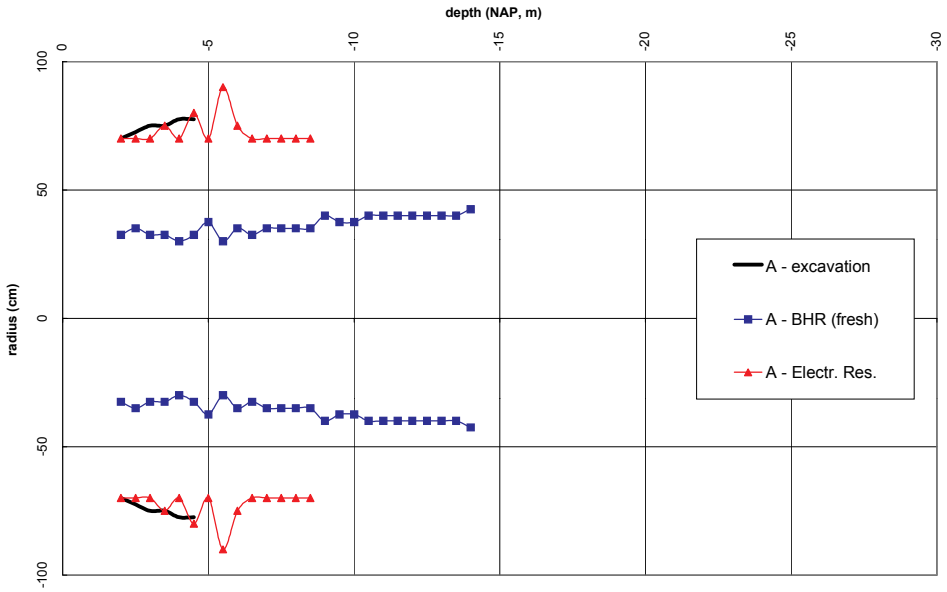


Figure 7.6 Interpreted Electrical Resistance Measurement and BHR Measurements Column A

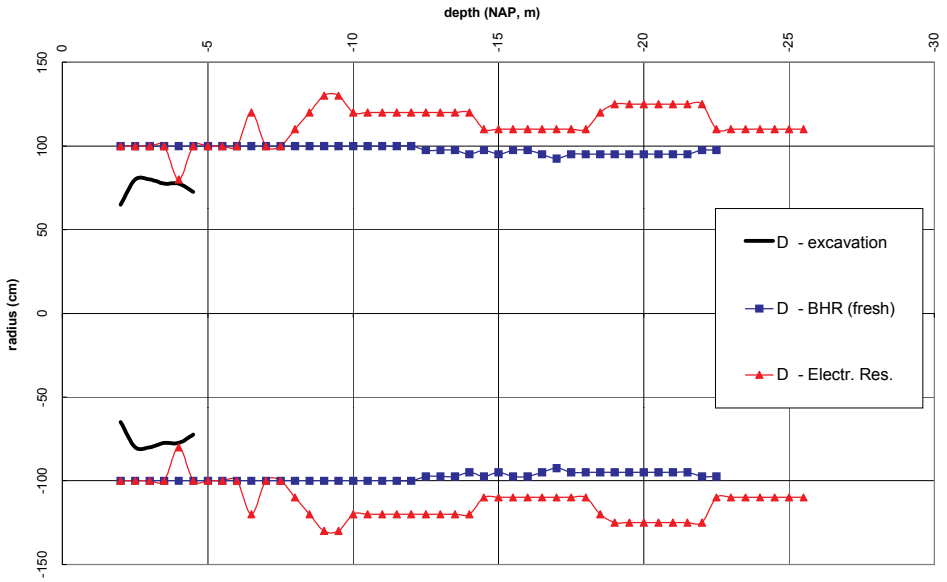


Figure 7.7 Interpreted Electrical Resistance Measurement and BHR Measurements Column D

GROUTING VERIFICATION METHODS

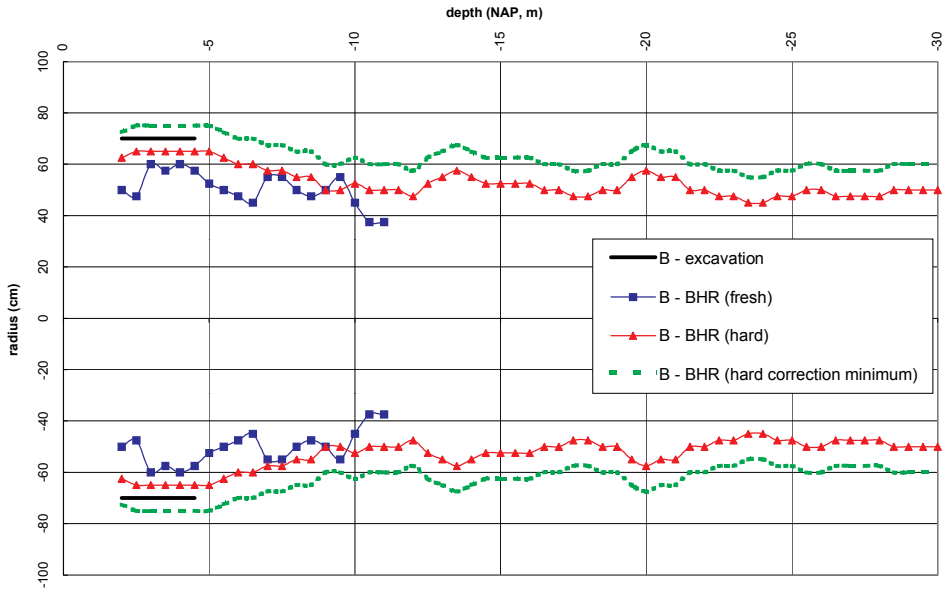


Figure 7.8 Interpreted BHR Measurements Column B

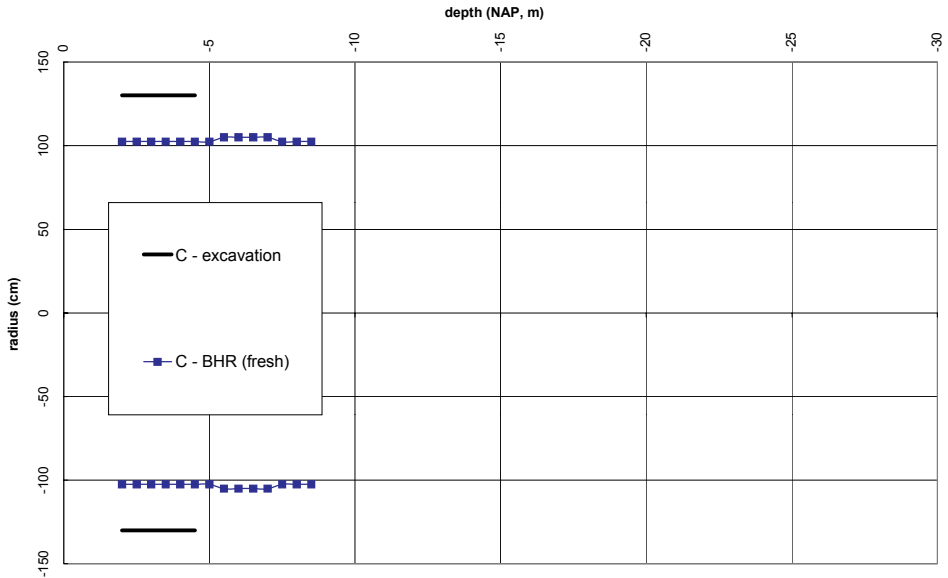


Figure 7.9 Interpreted BHR Measurements Column C

GROUTING VERIFICATION METHODS

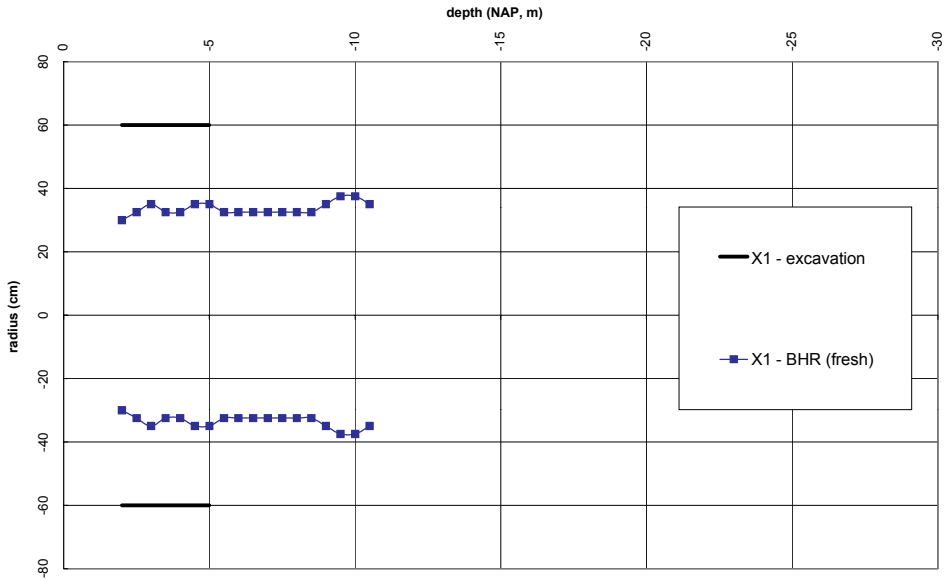


Figure 7.10 Interpreted BHR Measurements Column X1

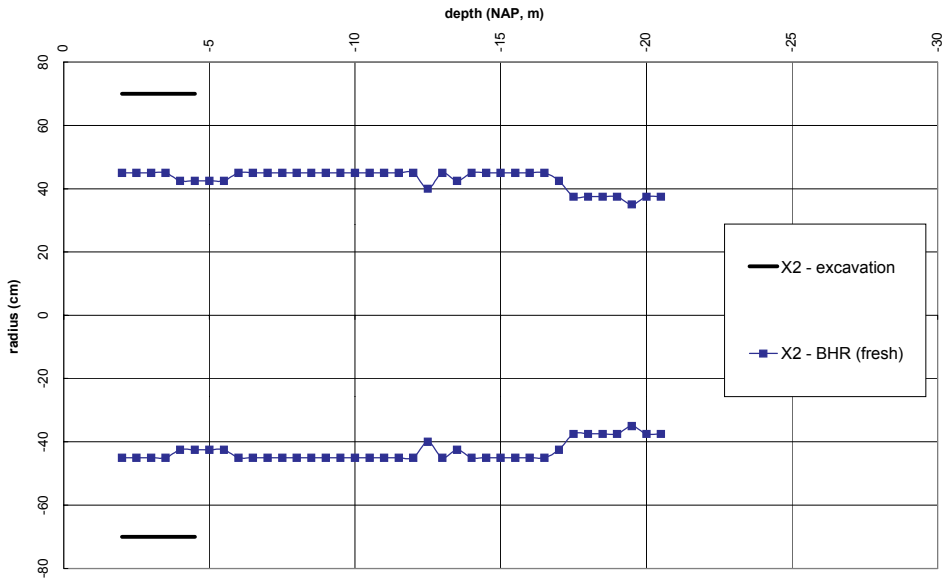


Figure 7.11 Interpreted BHR Measurements Column X2

7.5 Conclusions

In general, the results of electrical resistance measurement seem to be in fair accordance with the geometry of the grouted elements. The method however has disadvantages because of its limited applicability. The use of cables in permeation grouting applications is very costly. The use of PVC pipes in the fresh, jet grouted columns is restricted in depth and moreover, the best measurement results are obtained in a hardened column. This limits the possible use of this method as an active monitoring tool during jet grouting.

BHR measurements in permeation grouting applications are not considered feasible because of the poor contrast between the grouted material and virgin soil. BHR measurements in jet grouting columns show events in the data that provide evidence for grout presence in the subsurface, especially in the hardened grout columns. Verification of BHR measurements by comparison with the excavated column geometry generally resulted in an underestimation of the actual column diameter, which could be explained by a number of factors.

7.6 Future Perspective

It is strongly recommended that the electrical resistance method should be developed to provide a real time system for the verification of permeation grouting.

From discussion with T&A Radar it was concluded that the future of grouting verification lies in the development of real time BHR, inclinometer measurements and wireless communications. The following recommendations for hardware and software include:

- Modification of the BHR signal shape to a single pulse, which would lead to a much clearer definition of the transition between virgin soil and grouted soil (*hardware*).
- The use of a directional radar signal so that 3-dimensional measurements can be conducted instead of 2-dimensional measurements. In this way local irregularities can be detected (*hardware*).
- Applying a wireless connection (infrared) between antenna and inclinometer and the data acquisition system (*hardware*). This should be used in combination with automated interpretation of the acquired data (*software*) so that a real time image of the results can be obtained without the necessity for a specialist radar interpretation permitting jet grouting parameters to be instantly adjusted.

The modifications of the BHR, directional radar signals and interpretation software are currently being developed.

Chapter 8 SUITABILITY OF GROUTING FOR FOUNDATION IMPROVEMENT

8.1 Introduction

As discussed in Chapter 2, foundation *improvement* is a generic term that is used to define both the renovation and the preservation of foundations. In the specific case when settlements have been caused by overloading, foundation renovation implies increasing the bearing capacity of a pile foundation that has insufficient bearing capacity. In the case of foundation protection, the focus is on safeguarding the piles of the foundation against possible damage resulting from underground construction activities in the vicinity.

In the previous three chapters, the influence exerted by grouting on pile foundations has been discussed, taking into consideration the results of a test that was conducted in typical Amsterdam soil conditions. This chapter presents a more general discussion of the findings of the previous chapters in relation to the suitability of permeation grouting, jet grouting and compaction grouting for the purpose of foundation improvement. In the first section of this chapter, therefore, some general considerations regarding the influence of the test set-up on the results are given. To get a broader idea of the possible uses of grouting techniques for pile foundation improvement, the technical implications of the test results, the practical aspects and cost aspects will be discussed for each of the techniques under consideration. A distinction has been made between two typical types of structure. The *Historic Structure* represents structures like canal-side houses and old bridges, which will be renovated individually and which are positioned in such a way that working space will be limited. *Social Housing* represents mass production housing from the first half of the 20th century. Here the buildings will be renovated in groups. These buildings are easily accessible and there will be sufficient working space available.

8.2 Considerations Regarding the Influence of the Test Set-Up

Before the more general applicability of the results of the Full Scale Injection Test can be assessed, it is necessary to consider the influence of the test set-up and the typical Amsterdam soil conditions of the test.

The most important point of departure for the test was that the soft, stratified soil and end-bearing foundation pile conditions typical of Amsterdam had to apply. Because all the grouting methods used in the test change the properties of the soil at pile toe level, the most important factor to consider in other projects is that the piles on which grouting may be applied must be designed as **end bearing piles**. The material of the pile is less important; the mechanisms observed in the test may concern wooden, steel or concrete piles.

For all the grouting methods the settlement that occurred during the installation process should be considered with some restraint. Throughout the tests the jacks **maintained the working load** on all the piles, so the redistribution of loads was kept to a minimum. Vertical pile displacement as a function of time was obtained at constant load, thus being entirely dependent upon the injection process. This was important in the determination of the influence of the grouting process itself (eliminating other effects). During the test, settlement occurred as a result of the installation of the TAMs (permeation grouting), bringing the monitor to depth (jet grouting) and installation of the tubes (compaction grouting). As a result of the constant working load, these settlements give an overestimate of settlements that may occur during installation activities in other projects in which it may be assumed that some redistribution of loads will occur.

The **redistribution of loads** plays an important role in the designing of foundation improvements. Whether there will be a redistribution of loads when grouting is used in foundation improvement depends on the proximity of nearby piles and the stiffness and strength of the structure. When the adjacent piles are close enough, a pile that temporarily loses part of its bearing capacity owing to the grouting will redistribute part of its load. It is therefore very important, that piles that are located close

to each another should not be treated simultaneously. Where possible a primary/secondary sequence should be used: a pile next to another pile that has already been grouted should only be grouted when the grout near the first pile has hardened.

8.3 Using Permeation Grouting for Foundation Improvement

In Chapter 4 it was concluded that when installing permeation grouting TAMs using an uncased, rotary flush boring process, there is small (<1%) risk that a pile at a distance of 2m or closer will settle more than 2.5 mm when it is maintained under a constant working load. The pile reactions resulting from the actual grouting process were insignificant. When permeation grouting is used close to or at pile toe level, the bearing capacity and stiffness of the piles can be considerably (about 35%) increased. The piles in the test showed no signs of settlement due to consolidation effects and, since it is more likely that the grouted material will expand than that it will shrink, permeation grouting is considered a very suitable method for improvement of pile foundations.

The test results also showed that when the grouted element is located close to the pile and more elements are grouted near the piles, the positive effect on the bearing capacity increases considerably. This, in combination with the fact that when foundation improvement may be conducted the exact location of the foundation piles is often not available, promotes the use of grouting elements of at least 1 meter diameter at pile toe level.

It should be noted that it is only necessary to grout the piles that cause settlement problems. Usually these piles are located at the front or facade of the structure and thus easily accessible (see Section 2.1). When piles at the rear side of the structure also have to be grouted, accessibility problems start to play a role. When piles under the bearing wall, in the middle of the structure have to be grouted, problems may occur because of the necessary drilling inclination and the necessity to drill between the piles of the facade.

In Figure 8.1 a schematic presentation of a typical Amsterdam structure in which piles under the front (façade and about ¼ length of constructive walls) are treated by using permeation grouting is shown.

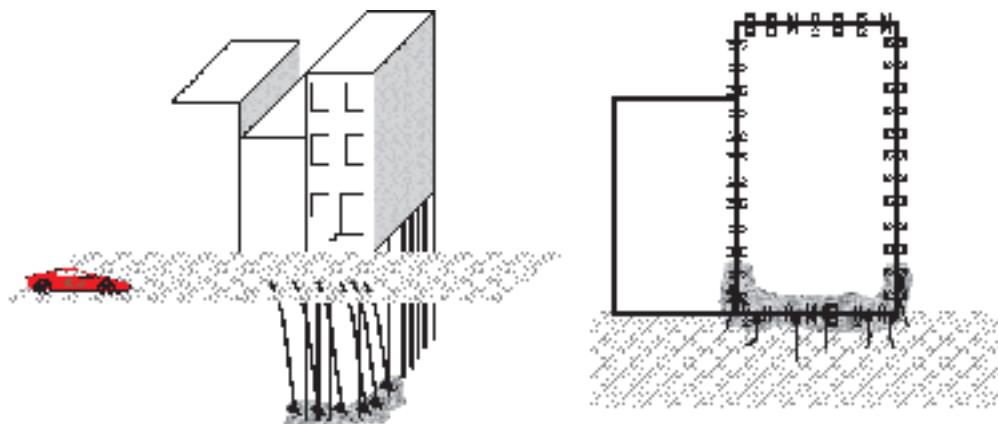


Figure 8.1 Schematic Presentation of Permeation Grouting Wooden Pile Foundation (Façade Only)

Figure 8.3 shows a similar solution for grouting all foundation piles (façade, back wall and both constructive walls) using permeation grouting.

When the depth of the permeation grouting treatment does not exceed 15 meters, relatively lightweight material can be used to install either TAMs or single injection points (Figure 8.2). Because the injection points can be installed from the outside, the working height usually is unlimited.

The single injection point is connected to a grout pump using a HDPE hose and is pushed down the bored hole by using a spring. The spring can be retrieved when the required depth has been reached. Because there are barbs on the injection point it will stay at the correct depth.

Special attention should be paid to the difference between load settlement behaviour in grouted and non-grouted piles that may occur as a result of the grouting. Because usually only a part of the structure suffers from inadequate pile bearing capacity, only this part of the structure has to be grouted. Based on the stiffness characteristics of the grouted piles obtained from the test, and considering the possibility of redistribution of loads to the non-grouted piles (that are considered to be in a good condition), no significant problems are expected to occur. To prevent problems concerning the difference in the load settlement behaviour of grouted and non-grouted piles, all the pile toes can be grouted. This is obviously more expensive, but there may be an additional advantage if the structure will react more stiffly to settlement induced by underground construction activities, like TBM tunnelling.

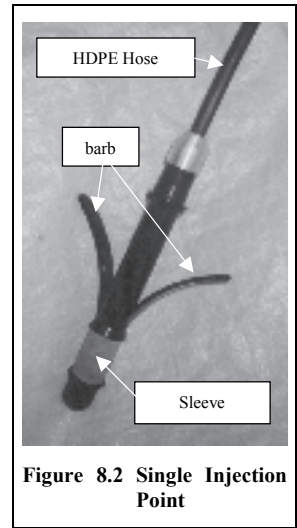


Figure 8.2 Single Injection Point

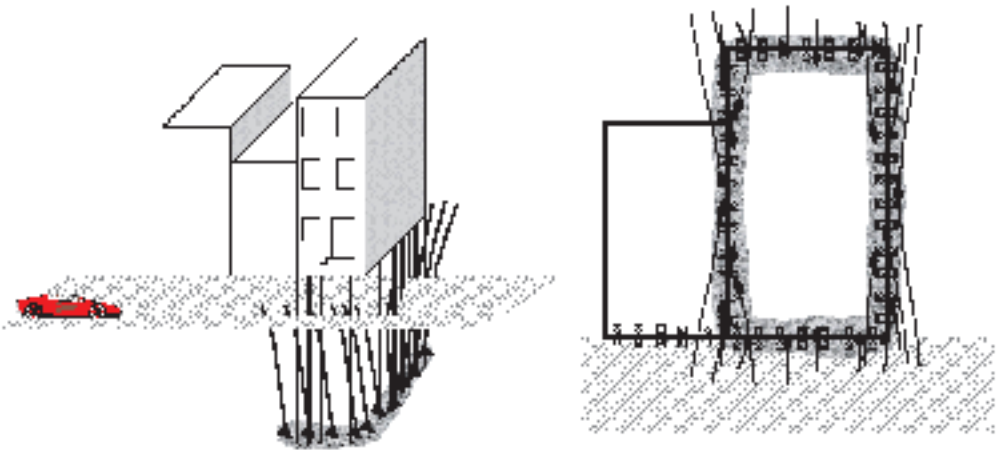


Figure 8.3 Schematic Presentation of Permeation Grouting Wooden Pile Foundation (Whole Structure)

A major advantage of permeation grouting, in comparison to conventional foundation improvement techniques, is that the **hindrance** of permeation grouting is much less. The grouted elements can be constructed from outside the structure, so the occupants do not have to be evacuated. Moreover, the level of noise pollution is kept to a minimum and access to the structure can easily be maintained. There will however be some hindrance to traffic in the street outside the structure, and possibly some services may have to be protected or diverted.

The **cost** of permeation grouting mainly depends on the total volume of soil to that has to be treated and the depth of foundation pile toes. Because grouting at a single level will usually be sufficient, a single injection point is the most cost efficient solution. Cost estimates, using cost indexes for small and large grouting projects, have indicated that the cost for permeation grouting (circa 0.7 m³ grouted soil per meter) for renovating the foundation of a historic structure lie between €15.000 and €25.000. The cost for permeation grouting for renovating the foundation of social housing lie between €5.000 and €10.000.

8.4 Using Jet Grouting for Foundation Improvement

The test results, dealt with in Chapter 5, indicate that the possibilities of using jet grouting for foundation renovation purposes are limited. Jet grouting under wooden piles did only significantly change the bearing capacity of one of the three piles. Based on the results of grouting under the concrete piles however, it is expected that jet grouting under wooden piles, when performed properly, should increase their bearing capacity. Since two of the three grouted columns caused significant pile displacements, jet grouting might then only be applied when the structure is so stiff that all pile loads can be redistributed.

Jet grouting under concrete piles also caused large pile displacements with sustained loading. Reducing the load to 80% of the working load showed that the pile displacements could be stopped and when the pile was fully reloaded 24 hours later, no additional displacements occurred. This indicated that for piles with considerable positive skin friction, grouting under the toe is feasible when load redistribution is possible.

Jet grouting for foundation protection, at 0.5 m or further from piles, caused settlement that did not exceed 1-2 mm for each grouted column. At this 0.5 m or further, neither the distance between the pile and the jet grouted column nor the column diameter seemed to influence the pile displacement, and consolidation effects did not seem to lead to additional settlement of the pile. After grouting, the piles initially exhibited a stiffer reaction and the ultimate bearing capacity did not significantly change (about 10% higher than before grouting). This indicates that jet grouting for foundation protection (see Figure 2.17 on page 19) is a suitable method.

If grouting is used the difference in load settlement behaviour that may occur as a result of the grouting plays a very important role. When jet grouting is applied to create pile extensions, the jet grouted piles, which are made of a different material than that used for the original piles, will be encased in grout and located in a deeper layer and hence their load settlement behaviour will also be different. Usually the piles with a jet-grouted extension will exhibit significantly stiffer load-settlement behaviour, because the grout is much stiffer than the soil. Because of the large difference in stiffness this is expected to give problems. Van Tol (1999) gives more general information on the interaction between existing and newly added piles.

Jet grouting causes significantly more environmental **hindrance** than permeation grouting or compaction grouting, because of the spoil production, the noise of the jet grouting rig and pumps and the risk and consequences of a blow-out. When the piles to be extended are located under the outer wall of the structure the grouted elements can be constructed from outside the structure. In this case, the hindrance caused by the jet grouting will be less than that caused by conventional foundation improvement techniques. There will also be hindrance in the street outside the structure, and possibly some service facilities may have to be protected or diverted. When piles inside the structure also have to be extended, the hindrance is comparable to that of conventional foundation improvement techniques.

The **cost** of jet grouting mainly depends on the total volume of soil to be treated, which in turn determines the grout volume and spoil volume. Using cost indexes for small and large grouting projects as a rough estimate, the cost per m³ of jet grouted soil varies from € 400 for large volumes of soil (>100m³) to be treated to € 1200 for small volumes of soil (<20m³) to be treated. The influence of the mobilization and demobilization costs makes jet grouting for smaller projects relatively unattractive in comparison to the other grouting methods. For instance, creating 10 pile extensions with a length of 10 m and a diameter of 0.5 m, requires the treatment of circa 20 m³ of soil at total cost of € 24.000.

The main advantage of jet grouting over permeation grouting and compaction grouting is that it can be used in any type of soil. This makes the jet grouting method suitable for the creation of new foundation piles, of piles under shallow foundations (Droof et al, 1995; Maertens, 1999) or of pile extensions for friction piles.

This method is only suitable for the creation of pile extensions for end bearing piles when the structure is strong and stiff enough to redistribute the loads from the grouted pile.

8.5 Using Compaction Grouting for Foundation Improvement

Compaction grouting will be most effective in thick sand layers with low cone resistance, because the level of compaction is then highest. Although the 1st sand layer in Amsterdam is only about 2 meters thick and the cone resistance is high (10-30 MPa), the most important conclusion drawn in Chapter 6 is that compaction grouting near a pile toe can considerably (up to 35%) increase the bearing capacity of a pile. The settlement that resulted from consolidation effects that occurred after the grouting led to the recommendation that the volume of the grouted element should be carefully controlled. Furthermore injections should be horizontally located at approximately 0.5 m from the pile toe and vertically within the 4D-8D area of the pile.

An example of how compaction grouting can be used under the façade of a typical Amsterdam structure is given in Figure 8.4.

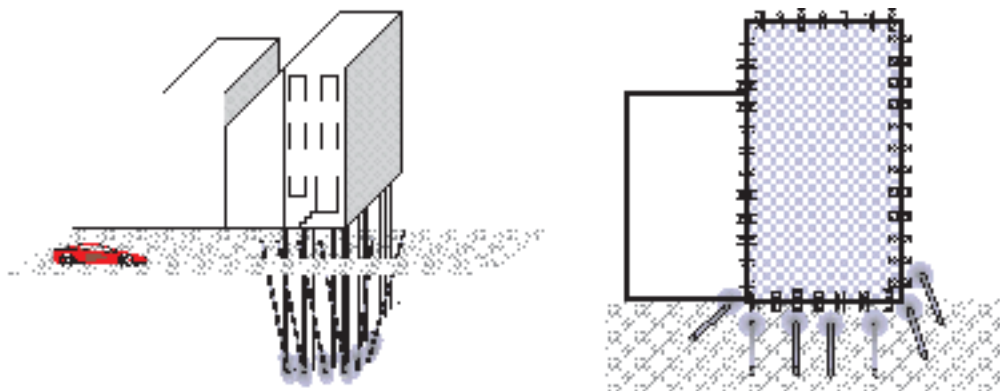


Figure 8.4 Example of Compaction Grouting used on a Typical Amsterdam Structure

There are many similarities between the use of compaction grouting and permeation grouting for foundation improvement. As with permeation grouting, special attention should be paid to the differences in load settlement behaviour that may occur as a result of the grouting. Because the grouted elements can be constructed from outside the structure the hindrance during the grouting procedure is also much less than that caused when using conventional foundation improvement.

The most significant difference is that for compaction grouting, after grouting tubes that have been used have to be withdrawn from the soil. This requires that a tube “pulling device” (usually the drilling rig) should be present during the whole grouting operation. Moreover, drilling the larger diameter compaction grouting tubes is slightly more difficult than installing injection point. When the working space is somewhat limited this can make compaction grouting more complicated and invasive than permeation grouting. If the drilling rig has to be present throughout the grouting operation, this will considerably increase the costs. However, it should be relatively simple to develop a “pulling device” to replace the drilling rig and this would considerably decrease the cost of the method. There will also be more obstruction on the street outside the structure because the pulling device is present throughout the operations and possibly also some service facilities will also have to be protected or diverted.

Other ways in which the process differs from that of permeation grouting are that it is very important that the grouted volume is controlled and that displacements of the grouted structure are monitored. These factors make compaction grouting more expensive than permeation grouting. Cost estimations that have been made, using cost indexes for small and large grouting projects, indicate that the cost for compaction grouting a historic structure (using 0.5 grout m³/m) lie between €20.000 and €30.000. The cost for compaction grouting social housing lie between €10.000 and €20.000.

8.6 Economic Feasibility of Grouting for Foundation Improvement

When comparing the costs of underpinning by using permeation grouting and compaction grouting with those of conventional underpinning methods, it can be concluded that a considerable reduction in costs and hindrance can be achieved by using the grouting methods. The total cost of the method is defined here as the sum of the construction cost and the economic damage.

The construction cost of grouting can be up to about 50% lower than the construction cost of conventional methods of underpinning a structure (€ 17.500 - € 35.000). Moreover, the hindrance due to grouting is marginal compared to the hindrance caused by conventional underpinning methods, thus the economic damage will also be significantly less. In Table 8.1 an attempt is made to quantify the economic damage, caused by the hindrance, for a structure with a commercial function (store, shop) or a residential function. For the commercial structure, the damage shown in the table is based on criteria of total stop in turnover for 2 months. For the residential function the damage is based on the provision of alternative housing and additional costs of moving and rehousing the residents for a period of 2 months. The obstruction of the street and services due to building activities during permeation grouting and compaction grouting is estimated for a 2-week period and is considered independent of the function of the structure.

Table 8.1 Indicative Economic Damage (€)

<i>Foundation Improvement Method</i>	<i>Historic Structure</i> individual restoration difficult to access	<i>Social Housing</i> mass production easy to access
<i>Conventional Underpinning</i>		
Commercial Function (per 50m ²)	32500	17500
Residential Function (per 100m ²)	3500	1500
<i>Permeation grouting</i>		
Obstruction Street/Services	750	250
<i>Compaction grouting</i>		
Obstruction Street/Services	1500	500

For structures with a commercial function, and more specifically for historical structures with a commercial function like shops in the city centre, the economic damage due to conventional underpinning can be enormous. In fact, in that case the cost of economic damage will be about equal to the construction costs of conventional underpinning.

8.7 Conclusions

Permeation grouting and compaction grouting can be useful and effective alternatives to conventional underpinning methods for renovating pile foundations. The methods may also be used for foundation protection. Jet grouting is suitable as an alternative method for creating foundation piles or for pile extensions for friction piles, but only suitable for use in the renovation of end bearing piles when the structure is strong and stiff enough to redistribute the loads from the grouted pile. Jet grouting is also very suitable to protect foundations, because it can be applied in any type of soil and at small distances from the existing foundations.

Considering the stiffness characteristics of the permeation and compaction grouted piles obtained from the test and also the possibility of the redistribution of loads to the non-grouted piles, no significant problems are expected to occur arising from the difference between the load settlement behaviour of grouted and non-grouted piles.

The construction cost of grouting can be up to about 50% lower than the construction cost of conventional methods of underpinning a structure (€ 17.500 - € 35.000). For structures with a commercial function, the conclusion is that when grouting for foundation renovation, the total cost, including economic damage, amount to 30% - 65% of the cost of conventional underpinning. For structures with a residential function, the total grouting cost amount to 50% - 80% of the cost of conventional underpinning. The effect of including economic damage for structures with a residential function is only marginal (<5%).

Finally, it is necessary to consider that grouting for foundation improvement and conventional underpinning are not fully comparable. In the first place, when making the cost calculations for the grouting methods, no economy of scale affects could be included, because the method is not yet used on a large scale. In the second place, conventional underpinning results in an entirely new foundation structure (piles and floor), whilst underpinning using grouting only reinforces the existing foundation structure. Therefore conventional underpinning certainly has added value over grouting for foundation improvement. However, when both may be applied, it is doubtful whether the cost of underpinning justifies this added value.

Chapter 9 CONCLUSIONS & FUTURE PERSPECTIVE

9.1 General

In some cases the differential settlement of structures is such that measures have to be taken to combat the effects of settlement. Moreover, in the event of later underground construction, the bearing capacity of the pile foundations of nearby structures can be negatively influenced, which calls for similar measures. The measures that have to be taken generally involve restoring the bearing capacity of the foundation. Before this restoration can take place, a foundation investigation program should be performed to carefully examine all possible causes of damage and then, by using the appropriate damage detection methods, to find the sources of the most serious damage.

Up till now foundation improvement has usually been done by using conventional foundation renovation methods to install additional foundation piles. Because these methods imply execution from inside the structure, causing significant hindrance and economic damage, the aim of this research has been to examine the use of grouting methods for pile foundation improvement.

9.2 Conclusions

Regarding the improvement of pile foundations, a distinction was made between foundation renovation (increasing the bearing capacity of a pile foundation that has insufficient bearing capacity) and foundation protection (safeguarding the piles of the foundation against possible damage resulting from underground construction activities in the vicinity). Analysis of the test results showed that permeation grouting and compaction grouting are suitable to be used for pile foundation renovation; jet grouting was only found to be suitable under certain conditions. For pile foundation protection both permeation grouting and jet grouting can be used.

Foundation improvement by means of grouting techniques can generally be executed from outside the structure and avoids the need to shore up the structure. However this application did evoke questions regarding the response of the foundation piles to the installation and grouting process, thus further research was considered to be necessary.

Existing theories used in modelling the grouting process have been examined and compared for all three grouting methods. Some efforts have also been made to use FEM analysis to increase understanding of the grouting process. It could be generally concluded that all grouting techniques, and especially jet grouting, are so complex that modelling serves only to increase understanding of the process. The existing models are not designed for use in engineering practice.

Because of the limitations of modelling, it was found necessary to perform a full-scale test in Amsterdam. The influence of grouting on pile foundations could then be examined by using the pile displacements, soil stresses, pore pressures and pile bearing capacity measured in this test.

When considering the use of grouting for pile foundation improvement purposes, the concern that may arise is that pile settlement can occur when installing the TAM/tube or positioning the jet grouting monitor close to the toes of the existing foundation piles. To isolate the effect of grouting from other effects, the pile loads were kept at a constant level during the test. However, when grouting is used for pile foundation renovation purposes, the load of the pile thus treated will be redistributed to the other piles. Therefore the pile settlements that result from this test form the upper limit of the settlements that will actually occur when grouting for pile foundation improvement.

There are many similarities between the processes of installing the permeation grouting TAMs or compaction grouting tubes and of drilling the jet grouting monitor to depth. Only insignificant changes in water and soil pressures occur during installation. Regarding pile displacements, there are only significant installation effects when the minimum distance between the TAM/tube/monitor and a wooden pile is less than 0.5 m.

CONCLUSIONS & FUTURE PERSPECTIVE

From the permeation groutability test it could be concluded that the applicability limits after Tausch (1985) for permeation grouting using a silica gel, have proved fairly correct for the Amsterdam situation. There was no clear difference in injection pressure applied in the different soil layers for any of the grouts used in the tests. The influence of grouting on pile displacements, total stresses and pore water pressures during the actual grouting process were insignificant, which corresponds to the non-disturbing character of the grouting process when properly conducted.

When permeation grouting is used for pile foundation protection, the bearing capacity of the piles will certainly not decrease. However, when permeation grouting is used for pile foundation renovation, the bearing capacity and stiffness of the piles can be increased. When the grouted element is located close to the pile toe and more elements are grouted near the piles, the positive effect on the bearing capacity may increase considerably.

During the jetting stage of the jet grouting process for pile foundation protection, pile settlement remained limited to 2 mm for each column. Neither the distance between the pile and the jet grouted column nor the diameter of the column seemed to influence the pile displacement. However, when grouting closer to the pile toe than 0.5 m for pile foundation renovation, the pile displacements increased exponentially, especially when grouting just below pile toe level. In this case also significant changes in pore water pressure and total stress were recorded. No coherent relation between the total stress change and the pile settlement could be detected.

After grouting for pile foundation protection, neither the bearing capacity nor the stiffness of the wooden piles was negatively influenced by the grouting. After grouting for pile foundation renovation the extended concrete piles showed almost exclusively elastic deformations and showed no sign of reaching their ultimate bearing capacity. It has not been possible to deduce an unambiguous relation for the change in cone resistance caused by the jet grouting.

From the samples obtained from the jet grouting columns, it could be deduced that although satisfactory strength and stiffness parameters were achieved, the variation coefficients of the grout parameters were high. Empirical relations derived from the test results were shown in Table 5.15

During the test, compaction grouting subsequently caused the piles to heave (caused by the large volumes of grout that were injected) and to settle (as a result of consolidation). The soil surface displacements were analogous to the vertical pile displacements. Generally the measurement points closest to the injection point showed the largest displacement and excess pore pressures. No apparent relation was found between the increase in excess pore pressures and the grouting pressures. When the excess pore pressures had dissipated the piles stopped settling.

Compaction grouting near a pile toe can considerably (at least 35%) increase the bearing capacity, which agrees with the calculations of the compaction ratio. Moreover, the load-settlement behaviour of all piles stiffened significantly.

For all methods, the dimensions of the grouted element play an important role in determining the influence of grouting. Geophysical verification methods can help determine these dimensions. On the whole, the results of electrical resistance measurement seem to be in accordance with the actual geometry of the grouted elements. However, the method does have disadvantages because of its limited applicability as an active monitoring tool during jet grouting. The use of Bore Hole Radar measurements in permeation grouting applications is not considered feasible. Verification by using BHR measurements in jet grouting columns showed that they usually underestimate the actual column diameter.

The construction cost of grouting can be up to about 50% lower than the construction cost of conventional methods of underpinning a structure. When grouting to renovate the pile foundations of structures with a commercial function, the total cost including economic damage amounts to 30% - 65% of the cost of conventional underpinning, while for structures with a residential function, the total grouting cost including economic damage amounts to 50% - 80% of the cost of conventional underpinning.

The main conclusion is therefore that permeation grouting and compaction grouting can be useful, economic and effective alternatives to conventional underpinning methods for renovating pile foundations. The methods may also be used for pile foundation protection. Jet grouting is only suitable for use in the renovation of end bearing piles when the structure is strong and stiff enough to redistribute the loads from the grouted pile. Jet grouting is very suitable for use in protecting pile foundations, because it can be applied in any type of soil.

Finally, it is necessary to consider that grouting for pile foundation improvement and conventional underpinning are not fully comparable. In the first place, when making the cost calculations for the grouting methods, no economy of scale affects could be included. Secondly, conventional underpinning results in an entirely new foundation structure (piles and floor), whilst underpinning using grouting only reinforces the existing foundation structure. Therefore, in comparison to grouting, conventional underpinning certainly has added value in pile foundation improvement. However, when both are equally suitable, it is doubtful whether the cost of underpinning justifies this added value.

9.3 Future Perspective

Until a database containing the relation between the jet grouting input and output parameters is available, it is highly recommended that trial columns should be made before the actual project is started. The diameter of the trial columns should be used to assess the influence radius of the jet grouting and thus predict the possible pile settlements.

Because of the wide scatter that is generally found when analysing jet-grouting strength and stiffness parameters, adequate risk assessments should be made or material factors of 2 to 3 should be used. In addition, because of the risk of blowouts, the significance of careful monitoring of the jet grouting process is emphasised. To counter this, the spoil return flow and the pressure at the monitor should be constantly monitored. Furthermore, the jet grouting rod could be supplied with integrated BHR equipment and a device capable of adjusting the drilling direction. To allow the application of the BHR, the radar signal should be shaped to a single pulse, a directional radar signal should be used and a wireless connection (infrared) between the BHR equipment and the surface should be developed. In combination with automated interpretation of the acquired data a real time image of the results can then be obtained.

The most important recommendations that follow from this research on compaction grouting are that the volume of the grouted element should be carefully controlled and that it is necessary to ensure that the installation procedure is accurate. Moreover, for piles at 12m depth, the grouted volume should be injected at approximately 0.5 m horizontally from the pile toe and vertically within the 4D-8D area of the pile. The diameter of the grouted element should not exceed 0.6 m (assuming a cylindrical shape) and the grouting pressures should not exceed 2.5 MPa at the injection point.

Because the small space between the piles complicated observation of the effects of each injection individually, it is recommended that to permit observation of consolidation phenomena, more research should be carried out with piles at a greater distance from each other and more time between individual injections. Experiments with a larger number of piles, different types of grout and grouted elements at varying distances should help to optimise this method.

LITERATURE REFERENCES

- Achterbosch**, L.A., 2001, *Compaction Grouting ter versterking van paalfunderingen*, Masters Thesis Delft University, in Dutch
- Al-Alusi**, H.R., 1998, *Compaction Grouting: From Practice to Theory*; Grouting : Compaction, Remediation and Testing; Geotechnical Special Publication No. 66, Edt. C. Vipulanandan, Proceedings of the ASCE Geo-Logan '97 Conference, ASCE, New York, pp. 43- 53
- Bandimere**, S.W., 1997, *Compaction Grout Mechanism – State of the Practice 1997*; Grouting : Compaction, Remediation and Testing; Geotechnical Special Publication No. 66, Edt. C. Vipulanandan, Proceedings of the ASCE Geo-Logan '97 Conference, ASCE, New York, pp. 18- 31
- Baker**, W.H., E.J. Cording & H.H. MacPherson, 1983, *Compaction grouting to control ground movements during tunnelling*, *Underground Space*, Vol.7, January, pp. 205-212
- Baker**, W.H., 1985, *Embankment Foundation Densification by Compaction Grouting*, Proceedings, Issues in Dam Grouting, ASCE, New York, pp. 104-122
- Battjes**, J.A., 1990, *Vloeistofmechanica Collegehandleiding*, Delft University Press Publ., in Dutch
- Boscardin**, M.D & E.J. Cording, 1989, *Building Response to Excavation Induced Settlement*, Journal of Geotechnical Engineering, Vol. 115, No.1
- Boulanger**, R.W. & R.F. Hayden, 1995, *Aspects of compaction grouting of liquefiable soil*, Journal of Geotechnical Engineering, Vol. 121, No.12, paper #10013, December, 1995, pp. 844-855
- Brauns**, J & A. Blinde, 1978, *Die Bedeutung der Untergrundsichtung bei der Ausbreitung von Injektionssuspensionen in fluvialen Sedimenten*, *Die Bautechnik* 7/1978, pp. 226-231
- Bruce**, D.A., 1994, *Small Diameter Cast-in-Place Elements for Load Bearing and In Situ Earth Reinforcement*, Ground Control and Improvement, John Wiley and Sons. Publ., pp. 406-492
- Bruce**, D.A., A.F. DiMillio & I. Juran, 1995, *Introduction to Micropiles: an international Perspective*, Foundation Upgrading and Repair, ASCE Geotechnical Special Publication #50, pp. 1-26
- Bruzzi**, D., A. Zattoni & G. Pezzetti, 1993, *Pressure cells: How to obtain better results*, Field Measurements in Geomechanics, Balkema Publ. Rotterdam, pp. 61-65
- Bolton**, M.D., Y.C. Lu and J.S. Sharma, 1996, *Centrifuge Models of Construction and Compensation Grouting*, Proceedings of the Congress on Geotechnical Aspects of Underground Construction in Soft Ground 1996, London, Balkema Rotterdam, pp. 403-408
- Borden**, R.H. & K.B. Ivanetich, 1997, *Influence of fines content on the behaviour of compaction grout*, Grouting : Compaction, Remediation and Testing; Geotechnical Special Publication No. 66, Edt. C. Vipulanandan, Proceedings of the ASCE Geo-Logan '97 Conference, ASCE, New York, pp. 62 – 75
- Brown**, D.R. & J. Warner, 1973, *Compaction Grouting*; Journal of the Soil Mechanics and Foundations Division, ASCE, Vol.99, August 1973, paper 9908
- Burland**, J.B., B.B. Broms & V.F.B. de Mello, 1977, *Behaviour of Foundations and Structures*, SOA Report, Session 2, Proc. 9th International Conference SMFE, Tokyo, pp. 495
- Burland**, J.B., & J.R. Standing, 1996, *Geotechnical Monitoring of Historic Monuments*, Proc. International Conference on Geotechnical Eng. For the preservation of Monuments & Historic Sites, pp. 321-341, Balkema Publ.
- Caron**, C., 1963, *The Development of grouts for the injection of fine sands*, Symposium on grouts and drilling muds in engineering practice, pp. 136-141
- Cambefort**, H., 1964, *Injection des sol*, Tome I & II, Principes et méthodes (in French) , 2nd ed., Eyrolles Paris Publ.
- Cambefort**, H., 1969, *Bodeninjektionstechnik, Einpressungen in Untergrund und Bauwerke (Injection des sols)*, übersetzt von Klaus Back, Berlin, Juli 1969
- Cambefort**, H., 1977, *The principles and applications of grouting*, Q.J.G.E., Vol. 10 (2), pp. 57-95
- Chin**, Fung Kee, 1978, *Diagnosis of pile condition*, Geotechnical Engineering Vol. 9, pp. 85-10
- Clough**, G.W. & T.D. O'Rourke, 1990, *Construction induced movements of insitu walls*, Design and performance of earth retaining structures, Ed. Lambe & Hansen, ASCE Publ.

LITERATURE REFERENCES

- Coomber**, D.B., 1985, *Tunnelling and soil stabilisation by jet grouting*, Tunnelling '85, The Institution of Mining and Metallurgy, pp.227-283
- Covil**, C.S., 1991, *Jet grouting: a state of the art review*, Masters Thesis, Imperial College of Science and Technology Publ.
- Droof**, E.R., A.J. Furth & J.A. Scarborough, 1995, *Jet grouting to support historic buildings*, Foundation Upgrading and Repair, ASCE Geotechnical Special Publication #50, pp. 27-41
- Engel**, H.J.J., 1975, *Praktijkervaringen bij het versterken van monumenten*, Cement XXVII nr.12, pp. 545-554
- Essler**, R.D., E.R.Drooff & E.Falk, 2000, *Compensation Grouting, Concept, Theory & Practice*, Advances in grouting and ground modification, Proceedings of sessions of Geo-Denver 2000, ASCE Geotechnical special publication #104, Denver, Colorado, pp. 1-15
- Evers**, G., 2000, Soletanche Bachy Research, Personal communication
- Faught**, K.L., 1997, *Compaction Grouting at tip of Sheet Piles*, Ground Treatment; Geotechnical Special Publication No. 69, Proceedings of the ASCE Geo-Institute, Logan, USA, pp.441-443
- Fujita**, K., 1994, *Soft ground tunnelling and buried structures*, XIII ICSMFE, New Delhi India, pp.89-108
- Fundamentum**, 2000, *Eindrapportage Praktijk Injectie Proef fase 1a, 1b & 1c*, " version C, S8170-RAP-024, 26-04-2000
- Gelderloos**, H.C., M.S. Bornhäuser and K.F. Brons, *het heffen van een verzakte caisson van de IJ-tunnel*, Bouw en Waterbouwkunde 15, 5 december 1969, pp. 181-188, in *Dutch*
- Glossop**, R., 1960, *The invention and development of injection processes*, Geotechnique, London, Vol. X, pp. 91-101 & Vol. XI, pp. 255-279 (1961).
- Goldscheider**, M., 1999, *Problems with old foundations*, Proceedings of the International Congress on Urban Heritage Building Maintenance, Foundations, Delft University of Technology Publ.
- Gouvenot**, D., 1996, *State of the art in European Grouting Technologies*, Grouting and Deep Mixing, Proceedings of the 2nd International Conference on Ground Improvement Geosystems, Tokyo, Balkema Publ. Rotterdam, May, pp. 833-850
- Graf**, E.D., 1969, *Compaction Grouting Technique*; Journal of the Soil Mechanics and Foundations Division, ASCE, Vol.95, September 1969
- Graf**, E.D., 1992, *Compaction Grout*, Grouting, Soil Improvement and Geosynthetics, Proceedings ASCE Geotech. Conference, Geotechnical Special Publication no. 30, New Orleans, February 1992, pp. 275-287
- Greenfield**, S.J., 1992, *Foundations in problem soil*, Prentice-Hall Publ.
- Gularte**, F.B., Taylor, G.E., Borden, R.H., 1992, *Temporary tunnel excavation support by chemical grouting*, Grouting, Soil Improvement and Geosynthetics, Proceedings ASCE Geotech. Conference, Geotechnical Special Publication no. 30, New Orleans, February 1992, pp. 423-435
- Hanrahan**, E.T., T.L. Orr & T.F. Widdis Edt., 1987, *Groundwater Effects in Geotechnical Engineering*, IX CEMSTF Dublin 1987, Balkema Publ., Session 7, pp. 639 – 745
- Harris**, D.I., R.J.Mair, J.P. Love, R.N. Taylor, T.O. Henderson, 1994, *Observations of ground and structure movements for compensation grouting during tunnel construction at Waterloo station*, Géotechnique, No.4., pp. 691-713
- Helbig**, T., 1999, *Technical report Jet Grouting works*, Eurosond/Soletanche-Bachy, Full Scale Injection Test Report
- Hoekstra**, J., 1974, *Funderingsonderzoek Dapperbuurt Amsterdam*, Rapportage Grondmechanica Delft, in *Dutch*
- Horvat**, E., C.R.M. Hogervorst & A.F. van Tol, 1977, *Basisrapport Funderingsversterking t.b.v. Stadsvernieuwing*, Concept 75-102/D, Rapportage Dienst van Gemeentewerken Grondmechanica Rotterdam, in *Dutch*
- Hopman**, V.J., A.E.C. van der Stoel & W. van Dalßen; 1999, *Geofysische meetmethoden bij grondverbetering: Praktijk Injectie Proef te Utrecht*, Geotechniek, 3^e jaargang, #1, in *Dutch*
- Hunt**, R, R.H. Dyer & R. Driscoll, 1991, *Foundation movement and remedial underpinning in low rise buildings*, Building Research Establishment
- Ichise**, Y, A. Yamakado, April 1974, *High Pressure Jet Grouting Method*, US Patent 3,802,203

LITERATURE REFERENCES

- Janssen, N.**, 1999, *Studie naar bodeminjectie ten behoeve van horizontale waterremmende lagen*, Masters Thesis, TU Delft, in Dutch
- Jörger, R.**, 2000, *Bilfinger + Berger Documentation HV-TIEF/MT Grs & Accurate grout Forecast* European Foundations Summer 1997
- Kaalberg, F.J.**, H.J. Lengkeek & E.A.H. Teunissen, 1999, *Evaluatie van de meetresultaten van het proefpalenproject ter plaatse van de Tweede Heinenoordtunnel, 1^e & 2^e passage*, Adviesbureau Noord/Zuidlijn Publ., in Dutch
- Kanematsu, H.**, 1980, *High pressure Jet Grouting method*, Doboku Sekoh Civil Engineering, vol. 21, nr. 13
- Karol, R.H.**, 1983, *Chemical Grouting*, Marcel Dekker Publ., New York & Basel, 465 pp.
- Kauschinger, L.J.**, R. Hankour, & E.B. Perry, 1992, *Methods to estimate composition of jet grout bodies*, Grouting, Soil Improvement and Geosynthetics, Proceedings ASCE Geotech. Conference, ASCE Geotechnical Special Publication no. 30, pp 194-205
- Krizek, R.J.**, Liao, H-J, Borden, R., 1992, *Mechanical properties of microfine cement/sodium grouted sand*, Grouting, Soil Improvement and Geosynthetics, Proceedings ASCE Geotech. Conference, Geotechnical Special Publication no. 30, New Orleans, February 1992, pp. 688-699
- Kudella, P.** 1994, *Mechanismen der Bodenverdrängung beim Einpressen von Fluiden zur Baugrundverfestigung*, Gudehus/Technische Universität Karlsruhe Publ., Heft 132, 191 pp.
- Kutzner, C.** 1996, *Grouting of rock and soil*, Balkema Rotterdam Publ., 271 pp.
- Lambe, T.W.** and R.V. Whitman. 1979, *Soil Mechanics, SI Version*, John Wiley & Sons Publ., New York, 553 pp.
- Linde, J.M.W. ter**, 1990a, *Rapport betreffende inspectie en beoordelingsmethodiek voor houten funderingen*, Fugro Leidschendam, in Dutch
- Linde, J.M.W. ter**, 1990b, *Inspectie- en beoordelingsmethodieken voor houten paalfunderingen*, Fugro Leidschendam, in Dutch
- Linde, J.M.W. ter**, 1997, *Funderingsherstel*, Funderingen A4600, Ten Hagen Stam Publ., in Dutch
- Littlejohn, G.S.**, 1985, *Chemical Grouting -1*, Ground Engineering, March, pp. 13-16
- Littlejohn, G.S.**, 1985, *Chemical Grouting -2*, Ground Engineering, April, pp.23-28
- Littlejohn, G.S.**, 1985, *Chemical Grouting -3*, Ground Engineering, May, pp. 29-34
- Lizzi, F.**, 1982, *Static Restoration of Monuments*, Sagep. Publ., Genoa, 146pp.
- Lizzi, F.**, 2000, <http://www.fondedile-foundations.ltd.uk/lizzilet.htm>
- Lunardi, P.**, 1997, *Ground Improvement by means of Jet Grouting*, Ground Improvement, Vol.1, pp. 65-85
- Maag, E.**, 1938, *Ueber die Verfestigung und Dichtung des Baugrundes (Injektionen)*, Erdbaukurs de E.T.H. 1938, Sammlung der Vorträge herausgegeben vom Institut für Erdbauforschung der eidg. Techn. Hochschule Zürich, Zürich
- Mace, N. & G.R. Martin**, 1996, *Ground remediation – Aspects of the theory and approach to compaction grouting*, Proceedings of the 6th Japan-U.S. Workshop on Earthquake Resistant Design of Lifeline Facilities and Countermeasures Against Soil Liquefaction, Tokyo, Japan
- Maertens, J.**, 1999, *Extending of shallow foundations by jet-grouting*, Proceedings of the International Congress on Urban Heritage Building Maintenance, Foundations, Delft University of Technology Publ.
- Mair, R.J.**, Taylor, R.N., Burland, J.B., 1996, *Prediction of ground movements and assessment of risk of building damage due to bored tunnelling*, Proceedings of the Congress on Geotechnical Aspects of Underground Construction in Soft Ground 1996, London, Balkema Rotterdam
- Mair, R.J.**, R.N. Taylor & A. Bracegirdle, 1993, *Subsurface settlement profiles above tunnels in clay*, Géotechnique 43, No. 2 , pp. 315-320
- Mair, R.J.**, D.I. Harris, , J.P. Love, D.Blakey, C.Kettle, 1994, *Compensation grouting to limit settlement during tunnelling at Waterloo station, London*, Tunnelling '94, Institution of Mining and Metallurgy, Chapman and Hall Publ., pp. 279-300
- Mayer, A.**, 1958, *Cement and clay grouting of foundations French grouting practice*, Proc. ASCE February, Paper 1550

LITERATURE REFERENCES

- Mitchel**, J.K., 1970, *In place treatment of foundation soils*, ASCE, Journal of the Soil Mechanics and Foundation Division 96(1)
- NEN 6743**, 1991, *Berekeningsmethoden voor funderingen op palen, Drukpalen*, Nederlands Normalisatie-instituut Publ.
- Nakanishi**, W., April 1974, *Method for forming a underground wall comprising a plurality of columns in the earth and soil formation*, US Patent 3,800,544
- Netzel**, H. & F.J. Kaalberg, 1999, *Settlement risk management with GIS for the Amsterdam North/South Metroline*, Proceedings of the ITA World Tunnel Congress 1999 Oslo Norway, Balkema Publ.
- Netzel**, H. & F.J. Kaalberg, 2000, *Numerical damage risk assessment studies on adjacent buildings due to TBM-tunnelling in Amsterdam*, GeoEng 2000, Melbourne
- Netzel**, H. & F.J. Kaalberg, 2001, *Monitoring of the North-South Metroline in Amsterdam*, Proceedings CIRIA conference July 2001, CIRIA Publ.
- Neville**, A.M., 1997, *Properties of concrete*, p.306, Essex Addison Wesley Longman Ltd. Publ.
- New**, B.M. & M.P. O'Reilly, 1991, *Tunnelling induced ground movement: predicting their magnitude and effects*, Invited review paper 4th International Congress on ground Movement and Structures
- Nichols**, S.G. & D.J. Goodings, 2000, *Effects of grout composition, depth and injection rate on compaction grouting*, Advances in grouting and ground modification, Proceedings of sessions of Geo-Denver 2000, ASCE Geotechnical special publication #104, Denver, Colorado, pp. 16-31
- Nonveiller**, 1989, *Grouting Theory and Practice*, Developments in Geotechnical Engineering no. 57, Elsevier Science Publ, 250 pp.
- Oversteegen**, M.J., 1999, *Experiment with foam concrete*, Proceedings of the International Congress on Urban Heritage Building Maintenance, Foundations, Delft University of Technology Publ.
- Paoli**, B. De, B. Bosco, R. Granata, D.A. Bruce, 1992a, *Fundamental observations on cement based grouts (1): Traditional materials*, Grouting, Soil Improvement and Geosynthetics, Proceedings ASCE Geotech. Conference, Geotechnical Special Publication no. 30, New Orleans, February 1992, pp. 474-485
- Paoli**, B. De, B. Bosco, R. Granata, D.A. Bruce, 1992b, *Fundamental observations on cement based grouts (2): microfine cements and the Cemill process*, Grouting, Soil Improvement and Geosynthetics, Proceedings ASCE Geotech. Conference, Geotechnical Special Publication no. 30, New Orleans, February 1992, pp. 486-499
- Peek**, R.D. & H. Willeitner, 1981, *Behaviour of Wooden Piling in Long Time Service*, Proceedings of the 10th International Conference Soil Mechanics And Foundation Engineering, Stockholm, June 1981, Balkema Publ., pp. 147-152
- Philips**, Caspar, 1768, *Grachtenboek*, original publications 1768/71 by Bernardus Mourik a/d Nes, reprints in 1922, 1930, 1936, 1962, 1979 (2x) and *Grachtenboek*, SDU (1991)
- Lundström**, R.B., 1981, *The Quality of The Wood in Timber Piles*, Proceedings of the 10th International Conference Soil Mechanics And Foundation Engineering, Stockholm, June 1981, Balkema Publ., pp. 131-132
- Müller**, R. & D.A. Bruce, 2000, *Equipment for Cement grouting: An Overview*, Advances in grouting and ground modification, Proceedings of sessions of Geo-Denver 2000, ASCE Geotechnical special publication #104, Denver, Colorado, pp. 155-172
- Peck**, R.B., 1969, *Deep excavations and tunnelling in soft ground*, Proceedings of the 7th. International Congress Soil Mechanics, Mexico, pp. 225-290
- Perbix**, W. & Teichert H.D., 1995, *Feinstbindemittel für Injektionen in der Geotechnik und im Betonbau*, Nachdruck aus Tunnelbau 1995, Sika AG
- PrEN12715**, Execution of special geotechnical works. Grouting, February 1997
- PrEN12716**, Execution of special geotechnical works. Jet grouting, February 1997
- Raffle**, J.F., D.A. Greenwood, 1961, *The relation between the rheological characteristics of grouts and their capacity to permeate soil*, Proceedings of the 5th International Conference on Soil Mechanics, Paris, pp. 789-793
- SBR-47**, 1975, *Negatieve kleef op funderingspalen*, Stichting Bouwresearch, Rapport # 47, Samson Publ., pp. 38-39

LITERATURE REFERENCES

- Schmertmann**, J.H. & J.F. Henry, 1992, *A Design Theory For Compaction Grouting*, Grouting, Soil Improvement and Geosynthetics, Proceedings ASCE Geotech. Conference, Geotechnical Special Publication no. 30, New Orleans, February 1992, pp. 215-228
- Sherard**, J.L., 1984, Dunningan, L.P., *Basic properties of sand and gravel filters*, Jet Grouting ASCE, Vol. 110, No. 6, June
- Speulman**, H., 1997, *Conservering en ommanteling kan houten paal redder*, Land + Water, Vol. 1/2, pp. 38-39
- Sagaseta**, C., 1987, *Analysis of undrained soil deformation due to ground loss*, Géotechnique 37, No. 3, pp. 301-320
- Scherer**, S.D., R.L. Gay, 2000, *Compaction Grouting: Three Midwest case histories*, Advances in grouting and ground modification, Proceedings of sessions of Geo-Denver 2000, ASCE Geotechnical special publication #104, Denver, Colorado, pp. 65-82
- Soga**, K., R.J. Mair, M.D. Bolton, M.R. Jafari, S.K.A. Au, S.W. Lee and K. Komiyama, 2001, *Laboratory Investigation of Compensation Grouting*, CIRIA Conference on Building Response to Tunnelling
- Standing**, J., 1999, *The assessment and building response to tunnelling, risk, damage and structural monitoring*, Proceedings of the International Congress on Urban Heritage Building Maintenance, Foundations, Delft University of Technology Publ.
- Stein**, J., 2000, Bohrabweichungsmessungen bei der Herstellung einer Düsenstrahlsole, Messen in der Geotechnik 2000, Technische Universität Braunschweig, Heft Nr.62, pp 209-222
- Stigt**, J. van, et al, 1995, *Renovatie en onderhoudstechnieken*, Delft University of Technology Publ., in Dutch
- Stoel**, A.E.C. van der, 1997, *Inventarisatie injectietechnieken & verdieping permeation grouting*, Deelrapportage promotieonderzoek, Ingenieursbureau Amsterdam – TU Delft, in Dutch
- Stoel**, A.E.C. van der, 1997b, *Dimensionering Injectielichamen*, Rapportage Adviesbureau Noord/Zuidlijn, intern rapport, in Dutch
- Stoel**, A.E.C. van der, 1998, *Soil Grouting: Full Scale Injection test North/South metro line Amsterdam*, Tunnels and Metropolises, Proceedings of the World Tunnel Congress 1998 on Tunnels and Metropolises São Paulo Brazil, Balkema Publ.
- Stoel**, A.E.C. van der; A.F. van Tol, 1998b, *Full Scale Injection Amsterdam: Results stage 1 and 2*, Proceedings of the ITA World Tunnel Congress 1999 Oslo Norway, Balkema Publ.
- Stoel**, A.E.C. van der; 1999a, *Praktijk Injectie Proef: resultaten en Evaluatie fase 0*, Adviesbureau Noord/Zuidlijn internal report R990786.D, in Dutch
- Stoel**, A.E.C. van der; 1999b, *Injection/grouting near pile foundations: Full Scale Test Amsterdam*, Geotechnical Aspects of Underground Construction in Soft Ground, IS'99 Tokyo Japan, Balkema Publ.
- Stoel**, A.E.C. van der; 2001, *Praktijk Injectie Proef: resultaten en Evaluatie fase 1*, Adviesbureau Noord/Zuidlijn internal report, in Dutch
- Stoel**, A.E.C. van der; 2001b, *Causes, Detection and Renovation of Pile Foundation Design*, Ingenieursbureau Amsterdam Publ., Amsterdam
- Soilex**, <http://www.byggforum.com/soilex>
- Tausch**, N., 1985, *A Special grouting Method to Construct Horizontal Membranes*, Symposium on Recent Developments in Ground Improvement Techniques, Bangkok 1983, pp 351-361
- Teunissen**, E.A.H. & M. Hutteman, 1998, *Pile surface settlement at full scale tests North/South metro line*, Tunnels and Metropolises, Proceedings of the World Tunnel Congress 1998 on Tunnels and Metropolises São Paulo Brazil, Balkema Publ.
- Tol**, A.F. van, 1982, *Funderingen: Funderingsonderzoek in de stadsvernieuwing*, Berichten over Stadsvernieuwing (Bos), 1982, Vol 7, #2, pp.14-19, in Dutch
- Tol**, A.F. van, 1994, *Hoe betrouwbaar is de paalfundering*, Intreerede 3-6-1994, TU Delft, in Dutch
- Tol**, A.F. van, 1996, *Funderingen en Constructie*, Lecture Notes, TU Delft, in Dutch
- Tol**, A.F. van, 1999, *Interaction between existing and newly added piles*, Proceedings of the International Congress on Urban Heritage Building Maintenance, Foundations, Delft University of Technology Publ.

LITERATURE REFERENCES

- Tol**, A.F. van & J.D. de Jong, 1999, *Paalfunderingen*, Praktijkboek Instandhouding Monumenten, #3 Sept.1999, in Dutch
- Tomlinson**, M.J., 1994, *Pile design and construction practice*, E & FN Spon Publ.
- Verhoef**, L.G.W., 1999, *Introduction*, Proceedings of the International Congress on Urban Heritage Building Maintenance, Foundations, Delft University of Technology Publ.
- Vesic**, A.S., 1972, *Expansion of Cavities in infinite soil mass*, Journal of the Soil Mechanics and Foundation Division, ASCE, Vol. 98 , SM3, Paper 8790, March 1972, pp. 265-290
- Vipulanandan**, C. & S. Shenoy, 1992, *Properties of cement grouts and grouted sands with additives*, Grouting, Soil Improvement and Geosynthetics, Proceedings ASCE Geotech. Conference, Geotechnical Special Publication no. 30, New Orleans, February 1992, pp. 500-511
- Vleeshauer** P. de & J. Maertens, 1999, *Jet-Grouting: Hoever staan we?*, Geotechniek, Vol. 2, pp. 17-22, in Dutch
- Warner**, J., 1972, *Strength Properties of Chemically Solidified Soils*, Journal of the Soil Mechanics and Foundation Division, ASCE., Vol. 11 November 1972, pp. 1163-1185
- Warner**, J. & D. Brown, 1974, *Planning and performing compaction grouting*, ASCE, Journal of Geotechnical Engineers, paper #10606, July 1974
- Warner**, J., 1978, *Compaction grouting - A significant case history*, ASCE, Journal of Geotechnical Engineers, vol. 104, paper #13897, July 1978
- Warner**, J., 1992, *Compaction Grout; Rheology vs. effectiveness*, Grouting, Soil Improvement and Geosynthetics, Proceedings ASCE Geotech. Conference, Geotechnical Special Publication no. 30, New Orleans, February 1992, pp.229-239
- Warner**, J., N. Schmidt, J. Reed, D. Shepardson, R. Lamb & S. Wong, 1992, *Recent Advances In Compaction Grouting Technology*, Grouting, Soil Improvement and Geosynthetics, Proceedings ASCE Geotech. Conference, Geotechnical Special Publication no. 30, New Orleans, February 1992, pp. 252-264
- Warner**, J., 1997, *Compaction Grout Mechanism – What do we know?*, Grouting : Compaction, Remediation and Testing; Geotechnical Special Publication No. 66, Edt. C. Vipulanandan, Proceedings of the ASCE Geo-Logan '97 Conference, ASCE, New York, pp. 1 – 17
- Weaver**, K.D., 1991, *Dam foundation grouting*, ASCE, New York
- Weele**, A.F. van, R. van Bueren & G.J. Maas, 1989, *Kwaliteit van houten paalfunderingen in Amsterdam*, Funderingstechniek, Vol.3 September 1989 , pp.34-43, in Dutch
- Weele**, A.F. van, 1993, *Moderne Funderingstechnieken*, 2e druk, Delft Univ. Press, in Dutch
- Weele**, A.F. van & B.M.L.G. Lencioni, 1999, *Het mislukken van een paalfundering is duur, maar leerzaam*, Geotechniek, Vol.3.1 Januari 1999 , pp.19-47, in Dutch
- Wit**, J.W.H.M. de, M. de Kant & J.C.S. Roelands, 1999, *Full scale test on environmental impact of diaphragm wall trench excavation in Amsterdam*, Geotechnical Aspects of Underground Construction in Soft Ground, IS'99 Tokyo Japan, Balkema Publ.
- Wit**, J.W.H.M. de, M. de Kant, H.J. Lengkeek, 2000, *Eindrapport Praktijkproef Openstaande Diepwandsleuven*, Adviesbureau Noord/Zuidlijn Publ., in Dutch
- Wong**, H.Y., 1973, *Compaction Grouting*, Journal of the Soil Mechanics and Foundations Division, GT5, ACSE Publ., 1974, May 1974, pp.556-559
- Yahiro**, T., 1973, *Induction grouting method using high speed water jet*, Proceedings of the 8th. International Conference on Soil Mechanics and Foundation Engineering, pp. 402-404
- Yonekura**, R., M. Kaga, 1992, *Current chemical grout engineering in Japan*, Grouting, Soil Improvement and Geosynthetics, Proceedings ASCE Geotech. Conference, Geotechnical Special Publication no. 30, New Orleans, February 1992, pp. 725-736
- Zanten**, D.van, S. Kay & ir. A.E.C. van der Stoel, 2001, *Jetgrouten naast een paalfundering, predicties en praktijkmetingen*, Geotechniek Vol.5 april, No.2, Educom Publ., pp. 96-103, in Dutch

APPENDICES

APPENDICES

APPENDIX I GROUTING VOCABULARY

Action radius: Theoretical distance travelled by the grout from the injection point.

Additive (Admixture): Any grout ingredient (e.g. liquefiers, stabilizers) other than the basic components of a grout mix (water, aggregates, or cementitious material), which is used to modify the liquid and solid state properties of the grout.

Batch: Quantity of grout mixed at one time.

Bentonite: A clay composed principally of minerals of the montmorillonite group, characterised by high water absorption capacity and a very large volume change upon saturation or drying. They are clays with a content of swellable smectites of at least 70% and a water absorption capacity of more than 500%. A distinction is made between natural, sodic, calcic, modified, and activated bentonites.

Bleeding: The autogenous flow of mixing water within, or its emergence from, newly placed grout.

Cement grout: A grout in which the primary bonding agent is cement.

Compaction grouting: A displacement grouting method that is intended to force forcing a mortar with high internal friction into the soil without fracturing it.

Compensation grouting: A term employed for controlled displacement grouting the aim of which is to counteract ground settlement induced by excavation works. This term refers to a number of grouting methods and is more-or-less a generic term for compaction grouting, displacement grouting and fracturing.

Consistency: The relative mobility or ability of freshly mixed mortar or grout to flow. The usual measurements are slump for stiff mixtures and flow for more fluid grouts.

Consolidation grouting: This term refers to several injection methods including impregnation, fissure grouting, bulk filling, hydraulic fracturing and compaction grouting, the aim of which is to strengthen the soil or rock mass.

Displacement grouting: Injection of grout into a host medium in such a manner as to move, compress, or displace the ground.

Double packer: A device consisting of a pair of seals (packers) fitted to a grouting pipe at a predetermined distance apart, used to limit grout injection to the ground between the two packers, i.e. the packed-off length or stage.

Downstage (Descending stage) grouting: A grouting technique where a given distance (stage) is drilled and grouted before the borehole is advanced by further drilling or in which packers are employed to start grouting at the top of the borehole and advance the grouting process progressively down the hole.

Filler: An inert material added to a grout to modify its properties or to replace a component.

Filtration: The process of passing a liquid through a filter. The filter impedes the flow of the liquid and may result in the deposition of a filter cake.

Flash set: The rapid development of rigidity in a freshly mixed grout, usually with the evolution of considerable heat. This rigidity cannot be dispelled nor can the plasticity be regained by further mixing without addition of water; also referred to as quick set or grab set.

(Hydraulic) fracturing: The fracturing of a formation initiated by the injection of water or grout a under pressure that is in excess of the local tensile strength and confining pressure; also called hydro-fracturing, hydro-splitting, hydro-jacking or claquage (French terminology).

Gel: The condition where a liquid grout begins to exhibit measurable shear strength. A colloidal material in which the dispersed substances form a continuous branching cohesive network. It may contain a proportion of liquid but possesses some properties of a solid. Some gels can be returned to the liquid phase by disturbance or mixing and will thereafter reform as a gel again (see Thixotropy).

Gel strength: The shear strength of a gel. This may be measured at a fixed time interval after mixing or breaking up of a gel or when the gel has fully developed.

Gel time: The measured time interval between the mixing of a grout and the formation of a gel.

Gravity grouting: Grouting under no applied pressure other than the height of fluid in the hole. Sometimes referred to as tremie grouting.

Grout: An injection fluid, generally referred to as **grout** is a pumpable material (suspension, solution, emulsion or mortar) injected into a soil or rock formation which stiffens and sets with time and thereby changes the physical characteristics of the formation.

Grouting pressure: A pressure monitored during the grouting process at defined locations (usually at the pump or the borehole collar).

Groutability ratio: The groutability ratio, GR, expresses the relationship between the particle size of the grout (suspension type grout) and the grain size of the soil to be grouted. The ratios, $GR = D_{15}/d_{85}$ or $GR = D_{10}/d_{90}$ are used, where: D_{15} = the size which 15% of the soil particles are smaller than, d_{85} = the size which 85% of the grout particles are smaller than.

Grout take: The measured quantity of grout injected into a unit volume of formation, or a unit length of grout hole, or a complete hole.

Hardener: In a two component chemical grout, the component that causes the base component to cure.

Hardening time: The time for a grout to reach its design strength.

Hydraulic binder: Finely ground inorganic material which, when mixed with water, forms a paste that sets and hardens by means of hydration and which, after hardening, retains its strength and stability even under water.

Injection valve: Openings along the injection string of a tube-à-manchette, usually covered by a flexible sleeve, the whole of which acts as valves.

Marsh viscosity: Viscosity tests are carried out with the Marsh cone. The duration of flow, of a given volume of liquid, expressed in seconds, is called the 'Marsh viscosity'.

Micro-fine or ultra-fine product: Very fine product having a uniform, steep particle size distribution curve, where $d_{95} < 20 \mu\text{m}$ (usually cement).

Packer: A device inserted into a droll hole or tube-à-manchette to isolate one part of the hole from another. A packer is usually an expandable device activated mechanically, hydraulically or pneumatically.

Penetration grouting: Filling of joints or fractures in rock, or pore spaces in soil with a grout, without displacing the ground.

Permeation (impregnation) grouting: The replacement of the interstitial water or gas in a porous medium with a grout at injection pressures low enough to prevent displacement.

Resin: A material that constitutes the base of an organic grout system, such as acryl, epoxy, polyester and urethane.

Rheological properties: The properties governing the flow of a fluid or plastic solid.

Set time (Setting time): The time between mixing and the achievement in a significant change in the rheological properties (formation of a gel). The setting time is volume and temperature dependent and can be measured in a number of ways.

Slump test: Test for assessing the consistency of a mortar by use of an Abram's cone. The cone is filled with mortar to a given height, the cone is then lifted and the distance between initial height of the cone and the final height of the mortar mound measured.

Solution: A liquid formed by completely dissolving a chemical in water to give a uniform fluid without solid particles. Solutions are Newtonian liquids with neither rigidity nor particles and harden in a predetermined period of time, called the 'setting time'. They can be true or colloidal solutions. In the case of colloidal solutions, large molecules are contained in the liquid.

Stable suspension: Stable suspensions are suspensions that in 2 hours exhibit less than 5 per cent bleeding of clear water at the top of a 1000 ml cylinder with an internal diameter of 60 mm at the temperature of 20°C.

Suspension: A mixture of liquid and solid materials. Behaves as a Bingham fluid during flow, possessing both viscosity and cohesion (yield strength). Particulate suspensions contain particles larger than clay size, while colloidal suspensions contain particles of clay size.

Syneresis: The expulsion of liquid (generally alkaline water) from a set gel that is not stressed, accompanied by contraction of the gel. Syneresis occurs over a period of a few months.

TAM or Sleeve Pipe grouting: Grouting method using tubes-à-manchette, which allow repetitive placement of grout. The method entails boring a hole and placing within it a smaller pipe (the tube-à-manchette) with groups of peripheral holes that are covered with a rubber sleeve to act as a valve.

Thixotropy: The property of a material that enables it to stiffen in a relatively short time when undisturbed, but upon agitation or manipulation to change to a very soft consistency or to a fluid of high viscosity, the process being completely reversible. The viscosity of thixotropic fluids decreases with increasing shear rate (loading) and returns to its initial value after a time of regeneration. Fluids that show an increase in apparent viscosity with time are called thixotropic. Thixotropy is common in non-Newtonian grouts.

Tube-à-manchette (TAM): A grout pipe perforated with rings of small holes at specified intervals. In most cases, each ring of perforations is enclosed by a short rubber sleeve fitting tightly around the pipe so as to act as a one-way valve when used with an inner pipe containing two packer elements that isolate a Stage for injection of grout.

Unconfined Compressive Strength (UCS): The load per unit area at which an unconfined prismatic or cylindrical specimen (height = 2 x width) of material will fail in a simple compression test performed without lateral support.

Viscosity: The internal fluid resistance of a substance which makes it resist a tendency to flow. A distinction is made between kinematic viscosity, ν , and dynamic viscosity, η , for which: $\nu = \eta/\rho$, where: ρ = density.

APPENDICES

APPENDIX II CHARACTERISTIC SOIL PARAMETERS

A.Table 1 Characteristic Soil Parameters

no.	Layer	Description	BS class	γ_{dry} [kN/m ³]	γ_{wet} [kN/m ³]	n [-]	e [-]	w [-]	D50 [\square m]	wL [%]	wP [%]	Ip [%]
2	Ford, Hydrobia clay	CLAY (grey), very sandy	CL	9	15.2	0.63	1.80	0.75	17	97	48	49
	Base peat	PEAT (brown), with some clay layers	PT	4.2	11.7	0.75	3.63	2.04				
4	1st sand layer	SAND (grey), moderately fine, limitedly silty	SW	17.1	20.0	0.34	0.52	0.17	155			
5	Intermediate layer	LOAM, very sandy	SM/SC	14.5	18.5	0.44	0.81	0.28	87	66	39	30
	Clay with sand layers	CLAY, moderately sandy, moderately humus, chalk	CL	12.4	17.2	0.52	1.11	0.40	78	49	27	23
	Trench fill sand with clay layers	SAND (moderately fine), with clay layers, shells, traces of peat	CL	14.8	18.6	0.43	0.79	0.27	200	55	32	31
6	2nd sand layer	SAND (grey), moderately fine to moderately coarse, chalk	SW	15.8	19.0	0.39	0.65	0.20	200			
7	Marine silty Eem sand	SAND (fine), grey, with clay layers	SM	15	18.6	0.42	0.74	0.24	200			
	Transition layer	CLAY, extremely silty, limitedly humus, chalk	CL	13.6	18.2	0.47	0.92	0.34	56	36	23	12
8	Marine Eem clay	CLAY (grey-green), limitedly silty to limitedly sandy	CL	13.1	17.9	0.50	0.99	0.36	29	41	24	17
	Transition layer sand	SAND, very fine, limitedly silty	SP	16.0	19.4	0.39	0.64	0.21	136			
	3rd sand layer	SAND, moderately fine, limitedly silty to limitedly gravelly	SW	17	19.6	0.35	0.55	0.16	457			

APPENDIX III INSTALLATION TIMES PERMEATION GROUTING

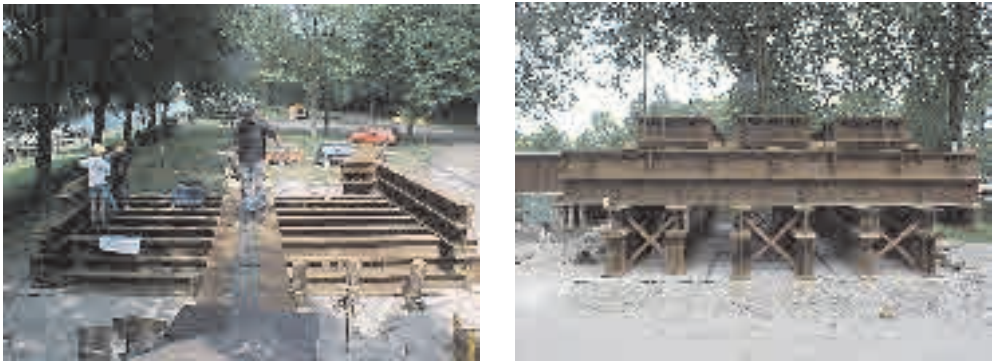
A.Table 2 Time of TAM installation

TAM	TAM type	Installation times reported the Contractor			Installation times after examination of the piezometer data		
		Start	End	duration	Start	End	duration
		date & time	date & time	(hh:mm)	Date & time	date & time	(hh:mm)
<i>Stage 3A permeation grouting</i>							
P1	Plastic 46 mm	2-09-99 9:45	2-09-99 10:15	0:30	2-9-99 9:45	2-9-99 10:45	1:00
P3	Plastic 46 mm	3-09-99 7:30	3-09-99 8:00	0:30	3-9-99 7:30	3-9-99 8:30	1:00
P5	Plastic 46 mm	3-09-99 14:55	3-09-99 15:18	0:23	3-9-99 14:55	3-9-99 15:45	0:50
P8	Plastic 46 mm	6-09-99 10:24	6-09-99 10:49	0:25	6-9-99 10:24	6-9-99 11:30	1:06
P9	Plastic 46 mm	6-09-99 19:40	6-09-99 20:10	0:30	6-9-99 19:40	6-9-99 21:00	1:20
PF10	Steel 42 mm	6-09-99 17:00	6-09-99 17:15	0:15	6-9-99 17:00	6-9-99 18:00	1:00
PF2	Steel 42 mm	6-09-99 12:13	6-09-99 12:32	0:19	6-9-99 12:13	6-9-99 13:15	1:02
PF4	Steel 42 mm	3-09-99 10:30	3-09-99 11:00	0:30	3-9-99 10:30	3-9-99 11:30	1:00
PF6	Steel 42 mm	6-09-99 15:00	6-09-99 15:25	0:25	6-9-99 15:00	6-9-99 16:00	1:00
F3	Steel 42 mm	6-09-99 7:45	6-09-99 8:07	0:22	6-9-99 7:45	6-9-99 8:45	1:00
<i>Stage 3C compensation grouting</i>							
C1	Steel 114.3 mm	12-10-99 13:00	12-10-99 15:00	2:00	12-10-99 11:00	12-10-99 14:00	3:00
C2	Steel 114.3 mm	12-10-99 9:00	12-10-99 11:00	2:00	12-10-99 8:00	12-10-99 10:30	2:30
C3	Steel 114.3 mm	8-10-99 10:00	8-10-99 12:00	2:00	8-10-99 10:00	8-10-99 13:00	3:00
F5	Steel 42 mm	5-10-99 15:00	5-10-99 16:00	1:00	5-10-99 14:00	5-10-99 17:00	3:00
F6	Steel 42 mm	4-10-99 12:30	4-10-99 15:00	2:30	4-10-99 14:30	4-10-99 17:30	3:00
F7	Steel 42 mm	5-10-99 13:00	5-10-99 14:00	1:00	5-10-99 9:00	5-10-99 13:00	4:00

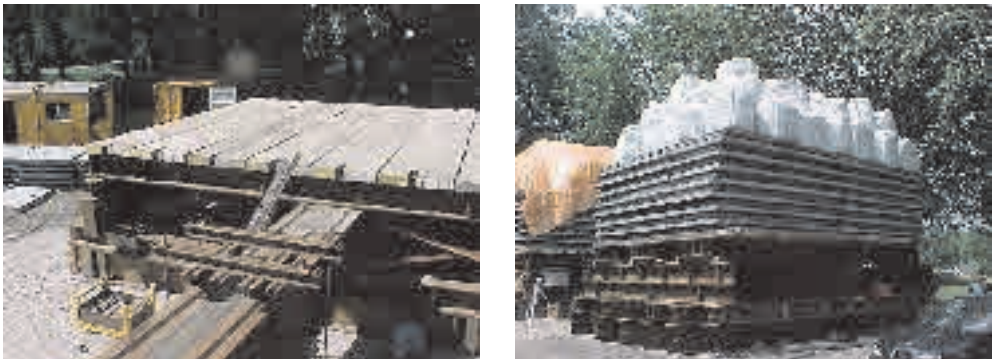
APPENDIX IV CHRONOLOGICAL SEQUENCE OF THE BALLAST FRAME CONSTRUCTION



A. Figure 1 Driving of Concrete (*left*) and Wooden (*right*) Piles



A. Figure 2 Placement of Stelcon Plates and Steel HE Profiles



A. Figure 3 Placement of Dragline Boards, and Stelcon & Sand Ballast

APPENDICES

APPENDIX V DATE OF JET GROUTING ACTIVITIES

A.Table 3 Dates of Jet Grouting: Drilling and Jetting Activities

Jet grouting Column		Start		End	
		Date	Time	Date	Time
A	Drilling	2-8-99	11:00	2-8-99	13:00
	jet grouting	4-8-99	8:45	4-8-99	15:15
B	Drilling	9-8-99	13:15	9-8-99	15:00
	jet grouting	10-8-99	8:00	10-8-99	14:00
C	Drilling	10-8-99	17:00	10-08-99	19:00
	jet grouting	11-8-99	10:30	11-08-99	20:00
D	Drilling	12-08-99	14:30	12-08-99	16:30
	jet grouting stage 1	13-08-99	7:00	13-08-99	10:30
	jet grouting stage 2	13-08-99	14:30	13-08-99	16:00
	jet grouting stage 3	13-08-99	18:45	13-08-99	21:00
E	drilling 1 st (1° time drilling angle 3°)	17-08-99	12:30	17-08-99	13:15
	drilling 2 nd (2° time drilling angle 5°)	17-08-99	13:35	17-08-99	14:25
F	jet grouting -22 to -17	17-08-99	17:22	17-08-99	17:59
	jet grouting -17 to -10	18-08-99	15:21	18-08-99	15:41
	Drilling	18-08-99	7:45	18-08-99	9:15
	jet grouting -22 to -17	18-08-99	13:20	18-08-99	13:41
X1	jet grouting -17 to -10	23-08-99	13:40	23-08-99	14:15
	Drilling	23-08-99	16:15	23-08-99	17:15
X2	jet grouting	24-08-99	8:30	24-08-99	11:40
	Drilling	24-08-99	14:15	24-08-99	14:45
X3 (W1)	jet grouting -22 to -12	25-08-99	7:30	25-08-99	9:00
	jet grouting -12 to -2	25-08-99	10:30	25-08-99	12:00
	Drilling (Re-drilled under different angle)	8-09-99	13:00	8-09-99	13:40
X4 (W2)	jet grouting	8-09-99	14:20	8-09-99	14:40
	Drilling	9-09-99	8:00	9-09-99	8:30
X5 (W3)	jet grouting	9-09-99	9:00	9-09-99	9:30
	Drilling	8-09-99	15:40	8-09-99	16:20
	jet grouting	8-09-99	17:30	8-09-99	17:55

A.Table 4 Date of Activities and Time Lap between the Different Activities of Jet Grouting

Column	Test	Date jet grouting	Date drilling cores	Time lap [days]	Date testing samples	Time lap [days]
A	UCS	04-08-1999	25-08-1999	21	05-11-1999	93
	Tensile	04-08-1999	25-08-1999	21	15-11-1999	103
	Triaxial	04-08-1999	25-08-1999	21	22-12-1999	140
B	UCS spoil	04-08-1999	25-08-1999	21	11-11-1999	99
	UCS	10-08-1999	30-08-1999	20	10-11-1999	92
	Tensile	10-08-1999	30-08-1999	20	15-11-1999	97
C	Triaxial	10-08-1999	30-08-1999	20	07-01-2000	150
	UCS spoil	10-08-1999	30-08-1999	20	11-11-1999	93
	UCS	11-08-1999	26-08-1999	15	05-11-1999	86
D	Tensile	11-08-1999	26-08-1999	15	15-11-1999	96
	Triaxial	11-08-1999	26-08-1999	15	07-11-1999	150
	UCS spoil	11-08-1999	26-08-1999	15	12-11-1999	93
X1	UCS	13-08-1999	31-08-1999	18	10-11-1999	89
	Tensile	13-08-1999	31-08-1999	18	15-11-1999	94
	Triaxial	13-08-1999	31-08-1999	18	22-12-1999	127
X2	UCS spoil	13-08-1999	31-08-1999	18	12-11-1999	91
	UCS	24-08-1999	06-09-1999	13	05-11-1999	73
	Tensile	24-08-1999	06-09-1999	13	15-11-1999	83
X3	Triaxial	24-08-1999	06-09-1999	13	22-12-1999	120
	UCS spoil	24-08-1999	06-09-1999	13	12-11-1999	80
	UCS	25-08-1999	07-09-1999	13	11-11-1999	78
X4	Tensile	25-08-1999	07-09-1999	13	16-11-1999	83
	Triaxial	25-08-1999	07-09-1999	13	07-01-2000	138
	UCS spoil	25-08-1999	07-09-1999	13	12-11-1999	79

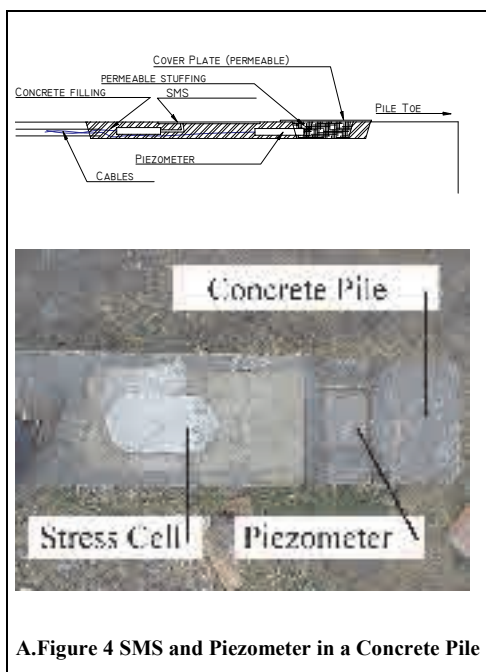
APPENDIX VI MONITORING EQUIPMENT

Stress Monitoring Stations and Piezometers Installed in Piles

The instrumentation in the monitored wooden and concrete piles consisted of a total pressure cell or Stress Monitoring Station (SMS) and a piezometer, which were placed at 0.50m and 0.25m from the pile toe respectively. In two of the concrete piles, additional SMS and additional piezometers were installed at the level of the 1st sand layer (NAP-13.25 m).

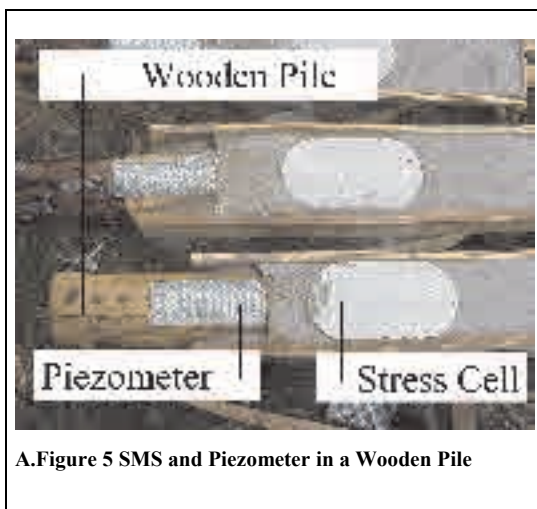
The SMS is basically formed from two stainless steel plates. The edges of the plates are welded together forming a sealed cavity which is filled with fluid, after which a pressure transducer is attached to the cell. The cell is installed with its sensitive surface in direct contact with the soil. The total pressure acting on that surface is transmitted to the fluid inside the cell and measured by the pressure transducer.

The three prefabricated *concrete piles* were specially equipped for the test. A PVC-tube was cast into the piles to accommodate the electronic data transfer cables running from the piezometer and SMS to the ground surface. For the piezometer and the SMS openings were created in the surfaces of the piles. A. Figure 4 shows the instruments cast-in-place in a concrete pile.



A. Figure 4 SMS and Piezometer in a Concrete Pile

Because the *wooden piles* are cylindrical and the SMS are flat, the possibility that the SMS might be damaged during the pile driving process was a concern. Boarding was placed along the pile and an opening was made in the pile into which the SMS and piezometer were placed. After the placing of the monitoring equipment the remaining space was filled with polyester. To ensure that the SMS and piezometers were not damaged the boarding was not removed from the pile. It was not expected that the slightly bigger shaft would significantly influence the bearing capacity of the wooden pile. A. Figure 5 shows the instruments in the wooden pile. An additional advantage of the boarding was that it prevented the pile from turning during the pile driving operation, thus ensuring the correct orientation of the monitoring equipment.



A. Figure 5 SMS and Piezometer in a Wooden Pile

Piezometers

Pore water pressures were measured across the test site by using piezometers (A.Figure 6). The piezometers were pushed into the soil (analogous with the CPT method). This method was chosen as there is evidence to suggest that more reliable measurements are obtained from these than from piezometers installed in boreholes. Most of the piezometers were installed in or just above the 1st sand layer at \pm NAP – 13 m.

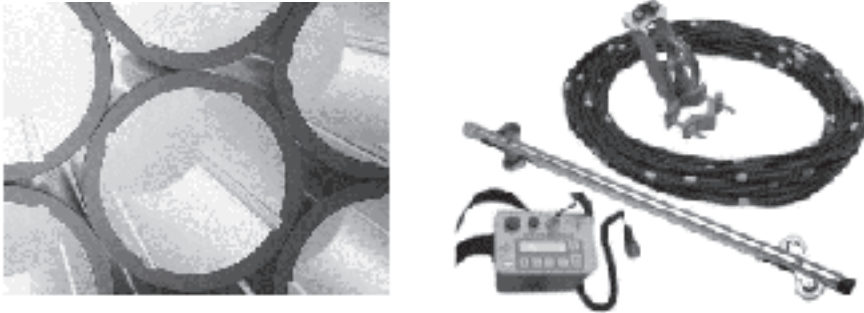


A.Figure 6 Piezometer

Inclinometers

Deformation inclinometers (A.Figure 7) were used to measure the lateral soil deformation.

The inclinometer casing is installed in a vertical borehole filled with bentonite cement that passes through the zones of movement into stable ground. The inclinometer probe, control cable, pulley assembly and readout A.Figure 7 (left) are used to survey the casing A.Figure 7 (right). The inclinometer casing is a special purpose, grooved pipe. The inclinometer casing provides access for the inclinometer probe, allowing it to obtain subsurface measurements, controls the orientation of the inclinometer probe and deforms with the adjacent ground or structure.



A.Figure 7 Inclinometer components (left) and PVC Inclinometer Casing (right)

A preliminary survey establishes the initial profile of the casing enabling subsequent surveys to identify changes in the profile resulting from ground movements. During a survey, the probe is drawn upwards from the bottom of the casing to the top, being halted in its travel at half-meter intervals to measure tilt. The inclination of the probe body is measured by two force-balanced servo-accelerometers. One accelerometer measures tilt in the plane of the inclinometer wheels, which track the longitudinal grooves of the casing. The other accelerometer measures tilt in the plane perpendicular to the wheels. Inclination measurements are converted into lateral deviations. Changes in lateral deviation, which are determined by comparing data from current and initial surveys, indicate ground movements.

Beacons

The beacons used for ground surface settlement monitoring consisted of a 0.5 by 0.5 m² steel base plate with a 2 m long steel bar welded to it on top of which the target was welded. The base plate was installed approximately 0.75 m under surface level.

Jointmeters

The frequency of measurements using the total station was limited, jointmeters (Figure 3.7 on page 28) were installed on all the pile heads to monitor pile displacement during grouting. These jointmeters could be monitored at a much smaller interval than the targets. The relative pile displacements are

measured by means of a mechanical gauge with an accuracy of 0.01 mm. The measuring signal is directed through a signal cable or to a terminal box and read by an automatic data acquisition system.

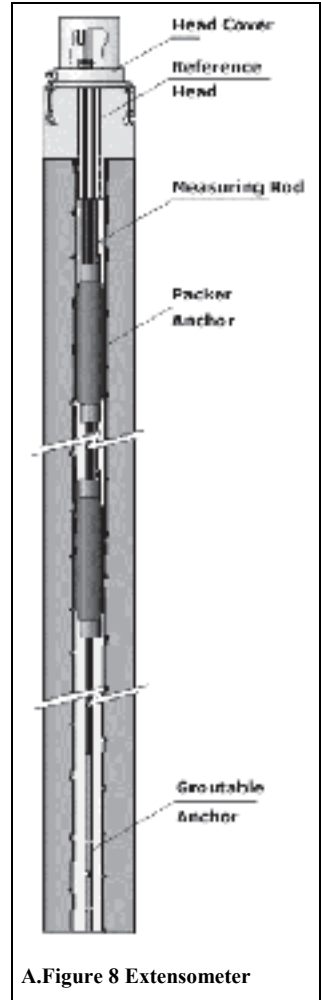
Soil Extensometers

To measure vertical soil deformations, borehole rod extensometers (A.Figure 8) were used. Two 2-point rod extensometers were installed; both with packer anchors filled with grout, at NAP-15.0 m and NAP-25.0 m. Each extensometer was installed in a $\varnothing 115$ mm borehole, with a waterproof head cover to protect the displacement transducers and reference heads. Protective tubing was installed with the rods to prevent bonding of the rods with the grout or surrounding soil. Each extensometer measures the distances between two anchor points in the borehole and the reference point at the borehole collar.

Automatic Levelling System

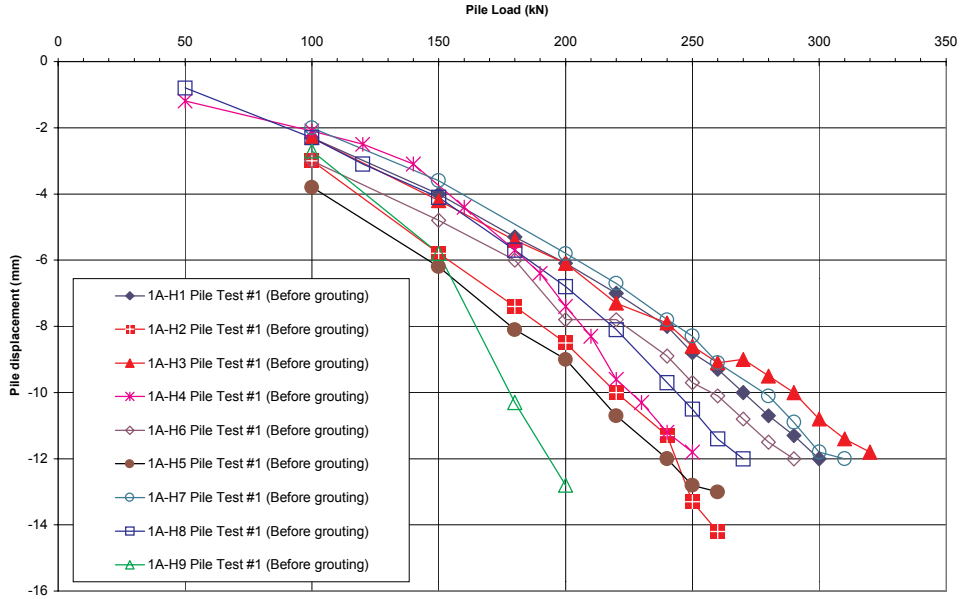
The automatic levelling system uses an automatic theodolite or ‘total station’ (A.Figure 9) to measure the position in 3D space of targets (Figure 3.7 on page 28) at a specified frequency. The frequency is dependent upon the number of targets the total station can measure. For the test on average 35 targets were monitored at a frequency of 5-6 measurement cycles per hour. The big advantage of this system is that is semi-continuous and can be programmed to retry measurements on targets that are temporarily invisible (blocked by equipment, workers, etc.).

Targets were placed on the piles, beacons, ballast frame (to measure settlement of the frame itself), extensometers & inclinometers, houses, lampposts, the quay and the lock (reference targets, to correct the movement of the Total Station).

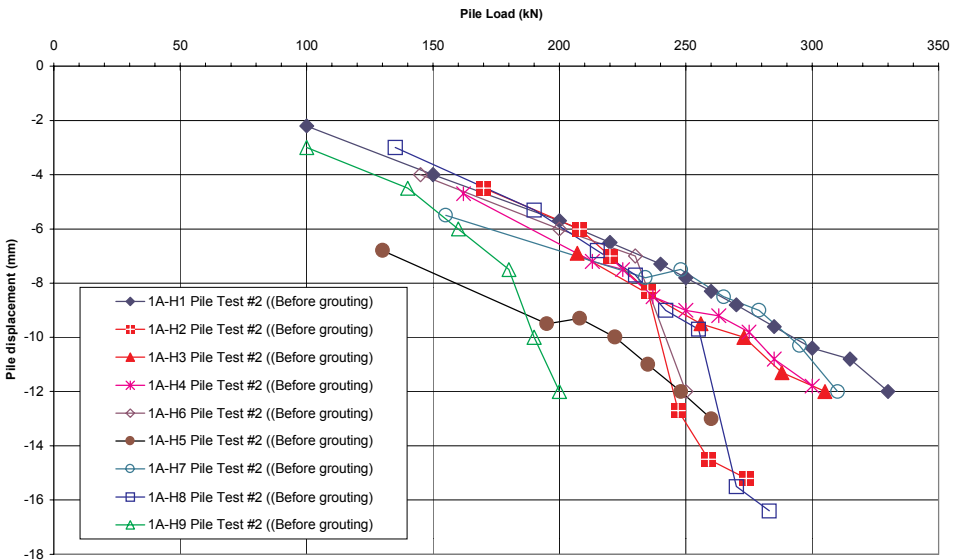


A.Figure 9 Total Station

APPENDIX VII RESULTS OF LOAD TESTS 1 AND 2

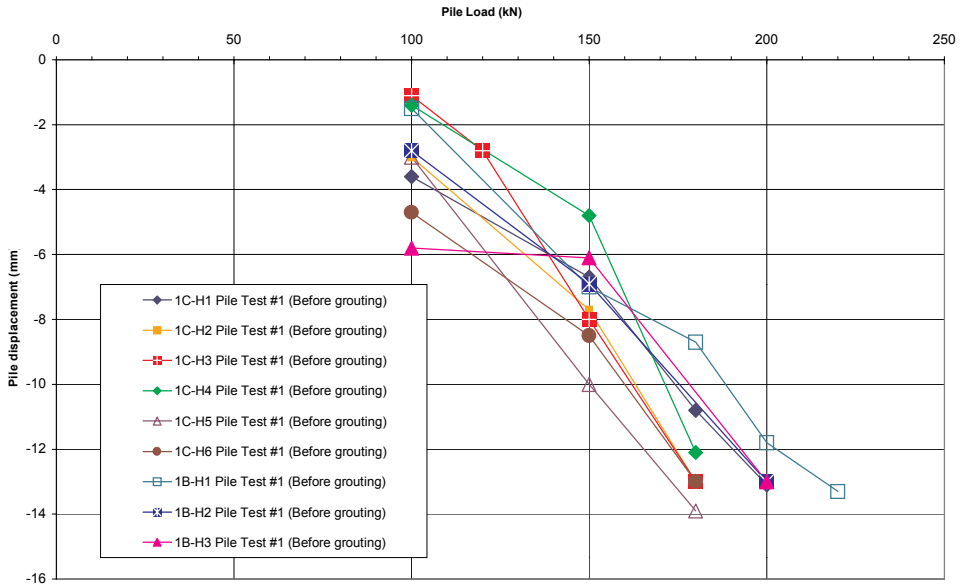


A. Figure 10 Pile Load Test 1 (Location A)

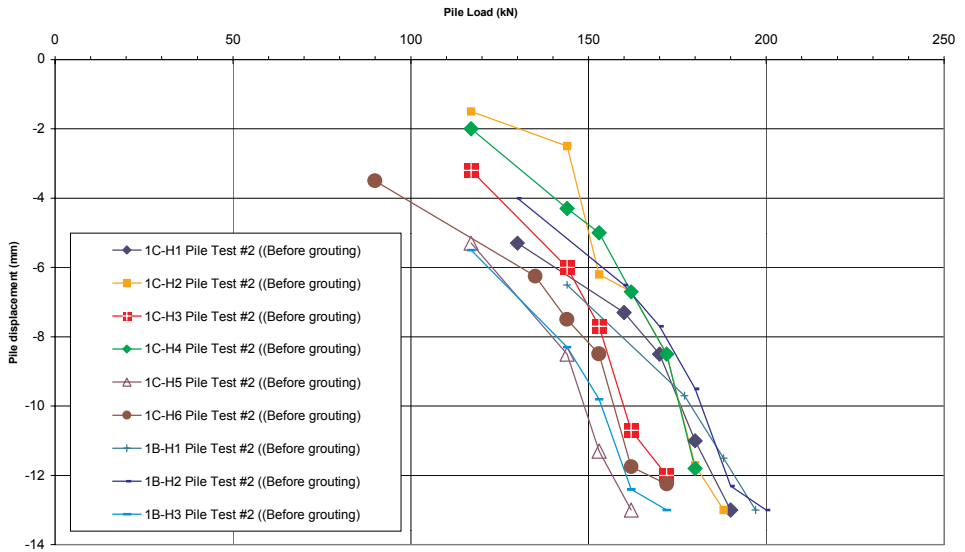


A. Figure 11 Pile Load Test 2 (Location A)

APPENDICES

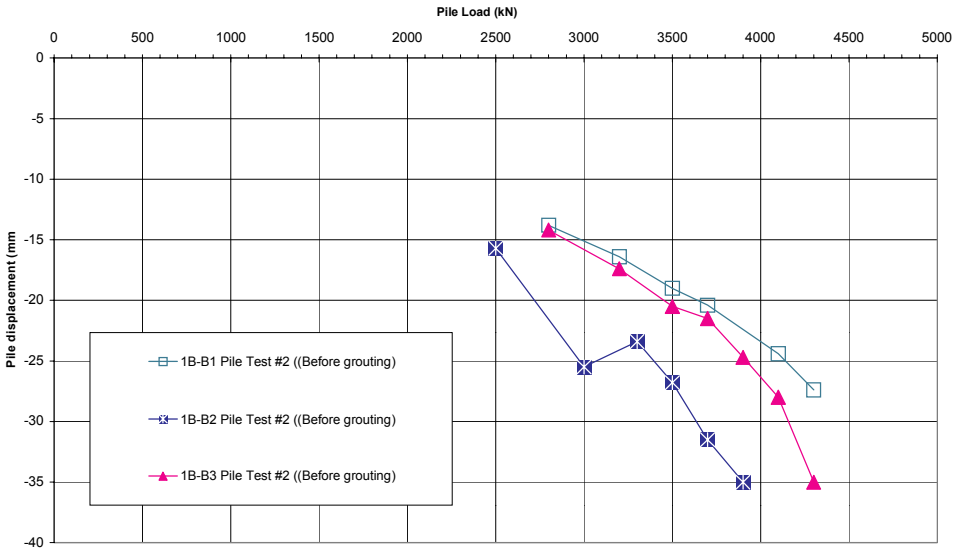


A. Figure 12 Pile Load Test 1 (Location B and C)



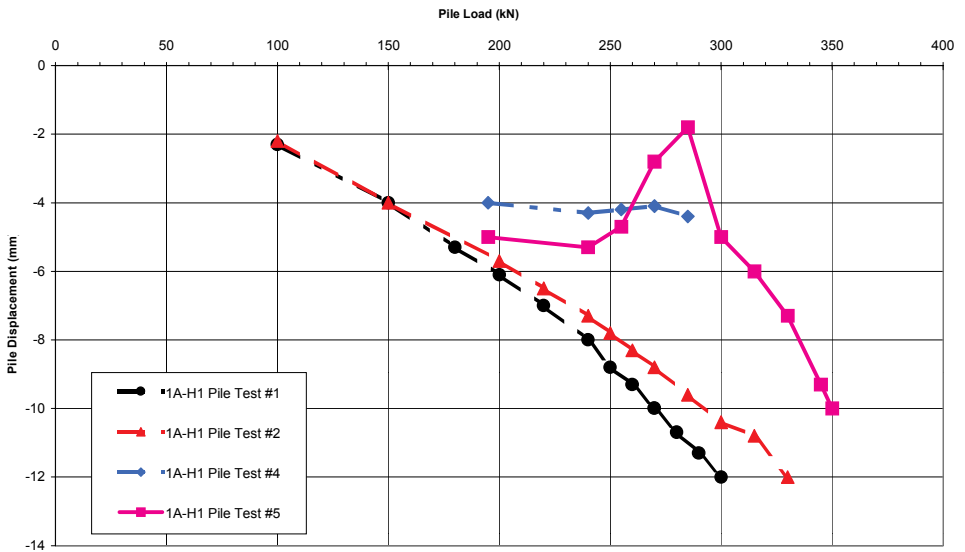
A. Figure 13 Pile Load Test 2 (Location B and C)

APPENDICES



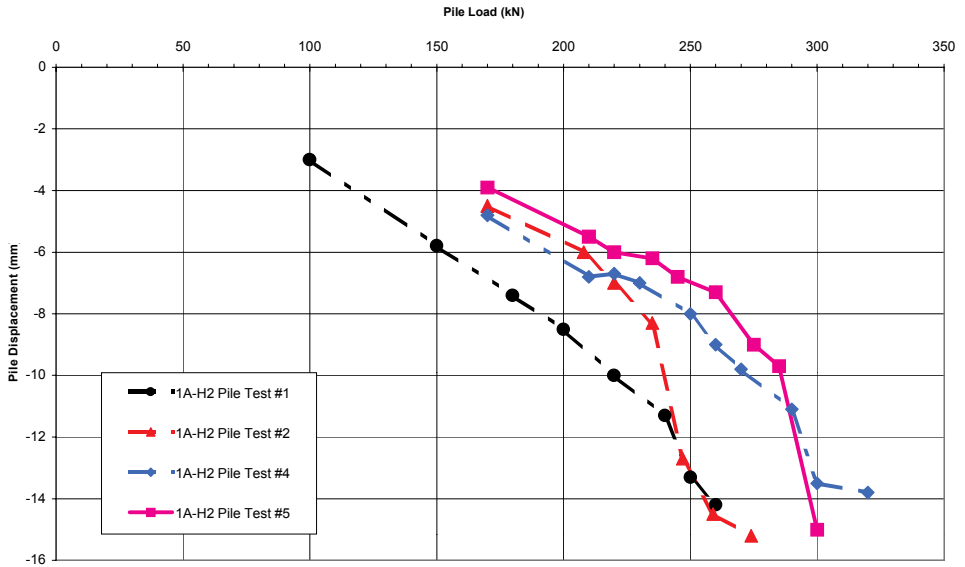
A. Figure 14 Pile Load Test 1 (Location B Concrete Piles)

APPENDIX VIII PILE LOAD TESTS BEFORE AND AFTER PERMEATION GROUTING

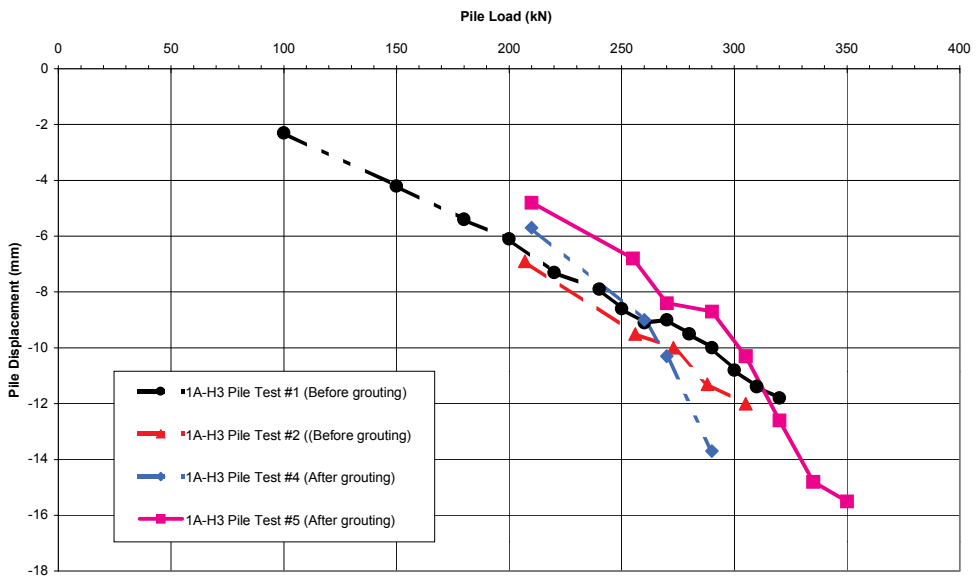


A. Figure 15 Pile Load Test Pile 1A-H1 after Permeation (#3) and Compensation Grouting (#4/5)

APPENDICES

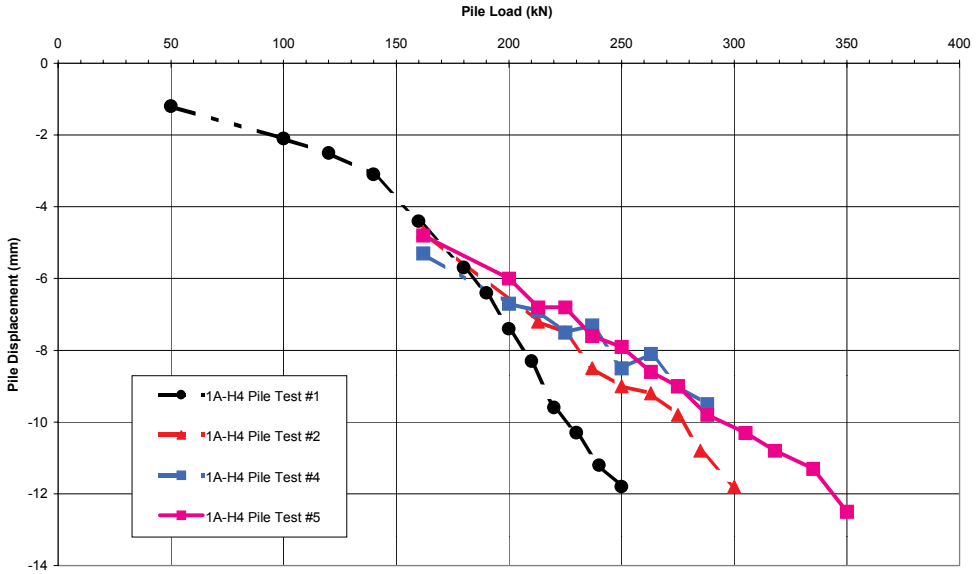


A. Figure 16 Pile Load Test Pile 1A-H2 after Permeation (#3) and Compensation Grouting (#4/5)

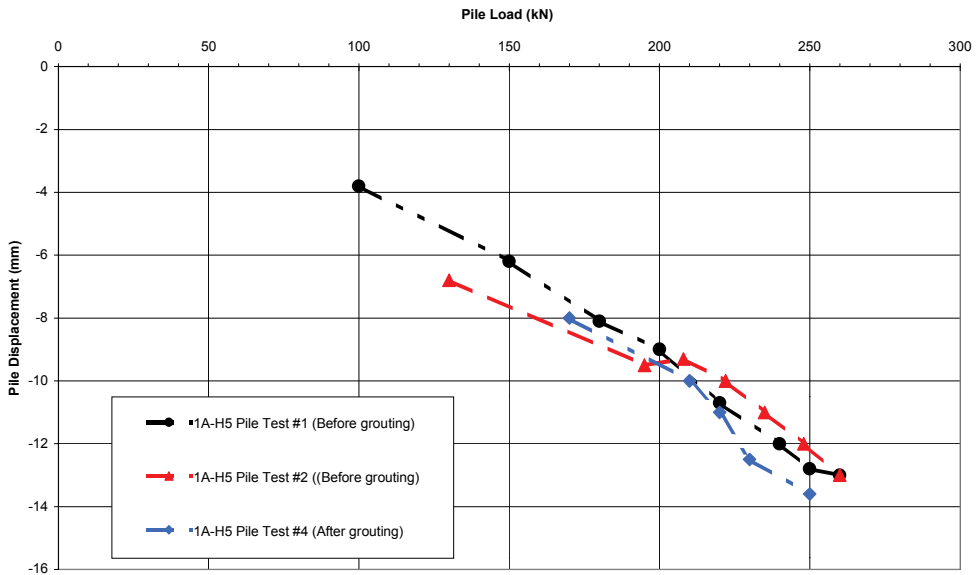


A. Figure 17 Pile Load Test Pile 1A-H3 after Permeation (#3) and Compensation Grouting (#4/5)

APPENDICES

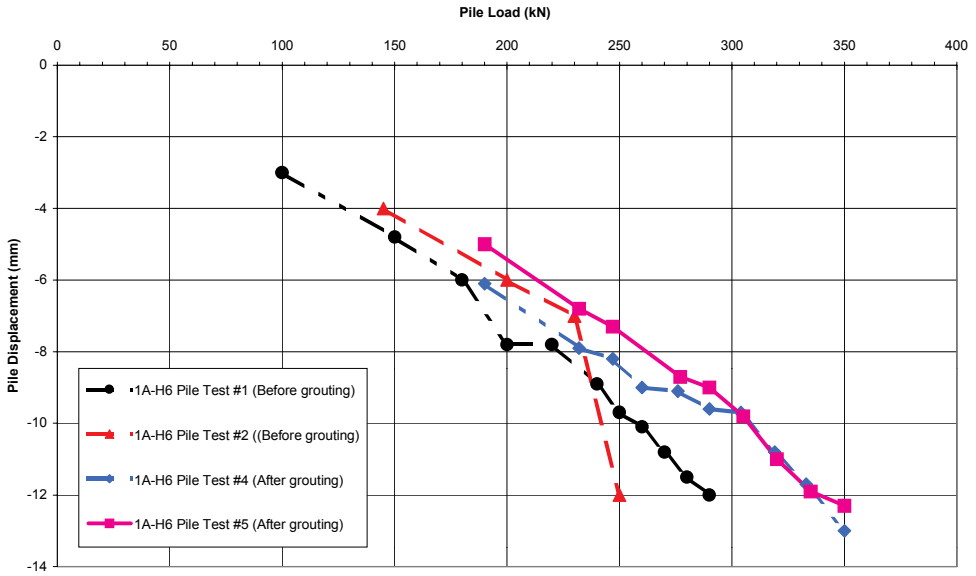


A. Figure 18 Pile Load Test Pile 1A-H4 after Permeation (#3) and Compensation Grouting (#4/5)

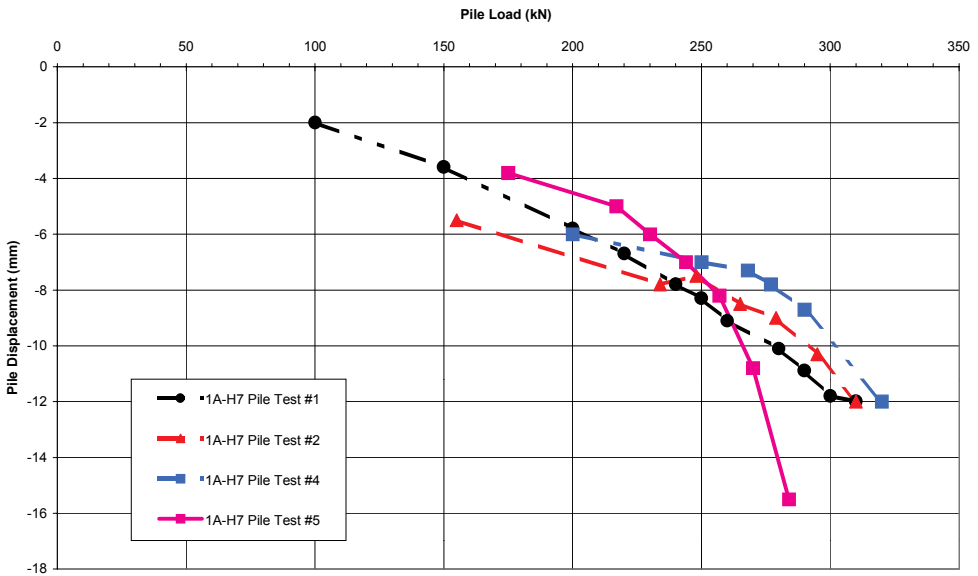


A. Figure 19 Pile Load Test Pile 1A-H5 after Permeation (#3) and Compensation Grouting (#4/5)

APPENDICES

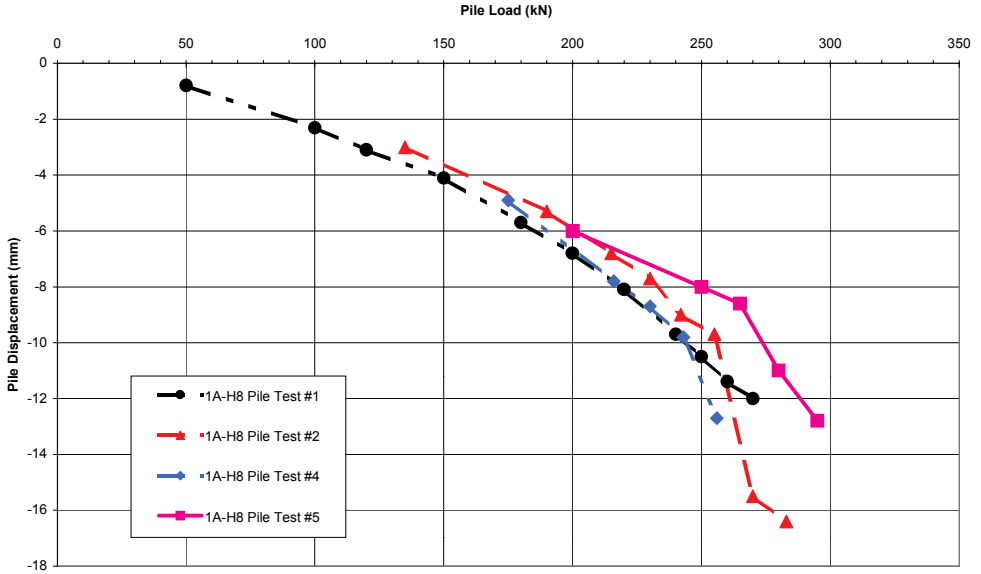


A. Figure 20 Pile Load Test Pile 1A-H6 after Permeation (#3) and Compensation Grouting (#4/5)

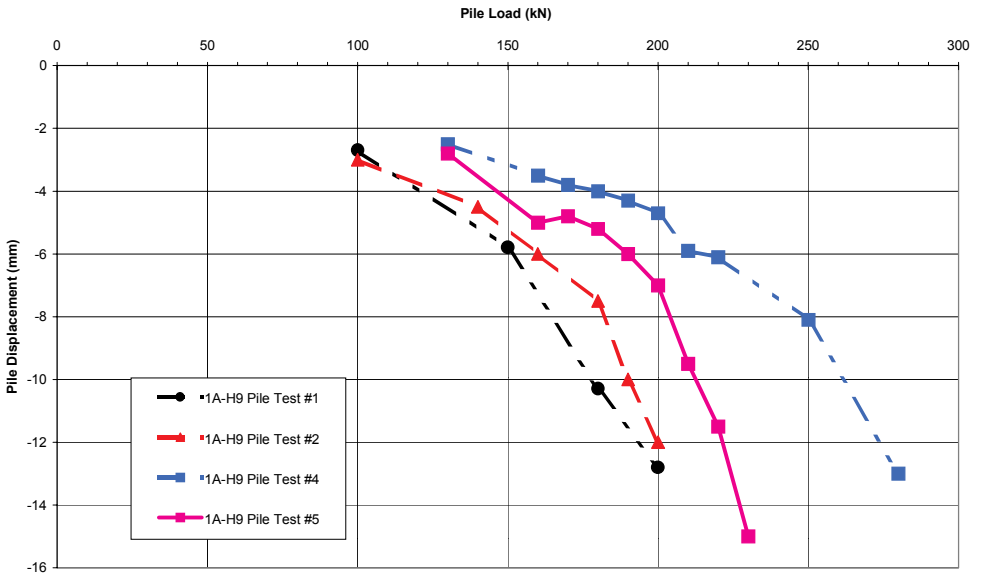


A. Figure 21 Pile Load Test Pile 1A-H7 after Permeation (#3) and Compensation Grouting (#4/5)

APPENDICES

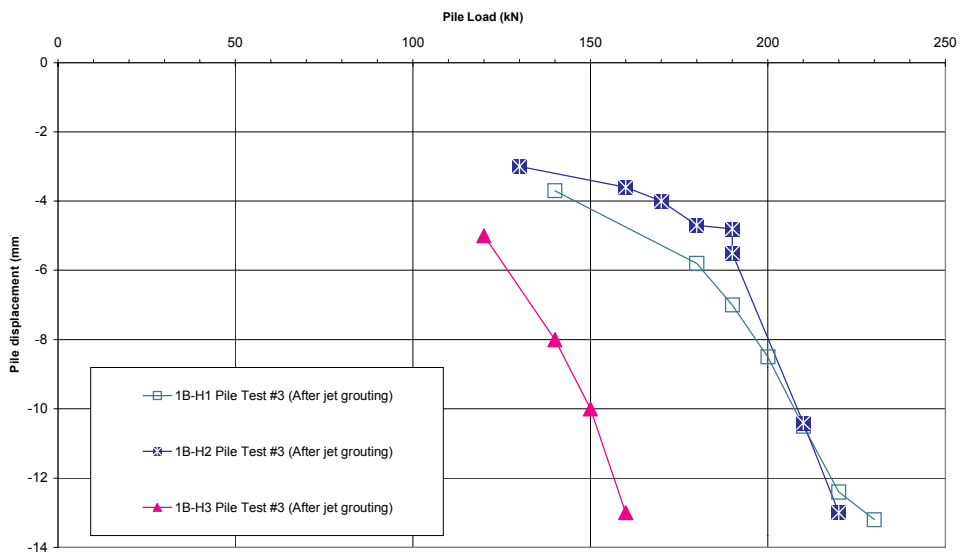


A. Figure 22 Pile Load Test Pile 1A-H8 after Permeation (#3) and Compensation Grouting (#4/5)

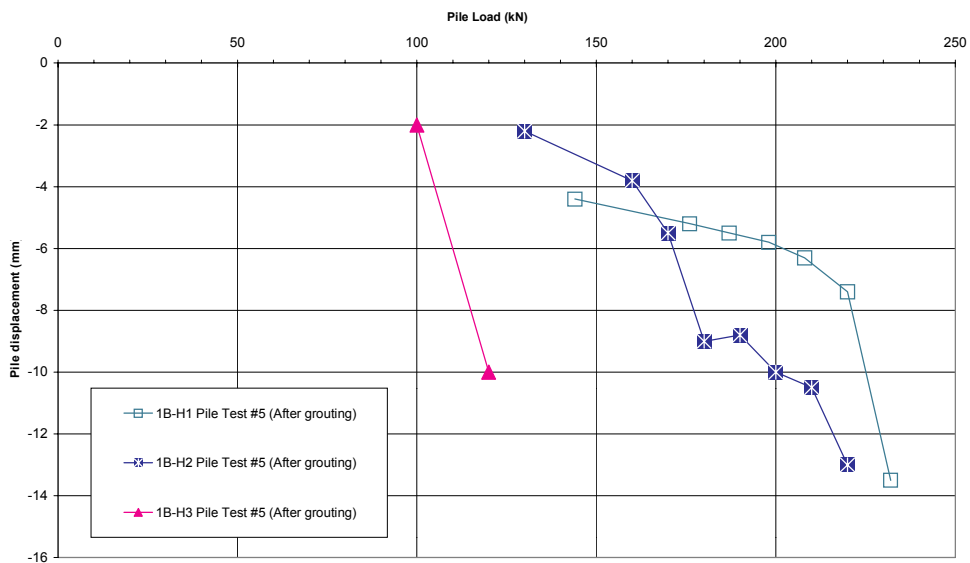


A. Figure 23 Pile Load Test Pile 1A-H9 after Permeation (#3) and Compensation Grouting (#4/5)

APPENDIX IX PILE LOAD TESTS BEFORE AND AFTER JET GROUTING

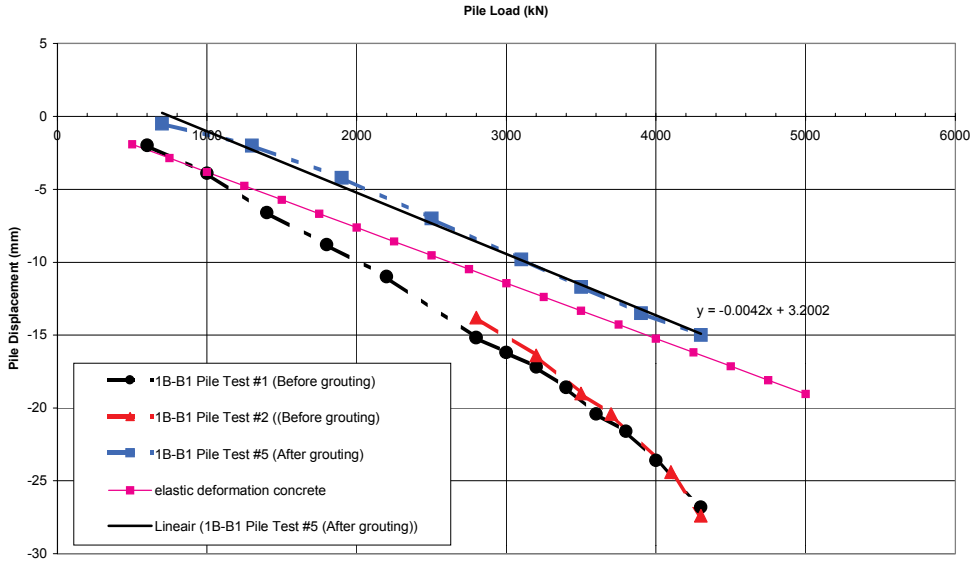


A. Figure 24 Pile load test on Wooden Piles after Jet Grouted Columns A, B, C, D

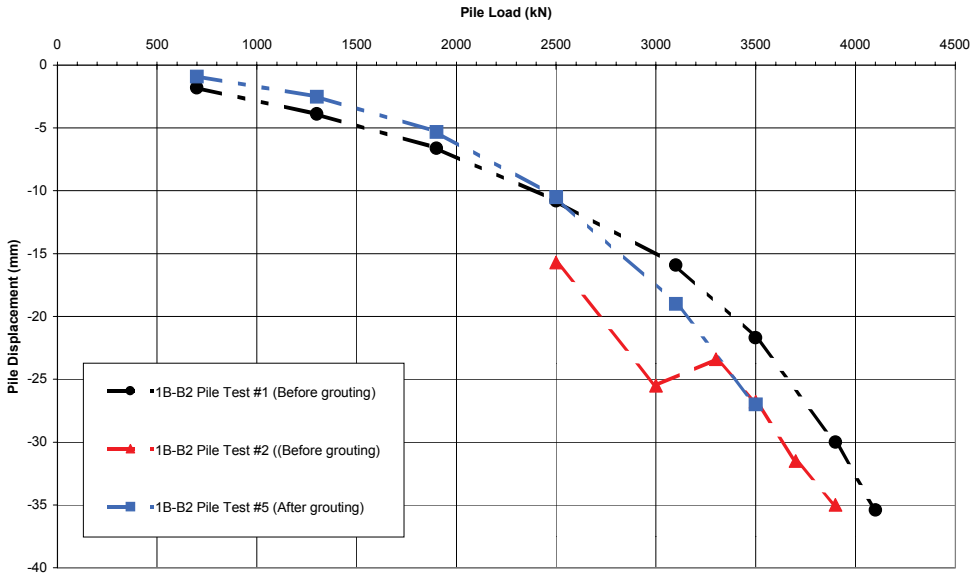


A. Figure 25 Pile load test on Wooden Piles after Jet Grouted Columns A – F, W1, W2 and W3

APPENDICES

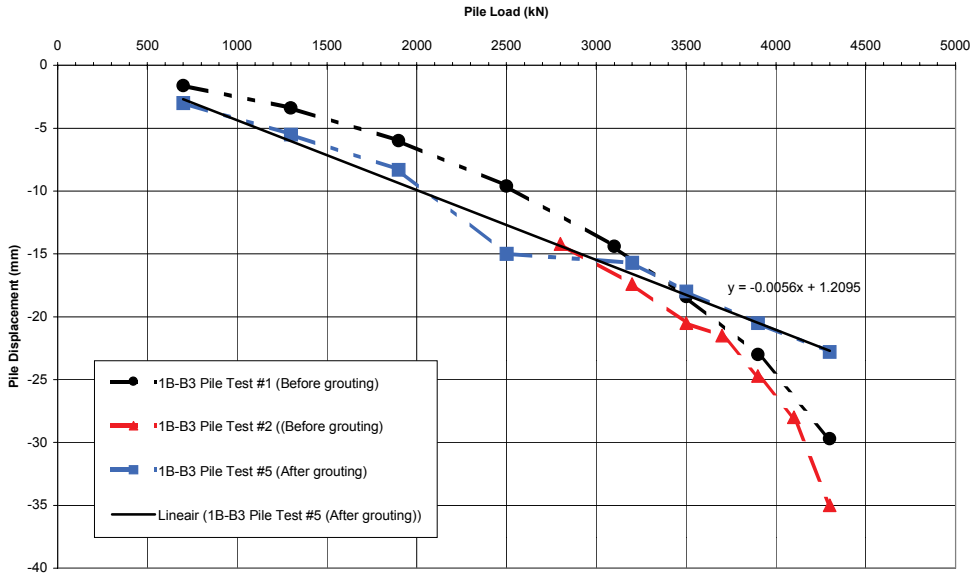


A. Figure 26 Pile Load Test 1B-B1

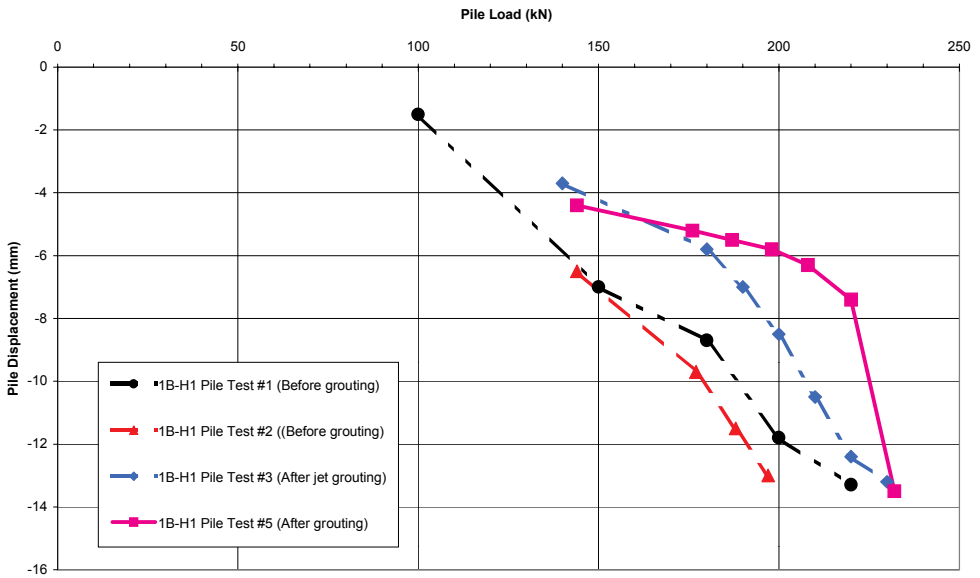


A. Figure 27 Pile Load Test 1B-B2

APPENDICES

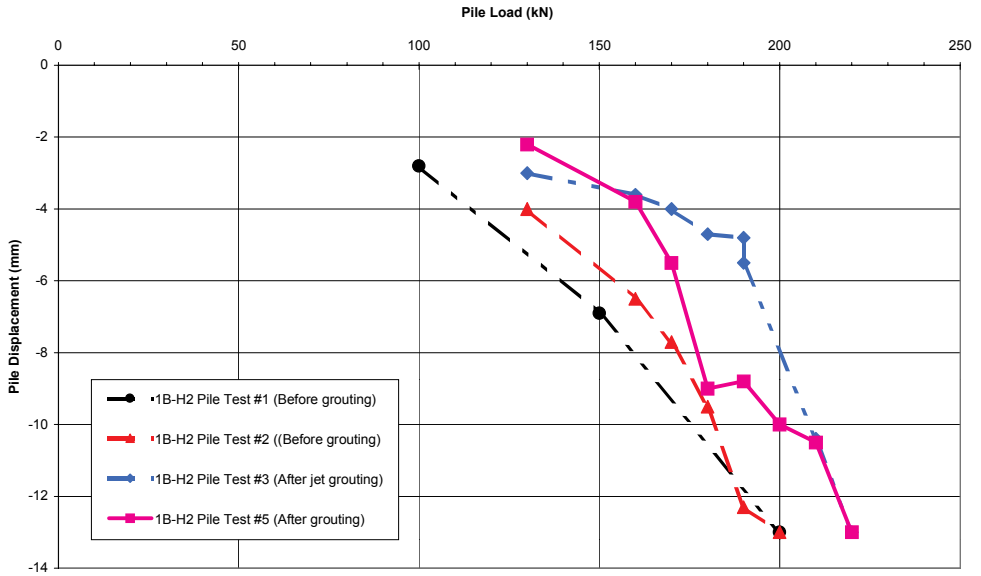


A. Figure 28 Pile Load Test 1B-B3

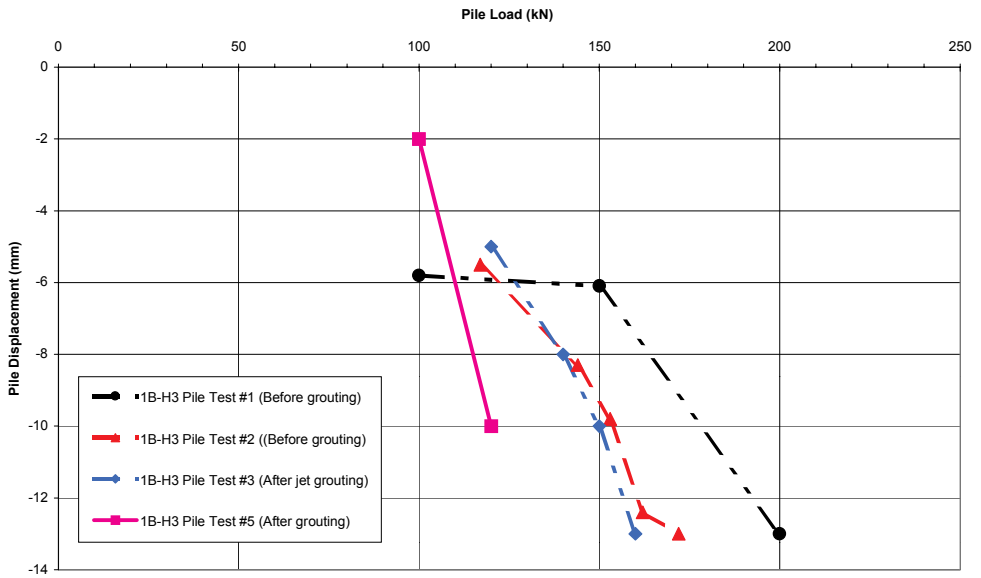


A. Figure 29 Pile Load Test 1B-H1

APPENDICES

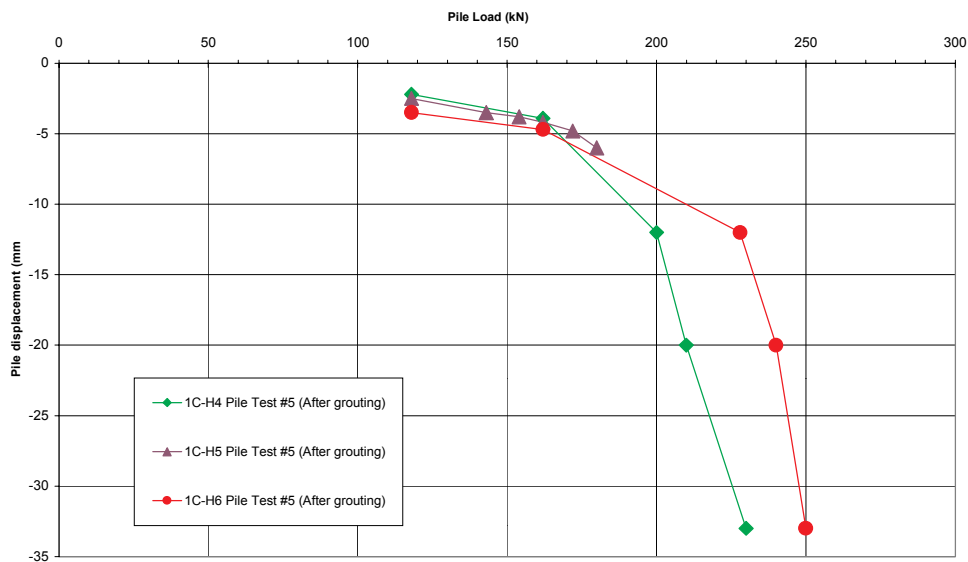


A. Figure 30 Pile Load Test 1B-H2

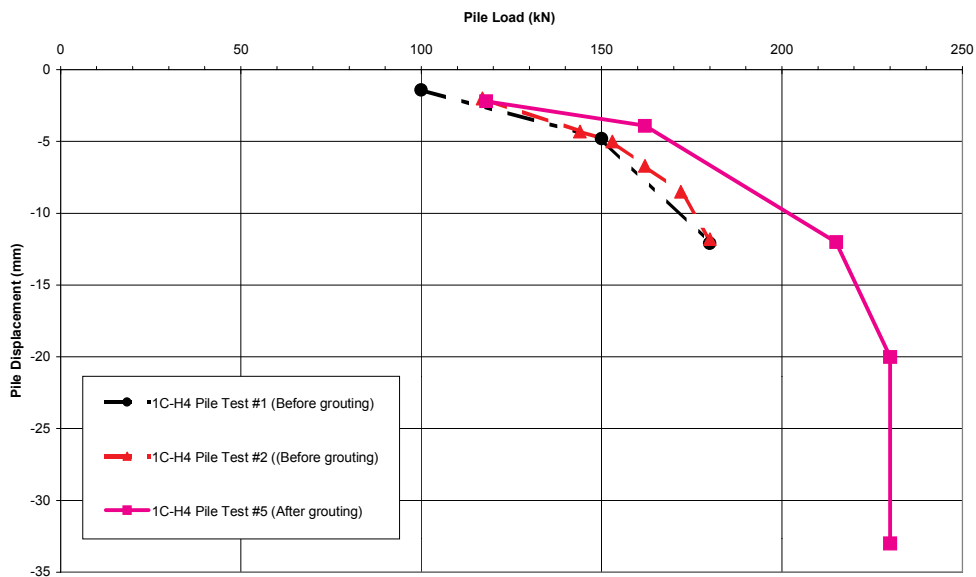


A. Figure 31 Pile Load Test 1B-H3

APPENDIX X PILE LOAD TESTS BEFORE AND AFTER COMPACTION GROUTING

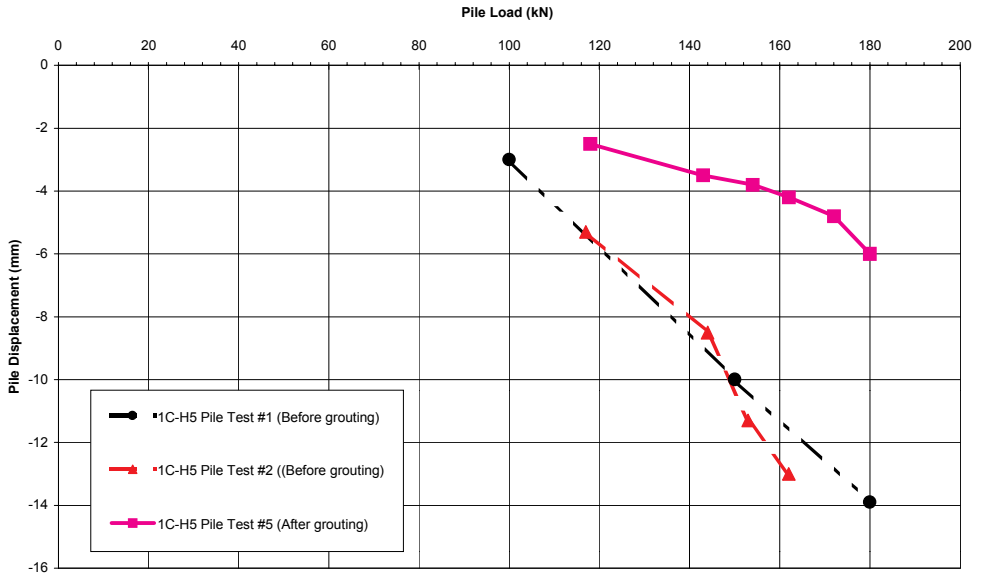


A. Figure 32 Results of Pile Load Test #5 on Pile 1C-H4, H5 and H6 after Compaction Grouting

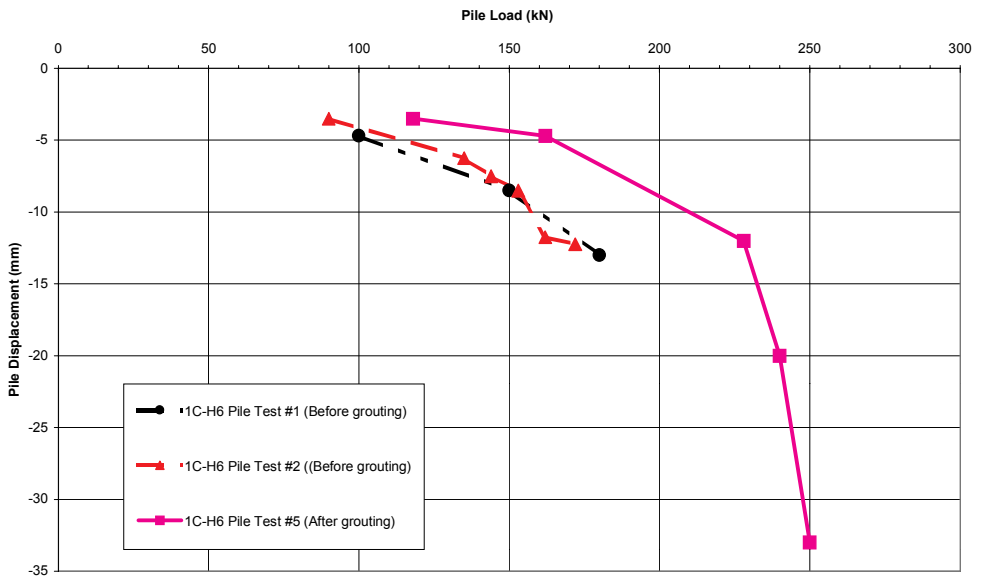


A. Figure 33 Pile Load Test Pile 1C-H4 after Compaction Grouting (#5)

APPENDICES



A. Figure 34 Pile Load Test Pile 1C-H5 after Compaction Grouting (#5)



A. Figure 35 Pile Load Test Pile 1C-H6 after Compaction Grouting (#5)

APPENDICES

APPENDIX XI DISTANCES BETWEEN PILES AND TAMS

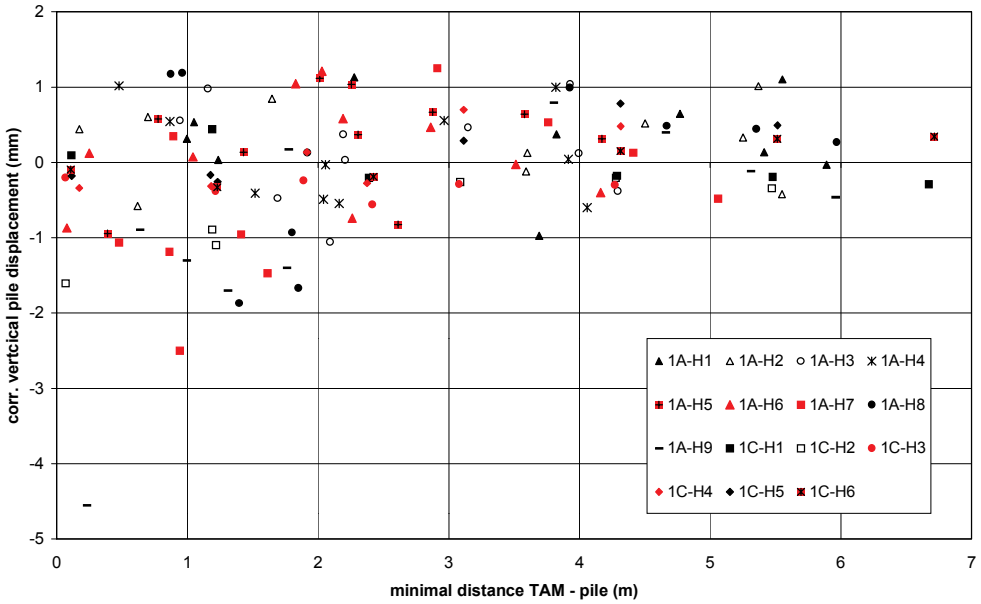
A.Table 5 Minimal distance between a TAM (design values) and a Pile/piezometer for Stage 3A

pile:	1A-H1	1A-H2	1A-H3	1A-H4	1A-H5	1A-H6	1A-H7	1A-H8	1A-H9	piezometers					
										WM-3	WM-4	WM-5	WM-6		
TAM															
F3	3.82	3.60	2.21	2.06	0.78	0.25	0.89	1.92	1.77	3.62	3.20	3.41	4.76		
P1	1.00	0.62	2.19	2.16	4.17	4.16	5.06	5.97	5.96	0.87	1.48	7.56	8.94		
P3	1.05	0.70	0.94	0.87	2.88	2.86	3.76	4.67	4.66	0.78	0.78	6.26	7.64		
P5	3.69	3.59	2.09	2.04	0.39	0.08	0.86	1.80	1.76	3.53	3.05	3.37	4.74		
P8	5.89	5.55	4.29	4.06	2.61	2.26	1.61	1.85	1.31	5.67	5.29	2.22	3.31		
P9	5.41	5.25	4.00	3.92	2.31	2.19	1.41	0.96	0.64	5.45	5.04	0.55	1.72		
PF10	5.55	5.37	3.93	3.82	2.01	1.83	0.94	0.87	0.23	5.33	4.86	1.63	2.98		
PF2	1.24	0.17	1.69	1.52	3.58	3.51	4.41	5.35	5.31	0.90	1.35	6.93	8.30		
PF4	2.28	1.65	1.16	0.48	2.25	2.03	2.91	3.93	3.80	1.90	1.79	5.42	6.78		
PF6	4.77	4.50	3.15	2.96	1.43	1.04	0.48	1.40	1.00	4.53	4.12	2.57	3.90		
				0.25	value between 0 and 0,5 m										
				0.75	value between 0,5 and 1,0 m										
				1.65	value between 1,0 and 2,0 m										

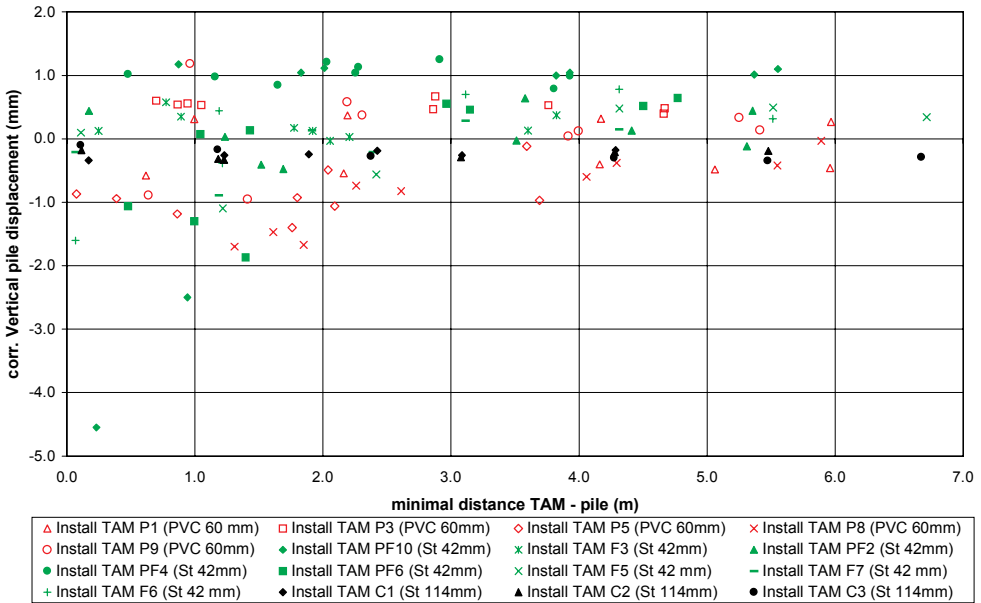
A.Table 6 Minimal distance between a TAM (design values) and a Pile/piezometer for Stage 3C

pile:	1C-H1	1C-H2	1C-H3	1C-H4	1C-H5	1C-H6	piezometers								
							WM-1	WM-12	WM-13	WM-14	WM-15	WM-16	WM-17	WM-2	
TAM															
C1	4.29	3.09	1.89	0.17	1.23	2.42	2.52	4.41	3.48	2.89	1.30	2.21	3.51	1.76	
C2	5.48	4.28	3.08	1.18	0.11	1.23	3.72	5.58	4.59	3.81	1.75	1.79	2.78	0.69	
C3	6.67	5.47	4.27	2.37	1.18	0.11	4.92	6.76	5.71	4.82	2.69	2.05	2.40	0.87	
F5	0.11	1.22	2.42	4.31	5.51	6.71	1.84	1.17	2.19	3.32	4.59	5.96	7.31	6.03	
F6	1.19	0.07	1.22	3.11	4.31	5.51	0.66	1.60	1.70	2.49	3.43	4.79	6.16	4.83	
F7	2.39	1.19	0.07	1.91	3.11	4.31	0.66	2.61	2.04	2.18	2.35	3.69	5.07	3.63	
				0.25	value between 0.0 and 0.5 m										
				0.75	value between 0.5 and 1.0 m										
				1.65	value between 1.0 and 2.0 m										

APPENDIX XII SCATTER PLOTS MINIMAL DISTANCE TAM/PILE VERSUS PILE DISPLACEMENT



A. Figure 36 Pile Scatter Plot Minimal Distance TAM-Pile vs. Pile Displacement



A. Figure 37 TAM Scatter Plot Minimal Distance TAM-Pile vs. Pile Displacement

APPENDIX XIII LIST OF FIGURES AND TABLES

Figures

Figure 1.1 Amsterdam Central Station, Beurs van Berlage and Amsterdam Royal Concert Hall (l→r).....	1
Figure 1.2 Amsterdam Mansions (Herengracht 174-150; Philips, 1769)	1
Figure 2.1 Early Cross Beam Pile Foundation (Bureau Monumentenzorg Amsterdam).....	4
Figure 2.2 Pile Driving in the 17 th Century	4
Figure 2.3 Building a Typical Amsterdam Canal-Side House	4
Figure 2.4 Amsterdam (<i>left</i>) and Rotterdam (<i>right</i>) Pile Foundation.....	5
Figure 2.5 Point Resistance, Positive Skin Friction and Negative Skin Friction Graphically Explained (after Van Tol, 1996)	6
Figure 2.6 Mechanical Processes of Pile Foundation Degradation	8
Figure 2.7 Schematic Representation of the Effect of an Embankment	9
Figure 2.8 Schematic Presentation of TBM Tunnelling under Existing Structures	10
Figure 2.9 Results of Visual Inspection of the Facades (<i>Entrepotdok</i> Amsterdam).....	12
Figure 2.10 Examples of Pile Types	15
Figure 2.11 Example Begijnhof Amsterdam	15
Figure 2.12 Example Entrepotdok Amsterdam; Stages	16
Figure 2.13 Example Entrepotdok Amsterdam; Cross Section of Tables	16
Figure 2.14 (a) Permeation Grouting (b) Jet Grouting (c) Fracturing (d) Compaction Grouting.....	17
Figure 2.15 Example of Jet Grouted Piles to Extend a Pile Foundation	18
Figure 2.16 Example of Compaction Grouting near a Pile Foundation	18
Figure 2.17 Example of Foundation Protection: TBM Tunnelling through a Grouted Structure.....	19
Figure 3.1 Map of Amsterdam Showing the Test Location	21
Figure 3.2 Typical CPT at Test Site.....	24
Figure 3.3 Grain Size Distribution of the Sand Layers and Intermediate Layer.....	25
Figure 3.4 Photograph of the Test Site	26
Figure 3.5 Typical Cross Section of the Ballast Frame Construction	27
Figure 3.6 Schematic Plan View of the Ballast Frame Construction	28
Figure 3.7 Wooden Pile during Testing.....	28
Figure 3.8 Relation Between Different Monitoring Equipment.....	29
Figure 3.9 Data Acquisition System (Fundamentum, 2000).....	30
Figure 3.10 Target Readings of the Reference Beam	31
Figure 3.11 Load Cell Readings During Permeation Grouting.....	33
Figure 3.12 Example of Total Station Irregularity.....	33
Figure 3.13 Displacement of Concrete Piles during Jet Grouting Instalation (Column C)	34
Figure 3.14 Concrete Pile during UBC Testing.....	35
Figure 4.1 Injection Unit: Pumps (left) and Controls & Registration Equipment (right).....	40
Figure 4.2 Principle of TAM and Double Packer Grouting	41
Figure 4.3 Double Packer	41
Figure 4.4 Viscosity Development in Time.....	42
Figure 4.5 Groutability Based on Grain Size Distribution (Covil, 1991 (after Cambefort, 1964)).....	46
Figure 4.6 Groutability Based on Grain Size Distribution (after Tausch, 1985).....	46
Figure 4.7 Vertical Overlap Grouted Elements.....	47
Figure 4.8 Relation between the Dimensionless Parameters R/r_0 and kht/er_0^2 for Different v	50
Figure 4.9 Relation between Grouting Pressure and Radius of the Grouted Element.....	51
Figure 4.10 Relation between Grouting Time and Radius of the Grouted Element.....	51
Figure 4.11 Relation Between the Strength (UCS) and the Percentage of Pores Filled (Kutzner, 1996).....	52
Figure 4.12 Test Set-up of Groutability Test	54
Figure 4.13 Groutability: Injection Pressure and Flow	55
Figure 4.14 Detailed Test Set-up: Plan View of the Piles, TAMs, Piezometers and Grout Elements	58
Figure 4.15 Typical Cross Section and Views of Piles, TAMs and Grout Elements	58
Figure 4.16 Typical Cross Section and Views of Piles, TAMs and Grout Elements	59
Figure 4.17 Definition Minimum Distance Between Pile Toe and TAM	60
Figure 4.18 Visualisation of the Grouted Element and the Influence Zone of the Pile	61
Figure 4.19 Monitoring Data of Pile 1A-H5 during TAM Installation	61
Figure 4.20 Jointmeter Readings during TAM Installation	62
Figure 4.21 Load and Displacement of Piles 1A-H7 and 1A-H9 during TAM Installation	62
Figure 4.22 Pile Reaction During \varnothing 150mm, Rotary Flushed Borings without Casing (TAM Installation)	63

APPENDICES

Figure 4.23 Probability of Pile Head Displacement during TAM Installation (Distance TAM –Pile < 2m).....	64
Figure 4.24 Piezometer & SMS Readings during TAM Installation.....	65
Figure 4.25 Piezometer and SMS Readings during Permeation Grouting.....	66
Figure 4.26 Example of Pile Load Test: Wooden Pile 1A-H6.....	67
Figure 5.1 Jet Grouting: High Pressure Cutting with Water (Shown at Surface Level).....	69
Figure 5.2 X-Jet.....	70
Figure 5.3 Monitor Used at the Test.....	71
Figure 5.4 Jet Grouting Process.....	71
Figure 5.5 Jet Grouting Systems: Principle Layout and Monitor Detail.....	72
Figure 5.6 Different Components of the Jet Grouting System.....	73
Figure 5.7 Jet Grouted Column (a) and Jet Grouted Panel (b,c).....	74
Figure 5.8 Jet Grouting Sequence: Fresh In Fresh (a) and Primary-Secondary (b).....	74
Figure 5.9 Jet Grouted Structures.....	75
Figure 5.10 Example of Work Diagram of Jet Grouting Pumps (De Vleeshauwer and Maertens, 1999).....	77
Figure 5.11 Relation Jet Grouting Pressure - Penetration Distance (De Vleeshauwer and Maertens, 1999).....	80
Figure 5.12 Indication of Jet Grouting Column Diameters (De Vleeshauwer and Maertens, 1999).....	80
Figure 5.13 Pressure Development of the Jet (De Vleeshauwer and Maertens, 1999).....	81
Figure 5.14 Details of Jet Grouting for Foundation Renovation: Columns E,F, W1, W2, W3 and with Alternative <i>wcr</i> for Columns X1 & X2.....	83
Figure 5.15 Details of Jet Grouting for Foundation Protection: Columns A-D.....	83
Figure 5.16 Detailed Test Set-Up: Cross Section of Columns A, B, C, D, X1 and X2 and Piles.....	84
Figure 5.17 Cross Section of Jet Grouting for Foundation Renovation: Pile Extension Columns E, F and W.....	84
Figure 5.18 Targets Attached to a Pole Mounted on the Inclinometers and Extensometers.....	86
Figure 5.19 Position of the Inclinometers, CPTs, Extensometers, Beacons and Piezometers in the Soil.....	86
Figure 5.20 Cores taken from Jet Grouted Sand Column B (<i>left</i>) and Jet Grouted Peat Column C (<i>right</i>).....	88
Figure 5.21 Position of the Cores taken from Columns A – D.....	88
Figure 5.22 Storage in Water Basin of Cores from Jet Grouted Columns.....	89
Figure 5.23 UCS Related to NAP Depth (m).....	90
Figure 5.24 Relation between Water Cement Ratio <i>wcr</i> and Compressive Strength f_u for Clay Layers.....	91
Figure 5.25 Relation between Water Cement Ratio <i>wcr</i> and Compressive Strength f_u for Sand Layers.....	91
Figure 5.26 Tensile Strength $f_{ct,sp}$ vs. Compressive Strength f_c for Jet Grouted Sand Layers.....	93
Figure 5.27 Tensile Strength $f_{ct,sp}$ vs. Compressive Strength f_c for Jet Grouted Clay Layers.....	93
Figure 5.28 Young's Modulus E_{cm} vs. Compressive Strength f_c for Jet Grouted Sand Layers.....	95
Figure 5.29 Young's Modulus E_{cm} vs. Compressive Strength f_c for Jet Grouted Clay Layers.....	95
Figure 5.30 Mass Density of the Jet Grouted Soil Layers.....	96
Figure 5.31 Displacement of Wooden Piles during Jet Grouting Column B.....	98
Figure 5.32 Close up of Displacement of Wooden Piles during Jetting Column B.....	99
Figure 5.33 Displacement of Concrete Piles during Jet Grouting Installation (Column B).....	99
Figure 5.34 Piezometer during Jet Grouting Column B.....	100
Figure 5.35 Piezometers in the Soil During Jet Grouted Columns B, C and D.....	101
Figure 5.36 Close Up of Piezometers in the Soil during Jet Grouting Columns B,C and D.....	101
Figure 5.37 Piezometers in the Piles During Jet Grouting Columns B, C and D.....	102
Figure 5.38 Maximum Increase in Pore Water Pressure versus Distance between the Piezometer and the Edge of the Jet Grouted Column (A,B,C,D).....	102
Figure 5.39 SMS in the Piles During Grouting Columns B, C and D.....	103
Figure 5.40 Extensometer Displacement during Jet Grouting Columns B and C.....	104
Figure 5.41 Surface Levelling Point Displacement during Jet Grouting Columns A,B,C,D.....	105
Figure 5.42 Example of Pile Load Test: Wooden Pile 1B-H1.....	106
Figure 5.43 Displacement of Concrete Piles during Jet Grouting Columns E and F.....	108
Figure 5.44 Displacement of Concrete Piles during Jet Grouting Column F (close up).....	109
Figure 5.45 Displacement of Wooden Piles during Jet Grouting Columns E and F.....	109
Figure 5.46 Displacement of Wooden Piles during Jet Grouted Columns W1 and W3.....	110
Figure 5.47 Displacement of Wooden Piles during Jet Grouting Column W2.....	111
Figure 5.48 Piezometers and SMS during Jet Grouting Columns E and F.....	112
Figure 5.49 SMS during Jet Grouting Columns E and F (close up).....	112
Figure 5.50 Piezometers and SMS during Jet Grouting Column W2 (close up).....	113
Figure 5.51 Test Results of Pile B1 and Elastic Deformation of a Concrete Pile with $E_c=30.000 \text{ N/mm}^2$	114
Figure 5.52 Pile Settlement versus Distance Pile - Outside Jet Grouted Column.....	116
Figure 5.53 Extra Influenced Zone by Jet Grouting a larger Diameter Column.....	117
Figure 5.54 Reduction of Cone Resistance as Function of the Distance from the Column.....	118

APPENDICES

Figure 5.55 View of Excavated Site (left) ; Top View of Column A (right).....	119
Figure 6.1 Very Stiff, Low Mobility Compaction Grout	123
Figure 6.2 Grout Composition (Bandimere, 1997).....	124
Figure 6.3 Bottom Up (<i>left</i>) and Top Down (<i>right</i>) Grouting of a Foundation Pile	127
Figure 6.4 Lateral Displacement of a Foundation Pile due to Compaction Grouting	127
Figure 6.5 Compaction Grouting next to a Foundation Pile, Densification and Possible Soil Movement.....	128
Figure 6.6 Expansion of a Cavity.....	130
Figure 6.7 Compaction Grouting Models for the Amsterdam Situation	131
Figure 6.8 Geometry (<i>left</i>) and Mesh (<i>right</i>)	132
Figure 6.9 Relative Shear Stress at Failure (<i>left</i>) and Plastic Points (<i>right</i>).....	133
Figure 6.10 Effective Stresses next to a Compaction Grouting Element	133
Figure 6.11 Total Displacements next to a Compaction Grouting Element	134
Figure 6.12 General Plan View of the Piles and Tubes.....	134
Figure 6.13 Typical Cross Section of Pile and Tube.....	135
Figure 6.14 Detailed Test Set-up: Plan View of the Monitoring Equipment	136
Figure 6.15 Typical Cross Section of Piles and Reference Frame	136
Figure 6.16 Position of the Grouted Element (<i>left</i>) and Causing of the Heave (<i>right</i>).....	137
Figure 6.17 Attachment of a Removable Plug at the Bottom End of the Tube.....	138
Figure 6.18 Installation of the Tubes	138
Figure 6.19 Grouting Equipment used for the Test	139
Figure 6.20 Cement Bentonite Sleeve Grout Backflow at Surface Level.....	140
Figure 6.21 Displacement of the Piles During Grouting.....	141
Figure 6.22 Vertical Displacements due to Grouting.....	142
Figure 6.23 Displacement of the Piles in Relation to Distance from the Grouting Centre of Gravity.....	142
Figure 6.24 Surface Levelling Point during Grouting.....	144
Figure 6.25 Surface Levelling Point during and 2.5 Days after Grouting.....	145
Figure 6.26 Surface Levelling Points: Maximum, after 1 Day and after 5 Days.....	145
Figure 6.27 Piezometer Readings during Compaction Grouting	146
Figure 6.28 Piezometer Readings after Compaction Grouting	147
Figure 6.29 Maximum Piezometer Readings as a Function of Distance to the Point of Injection	147
Figure 6.30 Reconstruction of the Horizontal Effective Stresses.....	148
Figure 6.31 Location of CPTs	149
Figure 6.32 Example of Pile Load Test: Wooden Pile 1C-H5	151
Figure 7.1 Principle Sketch and Photograph of Umbrella used in Amsterdam.....	154
Figure 7.2 Test Set-up Stage 1.....	155
Figure 7.3 Results of Electrical Resistance (left) Electromagnetic Measurements (right).....	156
Figure 7.4 Electrical Resistance Measurement Column C2.....	156
Figure 7.5 Image of a BHR Measurement in a Jet Grouted Column	158
Figure 7.6 Interpreted Electrical Resistance Measurement and BHR Measurements Column A.....	159
Figure 7.7 Interpreted Electrical Resistance Measurement and BHR Measurements Column D.....	159
Figure 7.8 Interpreted BHR Measurements Column B.....	160
Figure 7.9 Interpreted BHR Measurements Column C.....	160
Figure 7.10 Interpreted BHR Measurements Column X1.....	161
Figure 7.11 Interpreted BHR Measurements Column X2.....	161
Figure 8.1 Schematic Presentation of Permeation Grouting Wooden Pile Foundation (Façade Only).....	164
Figure 8.2 Single Injection Point.....	165
Figure 8.3 Schematic Presentation of Permeation Grouting Wooden Pile Foundation (Whole Structure)	165
Figure 8.4 Example of Compaction Grouting used on a Typical Amsterdam Structure	167

Tables

Table 3.1 Soil Characteristics at the Full-Scale Injection Test Site.....	25
Table 3.2 Pile Characteristics (average values).....	26
Table 3.3 Theoretical Bearing Capacity of the Piles.....	35
Table 3.4 Load Steps Pile Load Tests 1, 2 and 3.....	36
Table 3.5 Bearing Capacity Tests 1 and 2 of the Wooden and Concrete Piles.....	37
Table 3.6 Vertical Displacement of the Four Corners of the Ballast Frame (mm).....	38
Table 4.1 Indication of Average Unconfined Compressive Strength of Permeation Grouted Soil.....	53
Table 4.2 Soil Layers Tested Using Permeation Grouting.....	53
Table 4.3 Grout Types used for Testing.....	54
Table 4.4 Results of Laboratory UCS Tests on Permeation Grouting Elements.....	56
Table 4.5 Grout Elements and Accompanying TAM Code.....	59
Table 4.6 Permeation Grouting Characteristics.....	60
Table 5.1 Typical Average Unconfined Compressive Strength of Jet Grouted Soil.....	76
Table 5.2 Ranges of Jet Grouting Parameters (from prEN 12761).....	76
Table 5.3 Results of 3D-FEM Calculations for Jet Grouted Columns near Concrete Pile.....	80
Table 5.4 Dimensions of the Jet Grouted Columns.....	85
Table 5.5 Average Process Parameters used for Jetting the Columns.....	87
Table 5.6 Average and Standard Deviation UCS (f_c ; MPa).....	89
Table 5.7 Average and Standard Deviation Tensile Strength ($f_{ct,sp}$; MPa).....	92
Table 5.8 Average and Standard Deviation Young's Modulus (E_{cm} ; MPa).....	94
Table 5.9 Average Friction Angle and Shear Strength of the Grout.....	94
Table 5.10 Comparison Mass Density Soil versus Grouted Soil (kg/m^3).....	96
Table 5.11 Compressive Strength Grout vs. Spoil.....	97
Table 5.12 Calculation of Effective Stress Change from Total Stress and Pore Water Pressure Change.....	103
Table 5.13 Changing CPT value due to Jet Grouting (CPT after/CPT before * 100%).....	117
Table 5.14 Average Measured Diameter (Excavation).....	119
Table 5.15 Empirical Relations for the Relation between Various Grout Parameters.....	121
Table 6.1 Parameters used for PLAXIS 2D-FEM Calculations.....	132
Table 6.2 Piezometers.....	136
Table 6.3 Compaction Grout Composition.....	137
Table 6.4 Tube Installation and Grouting Data.....	139
Table 6.5 Vertical Displacements (mm) due to Compaction Grouting Tube Installation.....	140
Table 6.6 Maximum CPT Values Before and After Compaction Grouting.....	150
Table 8.1 Indicative Economic Damage (€).....	168

Annex Figures

A.Figure 1 Driving of Concrete (<i>left</i>) and Wooden (<i>right</i>) Piles	187
A.Figure 2 Placement of Stelcon Plates and Steel HE Profiles	187
A.Figure 3 Placement of Dragline Boards, and Stelcon & Sand Ballast	187
A.Figure 4 SMS and Piezometer in a Concrete Pile	189
A.Figure 5 SMS and Piezometer in a Wooden Pile	189
A.Figure 6 Piezometer	190
A.Figure 7 Inclinator components (<i>left</i>) and PVC Inclinator Casing (<i>right</i>)	190
A.Figure 8 Extensometer	191
A.Figure 9 Total Station	191
A.Figure 10 Pile Load Test 1 (Location A)	192
A.Figure 11 Pile Load Test 2 (Location A)	192
A.Figure 12 Pile Load Test 1 (Location B and C)	193
A.Figure 13 Pile Load Test 2 (Location B and C)	193
A.Figure 14 Pile Load Test 1 (Location B Concrete Piles)	194
A.Figure 15 Pile Load Test Pile 1A-H1 after Permeation (#3) and Compensation Grouting (#4/5)	194
A.Figure 16 Pile Load Test Pile 1A-H2 after Permeation (#3) and Compensation Grouting (#4/5)	195
A.Figure 17 Pile Load Test Pile 1A-H3 after Permeation (#3) and Compensation Grouting (#4/5)	195
A.Figure 18 Pile Load Test Pile 1A-H4 after Permeation (#3) and Compensation Grouting (#4/5)	196
A.Figure 19 Pile Load Test Pile 1A-H5 after Permeation (#3) and Compensation Grouting (#4/5)	196
A.Figure 20 Pile Load Test Pile 1A-H6 after Permeation (#3) and Compensation Grouting (#4/5)	197
A.Figure 21 Pile Load Test Pile 1A-H7 after Permeation (#3) and Compensation Grouting (#4/5)	197
A.Figure 22 Pile Load Test Pile 1A-H8 after Permeation (#3) and Compensation Grouting (#4/5)	198
A.Figure 23 Pile Load Test Pile 1A-H9 after Permeation (#3) and Compensation Grouting (#4/5)	198
A.Figure 24 Pile load test on Wooden Piles after Jet Grouted Columns A, B, C, D	199
A.Figure 25 Pile load test on Wooden Piles after Jet Grouted Columns A – F, W1, W2 and W3	199
A.Figure 26 Pile Load Test 1B-B1	200
A.Figure 27 Pile Load Test 1B-B2	200
A.Figure 28 Pile Load Test 1B-B3	201
A.Figure 29 Pile Load Test 1B-H1	201
A.Figure 30 Pile Load Test 1B-H2	202
A.Figure 31 Pile Load Test 1B-H3	202
A.Figure 32 Results of Pile Load Test #5 on Pile 1C-H4, H5 and H6 after Compaction Grouting	203
A.Figure 33 Pile Load Test Pile 1C-H4 after Compaction Grouting (#5)	203
A.Figure 34 Pile Load Test Pile 1C-H5 after Compaction Grouting (#5)	204
A.Figure 35 Pile Load Test Pile 1C-H6 after Compaction Grouting (#5)	204
A.Figure 36 Pile Scatter Plot Minimal Distance TAM-Pile vs. Pile Displacement	206
A.Figure 37 TAM Scatter Plot Minimal Distance TAM-Pile vs. Pile Displacement	206

Annex Tables

A.Table 1 Characteristic Soil Parameters	186
A.Table 2 Time of TAM installation	186
A.Table 3 Dates of Jet Grouting: Drilling and Jetting Activities	188
A.Table 4 Date of Activities and Time Lap between the Different Activities of Jet Grouting	188
A.Table 5 Minimal distance between a TAM (design values) and a Pile/piezometer for Stage 3A	205
A.Table 6 Minimal distance between a TAM (design values) and a Pile/piezometer for Stage 3C	205

DUTCH ABSTRACT / SAMENVATTING

Het doel van dit promotieonderzoek is geweest het gebruik van groutmethoden (*grouting*) als funderingsverbeteringsstelsysteem te onderzoeken. Onder funderingsverbeteringsstelsysteem wordt hier verstaan hetzij funderingsrenovatie (het verhogen van de draagkracht van paalfunderingen met onvoldoende draagvermogen), hetzij funderingsbescherming (het beschermen van paalfunderingen tegen mogelijke schade resulterend uit al dan niet ondergrondse bouwactiviteiten).

In sommige gevallen is de opgetreden verschuiving van een bouwwerk dusdanig dat maatregelen dienen te worden genomen om de negatieve effecten hiervan te bestrijden. Een andere reden voor het nemen van maatregelen kan zijn dat (ondergrondse) bouwactiviteiten de draagkracht van paalfunderingen onaanvaardbaar hebben aangetast. De maatregelen hebben over het algemeen het herstel van het draagvermogen van de fundering tot doel. Voordat herstel kan plaatsvinden dient een funderingsonderzoek uitgevoerd te worden om zorgvuldig alle mogelijke schadeoorzaken te kunnen bepalen. Vervolgens dienen, door gebruik te maken van geschikte schadedetectie-methoden, de ernstigste schadeoorzaken te worden bepaald.

Tot op heden is funderingsverbetering meestal toegepast in de vorm van de installatie van additionele palen (zogenaamde conventionele funderingsverbeteringsystemen). Omdat dergelijke systemen, die meestal vereisen dat de palen binnen het gebouw worden aangebracht, aanzienlijke hinder en economische schade tot gevolg kunnen hebben, is het doel van dit onderzoek geweest om vast te stellen in hoeverre groutmethoden geschikt zijn als funderingsverbeteringsstelsysteem.

Allereerst is een uiteenzetting gegeven van enkele definities en normen met betrekking tot paalfunderingen. Na een korte verhandeling over de geschiedenis van paalfunderingen volgen een inleiding betreffende de oorzaken en detectie van funderingsschade en een overzicht van mogelijkheden voor funderingsverbetering.

Een van de herstelmethoden, zijnde het gebruik van groutmethoden voor funderingsverbetering, kan over het algemeen van buiten het bouwwerk af worden uitgevoerd en voorkomt bovendien de noodzaak tot stutten. Vanwege de zeer beperkte ervaring met dergelijke funderingsverbeteringen (en dan met name de onzekerheid aangaande de reactie van de funderingspalen op het installatie- en groutproces) werd verder onderzoek noodzakelijk geacht. In Amsterdam is derhalve een proef op ware schaal uitgevoerd, waarvan in deze thesis o.a. de proefopzet en een analyse op de consistentie van de resultaten zijn gegeven. De invloed van de groutmethoden op de paalfunderingen is vastgesteld door de paalverplaatsingen, de grond- en waterspanningen en de verandering van het paal draagvermogen te onderzoeken.

Het zwaartepunt in deze studie wordt gevormd door het onderzoeken van drie groutmethoden, zijnde:

1. bodeminjectie (*permeation grouting*),
2. jetgrouten (*jet grouting*) en
3. grondverdringend grouten (*compaction grouting*).

Voor elk van de methoden zijn allereerst enkele algemene aspecten, zoals de historie, te gebruiken apparatuur, grout parameters en het toepassingsgebied gekenschetst. Vervolgens zijn bestaande theorieën voor het modelleren van het groutproces onderzocht en vergeleken en zijn enige Eindige Elementen Methode (EEM) berekeningen uitgevoerd. Dit heeft tot de algemene conclusie geleid dat alle groutmethoden, en in het bijzonder jetgrouten, dusdanig complex van aard zijn dat modelleren alleen van nut is om een beter begrip van het proces te ontwikkelen. Voor toepassing in de ingenieurspraktijk zijn deze methoden niet geschikt.

Een belangrijk uitgangspunt bij de proef is geweest dat de effecten van het grouten konden worden geïsoleerd van de effecten ten gevolge van belastingswijzigingen. Daarom is de gebruiksbelasting op de palen ten allen tijde gehandhaafd. Het gevolg is dat de resultaten van de proef een bovengrens vormen voor paalzettingen die zullen optreden wanneer grouten als funderingsverbetering-systeem wordt toegepast.

Er zijn vele overeenkomsten te vinden in het installatieproces voor de TAMs voor bodeminjectie, de buizen voor grondverdringend grouten of het op diepte brengen van de jetgrout monitor. Meestal traden slechts niet-significante veranderingen van grond- en waterspanningen op. De verplaatsingen waren slechts dan noemenswaardig wanneer de afstand tussen de TAM/buis/monitor en de houten paal minder dan 0,5 m bedroeg.

Uit de injecteerbaarheidstest voor bodeminjectie kon worden afgeleid dat de toepasbaarheid grenzen volgens Taush (1985) voor gebruik van een silicagel redelijk correct zijn voor de Amsterdamse situatie. Voor het grouten in de verschillende grondlagen werd geen significant verschil in injectiedruk gevonden. De invloed van het grouten op paalverplaatsingen en grond- en waterspanningen was niet significant, hetgeen gezien het niet verstorende karakter van het groutinjectie-proces, te verwachten was. Wanneer bodeminjectie wordt gebruikt voor funderingsbescherming, zal het draagvermogen van de palen zeker niet afnemen. Wanneer echter bodeminjectie wordt gebruikt voor funderingsrenovatie, kan het draagvermogen van de palen aanzienlijk worden verhoogd. Wanneer meer elementen dicht bij de paal zijn gepositioneerd neemt dit positief effect aanzienlijk toe.

Gedurende het jetgrouten voor funderingsbescherming zijn de paalverplaatsingen tijdens het jetten beperkt gebleven tot 2 mm voor elke aangebrachte jetgroutkolom. Noch de afstand tussen de funderingspaal en de jetgroutkolom, noch de diameter van de kolom leken invloed te hebben op de paalverplaatsing. Wanneer echter dichter dan 0,5 m bij paalpuntniveau werd gejet en dan in het bijzonder onder paalpuntniveau, namen de paalverplaatsingen exponentieel toe. In dat geval werden ook significante wijzigingen in de grond- en waterspanningen geregistreerd. Een coherente relatie tussen de veranderingen in grondspanning en de paalverplaatsingen kon echter niet worden gevonden.

Na het jetgrouten voor funderingsbescherming was noch het paal draagvermogen noch de stijfheid van de houten palen negatief beïnvloed door het grouten. Na het jetgrouten voor funderingsrenovatie toonden de met grout behandelde betonnen palen nagenoeg exclusief elastische vervormingen en geen enkel teken van het bereiken van hun bezwijkdraagvermogen. Het afleiden van een relatie voor de verandering in conusweerstand ten gevolge van het jetgrouten is niet mogelijk gebleken.

Voor wat betreft de monsters verkregen uit de boorkernen van de jetgroutkolommen kon worden geconcludeerd dat, hoewel afdoende sterkte en stijfheid waren bereikt, de variatiecoëfficiënt van de parameters hoog lag. Enige empirische relaties voor het verband tussen de verschillende parameters zijn afgeleid (zie Table 5.15 op pagina 121).

Gedurende de proef heeft het grondverdringend grouten achtereenvolgens gezorgd voor paal- en maaiveldheffingen (veroorzaakt door de grote geïnjecteerde groutvolumes) en -zettingen (veroorzaakt door consolidatie). De punten die het dichtst bij het injectiepunt lagen, vertoonden meestal de grootste verplaatsingen en wateroverspanningen; een relatie tussen de injectiedruk en de wateroverspanningen kon echter niet worden afgeleid. De paalzettingen stopten wanneer de wateroverspanningen gedissipeerd waren.

Het gebruik van grondverdringend grouten bij een paalpunt heeft het paal draagvermogen aanzienlijk (35%) kunnen vergroten, hetgeen overeenstemde met berekeningen van de *compactie ratio*. Bovendien vertoonden de palen een stijvere last-zakkings-karakteristiek.

Voor alle groutmethoden spelen de dimensies van het groutelement een belangrijke rol in het bepalen van de invloed van het grouten op de omgeving. Geofysische meetsystemen kunnen bij het bepalen van deze dimensies een nuttig hulpmiddel vormen. Over het geheel gezien lieten de elektrische weerstandsmetingen een geometrie zien die redelijk overeenstemde met de werkelijke vorm van de groutelementen. Deze methode heeft echter als nadeel minder geschikt te zijn als actief monitoringsinstrument tijdens jetgrouten. Het gebruik van boorgat-radar metingen bij bodeminjectietoepassingen wordt als niet haalbaar beschouwd. Boorgat-radar metingen in jetgroutkolommen hebben aangetoond dat deze methode de kolomdiameter over het algemeen onderschat.

Om te kunnen bepalen in hoeverre groutmethoden kunnen worden toegepast voor funderingsrenovatie zijn de kosten en hinder van groutmethoden vergeleken met die van conventioneel funderingsherstel. De constructiekosten van gROUTen kunnen tot circa 50% lager uitvallen dan de kosten van conventioneel funderingsherstel. Wanneer gROUTen wordt gebruikt voor het renoveren van bouwwerken met een commerciële functie, dan bedragen de kosten inclusief omzetting 30% - 65% van de kosten van conventioneel funderingsherstel. Voor bouwwerken met een woonbestemming is dit 50% - 85%.

Resumerend kan na de analyse van de proefresultaten en beschouwing van kosten en hinder van de groutmethoden de conclusie getrokken worden, dat bodeminjectie en grondverdringend gROUTen geschikte methoden voor funderingsrenovatie zijn. JetgROUTen werd alleen geschikt bevonden wanneer het bouwwerk stijf en sterk genoeg is om de heersende paalbelastingen her te verdelen. Voor funderingsbescherming komen alleen bodeminjectie en jetgROUTen in aanmerking, waarbij jetgROUTen vanwege de toepasbaarheid in nagenoeg alle grondsoorten en de betere sterkte- en stijfheidparameters een groter toepassingsgebied kent.

Ten slotte moet worden opgemerkt dat het gebruik van groutmethoden als funderingsverbeteringssysteem en conventioneel funderingsherstel niet zondermeer kunnen worden vergeleken omdat.

1. bij het maken van de kostenramingen voor de groutmethoden geen economische schaafeffecten konden worden meegenomen.
2. er bij conventioneel funderingsherstel een geheel nieuwe fundering (palen en vloer) wordt verkregen, terwijl bij de renovatie middels groutmethoden slechts de bestaande fundering wordt versterkt.

Het is daarom dat conventioneel funderingsherstel een meerwaarde kan hebben als verbeteringsmethode. Wanneer beide methoden echter even geschikt zijn, valt het te betwijfelen of de hogere kosten van conventioneel funderingsherstel deze meerwaarde rechtvaardigen.

Voor wat betreft het toekomstperspectief van jetgROUTen kan worden geconcludeerd dat zolang geen database voorhanden is waaruit de relatie tussen de invoer- en uitvoerparameters is af te leiden, afhankelijk van de omvang van het project een of meerdere proefkolommen dienen te worden geconstrueerd nog voor het wordt gestart. Vanwege de grote spreiding die over het algemeen wordt gevonden wanneer sterkte- en stijfheidparameters worden geanalyseerd, moet een gedegen risico inschatting worden gemaakt of dienen veiligheidsfactoren van 2 tot 3 te worden gebruikt. Daarnaast wordt het belang van nauwkeurig monitoren van het jetgROUTproces, om opbarsten te voorkomen, benadrukt. Om dit opbarsten tegen te gaan zouden bijvoorbeeld de retourspoeling en gROUTdruk bij de monitor constant gemeten kunnen worden.

De belangrijkste aanbeveling op het gebied van grondverdringend gROUTen is dat, om een nauwkeurige installatie te verzekeren, het volume van het geïnjecteerde element nauwkeurig gecontroleerd moet worden.

CURRICULUM VITAE

Almer Engelbert Carl van der Stoel

Geboren 1 September 1971 te Amsterdam



- 1983-1989 Atheneum-B (VWO), Waterlant College Amsterdam
Pre-University Education
- 1989-1993 HTS Weg- & Waterbouwkunde, Hogeschool van Amsterdam,
Technische & Maritieme Faculteit,
(afstudeerrichting Waterbouwkunde)
BSc Civil Engineering
- 1993-1996 TU Civiele techniek, *cum laude*, TU Delft
(afstudeerrichting Geotechniek)
MSc Civil Engineering
- 1994-1998 Deeltijd docent afdeling Civiele Techniek van de Hogeschool van Amsterdam
(voor de vakken Algemene Mechanica, Grondmechanica, Milieutechniek en
Vloeistofmechanica)
*Part-time Lecturer Amsterdam Polytechnic (Applied Mechanics, Soil
Mechanics, Environmental Engineering, Fluid Mechanics)*
- 1996 Extra certificaat TU Delft
(afstudeerrichting Ondergronds Bouwen)
Additional certificate MSc Civil Engineering
- 1997-2001 Promotieonderzoek aan de TU-Delft
(Faculteiten Bouwkunde en Civiele Techniek)
PhD Architecture & Civil Engineering
- 1996-heden Geotechnisch adviseur Ingenieursbureau Amsterdam,
gedetacheerd als ontwerpleider mitigerende maatregelen bij het Adviesbureau
Noord/Zuidlijn te Amsterdam
Geotechnical Consultant / Mitigating Measures Noord/Zuidlijn Amsterdam